IAEA TECDOC SERIES

IAEA-TECDOC-1741

Guidelines for Using Fallout Radionuclides to Assess Erosion and Effectiveness of Soil Conservation Strategies

Joint FAO/IAEA Programme
Nuclear Techniques in Food and Agriculture

IAEA
International Atomic Energy Agency

GUIDELINES FOR USING FALLOUT RADIONUCLIDES TO ASSESS EROSION AND EFFECTIVENESS OF SOIL CONSERVATION STRATEGIES

IAEA-TECDOC-1741

GUIDELINES FOR USING FALLOUT RADIONUCLIDES TO ASSESS EROSION AND EFFECTIVENESS OF SOIL CONSERVATION STRATEGIES

PREPARED BY THE
JOINT FAO/IAEA DIVISION OF NUCLEAR TECHNIQUES IN FOOD AND AGRICULTURE

INTERNATIONAL ATOMIC ENERGY AGENCY
VIENNA, 2014

COPYRIGHT NOTICE

For further information on this publication, please contact:

Soil and Water Management and Crop Nutrition Section
International Atomic Energy Agency
Vienna International Centre
PO Box 100
1400 Vienna, Austria
Email: Official.Mail@iaea.org

Printed by the IAEA in Austria
June 2014

IAEA Library Cataloguing in Publication Data

Guidelines for using fallout radionuclides to assess erosion and effectiveness of soil conservation strategies. — Vienna : International Atomic Energy Agency, 2014.
p. ; 30 cm. — (IAEA-TECDOC series, ISSN 1011–4289 ; no. 1741)
ISBN 978–92–0–105414–2
Includes bibliographical references.

1. Radioactive tracers in soil science. 2. Radioisotopes in soil chemistry. 3. Soil conservation — Research. I. International Atomic Energy Agency. II. Series.

IAEAL 14–00907

FOREWORD

Soil degradation currently affects 1.9 billion hectares of agricultural land worldwide, and the area of degraded land is increasing rapidly at a rate of 5 to 7 million hectares each year. Most of this degradation is caused by inappropriate and poor land management practices in agriculture and livestock production. Among all degradation processes, including soil acidification, salinization and nutrient mining, soil erosion is by far the most common type of land degradation, accounting for 84% of affected areas, with more than three quarters of the affected surface land area located in developing countries.

Current concerns about the impacts of soil erosion on crop productivity and the environment, as well as the deployment of effective soil conservation measures, have generated an urgent need to obtain reliable quantitative data on the extent and actual rates of soil erosion to underpin sustainable soil conservation strategies. The quest for new approaches for assessing soil erosion to complement conventional methods has led to the development of methodologies based on the use of fallout radionuclides (FRNs) as soil erosion tracers.

With increasing attention being paid to land degradation worldwide, this publication explains and demonstrates FRN based methods to trace soil movement and to assess soil erosion at different spatial and temporal scales, and to evaluate the effectiveness of soil conservation strategies to ensure sustainable land management in agricultural systems. This publication summarizes the experiences and knowledge gained since the end of the 1990s in the use of FRNs by the IAEA and by scientists from both developed and developing countries involved in IAEA research networks. This publication provides guidance in the application of FRNs to stakeholders involved in sustainable agricultural development.

The IAEA wishes to thank the contributors involved in the preparation of this publication. The IAEA officers responsible for this publication were L. Mabit and G. Dercon of the Joint FAO/IAEA Division of Nuclear Techniques in Food and Agriculture.

EDITORIAL NOTE

This publication has been prepared from the original material as submitted by the contributors and has not been edited by the editorial staff of the IAEA. The views expressed remain the responsibility of the contributors and do not necessarily represent the views of the IAEA or its Member States.

Neither the IAEA nor its Member States assume any responsibility for consequences which may arise from the use of this publication. This publication does not address questions of responsibility, legal or otherwise, for acts or omissions on the part of any person.

The use of particular designations of countries or territories does not imply any judgement by the publisher, the IAEA, as to the legal status of such countries or territories, of their authorities and institutions or of the delimitation of their boundaries.

The mention of names of specific companies or products (whether or not indicated as registered) does not imply any intention to infringe proprietary rights, nor should it be construed as an endorsement or recommendation on the part of the IAEA.

The IAEA has no responsibility for the persistence or accuracy of URLs for external or third party Internet web sites referred to in this publication and does not guarantee that any content on such web sites is, or will remain, accurate or appropriate.

CONTENTS

SUMMARY

The conservation of soil and water resources has become a major concern for ensuring global food production. Soil erosion is a worldwide threat and represents the main mechanism of land degradation in both developed and developing countries. To control soil erosion, there is a need to monitor the impacts of land use and assess the effectiveness of specific soil conservation technologies. Fallout radionuclides (FRNs) have proven to be a cost effective tool to trace soil redistribution due to erosion within the landscape from plot to basin scale and can complement the information provided by conventional erosion measurements and modelling.

The purpose of this publication is to provide up to date information on the use of FRNs, such as caesium-137 (^{137}Cs), lead-210 (^{210}Pb) and beryllium-7 (^{7}Be), to assess soil erosion magnitude in agricultural land. It summarizes the state of the art in the use of these fallout radionuclides as tracers, the main assumptions, the requirements and their limitations, which have to be recognised when using FRNs as soil tracers.

This publication includes nine papers. The first paper provides background information and highlights the specificity and usefulness of ^{137}Cs, ^{210}Pb and ^{7}Be, compared to conventional non-nuclear approaches for measuring soil redistribution in agricultural landscapes and quantifying the effectiveness of soil conservation strategies in controlling and reducing soil erosion.

The next three papers cover the theoretical basis and demonstrate the use of each FRN as a soil tracer: i.e. ^{137}Cs ('^{137}Cs: A widely used and validated medium term soil tracer'), ^{210}Pb ('The use of excess ^{210}Pb (^{210}Pb$_{ex}$) as a soil and sediment tracer') and ^{7}Be ('The use of ^{7}Be as a short term soil redistribution tracer'). The most well-known conservative and validated anthropogenic radionuclide used to investigate medium-term (50 years) soil redistribution and degradation is ^{137}Cs. Therefore the main paper of this TECDOC (i.e. '^{137}Cs: A widely used and validated medium term soil tracer') is dedicated to the use of this radionuclide. The paper on 'The use of excess ^{210}Pb (^{210}Pb$_{ex}$) as a soil and sediment tracer' focuses on lead-210 (^{210}Pb) as environmental tracer. For more than five decades ^{210}Pb, which is one of the fallout radionuclides offering the broadest spectrum for environmental applications due to its geogenic origin and relatively long half-life (22 years), has been widely used for dating sediments and investigating sedimentation processes. Since the 1990s it has been used as well to provide information about the magnitude of soil and sediment redistribution. As highlighted in this paper, the analysis of this radionuclide should be undertaken with care, the accurate measurement of ^{210}Pb$_{ex}$ activity (the ^{210}Pb commonly termed unsupported or excess ^{210}Pb, which is deposited as fallout and not in equilibrium with the parent ^{226}Ra) being a fundamental requirement for using this nuclear tool as soil tracer. The next paper ('The use of ^{7}Be as a short-term soil redistribution tracer') explains how to use ^{7}Be for assessing short-term soil redistribution magnitude and for evaluating the impact of short-term (up to 6 months) changes in land use practices and the effectiveness of soil conservation measures for sustainable management. It should be recognized that ^{7}Be is still in its infancy as contemporary tracer of erosion and sedimentation processes. This cosmogenic radionuclide requires further investigation before its full potential can be exploited with confidence at large scale.

The fifth paper ('Conversion models and related software') is dedicated to the different conversion models used to convert FRN inventories into estimates of soil redistribution rates. Conversion models are a major requirement in the use of FRNs to obtain information on soil erosion and sedimentation magnitudes, since they are able to convert measurements of the

reduction or increase in the radionuclide inventory of a sampling point, relative to the local reference inventory, into a quantitative estimate of erosion or deposition rates. This paper is therefore a key paper of this TECDOC that delivers a detailed overview of the nine commonly used conversion models for use with ^{137}Cs, ^{7}Be, ^{210}Pb and the development of user-friendly software for model implementation.

The following three papers present case studies conducted respectively in Morocco, Chile, and Switzerland. The first study illustrates the potential of the combined use of fallout ^{137}Cs, ^{210}Pb and the widely applied Revised Universal Soil Loss Equation (RUSLE) to estimate medium and long-term (from 50 to 100 years) soil erosion rates and to establish sediment budgets in agricultural fields under Mediterranean climatic conditions in Morocco. The second study reports several research results obtained by using both ^{137}Cs and ^{7}Be in Chile. The combined use of these fallout radionuclides was applied for studying the effects of land use and the shift in tillage systems, i.e. from conventional to no-tillage. This paper demonstrates the clear reduction of soil loss when adopting no-tillage. In the last case study, a combined application of ^{137}Cs, stable isotope techniques (based on the use of carbon-13) and traditional erosion models, such as the Universal Soil Loss Equation (USLE) and the Water Erosion Prediction Project (WEPP) model, have been used to evaluate soil redistribution in mountainous grasslands in Switzerland. This innovative investigation has improved the understanding of winter and snow processes triggering soil erosion for future modelling of alpine systems.

The TECDOC concludes with a paper which presents current and future trends and opportunities in the use of FRNs to document agricultural soil redistribution from field to landscape scales across the short, medium and long term.

This TECDOC delivers a comprehensive step by step guidance in the application of FRNs for investigating soil erosion and soil redistribution affecting agro-ecosystems to an audience of scientists and technicians from disciplines, such as soil science, ecology, and agronomy, as well as extension workers, undergraduate and graduate students, and staff of non-governmental organizations involved in agricultural development at local, national, regional and international level.

ASSESSMENT OF SOIL EROSION AND SEDIMENTATION: THE ROLE OF FALLOUT RADIONUCLIDES

L. MABIT, F. ZAPATA, G. DERCON
Soil and Water Management and Crop Nutrition Subprogramme, Joint FAO/IAEA Division of Nuclear Techniques in Food and Agriculture,
Vienna - Seibersdorf

M. BENMANSOUR
Centre National de l'Energie, des Sciences et des Techniques Nucléaires (CNESTEN), Rabat, Morocco

C. BERNARD
Ministère de l'Agriculture, des Pêcheries et de l'Alimentation du Quebec,
Quebec, Canada

D.E. WALLING
Geography, College of Life and Environmental Sciences, University of Exeter, Exeter, United Kingdom University of Exeter, School of Geography,
Exeter, United Kingdom

Abstract

Worldwide soil degradation is affecting 1.9 billion hectares and is increasing at a rate of 5 to 7 million hectares each year. About 80% of the world's agricultural land suffers moderate to severe erosion, and 10% suffers slight to moderate erosion. As a result of climate change and global warming, water erosion risk is even expected to increase. Land degradation by soil erosion has also wider negative ecological and socio-economic impacts and the economic costs of both on-site and off-site impacts of soil erosion in agricultural land have been estimated at $400 billion per year. The current concerns about declining soil productivity, increasing downstream sedimentation, and its related environmental pollution problems in agro-ecosystems, generate an urgent need for obtaining reliable quantitative data on the extent and rates of soil erosion. To efficiently control and mitigate soil losses by erosion and reduce their environmental impacts, soil conservation measures need to be targeted to areas with high erosion and sediment transfer. For this purpose, reliable and comprehensive data on the magnitude and spatial extent of soil redistribution are needed. Traditional monitoring and modelling techniques to quantify soil erosion and sedimentation are capable of meeting some of the information requirements, but they have a number of important limitations.

The quest for alternative techniques of soil erosion assessment to complement existing methods and to meet new requirements has directed attention to a particular group of environmental radionuclides, namely fallout radionuclides (FRNs). These natural and anthropogenic radioisotopic tracers represent effective and valuable tools for the assessment of erosion and deposition within the landscape at several temporal and spatial scales. The use of FRNs can complement and in some cases even substitute conventional measurements to evaluate erosion and sedimentation processes for developing and improving land management and soil conservation measures.

1. Introduction

Soil erosion and associated sedimentation are natural landscape forming processes. However, they can be accelerated by human activities that can have negative impacts on agricultural production as well as watershed management and conservation of natural resources [1-2]. At present, the rate of soil erosion exceeds the rate of soil formation over extensive areas of the globe, leading to the degradation of the soil resource and a decline in its productive potential. This disparity between soil erosion and formation rates is a common result of human activities [3].

Land degradation and soil erosion by water are associated with the irretrievable loss of the basic soil resource and thus have a major impact on water and biogeochemical cycles, biodiversity and plant primary productivity. Soil erosion and deposition also have negative ecological and socio-economic effects. Several reports have highlighted the seriousness of land degradation by various processes, in particular soil erosion, at the global and regional levels. Current concerns about the effects and impacts related to accelerated soil erosion generate an urgent need for obtaining reliable quantitative data on the extent and actual rates of soil erosion worldwide [4-6]. This paper provides a brief background to soil erosion/sedimentation processes and the need for quantitative information. Soil erosion assessment methods are explored with particular reference to the use of nuclear techniques, i.e. using fallout radionuclides (FRNs) to measure soil redistribution in agricultural landscapes. The paper also provides an account of methodological developments and applications related to the use of FRNs in soil erosion and sedimentation studies.

2. Erosion and sedimentation: processes and problems

2.1. Factors influencing soil erosion rates

The main factors influencing soil erosion can be grouped into three categories: a) energy, b) resistance, and c) protection [7].

(i) Energy factors

These are related to the capacity of several agents such as rainfall, runoff, wind, ice, gravity and also mechanical tools (machinery) to generate erosion. In this regard, erosivity is the potential aggressivity of the causal agent. Landscape morphological features (e.g. slope gradient, aspect, form and length) are intrinsically linked to these energy factors.

Water erosion has been identified as one of the major causes of soil degradation in both developed and developing countries [8-10]. On any given slope, surface runoff characteristics, and hence water erosivity, are closely related to rainfall event characteristics (e.g. rainfall intensity, event duration, raindrop size), antecedent conditions and the hydrological properties of the soil surface and shallow subsurface (for a detailed discussion of runoff generation processes and soil erosion see [11]. Water erosion occurs as laminar or sheet erosion, rill/interrill erosion and gully erosion (Fig.1). Changes in vegetation and soil hydrological conditions can also produce surficial mass movements on sloping lands and lands with low soil stability [12].

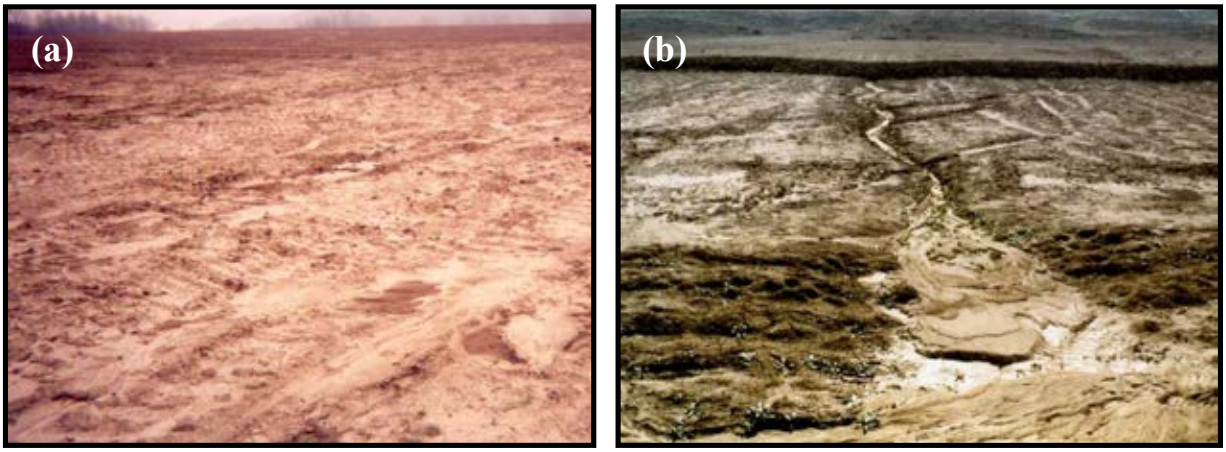

FIG. 1. (a) Sheet erosion affecting soil after crop harvest and (b) Intense sheet erosion on arable land, generating excessive waterlogging and sediment deposition [13].

Wind velocity and evaporation are the main factors controlling spatial patterns and rates of wind erosion. Wind selectively mobilizes and transports soil particles to nearby areas via processes of rolling and saltation as well as to remote locations as dry deposition/dust carried in suspension [14].

Processes of mechanical erosion include tillage, land levelling, and harvesting of root and tuber crops where machinery causes the soil movement and losses [15-17]. In agricultural landscapes, tillage erosion has been identified as an additional important global soil degradation process that has to be accounted for when assessing the erosional impacts on soil productivity, environmental quality or landscape evolution (e.g. [18]).

(ii) Resistance factors

These are related to the soil erodibility or the susceptibility of the soil to be eroded. Soil erodibility is directly dependent on the physico-mechanical properties of the soil (e.g. degree of aggregate stability) and indirectly dependent on other properties (linked to chemical, physico-chemical, and biological factors) that affect the former (for more information on this topic see e.g. [19-24]).

(iii) Protection factors

In practice, several types of erosion can occur in a given location according to the local land use and management practices [12] but there are also a range of factors that can reduce erosivity. Interception of rainfall is a major factor in this regard and good cover of plant biomass (vegetation or crop residues) will protect the soil from water and wind and the erosion losses will accordingly be reduced. In contrast, removal of vegetation by deforestation and overgrazing will result in enhanced erosion and deposition off-site. The loss/removal of scarce natural vegetation in arid zones leaves the soil prone to wind and water erosion and promotes desertification. In many parts of the developing world, resource-poor farmers who practice subsistence agriculture on communal lands do not have sufficient economic and technical resources to permit adequate soil management and conservation, and they cannot make investments to improve soil quality. It is therefore necessary to consider the importance of socio-economic and political factors that are drivers of the degradation of soil resources by

erosion. The availability of resources and the economic incentives provided by relevant bodies and associated agricultural policies also exert a very important influence on land use and its intensification. These factors can have a great influence on soil erosion [25, 26].

2.2. Effects and impacts of soil erosion

Accelerated erosion decreases soil productivity (on-site impacts), increases downstream sedimentation, and is related to environmental pollution problems (off-farm impacts) in agro-ecosystems [27, 28]. On-site and off-site impacts of erosion can be summarised as follows.

(i) On-site effects

Soil erosion affects farmers particularly through soil (including colloidal particles), nutrient and organic matter losses with consequent decline in soil fertility/productivity and crop yield reduction. These problems may occur as a consequence of two major processes. First, continual removal of surface soil by erosion, which leads to soil degradation reflected in the reduction of soil fertility and breakdown of soil structure [29, 30]. Compaction and poor internal drainage can act to exacerbate this problem by reducing the infiltration capacity of the soil and enhancing surface runoff. Secondly, extensive rills and gullying may lead to a reduction of the cultivable areas. The impact of this process has been widely recognised and various estimates of its severity have been established [31-32]. In the long-term, soil redistribution leads to spatial variability in soil quality, i.e. depletion or removal of soil particles and constituents, such as nutrients and organic matter, in eroding areas and enrichment in depositional areas [30, 33-34].

(ii) Off-site effects

Sediment and associated potential pollutants (mainly nutrients, pesticides, and pesticide metabolites) can reach watercourses and contribute to the eutrophication and contamination of water resources affecting aquatic ecosystems and wetlands (e.g. Fig. 2). They can also increase or create siltation problems and other major off-site impacts such as muddy floods and mudflows which can damage human infrastructure and habitation [35]. The presence of increased sediment concentrations in stream systems and lakes can also cause degradation of aquatic ecosystems and habitats, through, for example, the silting of fish spawning gravels and the mantling of aquatic vegetation with sediment deposits. In both developed and developing countries, the problem of sedimentation in water conveyance systems and reservoirs increases costs of water treatment and management of dams.

Land degradation by soil erosion and deposition also has wider negative ecological and socio-economic impacts. These are directly related to food insecurity and increased malnutrition leading often to higher levels of poverty, rural migration, social unrest and overall poor economic development [36-37]. Productivity losses have been estimated for several regions based on an annual average loss of 0.3% of the total global value of selected crops [38]. Off-site economic losses in the USA due to sedimentation were estimated to be about $6 billion annually two decades ago [39]. According to [40], these off-site economic losses are underestimated and it is widely accepted that global off-site impacts are far greater than on-farm productivity losses. Biodiversity losses and greenhouse gas emissions have been attributed to the increased sedimentation. However, it is difficult to estimate these impacts [38]. Worldwide economic costs of both on- and off-site impacts of soil erosion in agricultural land have been estimated at $400 billion per year [27].

FIG. 2. Land use change/intensification in the uplands of Southeast Asia causes severe soil losses and resulting sediment mobilisation and deposition of sediment on fertile rice paddy soils in the lowlands (Photo by P. Schmitter, University of Hohenheim).

2.3. Magnitude and extent of land degradation by soil erosion

Several reports highlight the seriousness of land degradation, in particular soil erosion, at the regional and global levels. Worldwide soil degradation is currently affecting 1.9 billion hectares and is increasing at a rate of 5 to 7 million hectares each year [41]. More than three quarters of this degradation is caused by bad management practices in agriculture and livestock production or by conversion of forest to cropland. Estimates of the extent of soil degradation by water and wind erosion in developing countries are shown in Table 1.

TABLE 1. EXTENT OF SOIL DEGRADATION (MILLION HECTARES) BY WATER AND WIND EROSION [1, 42]

Region	Soil degradation area (in million hectares)		
	Water erosion	Wind erosion	Total erosion
Africa	227.3	187.8	415.1
Asia	435.2 (39.6%)*	224.1 (40.7%)	659.3 (40.0%)
Central America and Mexico	46.5	4.4	50.9
South America	124.1	41.4	165.5
Subtotal of third world countries	833.1 (75.7%)	457.7 (83.2%)	1290.8 (78.2%)
Total worldwide	1100.0	550.0	1650.0

**Data in parentheses are % of the total worldwide affected*

More than three quarters of the surface land area affected by erosion is in developing countries of Africa, Asia and Latin America, with 40% of the total occurring in Asia. Worldwide, 1100 million hectares are affected by water erosion and 550 million hectares are affected by wind erosion. Soil losses by water are more serious than those by wind across all regions.

According to the Global Assessment of Soil Degradation (GLASOD) survey, among the several degradation processes, soil erosion is by far the most common type of land degradation, accounting for 84% of the affected area [8, 43-44]. About 80% of the world's agricultural land suffers moderate to severe erosion, and 10% suffers slight to moderate erosion [45]. In the USA alone, about 23 million hectares of fragile cropland experience excessive erosion, and about 20 million hectares of cropland have erosion rates that exceed the tolerable soil-loss rate [3]. Soil erosion continues to threaten the productive capacity of nearly one-third of the cropland and at least one-fifth of all rangeland in the USA [3]. In Europe, erosion by wind and water is the major threat to soil resources and represents the main mechanism of landscape degradation. Indeed, around 115 million hectares of farmland, 12% of the total area of Europe, is highly affected by erosion processes [46]. In developing countries, soil erosion by water and tillage is particularly severe on small farms that are often located on marginal lands due to poor soil quality and steep topography [36]. Reported soil erosion rates are highest in Asia, Africa and South America, averaging 30 to 40 t $ha^{-1}yr^{-1}$, and lowest in the USA and Europe, averaging about 17 t ha^{-1} yr^{-1} [27, 47]. These relatively lower rates reported in the USA and Europe, however, greatly exceed the average rate of soil formation of about 1 t ha^{-1} yr^{-1} [48].

A global soil erosion survey was conducted for different regions of the world by [49], using the Revised Universal Soil Loss Equation (RUSLE) and global spatial datasets for estimating erosive parameters. The estimated global mean soil erosion rate was about 11.5 t ha^{-1} yr^{-1}. The average soil erosion rate was highest in South America (16.7 t ha^{-1} yr^{-1}) followed by Asia (15.8 t ha^{-1} yr^{-1}) and Europe (13.4 t ha^{-1} yr^{-1}). The average soil erosion rates in North America and Africa were found to be 6.9 and 5.8 t ha^{-1} yr^{-1}, respectively, while Australia had the lowest rate of 3.9 t ha^{-1} yr^{-1}.

As a result of climate change and global warming, the water erosion risk is expected to increase in the USA [50] and the European Union (EU) by the year 2050 for about 80% of the agricultural areas. This pressure will mainly take place in the areas where soil erosion is currently already severe [5, 51]. Using climate change simulation models, a geo-referenced RUSLE model, and considering future changes in land cover based on actual and historical land use data, [52] estimated a world average increase in soil loss of 14% under climate change.

2.4. Controlling soil erosion

In spite of the soil erosion problems and its ecological and socio-economic impacts, it is also important to recognize that effective soil conservation programmes can successfully counter soil erosion and contribute significantly to environmental sustainability as shown in the USA [53]. However, most developing countries do not have the resources to establish institutionalized land care/watershed development programmes for implementing long-term soil conservation activities. Existing land development programmes focus their activities on conducting inventories of land resources and monitoring rapid land use/management changes. In many cases when international aid is received, specific watershed development/soil conservation project activities are set up in a given area usually for a defined short-term period. Since most of the indirect benefits occur beyond the project life, evaluation and

monitoring work is normally concentrated on its accomplishments, and its short-term and direct benefits [54]. Moreover, while some countries have spent huge amounts of money in implementing soil conservation technologies to arrest soil erosion, few attempts have been made to evaluate the effectiveness of such conservation projects due to the absence of an adequate evaluation methodology. Soil erosion generally does not have a great influence on farmers' decisions to adopt or not adopt soil conservation practices, unless erosion reaches high levels. Economic arguments linked to soil quality changes and productivity decline can be a more convincing [35].

2.5 Assessment of soil erosion/sedimentation

Current concerns about both on-site and off-site adverse effects associated with accelerated soil loss, generate an urgent need for obtaining reliable quantitative data on the extent and actual rates of soil erosion worldwide. Such data are required for a more comprehensive assessment of the magnitude of erosion effects, to (i) obtain a better understanding of the processes and the main controlling factors, (ii) validate new soil erosion/sedimentation prediction models, and (iii) provide a basis for developing scientifically sound land use policies and selecting effective soil conservation measures and land management strategies, including assessment of their economic and environmental impacts [2, 3].

Despite extensive literature on the global, regional, and national problems of soil erosion, reliable quantitative data on the extent and rates of soil erosion are scarce for many regions of the world. Since soil erosion research is capital and labour intensive as well as a time-consuming exercise, well-designed experiments using standardized methodologies should be performed so that the data obtained are comparable and representative of the study areas [55-56, 61].

Existing methods for assessing soil erosion can be grouped into two main categories: (i) erosion measurement methods and (ii) erosion modelling and prediction methods. In both cases, there is a need for direct measurement of soil erosion, which can be undertaken using erosion plots, surveying methods and nuclear techniques. The selection of the method to be used basically depends on the objectives of the study and the availability of resources [57]. Soil erosion studies were initially conducted in the first half of the twentieth century, and commonly used conventional measurements of sediment export at spatial scales ranging from micro-plots to large-sized plots (under simulated or natural rainfall). More recently, these studies have been scaled up to the watershed level. A range of approaches exist and have been used worldwide to measure erosion [9-11, 35, 58-64]. These include:

- *Erosion pins*: This method consists of driving pins into the soil so that the top of the pin gives a starting point in time from which changes in the soil surface level (soil removal and deposition) can be measured;

- *Erosion plots*: This approach is used to measure runoff and sediment produced by water erosion from small confined (delineated) plots under natural precipitation or simulated rainfall, often with different vegetation cover;

- *Volumetric measurements of soil removal*: Estimates of soil loss are based on three-dimensional measurements of the volume of rills or gullies and measurements or estimates of the deposited volume of an outwash fan or in a catch pit or reservoir;

- *Use of conventional markers*: Marked stones can be used as tracers to estimate soil translocation by tillage operations;

- *Sediment production in watershed/catchment studies*: Estimates and measurements of sediment yield are obtained using gauging stations, suspended sediment samplers, sediment traps, and reservoir silting/check dam measurements.

From the late 1960s until the present, many modelling studies have been conducted focussing on predicting soil erosion rates using field and laboratory data for validation, e.g. the 'Universal Soil Loss Equation' (USLE) [65]. To predict or understand spatial patterns and trends in soil erosion and sediment transfer, numerous erosion and sediment transport models supported by Geographical Information Systems (GIS) and remote sensing technologies have been developed at different scales. These include empirical and conceptual models (e.g. USLE, SEDD, AGNPS, and LASCAM) and physically-based modelling techniques (e.g. ANSWERS, LISEM, CREAMS, WEPP, EUROSEM, KINEROS, RUNOFF, WESP, CASC2D-SED, SEM, SHESED, etc.). The main applications of the models commonly used in soil erosion studies have been recently reviewed by [66].

Existing classical techniques such as erosion plots and surveying methods for monitoring soil erosion are capable of meeting some of the information requirements but they have a number of important limitations in terms of the representativeness of the data obtained, their spatial resolution, their potential to provide information on long-term rates of soil erosion, associated spatial patterns over extended areas, and the costs involved [67-68]. Traditional monitoring and modelling techniques for soil erosion/sedimentation require many parameters and in turn many years of measurements [10, 69] for example, to obtain long-term erosion data in agro-ecosystems, experimental plots have to be carried out over decades to integrate the inter-annual variability of climate and cropping practices. In addition, advances in the use of distributed numerical models and the application of GIS and geostatistics to erosion modeling have highlighted the need for spatially distributed data that represent the spatial variability of soil erosion and deposition rates within the landscape, in response to the local topography and land use/management [2]. The quest for alternative techniques of soil erosion assessment to complement existing methods and to meet new requirements has directed attention to the use of radionuclides, in particular anthropogenic fallout ^{137}Cs, as tracers for documenting rates and spatial patterns of soil redistribution within the landscape [70-71].

3. Use of fallout radionuclides as soil tracers for soil erosion and sedimentation studies

The background to the use of fallout radionuclides to assess erosion and sedimentation processes is described in this paper.

3.1. Introduction to radioactivity

(i) Atom, nucleus and radioactivity

An atom consists of a central nucleus (proton and neutron), which is relatively heavy and carries a positive electrical charge (proton), surrounded by a cloud of low mass, negatively-charged electrons. A complete atom is electrically neutral, which means that the number of electrons or their negative charge are equal to the amount of (opposite) positive charge on a proton in the nucleus, and there is no overall charge on the neutral atom.

The nucleus of an atom is made of particles collectively named nucleons. There are two types of nucleons: protons (p) and neutrons (n). They have practically equal masses but protons carry a positive electrical charge and neutrons possess no charge. The number of proton plus

neutrons is referred to as the mass number (A). The number of protons (Z) determines the charge of the nucleus and is referred to as the atomic number. The neutron number (N) is defined as A minus Z. Isotopes of a particular element are defined as containing the same number of protons but may have different numbers of neutrons. Thus, isotopes with different numbers of neutrons in their nuclei but the same number of protons have similar chemical properties.

Most of the approximately one thousand known isotopes are stable and do not disintegrate with time. The presence of neutrons keeps the proton together and so stabilises the nucleus. However, when the ratio of neutrons to protons is outside a particular value, which varies with each isotope, the nucleus becomes unstable and spontaneously emits particles and/or electromagnetic radiation. This phenomenon, which characterizes radionuclides, is called radioactive decay and is a statistical process in which the decay rate is proportional to the number of radioactive nuclei of a particular type present at any time t and is usually accompanied by the emission of charged particles and/or gamma rays.

(ii) Modes of radioactive decay

Three main types of emitted radiation exist: alpha, beta, and gamma. Since most commonly used radionuclides in soil erosion studies are gamma-emitters, we describe in this paper only gamma radiation (γ). Alpha or beta decay processes may leave the product nucleus either in its ground state or more frequently in an excited state. A nucleus in an excited state may give up its excitation energy and return to ground state in a variety of ways. The most common is by the emission of electromagnetic radiation called gamma radiation. These are photons or quanta packages of energy transmitted in the form of wave motion with energies typically from several keV to several MeV. They are distinguished from only by the fact that they come from the nucleus. Most gamma rays are somewhat higher in energy than x-rays and are, therefore, very penetrating. Gamma radiation can travel very large distances and lose its energy by interacting with atomic electrons. Depending on their energies, they can be stopped by a thin piece of aluminium foil, or can penetrate through several centimetres of lead.

(iii) Law of radioactivity

The probability that any particular atom within a large number of radioactive atoms *(N)* will disintegrate is termed the decay constant (λ). The activity of these radioactive atoms, which is the total number of disintegrations per unit time, will be λN. The rate of depletion (*dN/dt)* is equal to the activity (*A)* as long as there is no new supply of radioactive atoms. *N* decreases with increasing time. The decay process is given by the following Equation:

$$dN/dt = -Nl = -A \quad (1)$$

This Equation can be solved as follows:

$$N = N_0 e^{-\lambda t} \quad (2)$$

where:

N_0 is the initial number of the radioactive atoms at $t = 0$;
N is the number of remaining radioactive atoms at time t.

$N_0\lambda$ is the activity at $t = 0$, A_0 , the latter Equation can be expressed in terms of activity ratios as:

$$A/A_0 = N\lambda/N_0\lambda = e^{-\lambda t} \quad (3)$$

The half-life ($t_{1/2}$) is the time interval over which the initial number of radioactive atoms (N_0) is exactly halved: $N = N_0/2$. $t_{1/2}$ is related to decay by $t_{1/2} = \ln 2/\lambda$.

If the competing modes of decay of any nuclide have probabilities $\lambda_1, \lambda_2, \lambda_3 \ldots$ per unit time, then the total probability of decay is represented by the total decay constant λ, which is the linear sum of all the partial decay constants. The partial activity of a sample of N nuclei, if measured by a particular mode of decay characterised by λ_i, is then given by the Equation 1.4 and the total activity is given by the Equation 1.5:

$$dN_i/dt = -\lambda_i N = \lambda_i N_0 e^{-\lambda t} \quad (4)$$

$$dN/dt = \sum dN_i/dt = N\sum \lambda_i = \lambda N_0 e^{-\lambda t} \quad (5)$$

In many cases, a parent radionuclide 1 decays into a daughter radionuclide 2, which is itself radioactive and decays into a daughter 3 until daughter radionuclide M decays into daughter radionuclide N. In this case, if at time $t = 0$, there is only the parent nuclide and no atoms of its series, and if the corresponding decay constants are $\lambda_1, \lambda_2, \ldots\lambda_m, \lambda_n$ at any time t, the relation between number N_n *and* N_m is given by the following Equation:

$$dN_N/dt = N_m\lambda_m - N_n\lambda_n \quad (6)$$

More details on the resolution of these Equation series, called Batmen Equations, are provided by [72].

(iv) Units of radioactivity

The SI unit of activity is the Becquerel (Bq), which is defined as one nuclear disintegration per second. Before the introduction of SI units, the most commonly used radioactivity unit was the Curie (Ci) corresponding to 3.7×10^{10} nuclear disintegrations per second.

3.2. Fallout radionuclides in soil erosion and sedimentation studies

In the investigations of soil erosion and sedimentation, work has focused on the use of a particular group of environmental radionuclides, namely fallout radionuclides (FRNs), which include artificial radionuclides such as ^{137}Cs originated from thermonuclear weapon tests in the 1950s-1960s, and geogenic radioisotopes such as ^{210}Pb and also more recently cosmogenic radioisotopes such as ^{7}Be (Fig. 3). They have been used worldwide to obtain rates and patterns of soil erosion and deposition at several temporal and spatial scales [73-75].

The basic principles for the application of these FRNs in soil erosion and sedimentation studies are similar. FRNs reach the land surface by fallout from the atmosphere. It is assumed that such fallout input is spatially uniform, at least over a relatively small area. Because these radionuclides are rapidly and strongly adsorbed by fine soil particles, they accumulate at or near the soil surface. Documenting the subsequent redistribution of the radionuclide tracer,

which moves across the landscape in association with soil or sediment particles primarily through physical processes, affords a very effective means of tracing rates and patterns of erosion and deposition within agricultural landscapes. In essence, the fallout radionuclide is equivalent to artificial labelling by the application of a radioisotope tracer to the surface of a given area.

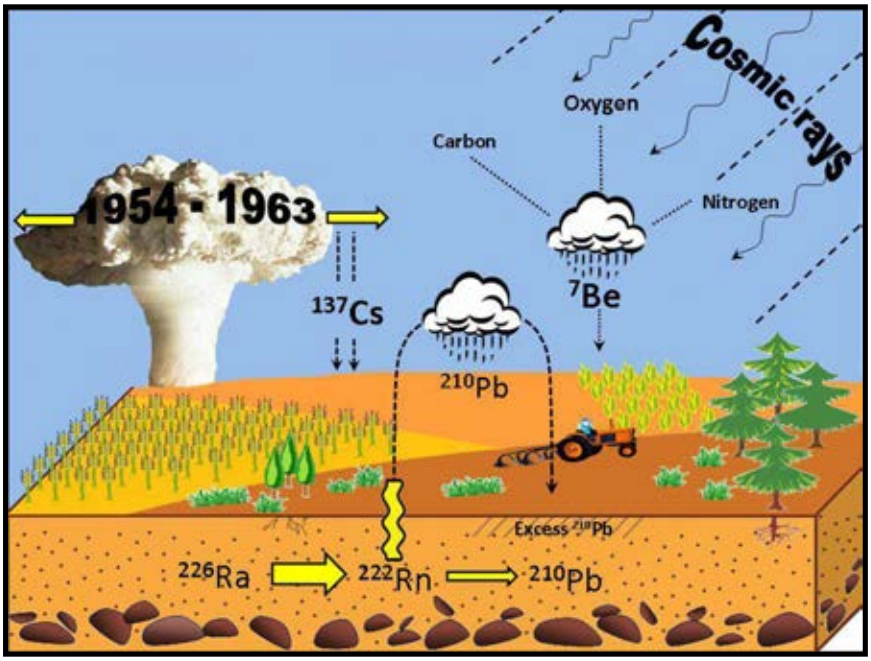

FIG. 3. Origin of fallout radionuclides (^{137}Cs, ^{7}Be, and $^{210}Pb_{ex}$) used as soil tracers in erosion and sedimentation studies [76].

3.3. The application of the FRN ^{137}Cs technique

The application of the ^{137}Cs technique for determining rates and patterns of soil loss is based on several assumptions. The key assumptions and requirements of the ^{137}Cs technique have been fully described in many publications [70, 77-80]. The redistribution assessment is commonly based on the ^{137}Cs inventory (total radionuclide activity per unit area) measured at a given sampling site compared with a reference site (inventory representing the cumulative atmospheric fallout input at the site, taking due account of the different behaviour of cultivated and non-cultivated soils). Because direct long-term measurements of atmospheric fallout are rarely available, the cumulative input or reference inventory is usually established by sampling adjacent stable and nearly undisturbed sites, where neither significant erosion nor additional deposition have occurred (Fig. 4).

The determination of ^{137}Cs inventories requires soil cores to be taken according to a carefully planned field sampling design. Measurement of ^{137}Cs concentration vs. depth is required for cores representative of each landscape unit within the study site. It is essential to determine the inventory of ^{137}Cs at a reference site (i.e. a location undisturbed by erosion or sedimentation) near to the study area [74]. Sampling sites can be characterised as erosional or depositional by comparing the ^{137}Cs inventory of the given site with that of the reference site. Inventories lower than the reference value represent soil losses by erosion and those in excess of the reference level indicate deposition (accumulation) of soil [81].

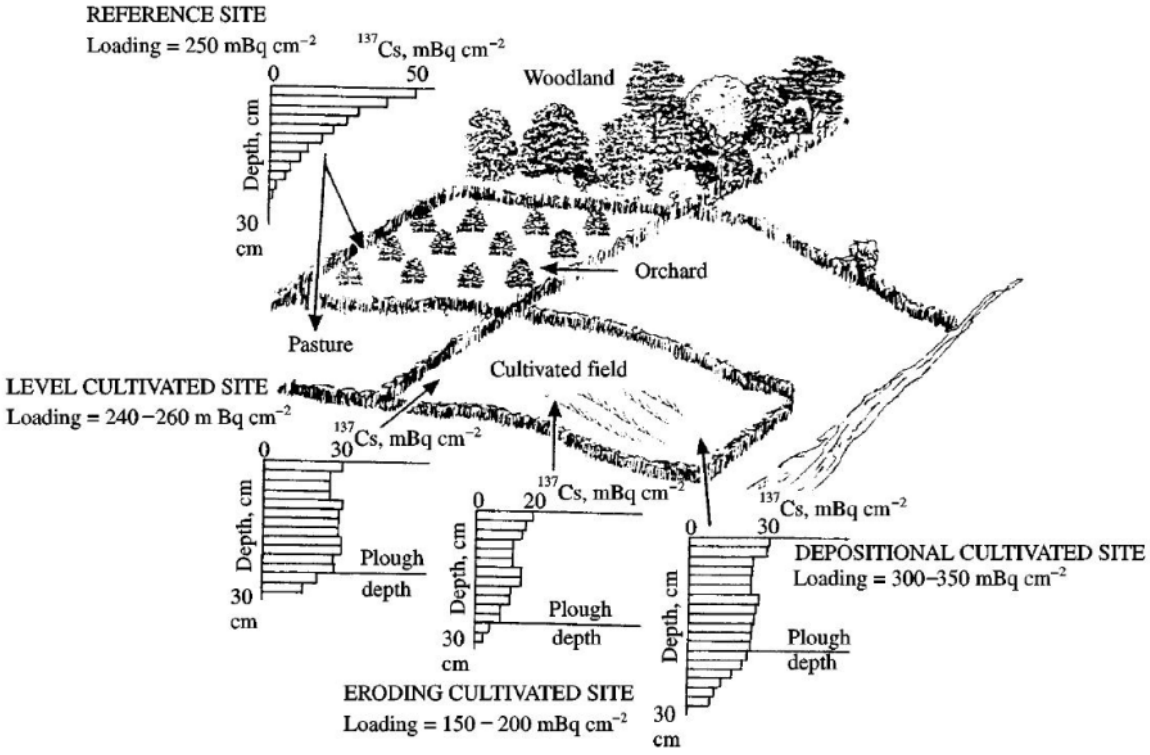

FIG. 4. Diagram illustrating the application of the ^{137}Cs method to study soil erosion and deposition within a landscape [82].

To derive quantitative estimates of soil erosion and deposition rates from ^{137}Cs measurements, it is necessary to use conversion models that are developed on the basis of physical processes influencing the relationship between magnitude of the reduction or increase in the ^{137}Cs inventory and the soil redistribution [81, 83]. The soil redistribution data obtained (soil erosion and sedimentation rates and patterns) represent an integrated measurement of all effects leading to soil redistribution occurring during the period extending from the main phase of atmospheric fallout input to the time of sampling. When using several FRNs, soil redistribution data over different time scales can be obtained using a single sampling campaign, thereby avoiding time-consuming, costly installations and procedures commonly required to monitor study sites over extended periods. The ^{137}Cs method is the most widely used and validated for medium-term (50 years) soil erosion assessment. The use of $^{210}Pb_{ex}$ has been extended from the previous sediment dating application to provide a method for longer-term (100 years) soil and sediment redistribution studies [84]. Recent developments of the ^{7}Be application permit short-term (days to months) soil erosion assessment in connection to individual rainfall events and seasonal changes in land use/management practices [85-87].

3.4. Advantages and limitations of FRN techniques for assessing erosion and sedimentation

To efficiently control and mitigate soil losses by erosion and reduce their environmental impacts, soil conservation measures need to be targeted to areas with high erosion and sediment transfer. For this purpose, reliable and comprehensive data on the magnitude and spatial extent of soil redistribution (erosion/sedimentation) in the landscape are needed.

Effective erosion control demands knowledge of soil erosion rates and processes and their main influencing factors in the study area. Besides the objectives of the study and the availability of resources, the choice of a particular method for measuring soil erosion requires a thorough knowledge of the advantages and limitations of the technique used. The following section summarizes the main advantages and limitations of FRN techniques in soil erosion/sedimentation studies [2, 74-75, 88-89]

- FRNs are present in the environment (or landscape) worldwide and while occurring at very low levels, they can be readily measured;

- FRN techniques provide information on soil erosion and sedimentation rates and patterns at various temporal scales, depending on the FRN used, integrating from a single event up to a period of 100 years;

- Erosion estimates are retrospective and can be obtained opportunistically on the basis of a single visit to the site for soil sampling, which can be completed in a relatively short time. Site disturbance during sampling is minimal and does not interfere with normal cropping operations;

- There are no major scale (plot to watershed) constraints, apart from the number of samples to be analysed;

- Time-consuming, costly and long-term monitoring/maintenance programs, which are required in conventional methods, can be avoided;

- Soil redistribution rates represent the integrated effects of all landscape processes resulting in movement of soil particles under defined land use/management;

- Information can be obtained from individual sampling points or integrated across landscape units allowing estimated rates and spatial patterns of soil redistribution to be assembled and mapped;

- Since radionuclide-based measurements provide information on the spatial distribution of erosion/sedimentation rates, they can be used to validate the results of spatially distributed soil erosion models.

Among the limitations, the following should be considered by workers planning to use FRNs:

- A multi-disciplinary team (soil and nuclear sciences) is often required for proper application of the technique. This may be a particular limitation in developing countries with limited scientific staff;

- Suitable sample preparation, high precision gamma detection facilities, and skilled staff are required for analysing the samples. This includes quality assurance/control for low level gamma spectrometry. Very low FRN inventories reported in some study areas demand long counting times and increase uncertainty of the measurements;

- The FRN technique is an indirect approach that depends on the relationship between measured FRN inventories and estimated soil redistribution. Hence, specialised data processing is required to derive estimates of soil redistribution rates (see Paper 5 of this TECDOC).

While some limitations are inherent in the FRN technique, others have been successfully addressed within the framework of the IAEA-supported research networks described below. Considering the limitations of other techniques, the FRN techniques have great potential as a complementary approach in soil erosion/sedimentation studies.

3.5. A brief history of FRN methodological developments

The International Atomic Energy Agency (IAEA) has played a key role in these methodological developments and applications. The Soil and Water Management and Crop Nutrition (SWMCN) Sub-programme of the Joint FAO/IAEA Division of Nuclear Techniques in Food and Agriculture has strengthened national capacities for using these nuclear-based techniques and has disseminated them through international co-operation in research, training and other outreach activities in FAO and IAEA Member States. In this way, both UN organizations meet their mandates and contribute to their commitment towards achieving the UN Millennium Development Goals of Extreme Poverty and Hunger Eradication and Environmental Sustainability [90].

(i) Initial development of FRN techniques

Early applications of the ^{137}Cs technique in soil erosion research were made by several groups in Australia [80, 91-93] Canada [79, 94-95], England [77, 96, 83-84], and the USA [70, 97-98]. These pioneering groups provided a solid foundation for the application of the ^{137}Cs technique to measure soil redistribution in agricultural and natural landscapes. One important lesson learned from these early studies was that there is a need for harmonized protocols for a worldwide and consistent application of this technique.

In view of the increasing concern of soil erosion and sedimentation as a serious threat to sustainable watershed management, the IAEA has been actively involved on the development of nuclear techniques in soil erosion and siltation studies since the mid-1990s [99-100]. From 1995 to 2001, the IAEA implemented two co-ordinated research projects (CRPs): (1) "*Assessment of soil erosion through the use of ^{137}Cs and related techniques as a basis for soil conservation, sustainable production, and environmental protection*" that was co-ordinated by the Soil and Water Management and Crop Nutrition Section and (2) "*Sedimentation assessment by environmental radionuclides and their application to soil conservation measures*", that was co-ordinated by the Isotope Hydrology Section of the IAEA [56, 75]. Through these two closely linked projects, refined and standardized methods and protocols for the worldwide application of the ^{137}Cs technique were developed and a wealth of information on soil erosion/sedimentation rates was obtained [75, 88, 101-102]. Conversion models for deriving soil erosion/sedimentation rates from ^{137}Cs measurements were developed and tested [83], and specific approaches developed to take due account of the Chernobyl fallout in Russia [103].

(ii) Recent development of FRN techniques

The development, refinement and calibration of the ^{137}Cs technique have provided a universal tool to quantify soil redistribution rates in a range of natural and agro-ecosystems, and have paved the way for a wider application of the technique, particularly in assessing the

effectiveness of soil conservation technologies in controlling or mitigating soil erosion and associated degradation processes. Recent studies were conducted from 2002-2007 within the framework of the IAEA Co-ordinated Research Project "*Assessment of the effectiveness of soil conservation technologies using fallout radionuclides*" [104]. These studies have emphasized the combined use of FRNs such as ^{137}Cs, ^{210}Pb, and ^{7}Be, which enables the determination of erosion rates at several time scales (from short- to long-term) and under different local conditions (from hill slopes to small watersheds) [105]. An account of recent FRN methodological developments is given by [74].

Erosion and sedimentation rates estimated using FRN measurements have been successfully validated using other more conventional methods (erosion plots, erosion pins, erosion-sedimentation modelling, and catchment sediment yields) in a range of environments. Examples of the selected comparative assessment of soil erosion studies using FRNs and conventional methods are presented in Table 2.

(iii) Future research

Current concerns related to the impacts of agricultural land use on the environment have highlighted the important role of sediment (and associated nutrient/chemicals) in degrading water quality and in a range of other environmental problems [106]. The loss of topsoil and associated nutrients/chemical inputs as well the potential degradation of water quality through land erosion enhanced by human activity is a serious threat to food security and sustainable agricultural production in many regions worldwide.

TABLE 2. EXAMPLES OF THE COMPARISON OF NET EROSION RATES OBTAINED FROM FRNS AND CONVENTIONAL MEASUREMENTS

Study scale	Fallout radionuclides			Conventional measurement		
	FRN(s)	Net erosion rate (t^{-1} ha^{-1} yr^{-1})	References	Method	Net erosion rate (t^{-1} ha^{-1} yr^{-1})	References
Basin, 217 km^2	^{137}Cs	2.8	[107]	USLE	3	[108]
Field, 1 ha	^{137}Cs $^{210}Pb_{ex}$	12.1 to 14.3	[109]	RUSLE 2	12.1	[109]
Small watersheds 1 to 2 ha	^{137}Cs	8.9 to 14.7	[110-111]	Sediment measurements at the outlet	7.8 to 19.2	[110-111]

These impacts are likely to increase further due to the anticipated intensification of climate variability. Sediment transport is the key to understanding the movement and fate of many nutrients (e.g. soil organic carbon and phosphorus) and contaminants [112-113] and carbon storage and mobilization within the watershed [114]. These substances drive eutrophication, decrease agricultural productivity and cause environmental degradation. Therefore, there is a clear need to develop comprehensive area-wide sediment budgets for better understanding of sediment mobilization, transfer and storage in watersheds from source to sink [115-116]. Planning and implementing effective control measures to reduce soil loss/sediment transport and related environmental problems requires i) quantification of sediment loads, ii) identification and apportioning of sediment sources, and iii) evaluation of the fate of sediment-associated pollutants at the watershed scale. The interaction of sediment sources,

transfers and sinks across the landscape of a watershed is highly complex. FRN techniques will need to be further developed to enable quantitative determination of the mobilization, transfer and storage of sediment on an area-wide basis over different timescales. Furthermore, there is an opportunity to link FRN-derived data to that from compound specific stable isotope (^{13}C and ^{15}N) techniques (CSSI). These have been shown to be successful in identifying the sources of sediments deposited in an estuary [117-118]. Such applications will help to identify risk areas of soil loss/sediment production to target soil conservation technologies [119], and thus establish guidelines for sustainable management of land and water resources [116, 120].

3.6. Application of FRN techniques in soil erosion/sedimentation studies: current status

According to a bibliographic survey on the use of FRNs to assess erosion and sedimentation, this method has been used in more than 4000 research papers over the last 40 years to assess soil erosion in various agricultural and natural ecosystems [121]. An overview of selected applications of FRN techniques in a wide range of soil erosion/sedimentation studies has been presented by [73].

To develop and widen the use of these techniques, the transfer of nuclear technology is facilitated by the IAEA through national and regional field projects, Technical Co-operation Projects and other dissemination means. At present, there are 38 national and regional Technical Co-operation (TC) projects using FRNs to address issues relating to sustainable land management in developing Member States. For example, one major regional TC/RCA project (RAS5043) on *"Sustainable Land Use and Management Strategies for Controlling Soil Erosion and Improving Soil and Water Quality"* was implemented from 2005 through 2009 in the Asia and the Pacific region. The FRN technology has been successfully used by the 14 national teams from the participating countries (Australia, , China, India, Indonesia, Republic of Korea, Malaysia, Mongolia, Myanmar, Pakistan, Philippines, Sri Lanka, Thailand, and Vietnam) (i) to assess soil erosion, (ii) to evaluate the efficiency of soil conservation measures (e.g. reforestation, terracing, contour cropping and contour hedgerow systems), and (iii) to better understand the link between soil redistribution and soil quality (e.g. soil organic matter) in the landscape. The skills and expertise gained in the project can be used to further train scientists and technicians from the region. Partnerships have also been established with related policy-making and development-oriented institutions for disseminating the FRN technology to assess soil redistribution and improve land management practices. The information generated in the project has been used by the national teams and their partners as a basis to formulate land development projects for enhancing the adoption of improved soil conservation and water management practices.

The success outlined in the above example has stimulated additional commitment from the IAEA in responding to requests from Member States. For example, a regional TC project (RLA5051) on "*Using Environmental Radionuclides as Indicators of Land Degradation in Latin American, Caribbean and Antarctic Ecosystems*", was implemented with 14 participating countries of the region for a-five year duration (2009 - 2013). Land degradation affects about 300 million hectares in the Latin American and Caribbean region. Out of this, 51% (180 million hectares) is agricultural land. The project aimed to enhance soil conservation and environmental protection in Latin American, Caribbean and Antarctic environments in order to ensure sustainable agricultural production and reduce on- and off-site impacts of land degradation.

A five-year on-going regional technical co-operation project (2012-2015) on *'Supporting Innovative Conservation Agriculture Practices to Combat Land Degradation and Enhance Soil Productivity for Improved Food Security'* focuses on the use of FRNs (primarily ^{137}Cs, secondarily ^{210}Pb and ^{7}Be) as means for obtaining quantitative information on African soil degradation, soil erosion and sedimentation redistribution rates within agricultural landscapes, over a range of different time scales. The overall objective of this project (i.e. RAF5063) that involves 10 countries (i.e. Algeria, Benin, Côte d'Ivoire, Madagascar, Mali, Morocco, Senegal, Tunisia, Uganda and Zimbabwe) is to develop a regional network for strengthening conservation agriculture practices in Africa to combat land degradation and enhance soil quality and productivity.

4. Concluding remarks

The use of FRN techniques affords an effective and valuable tool for the assessment of surface erosion and deposition within the landscape over several spatial and temporal scales. The key advantage of this approach is that it can provide time-integrated estimates of rates of erosion/deposition and spatial patterns of soil redistribution without the need for long-term monitoring programs. Significant progress has been made in harmonizing the protocols for application of FRNs in soil erosion research through cooperation of specialist teams and coordination by the IAEA. The developed methods and protocols provide a standardized framework for the application of these techniques worldwide. This work is an essential pre-requisite to obtain directly comparable and representative information on soil erosion rates in a wide range of environments, and to understand the influence of the main factors affecting soil loss/sediment production in the landscape. Furthermore, this information is required to underpin the scientifically-sound management of land and water to mitigate/control soil erosion and associated problems. The efficacy of the approach has been increasingly recognized in other studies and a range of expanding applications at the watershed scale demonstrates its value. Current developmental work focuses on integrated approaches that combine these FRN techniques with advanced sediment fingerprinting techniques to identify soil loss and sediment production in critical source areas. Techniques, models and guidelines will be provided to establish comprehensive sediment budgets and foster sustainable land and water management at the watershed scale.

REFERENCES

[1] LAL, R., Soil management in the developing countries. Soil Science 165 (2000) 57–72.

[2] WALLING, D.E., Recent advances in the use of environmental radionuclides in soil erosion investigations. In: IAEA (Ed.), Nuclear Techniques in Integrated Plant Nutrient, Water and Soil Management. Proc. FAO/IAEA Int. Symp. Vienna, October 16-20, 2000. IAEA-CSP-11P, Vienna, Austria (2001) 279–301.

[3] TOY, T.J., FOSTER, G.R., RENARD, K.G., (EDS). Soil Erosion: Processes, Prediction, Measurement, and Control. John Wiley & Sons, Inc., New York, USA (2002) 352.

[4] BOARDMAN, J., Soil erosion science: Reflections on the limitation of current approaches. Catena 68 (2-3) (2006) 73–86.

[5] European Environmental Agency. Down to earth: soil degradation and sustainable development in Europe. A challenge for the 21st century. Environmental Issue series, No. 16, Copenhagen (2002) 32.
[6] Food and Agriculture Organization of the United Nations. Conservation Agriculture (2010).
[7] MORGAN, R.P.C., Soil Erosion: Topics in Applied Geography 99, 2nd Edition. Longman, New York, USA (1980) 113.
[8] Food and Agriculture Organization of the United Nations. National Soil Degradation Maps. Soil Degradation Map of Austria. FAO/AGL. GLASOD (2005).
[9] MABIT, L., BERNARD, C., LAVERDIERE, M.R., L'étude de l'érosion hydrique au Québec. Vecteur environnement 33 (2000) 34–43.
[10] MABIT, L., LAVERDIERE, M.R., BERNARD, C., L'érosion hydrique: méthodes et études de cas dans le nord de la France. Cah. Agri. 11 (2002) 195–206.
[11] MORGAN, R.P.C., Soil Erosion and Conservation, 3rd Edition. Longman Group, Harlow Essex, New York, USA (2005) 198.
[12] TORRI, D., An overview of the current research needs for improving soil erosion control, In: Francaviglia, R. (Ed.): Agricultural Impacts on Soil Erosion and Soil Biodiversity: Developing Indicators for Policy Analyses. Proc. OECD Expert Meeting, March 2003, Rome, Italy (2004) 59–74.
[13] Food and Agriculture United Nations Organization. Photo library on soil erosion processes. FAO Land and Water Digital Media Series 28, FAO, Rome, Italy (2004).
[14] GOOSENS, D., The on-site and off-site effects of wind erosion, In: Warren, A. (Ed.): Wind Erosion in Agricultural Land. Research Results for Land Managers. EC-DG Research, Environment and Sustainable Development Programme. EU official publication, Luxembourg (2002) 29–38.
[15] LINDSTROM M.J., NELSON, W.W., SCHUMACHER, T.E., Quantifying tillage erosion rates due to moldboard plowing. Soil Till. Res. 24 (1992) 243–255.
[16] LOBB, D.A., KACHANOSKI R.G., MILLER, M.H., Tillage translocation and tillage erosion on shoulder slopes landscape positions measured using ^{137}Cs as a tracer. Can. J. Soil Sci. 75 (1995) 211–218.
[17] POESEN, J., VERSTRAETEN, G., SOENENS, R., SEYNAEVE, L., Soil losses due to harvesting of chicory roots and sugar beets: an under-rated geomorphic process? Catena 43 (2001) 35–47.
[18] VAN OOST, K., GOVERS, G., DE ALBA, S., QUINE, T.A., Tillage erosion: a review of controlling factors and implications for soil quality. Progress in Physical Geography 30 (2006) 443–466.
[19] BARTHÈS, B., ROOSE, E., Aggregate stability as an indicator of soil susceptibility to runoff and erosion; validation at several levels. Catena 47 (2002) 133–149.
[20] BRONICK, C.J., LAL, R., Soil structure and management: a review. Geoderma 124 (2005) 3–22.
[21] BRYAN, R.B. Soil erodibility and processes of water erosion on hillslope. Geomorphology 32 (2000) 385–415.
[22] KNAPEN, A., POESEN, J., GOVERS, G., GYSSELS, G., NACHTERGAELE, J., Resistance of soils to concentrated flow erosion: A review. Earth-Sci. Rev. 80 (2007) (1-2) 75–109.
[23] LIPIEC, J., HATANO, R., Quantification of compaction effects on soil physical properties and crop growth. Geoderma 116 (2003) 107–136.
[24] SEYBOLD, C.A., HERRICK, J.E., Aggregate stability kit for soil quality assesments. Catena 44 (2001) 37–45.
[25] STOCKING, M., Tropical soils and food security: The next 50 Years. Science 302 (2003) 1356–1359.

[26] BOARDMAN, J., POESEN, J., EVANS, R., Socio-economic factors in soil erosion and conservation. Environ. Sci. Policy 6 (2003) 1–6.
[27] PIMENTEL, D., HARVEY, C., RESOSUDARMO, P., SINCLAIR, K., KURZ, D., MCNAIR, M., CRIST, S., SHPRITZ, L., FITTON, L., SAFFOURI, R., BLAIR, R., Environmental and economic costs of soil erosion and conservation benefits. Science 267 (1995) 1117–1123.
[28] SCHMITTER, P., DERCON, G., HILGER, T., THI LE HA, T., HUU THANH, N., LAM, N., DUC VIEN, T., CADISCH, G., Sediment induced soil spatial variation in paddy fields of Northwest Vietnam. Geoderma 155 (2010) 298–307.
[29] ELWELL, H.A., Sheet erosion from arable land in Zimbabwe: prediction and control. In: Walling, D.E. (Ed.), Challenges in African Hydrology and Water Resources. Proceedings of the Harare Symposium, July 1984. IAHS Publication No. 144, IAHS Press, Wallingford, UK (1984) 429–438.
[30] MABIT, L., BERNARD, C., Relationship between soil inventories and chemical properties in a small intensively cropped watershed. *Comptes Rendus de l'Académie des Sciences Série IIa* Earth Planet Sci. 327 (1998) 527–532.
[31] WHITLOW, R., Mapping erosion in Zimbabwe: a methodology for rapid survey using aerial photographs. Applied Geography 6 (1986) 149-162.
[32] VALENTIN, C., POESEN, J., LI, Y., Gully erosion: Impact, factors and control. Catena 63 (2005) 132–153.
[33] MABIT, L., BERNARD, C., MAKHLOUF, M., LAVERDIÈRE, M.R., Spatial variability of erosion and soil organic matter content estimated from ^{137}Cs measurements and geostatistics. Geoderma 145 (2008) 245–251.
[34] PANSAK, W., HILGER, T.H., DERCON, G., KONGKAEW, T., CADISCH, G., Changes in the relationship between soil erosion and N loss pathways after establishing soil conservation systems in uplands of Northeast Thailand. Agriculture, Ecosystems & Environment 128 (2008) 167–176.
[35] BOARDMAN, J., POESEN, J., (Eds). Soil Erosion in Europe. Wiley, Chichester, UK (2006) 855.
[36] PIMENTEL, D., Soil erosion: A food and environmental threat. Environment, Development and Sustainability 8 (2006) 119–137.
[37] United Nations Environment Programme. Global Environment Outlook: Environment for Development GEO-4. Summary for Decision Makers (2007) 36.
[38] LAL, R., DEN BIGGELAAR, C., WIEBE, K.D., Measuring on-site and off-site effects of soil erosion on productivity and environmental quality. In: Francaviglia, R. (Ed.), Agricultural Impacts on Soil Erosion and Soil Biodiversity: Developing Indicators for Policy Analyses. Proceeding OECD Expert Meeting, March 2003, Rome, Italy (2004) 75–86.
[39] CLARK, E.H., The off- site cost of soil erosion. J. Soil Water Conserv. 40 (1985) 19–22.
[40] CROSSON, P., The economics of soil erosion and maintaining soil biodiversity. In: Francaviglia, R. (Ed.), Agricultural Impacts on Soil Erosion and Soil Biodiversity: Developing Indicators for Policy Analyses. Proc. OECD Expert Meeting, March 2003, Rome, Italy (2004) 13–20.
[41] LAL, R., Encyclopaedia of Soil Science. 2nd Edition, CRC Press (2006).
[42] OLDEMAN, L.R., The global extent of soil degradation. In: Greenland, D.J., Xzabolcs, L. (Eds). Soil Resilience and Sustainable Land Use. CAB International, Wallingford, UK (1994) 99–118.
[43] OLDEMAN, L.R., HAKKELING, R.T.A., SOMBROEK, W.G., World Map of the Status of Human-Induced Soil Degradation: An Explanatory Note. ISBN 90-6672-042-5. ISRIC and UNEP, Wageningen, The Netherlands (1990) 27.

[44] International Soil Reference and Information Centre. GLASOD – SOTER Newsletter, Wageningen, The Netherlands (1992).
[45] SPETH, J.G., Towards an Effective and Operational International Convention on Desertification. United Nations. International Convention on Desertification, International Negotiating Committee. New York, USA (1994).
[46] Commission of the European Communities. Thematic Strategy for Soil Protection. Communication from the Commission to the Council, the European Parliament, the European Economic and Social Committee, and the Committees of the Region – COM Brussels, Belgium 231 (2006) 12.
[47] BARROW, C.J., Land Degradation: Development and Breakdown of Terrestrial Environments. Cambridge Univ. Press, Cambridge, UK (1991) 295.
[48] TROEH, F.R., THOMPSON, L. M., Soils and Soil Fertility, 5th Edition. Oxford Univ. Press, New York, USA (1993).
[49] NAM, P.T, YANG, D., KANAE, S., OKI, T., MUSIAKE, K., Global soil erosion estimate using RUSLE model: The use of global spatial datasets on estimating erosive parameters. Geoinformatics 14 (2003) 49–53.
[50] Soil and Water Conservation Society. Conservation implications of climate change: soil erosion and runoff from cropland. Soil and Water Conservation Society Report. Ankeny, Iowa, USA (2003).
[51] European Environmental Agency. Environment in the European Union at the turn of the century. Environmental Issue series, No. 2, Copenhagen (1999) 448.
[52] YANG, D., KANAE, S., OKI, T., KOIKE, T., MUSIAKE, K., Global potential soil erosion with reference to land use and climate change. Hydrol. Process. 17 (2003) 2913–2928.
[53] BERNARD, J.M., IIVARI, T.A., Sediment damages and recent trends in the United States. Int. J. Sediment Res. 15 (2000) 135–148.
[54] SHENG, T. C., Principles and practices of monitoring and evaluation for watershed and conservation projects, In: de Graaff, J., *et al.* (Eds). Monitoring and Evaluation of Soil Conservation and Watershed Development Projects, Science Publishers, Enfield, New Hampshire, USA (2007) 13–25.
[55] Food and Agriculture Organization of the United Nations. Assessing Soil Degradation. Soils Bulletin No. 34. FAO, Rome. Italy (1977).
[56] ZAPATA, F., GARCIA AGUDO, E., HERA, C., ROZANSKI, K., FROEHLICH, K., Use of nuclear techniques in soil erosion and siltation studies. In: IAEA (Ed.), Nuclear Techniques in Soil-Plant Studies for Sustainable Agriculture and Environmental Preservation. Proc. FAO/IAEA Int. Symp. Vienna, October 17-21, 1994. IAEA Proceedings Series STI/PUB/947, IAEA, Vienna (1995) 631–642.
[57] ELLIOT, W.J., FOSTER, G.R., ELLIOT, A.V., Soil erosion: Processes, impacts and prediction. In: Lal, R., Pierce, F.J. (Eds), Soil Management for Sustainability. Soil Water Conserv. Soc., Edmonton, Alberta, Canada (1991) 25–34.
[58] CROKE, J., NETHERY, M., Modelling runoff and soil erosion in logged forests: scope and application of some existing models. Catena 67 (2006) 35–49.
[59] STROOSNIJDER, L., Measurement of erosion: Is it possible? Catena 64 (2005) 162–173.
[60] HUDSON, N.W., Field Measurement of Soil Erosion and Runoff. FAO Soils Bulletin Vol. 68. FAO, Rome, Italy (1993).
[61] LAL, R. Soil Erosion Research Methods, 2nd Edition. Soil and Water Conservation Society, Ankeny, IA, USA (1994).
[62] AKSOY, H., KAVVAS, M.L., A review of hillslope and watershed scale erosion and sediment transport models. Catena 64 (2005) 247–271.

[63] DERCON, G., GOVERS, G., POESEN, J., SANCHEZ, H., ROMBAUT, K., VANDENBROECK, E., LOAIZA, G., DECKERS, J. Animal-powered tillage erosion assessment in the southern Andes region of Ecuador. Geomorphology 87 (2007) 4–15.
[64] MABIT, L., KLIK, A., BENMANSOUR, M., TOLOZA, A., GEISLER A., GERSTMANN, U.C., Assessment of erosion and deposition rates within an Austrian agricultural watershed by combining ^{137}Cs, $^{210}Pb_{ex}$ and conventional measurements. Geoderma 150 (2009) 231–239.
[65] WISCHMEIER, W.H., SMITH, D.D., Predicting Rainfall Erosion Losses - A Guide to Conservation Planning. United States. Department of Agriculture, Agricultural Handbook 537. U.S. Government Printing Office, Washington D.C, USA (1978).
[66] AUERSWALD, K., Water erosion. In: Chesworth, W. (Ed.), The Encyclopedia of Soil Science. Springer, Dordrecht (2008) 817–822.
[67] LOUGHRAN, R.J., The measurement of soil erosion. Progress in Physical Geography 13 (1989) 216–233.
[68] HIGGITT, D.L., Soil erosion and soil problems. Prog. Physical Geography 15 (1991) 91–100.
[69] MABIT, L., BERNARD, C., LAVERDIÈRE, M.R., Quantification of soil redistribution and sediment budget in a Canadian watershed from fallout caesium-137 (^{137}Cs) data. Can. J. Soil Sci. 82 (2002) 423–431.
[70] RITCHIE, J.C., MCHENRY, J.R., Determination of fallout ^{137}Cs for measuring soil erosion and sediment accumulation rates and patterns: J. Environ. Qual. 19 (1990) 215-233.
[71] WALLING, D.E., QUINE, T.A., The use of fallout radionuclide measurements in soil erosion investigations. In: IAEA (Ed.), Nuclear Techniques in Soil-Plant Studies for Sustainable Agriculture and Environmental Preservation. Proc. FAO/IAEA Int. Symp. Vienna, October 17-21, 1994. IAEA Proc. Series STI/PUB/947, Vienna, Austria (1995) 597–619.
[72] IVANOVICH, M., HARMON, R.S., The phenomenon of radioactivity. In: Uranium-series Disequilibrium: Applications to Earth, Marine and Environmental Sciences, 2nd Edition, Clarendon Press, Oxford, UK (1992) 1–33.
[73] ZAPATA, F., NGUYEN, M.L., Soil erosion and sedimentation studies using environmental radionuclides. In: Froehlich, K. (Ed.), Environmental Radionuclides: Tracers and Timers of Terrestrial Processes, Book series. Radioact. Environ. 16 (2009) 295–322.
[74] MABIT, L., BENMANSOUR, M., WALLING, D.E., Comparative advantages and limitations of fallout radionuclides (^{137}Cs, ^{210}Pb and ^{7}Be) to assess soil erosion and sedimentation. J.Environ. Radioact. 99 (2008) 1799–1807.
[75] ZAPATA, F. (Ed.). Handbook for the Assessment of Soil Erosion and Sedimentation using Environmental Radionuclides. Kluwer, Dordrecht, The Netherlands (2002) 219
[76] ZUPANC, V., MABIT, L., Nuclear techniques support to assess erosion and sedimentation processes: A preliminary step in investigating the use of ^{137}Cs as soil tracer in Slovenia. Dela 33 (2010) 21–36.
[77] WALLING, D.E., QUINE, T.A., Use of caesium-137 measurements to investigate soil erosion in arable fields in the UK: potential applications and limitations. European Journal of Soil Science 42 (1991) 147–165.
[78] WALLING, D.E., QUINE, T.A., Use of ^{137}Cs as a tracer of erosion and sedimentation: Handbook for the application of the ^{137}Cs technique. Report to the UK Overseas Development Administration, Exeter, UK (1993).
[79] DE JONG, E., BEGG, C.B.M., KACHANOSKI, R.G., Estimates of soil erosion and deposition for some Saskatchewan soils. Can. J. Soil Sci., 63 (1983) 607–617.

[80] LOUGHRAN, R.J., ELLIOTT, G.L., CAMPBELL, B.L., SHELLY, D.J., Estimates of soil erosion from caesium-137 measurements in a small cultivated catchment in Australia. Appl. Radiat. Isot. 39 (1988) 1153–1157.
[81] WALLING, D.E., HE, Q., APPLEBY, P.G., Conversion models for use in soil-erosion, soil-redistribution and sedimentation investigations. In: Zapata, F. (Ed.), Handbook for the Assessment of Soil Erosion and Sedimentation using Environmental Radionuclides. Kluwer, Dordrecht, The Netherlands (2002) 111–164.
[82] WALLING, D.E., QUINE, T.A., Use of caesium-137 to investigate patterns and rates of soil erosion on arable fields. Soil Erosion on Agricultural Land (1990) 33-53.
[83] WALLING, D.E., HE, Q., Improved models for estimating soil erosion rates from cesium-137 measurements. J. Environ. Qual. 28 (1999) 611–622.
[84] WALLING, D.E., HE, Q., Use of fallout ^{210}Pb measurements to estimate soil erosion on cultivated land. Soil Sci. Soc. Am. J. 63 (1999) 1404–1412.
[85] BLAKE, W.H., WALLING D.E., HE, Q., Fallout beryllium-7 as a tracer in soil erosion investigations. Appl. Radiat. Isot. 51 (1999) 599–605.
[86] SEPÚLVEDA, A., SCHULLER, P., WALLING, D.E., Use of ^{7}Be to document erosion associated with a short period of extreme rainfall. J. Environ. Radioact. 99 (2008) 35–49.
[87] WALLING, D. E., SCHULLER, P. ZHANG, Y., IROUME, A., Extending the timescale for using beryllium-7 measurements to document soil redistribution by erosion. Water Resour. Res. 45 (2009) W02418, doi:10.1029/2008WR007143.
[88] ZAPATA, F., (Ed.), Field Application of the Cs-137 Technique in Soil Erosion and Sedimentation. Special Issue. Soil & Tillage Research 69 (2003) 153.
[89] BERNARD, C., MABIT, L., LAVERDIERE, M.R., WICHEREK, S., Césium-137 et érosion des sols. Cahiers Agricultures, 7 (3) (1998) 179–186.
[90] United Nations. UN Millennium Development Goals (2009).
[91] CAMPBELL, B.L., LOUGHRAN, R.J., ELLIOTT, G.L., Caesium-137 as an indicator of geomorphic processes in a drainage basin system. Australian Geography Studies, 20 (1982) 49–64.
[92] ELLIOTT, G.L., CAMPBELL, B.L., LOUGHRAN, R.J., Correlation of erosion measurement and soil caesium-137 content. Appl. Radiat. Isot. 41 (1990) 713–717.
[93] WALLBRINK, P.J., MURRAY, A.S., The use of fallout radionuclides as indicators of erosion processes. Hydrol. Process. 7 (1993) 297–304.
[94] KACHANOSKI, R.G., Estimating soil loss from changes in soil caesium-137. Can. J. Soil. Sci. 73 (1993) 515–526.
[95] PENNOCK, D.J., LEMMON, D.S., DE JONG, E., Caesium-137 measured erosion rates for five parent material groups in southwestern Saskatchewan. Can. J. Soil Sci. 75 (1995) 205–210.
[96] WALLING, D.E., BRADLEY, S.B., The use of caesium-137 measurements to investigate sediment delivery from cultivated areas in Devon. In: IAHS Publication No. 174, IAHS Press, Wallingford, UK (1988) 325–335.
[97] RITCHIE, J.C., MCHENRY, J.R., Determination of fallout Cs-137 and natural gamma-ray emitting radionuclides in sediments. Appl. Radiat. Isot. 24 (1973) 575–578.
[98] RITCHIE, J.C., MCHENRY, J.R., Fallout Cs-137: a tool in conservation research. J. Soil Water Conserv. 30 (1975) 283–286.
[99] INTERNATIONAL ATOMIC ENERGY AGENCY. Use of Nuclear Techniques in Studying Soil Erosion and Siltation. IAEA-TECDOC-828, IAEA, Vienna, Austria (1995).
[100] INTERNATIONAL ATOMIC ENERGY AGENCY. Use of ^{137}Cs in the Study of Soil Erosion and Sedimentation. IAEA TECDOC-1028, IAEA, Vienna, Austria (1998).

[101] QUERALT, I., ZAPATA, F., GARCIA AGUDO, E., (Eds), Assessment of soil erosion and sedimentation through the use of the ^{137}Cs and related techniques. Special issue. Acta Geologica Hispanica 35 (2000) 195–367.
[102] ZAPATA, F., GARCIA AGUDO, E., Future prospects for the ^{137}Cs technique for estimating soil erosion and sedimentation rates. Acta Geologica Hispanica 35 (2000) 197–205.
[103] GOLOSOV, V., Application of Chernobyl-derived ^{137}Cs for the assessment of soil redistribution within a cultivated field. Soil Till. Res. 69 (2003) 85–97.
[104] ZAPATA, F., Use of environmental radionuclides to monitor soil erosion and sedimentation in the field, landscape and catchment level before, during and after implementation of soil conservation measures. In: de Graaff, J., *et al.* (Eds), Monitoring and Evaluation of Soil Conservation and Watershed Development Projects. Science Publishers, USA (2007) 301–317.
[105] ZAPATA, F., LI, Y., Report of the Fourth and Final Research Coordination Meeting of the FAO/IAEA Coordinated Research Project "Assess the Effectiveness of Soil Conservation Techniques for Sustainable Watershed Management Using Fallout Radionuclides". IAEA-311-D1-RC-888, IAEA, Vienna (2007).
[106] HOROWITZ, A.J., WALLING, D.E., (Eds). Sediment Budgets 1 & 2, Proceedings International Symposium on Sediment Budgets, Foz do Iguacu, Brazil, April 2005. IAHS Publication No. 291 & 292, IAHS Press, Wallingford, UK (2005) 366 & 342
[107] MABIT, L., BERNARD, C., LAVERDIÈRE, M.R., Assessment of erosion in the Boyer River watershed (Canada) using a GIS oriented sampling strategy and ^{137}Cs measurements. Catena 71 (2007) 242–249.
[108] LANDRY, I., Analyse par Géomatique des Bilans et des Flux d'Azote et de Phosphore dans un Bassin Versant Agricole: Le Cas de la Rivière Boyer. M.Sc. Thesis, Université du Québec, INRS-Eau. Québec, Canada (1998).
[109] BENMANSOUR, M., NOUIRA, A., BENKDAD, A., IBN MAJAH, M., BOUKSIRAT, H., EL OUMRI, M., MOSSADEK, R., DUCHEMIN, M., Estimates of long and short term soil erosion rates on farmland in semi-arid West Morocco using caesium-137, excess lead-210 and beryllium-7 measurements. In: Impact of soil conservation measures on erosion control and soil quality. IAEA-TECDOC-1665 (2011) 159–174.
[110] PORTO, P., WALLING, D.E., FERRO, V., DI STEFANO, C., Validating erosion rate estimates provided by caesium-137 measurements for two small forested catchments in Calabria, Southern Italy. Land Degradation and Development 14 (2003) 389–408.
[111] PORTO, P., WALLING, D.E., TAMBURINO, V., CALLEGARI, G., Relating caesium-137 and soil loss from cultivated land. Catena 53 (2003) 303–326.
[112] MCDOWELL R.W., SHARPLEY, A.N., FOLMAR, G., Phosphorus export from an agricultural watershed: linking source and transport mechanisms. J. Environ. Qual. 30 (2001) 1587–1595.
[113] MCDOWELL R.W., SHARPLEY, A.N., Uptake and Release of Phosphorus from Overland Flow in a Stream Environment . J. Environ. Qual. 32 (2003) 937–948.
[114] LAL, R., Farming carbon. Soil Till. Res. 96 (2007) 1–5.
[115] WALLING, D.E., OWENS, P.N., LEEKS, G.J.L., The role of channel and floodplain storage in the suspended sediment budget of the River Ouse, Yorkshire, UK. Geomorphology 22 (1998) 225–242.
[116] NGUYEN, M.L., Integrated Approaches for the Assessment of Land Use Impacts on Soil Loss/Sediment Production and Related Environmental Problems. Report of the Consultants' Meeting held in Vienna, Austria, November 5-7, 2007, IAEA, Vienna, Austria (2008).

[117] GIBBS, M., Sediment Tracking Method Refinement. Technical Publication 294. Auckland Regional Council, New Zealand (2005).
[118] GIBBS, M., Sediment Source Mapping in Mahurangi Harbour. Technical Publication 321. Auckland Regional Council, New Zealand (2006).
[119] DELGADO, J.A., BERRY, J.K., Advances in precision conservation. Advances in Agronomy 98 (2008) 1–44.
[120] NGUYEN, M.L., ZAPATA, F., DERCON, G., 'Zero-tolerance' on land degradation for sustainable intensification of agricultural production. In: Zdruli, P. *et al.* (Eds), Land Degradation and Desertification: Assessment, Mitigation and Remediation. Springer, Berlin (2010) 37–48.
[121] RITCHIE, J.C., RITCHIE, C.A., Bibliography of publication of ^{137}Cs studies related to erosion and sediment deposition (2008). http;//www.ars.usda.gov/Main/docs.htm?dosid=15237

^{137}Cs: A WIDELY USED AND VALIDATED MEDIUM TERM SOIL TRACER

L. MABIT, S. CHHEM-KIETH, P. DORNHOFER, A. TOLOZA
Soil and Water Management and Crop Nutrition Subprogramme, Joint FAO/IAEA Division of Nuclear Techniques in Food and Agriculture,
Vienna - Seibersdorf

M. BENMANSOUR
Centre National de l'Energie des Sciences et des Techniques Nucléaires (CNESTEN), Rabat, Morocco

C. BERNARD
Ministère de l'Agriculture des Pêcheries et de l'Alimentation du Quebec,
Quebec, Canada

E. FULAJTAR
Soil Science and Conservation Research Institute,
Bratislava, Slovakia

D.E. WALLING
Geography, College of Life and Environmental Sciences, University of Exeter,
Exeter, United Kingdom

Abstract

Radioactive Caesium-137 (^{137}Cs) is found globally in the environment due to fallout after nuclear weapon testing in the fifties and sixties, and nuclear accidents in the more recent past. The properties and particular features of ^{137}Cs (half-life of about 30 years), such as its strong adsorption to soil particles, make it an exceptional and the most widely used soil tracer for studying soil movement processes. The ^{137}Cs method that possesses a number of major advantages over traditional approaches to document erosion and deposition rates, provides estimates of soil redistribution averaged over a period of several decades. It has been employed to study soil redistribution under different agro-ecological conditions in many different areas of the world. ^{137}Cs has been also used in soil erosion investigations over a wide range of geographic scales, extending from experimental plots, through fields of a few hectares to small watersheds of several km^2. This method has been validated by many international peer-reviewed studies that compared erosion rates obtained with ^{137}Cs, other tracers, direct measurements at various scales and/or traditional soil erosion modelling. Significant progress has been made in harmonizing protocols for application of ^{137}Cs-based soil erosion research through cooperation of specialist teams and coordination by the International Atomic Energy Agency (IAEA). The development, refinement and calibration of the ^{137}Cs method have provided a universal and mature tool to quantify soil redistribution rates in a range of natural and agro-ecosystems, and have paved the way for a wider application of the technique, particularly in assessing the effectiveness of soil conservation technologies in controlling or mitigating soil erosion and associated degradation processes. This paper explains the fundamental principles of the use of fallout radionuclides for soil erosion assessments based on the example of ^{137}Cs.

1. General information and basis

The properties and particular features of the origin of radioactive ^{137}Cs in the environment make it an exceptional tracer for studying soil erosion and deposition processes. ^{137}Cs is the most widely used of the fallout radionuclide (FRN) soil tracers and has been employed to study the soil erosion and deposition redistribution under different agri-environmental conditions in many different areas of the world e.g. [1-7].^{137}Cs has also been used to determine medium-term (i.e. since the mid-1950s) sediment accumulation rates in a wide variety of depositional environments, such as lakes, reservoirs and river floodplains [8, 9]. Its great utility is demonstrated by the bibliography on the use of ^{137} Cs in soil erosion studies [4], which includes in excess of 4000 items.

1.1. ^{137}Cs origin and characteristics

Caesium (or caesium) (Cs) is the 55th atomic element of Mendeleyev's periodic table. It is the most electropositive and the most alkaline element among alkali metals. Its atomic mass is variable from 125 to 145. Only the stable isotope of caesium, ^{133}Cs, is natural. The most well-known radioactive isotopes of caesium are^{134}Cs ($t_{1/2}$=2.06 years) and ^{137}Cs ($t_{1/2}$=30.17 years).

There are no natural sources of ^{137}Cs. Indeed, it is an artificial or 'man-made' radionuclide generated as a product of nuclear fission. ^{137}Cs is a component of the ^{137}I decay chain as outlined in Equation (1). It emits a strong gamma-ray (662.66 KeV) making its measurement in environmental samples using gamma detector facilities relatively easy without the need for special chemical preparation or separation [8].

$$^{137}I \rightarrow {}^{137}Xe \rightarrow {}^{137}Cs \rightarrow {}^{137\,m}Ba \rightarrow {}^{137}Ba \qquad (1)$$

The main sources of ^{137}Cs present in the environment are (i) atmospheric nuclear weapons tests carried during the period from the late 1950s to the 1970s, (ii) releases from the Chernobyl nuclear power plant accident in 1986 and (iii) local releases from nuclear reactor and waste reprocessing plants.

Bomb-derived ^{137}Cs was injected into the stratosphere where it circulated globally before reaching the soil surface as fallout [10]. The fallout was associated primarily with precipitation, but locally, around the nuclear test sites, dry fallout was also significant [8]. The global deposition of ^{137}Cs fallout extended from the mid-1950s until the 1970s, with maximum fallout occurring in 1963 in the northern hemisphere and slightly later in the southern hemisphere. After moratoriums on testing and the Test Ban Treaty signed in 1963, global radioactive fallout rates decreased steadily, except for minor periods in 1971 and 1974 caused by nuclear testing by non-treaty countries.

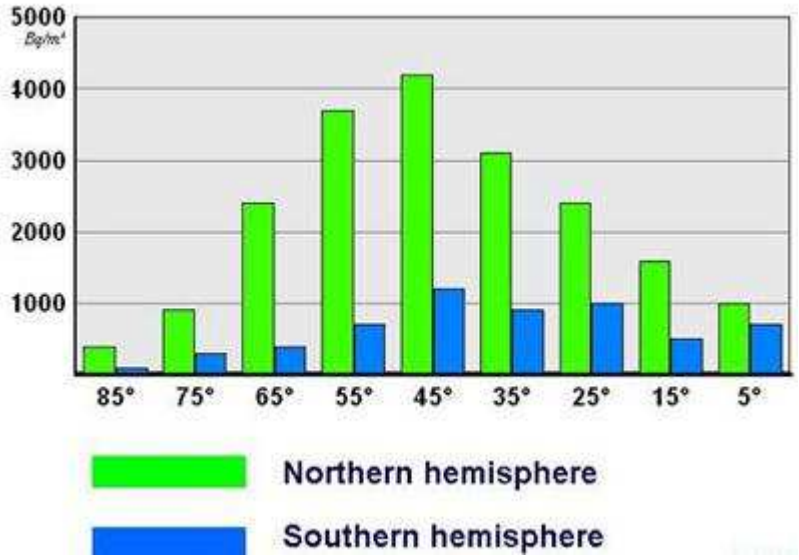

FIG. 1. Latitudinal variability of ^{137}Cs deposition at the global scale [11].

The spatial distribution of ^{137}Cs fallout was determined by the location of the weapons testing, the pattern of stratospheric circulation and transport and the amount of annual precipitation. Fallout patterns show a clear latitudinal zoning [12]. This zonal distribution has a strong correlation with the latitudinal rainfall distribution [11, 13]. Total fallout in the northern hemisphere was substantially greater than in the southern hemisphere (Fig. 1).

The two major reasons for this latitudinal difference are, firstly the location of most nuclear weapon tests in the northern hemisphere and secondly the limited intensity of air exchange between both hemispheres. ^{137}Cs inventories in the southern hemisphere are, however, still measurable using appropriate detectors and counting times. The global pattern of bomb-derived ^{137}Cs fallout indicates that inputs ranged between approximately 160 and 3200 Bq m^{-2}, depending on latitude [14, 15]. An approximate global distribution of bomb-derived ^{137}Cs fallout inventories is illustrated in Fig. 2.

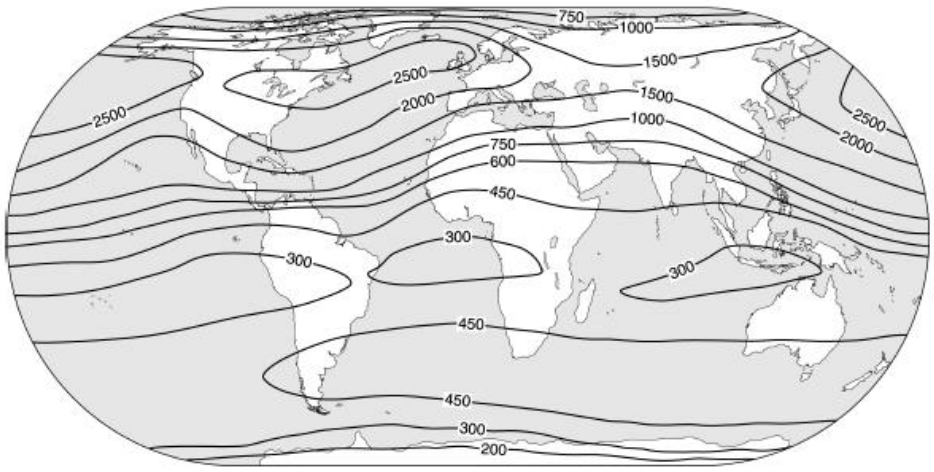

FIG. 2. Global distribution of bomb-derived ^{137}Cs fallout inventories (Based on [16]).

The fallout of ^{137}Cs released into the atmosphere by nuclear accidents, such as the Chernobyl incident, is characterized by a more localised and heterogeneous spatial distribution, reflecting the atmospheric circulation and precipitation distribution immediately after the release. In some locations in Europe, Chernobyl fallout increased the existing bomb-derived ^{137}Cs inventories by several orders of magnitude [17-20]. In Central Russia, for example, the ^{137}Cs inventories after the Chernobyl accident reached 500 kBq m^{-2} [21]. Such inventories were more than two orders of magnitude greater than those associated with bomb fallout. Other releases from nuclear plants have been very small in comparison to the Chernobyl accident with restricted local effects. The occurrence of Chernobyl fallout can impact on the implementation of the ^{137}Cs method.

1.2. Behaviour of ^{137}Cs in soil

For the use of ^{137}Cs as a soil erosion tracer it is important that ^{137}Cs has a limited mobility in soil. After its deposition at the soil surface it is rapidly and strongly adsorbed on the cation exchange sites of fine soil particles (clay and organic particles) and can thus be considered as being essentially non-exchangeable [8, 13, 22, 23]. The ^{137}Cs intercepted by the plant canopy can be transferred to the soil via wash-off and the biological uptake from soils by vegetation can be considered negligible [24]. If adsorbed by the vegetation, the ^{137}Cs is released to soils when the vegetation dies and decays [13, 24-26].

The vertical distribution or profile of ^{137}Cs in soils reflects a range of physical, physico-chemical and biological processes operating in the soil system [27]. The importance of physico-chemical processes is higher in some extreme environments, where the biological activity is low and climatic or geological factors play a key role. In arctic soils, for example, freeze-thaw is an important process and in vertisols, wetting and drying result in important soil redistribution processes. In most undisturbed soils, physico-chemical processes and bio-perturbation are the major factors responsible for the redistribution of fallout ^{137}Cs in the soil profile, while in cultivated soils, the redistribution of ^{137}Cs is primarily the result of mechanical mixing associated with cultivation. Lateral redistribution of ^{137}Cs in soils by biological and chemical processes is insignificant in comparison with the movement of ^{137}Cs by physical processes i.e. erosion and transport by water and wind [8]. For these reasons, and since ^{137}Cs fallout was relatively uniformly distributed across the landscape and strongly adsorbed by soil particles, it can be used as a tracer for studying the physical processes of erosion and sedimentation. The spatial variability of ^{137}Cs inventories can provide quantitative information on rates and patterns of erosion and sedimentation.

A typical example of the vertical distributions of the^{137}Cs inventories in an undisturbed area and in eroded and depositional areas of a cultivated soil is presented in Fig. 3. In undisturbed soils the ^{137}Cs areal activities below the upper few cm typically decrease exponentially with depth (profile A). More than 80% of the total inventory occurs in the top 15 cm. At cultivated sites (profile B), areal activities per increment can be expected to be more or less uniform within the plough layer due to mixing caused by cultivation practices. The ^{137}Cs inventories found in agricultural areas are generally reduced on convex slopes, which constitute eroding areas (profile B), and increased in depressions or small valleys and at the base of the slopes (profile C) where deposition occurs.

The depth distribution profiles can also be represented in terms of the ^{137}Cs concentration profile (activity in Bq kg^{-1}vs. depth in cm) instead of ^{137}Cs areal activity (Fig. 4). In this case the exponential decrease of ^{137}Cs concentration does not always commence immediately at the surface. In some areas with intensive bio-perturbation, the uppermost part of the profile is homogenised. In cultivated areas, the depth of the layer characterized by near homogeneous ^{137}Cs concentrations depends on the tillage implements used. In areas with mechanized

agriculture it usually extends to about 25-30 cm, which represents the plough depth. In areas where tillage involves human or animal power, it will be considerably thinner (10-20 cm). In areas where special deep cultivation practices occur, such as trenching in vineyards, the depth of the homogenised layer can reach up to 60 cm. If the deep cultivation is carried out only occasionally, homogenisation may not be achieved and the depth distribution of ^{137}Cs concentrations may show more irregularity.

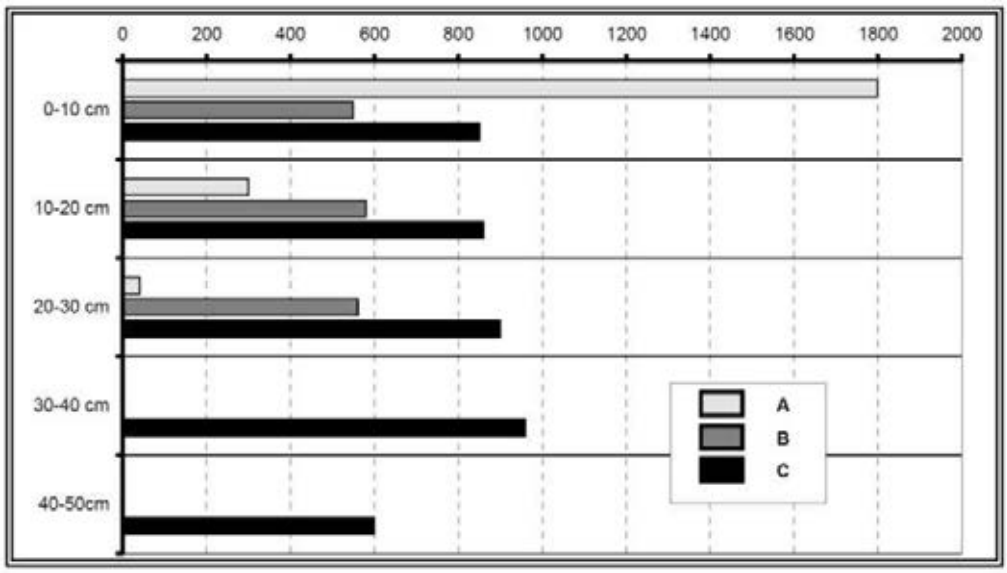

FIG. 3. The vertical distribution of ^{137}Cs (Bq m^{-2}) in a soil in northern France (Adapted from [28]) where: A = undisturbed area - reference site 2200 Bq m^{-2}; B = Eroded agricultural site 1700 Bq m^{-2}; C = Depositional agricultural site area 4000 Bq m^{-2}.

Overall, ^{137}Cs redistribution by biological and chemical processes is generally insignificant when compared with the lateral transport of ^{137}Cs by physical processes (especially water and wind) [8]. Therefore ^{137}Cs can be used as a tracer for studying the physical processes of erosion and sedimentation and it can provide quantitative information on their rates and spatial patterns.

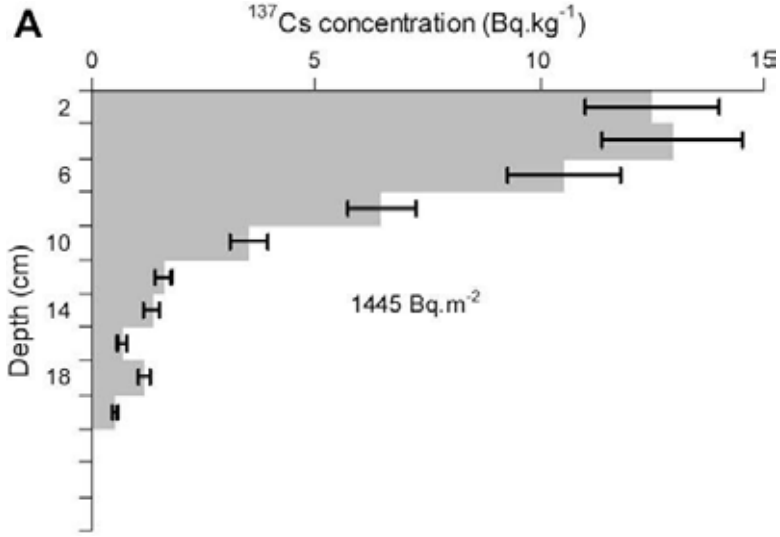

FIG. 4. An example of the vertical distribution of ^{137}Cs (Bq kg^{-1}) in an undisturbed soil in Morocco [29].

1.3. General principles of the ^{137}Cs method used for soil erosion and sedimentation assessment

The principles associated with the use of ^{137}Cs for the assessment of soil redistribution have been described in several publications (see [30]). The basic principle of the method is simple, but there are some methodological issues which require careful consideration and some pitfalls which can present serious obstacles for the successful use of this method, if the user is not aware of them. The representativeness and accuracy of the results obtained, depends heavily on the correct implementation of the ^{137}Cs method.

The key feature of ^{137}Cs behaviour in the soil, on which the method is founded, is the strong bonding of ^{137}Cs to soil particles and its chemical stability in soil environments. This makes it possible to make the fundamental assumption that ^{137}Cs can move only together with soil particles to which it is bound and that the major processes causing its redistribution in the landscape are key mechanical processes such as water, wind and tillage.

As illustrated in Fig. 5, the post fallout redistribution of ^{137}Cs across the landscape can be used to estimate soil redistribution rates and patterns based on a comparison of the total ^{137}Cs inventory (areal activity) in eroding or depositing sites with the ^{137}Cs inventory at undisturbed stable areas known as 'reference sites' It is important that no soil erosion or deposition has occurred at the reference site to ensure that the reference inventory reflects the original fallout input [30, 31].

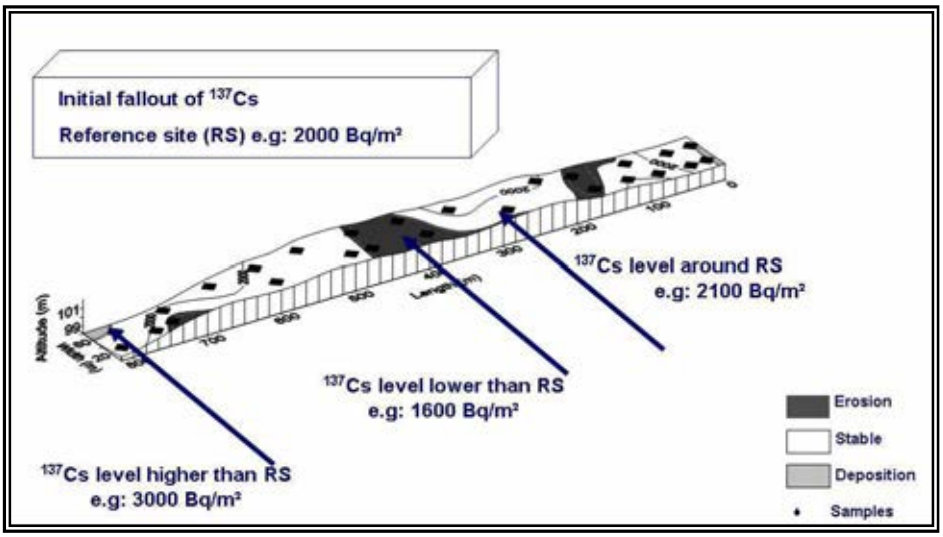

FIG. 5. The guiding principles of the ^{137}Cs method (Adapted from [27]).

To obtain quantitative estimates of soil erosion and deposition rates from ^{137}Cs measurements, a number of theoretical conversion models have been developed (see [32]). A set of selected models for cultivated and uncultivated land is described in Paper 5 of this TECDOC.

The ^{137}Cs method provides estimates of soil redistribution averaged over a period of several decades (i.e. from the beginning of global fallout in the mid-1950s until the time of sampling). It is therefore particularly useful for providing estimates of medium-term total and mean annual soil erosion and deposition rates. In most applications, it is necessary to assume that land use and erosion rates have remained essentially constant over this period. However,

Schuller et al. [33] presented an interesting approach allowing the discrimination of soil redistribution rates for a conventional tillage period followed by a no-till management period, within the overall ca. 50 year period (see Paper 7 of this TECDOC).

^{137}Cs has been used in soil erosion investigations over a range of different scales, extending from experimental plots, through fields of a few hectares to small watersheds of several km^2 [30]. To date, one of the largest scale investigations using ^{137}Cs is a study in a 200 km^2 watershed in Quebec, Canada, reported by [34], where ^{137}Cs and geographic information system (GIS) approaches were combined to assess erosion and sedimentation rates within the watershed and to investigate off-site impacts through assessment of the net sediment output at the catchment outlet.

1.4. Advantages and limitations

The ^{137}Cs technique possesses a number of major advantages over traditional approaches to document erosion and deposition rates. They can be summarized as follows [6, 30, 35].

(a) The approach provides retrospective information. Past erosion rates can be estimated from samples collected at the present time;

(b) The technique provides estimates of medium-term average (50 years) rates of soil redistribution and therefore integrate land use and climatic variability, including extreme events;

(c) The technique provides information on both erosion and deposition and therefore permits quantification of net erosion and sediment export;

(d) The assessment of soil redistribution provided by ^{137}Cs integrates all processes involving soil particle movements (water, wind and tillage erosion);

(e) The technique permits the quantification of soil loss and deposition associated with sheet erosion, which is difficult to assess using other classical approaches at the field scale, due to the limited depths of soil removal and accumulation commonly involved;

(f) Estimates are based on individual sampling points within the landscape, and spatially distributed information on rates and patterns of soil redistribution can therefore be generated;

(g) The technique does not require costly and labour intensive long-term monitoring programs. The results can be obtained from a single visit to the site for soil sampling;

(h) Although ^{137}Cs is commonly used retrospectively, by comparing the inventories measured at a study site with the local reference inventory, it can also be used for ongoing monitoring of soil redistribution by comparing the inventories measured at specific points within the study site between successive sampling campaigns separated by a period of several years e.g. [36-38];

(i) Sampling is relatively simple and cost-effective and can be completed in a relatively short time, depending on the sampling density and the size of the area investigated;

(j) The site disturbance during sampling is minimal and will not interfere with seeding and cultivation operations. Furthermore, there is no disturbance of natural runoff and erosion processes, such as might occur with the installation of bounded erosion plots. Whole fields and the complete slope profile can be sampled.

The main constraints or limitations are listed below [30]:

(a) In some areas, especially in the southern hemisphere, ^{137}Cs inventories are low and gamma analyses will require greater count times to obtain an acceptable precision for the measurements;

(b) The Chernobyl accident provided additional fallout inputs in some areas. These inputs must be taken into account, when using ^{137}Cs measurements to estimate soil redistribution rates. Unless the Chernobyl input is considerably greater than the input of ^{137}Cs associated with 'bomb fallout', such that the ^{137}Cs measurements will primarily reflect erosion occurring after 1986, the conversion models used must be modified to take account of both bomb fallout and the additional Chernobyl fallout input in 1986;

(c) The technique is primarily suited to estimating medium-term (i.e. 50 years) average erosion rates and cannot readily provide the information needed to document changes in erosion rates linked to short-term changes in land use and management practice;

(d) The commonly used approach involves comparison of measured inventories with a reference value, representing the inventory associated with a point experiencing neither erosion nor deposition. In view of its central importance to the reliability of the estimates of soil redistribution rates obtained, it is important that the reference inventory should be accurately determined. It is important to ensure that the sampling site used to establish the reference inventory provides a representative estimate of the local reference inventory [39]. This may cause problems in mountain regions, where rainfall may be characterized by high spatial variability, in areas with stony soils, in areas under intensive cultivation where few undisturbed areas exist, in areas where snow represents a substantial proportion of the annual precipitation and where significant drifting may occur, and in arid and semi-arid areas with poor vegetation cover, where redistribution of soil by aeolian processes can cause the accumulation of additional ^{137}Cs labelled sediment at the reference site;

(e) There is a need to take account of sampling representativeness and sample variability (see [40]). Multiple or replicate samples are normally collected to determine the reference inventory value. A guideline on the number of reference samples required will be discussed in the following section.

2. Sampling design

2.1. Sampling objectives

The design of effective and appropriate sampling strategies is an important and critical step for successfully applying ^{137}Cs or other FRNs in soil erosion and sedimentation studies. The strategy will depend on the study objectives. According to Pennock and Appleby [41], investigations can be classified into three different categories: soil redistribution studies, floodplain/lake and reservoir sedimentation studies, and integrated catchment studies.

Soil redistribution studies focus on soil erosion and deposition due to physical processes that remove a fraction of the ^{137}Cs-labelled soil and deposit it elsewhere. ^{137}Cs is used to study the rates and patterns of the three main agents of soil erosion: water, wind and tillage. The second type of studies concerns the application of FRNs − especially ^{137}Cs and $^{210}Pb_{ex}$ − to estimate sedimentation rates in floodplains, lakes and reservoirs. The third category involves the integration of terrestrial and aquatic environments and focuses on the establishment of a full sediment budget within the whole catchment. It may involve sampling of active erosion and sedimentation areas in the upstream areas which are responsible for sediment transport and

deposition within the catchment. All sampling strategies should be established in accord with the study objectives.

Eberhardt and Thomas [42] identified three categories of field studies that use the ^{137}Cs technique: (i) descriptive studies; (ii) analytical studies and (iii) pattern-development studies.

(i) Descriptive studies

In descriptive studies the objective of the sampling is to determine a measure of central tendency such as the mean value (e.g. inventories at the reference site) and the standard deviation or coefficient of variation for the population. Sample numbers are chosen to ensure that the confidence interval around the mean value is as small as possible to represent spatial variability within the site.

(ii) Analytical studies

Analytical studies involve comparison of soil erosion and deposition rates between two or more data sets based on structured hypothesis testing e.g. comparisons of soil redistribution rates associated with (a) different slope positions, e.g. [43-47], (b) different parent materials [48], or (c) different land uses e.g. [49, 50]. Sample numbers for each group are chosen to maximize the robustness of the comparison between the groups.

(iii) Pattern-development field studies

For pattern-development field studies, the final step is to map spatial patterns in the property under investigation (e.g. ^{137}Cs distribution, soil redistribution rates, etc.). An adequate number of samples must be obtained to ensure the establishment of a reliable and meaningful map of the ^{137}Cs spatial variability, integrating specific site parameters (topography, soil, etc.).

The sampling strategy described in the following sections is related to soil redistribution studies and involves collection of soil samples at the reference site and at the study site.

2.2. Selection of the study site and the background data collection

The selection of an appropriate site is a key requirement in any study. It is recommended that several sites are visited to support selection of a site that is representative of the wider landscape or land use type under investigation. If the study is to be carried out in a country or region where the ^{137}Cs method has not previously been applied, or if the study is to be carried by a research team which does not have experience of the method, it is recommended that a small site is selected and that geographical conditions and the dynamics of soil redistribution are not too complex. Application of the ^{137}Cs method and interpretation of the results obtained is much easier for smaller sites with relatively simple geographical conditions and limited variability of soil redistribution processes.

Before formulating the sampling strategy, a reconnaissance survey to include background data collection will be required. This requires two main actions:

(i) Enquiries, collection and compilation of background environmental and socio-economic information.

This task can be achieved using existing references, official documents and governmental reports. It is recommended that any parameter which can be related to erosion and sedimentation processes, impact or assessment is collected. The major datasets that will be of use (see [41, 51]) can be listed as follows:

(a) *Climatic data (over several years)*: rainfall, temperature, etc.;

(b) *Geomorphology and pedology*: topography, typical landforms of the region, soil type and texture;

(c) *Land use*: type of land use since the 1950s, type and frequency of tillage, specific soil conservation practices if applied;

(d) *Messages or records:* earlier erosion events, flooding or extreme weather events, conditions of their occurrence and their characteristics (spatial extension, duration, etc.).

(ii) A reconnaissance survey of the selected study area:

The objective is to recognize the specific environmental conditions of the study area including the identification of potential suitable reference sites, the typical topography of the study area, soil types and land use. This is a key step that will allow refinement of the sampling strategy.

2.3. Sampling strategy at the reference site

One of the major issues related to the use of ^{137}Cs as a soil tracer is the choice of the reference site which is used to estimate the total^{137}Cs fallout input or reference inventory, which is a key component of the conversion models used to estimate erosion and sedimentation rates from the assembled data. Hence, before implementing any study, a suitable reference site should be identified. At present, no detailed protocol for the selection of an appropriate reference site is readily available. Therefore, a protocol for the selection and the evaluation of the validity of reference sites will be presented in this section.

(i) Criteria for reference site selection

The estimation of net erosion from ^{137}Cs measurements is founded on the hypothesis that the local fallout of ^{137}Cs was uniform in space. The ^{137}Cs activities of individual sampling points are compared with that of the control or reference site to estimate the amount of erosion or deposition that has occurred since initial fallout.

Measurements undertaken for reference sites usually show some variability in^{137}Cs inventory. Owens and Walling [40] stated that the observed variability in^{137}Cs reference values could be related to: (i) random spatial variability in soil properties that influence ^{137}Cs micro-variability (e.g. infiltration capacity linked to soil bulk density, cracking and stoniness), the effects of vegetation cover and roots, micro-topography, and human and animal disturbance, (ii) apparent systematic spatial variability at a regional scale, where variations in rainfall and wind flows may have affected the initial ^{137}Cs fallout, (iii) sampling variability, a function of the surface area over which the samples are collected and (iv) measurement precision.

To minimise the variability and to maximize the representativeness of the reference inventory value the following selection criteria should be applied (adapted from [30]):

(a) The reference site should not have been cultivated or disturbed since the beginning of the 1950s. The site should have been stable since the first global occurrence of ^{137}Cs fallout (1954). These undisturbed sites should ideally be selected in protected areas of permanent grassland, abandoned pasture which have not been ploughed for the last 50 years;

(b) In order to represent the initial ^{137}Cs input, the site needs to be selected within the study area (field or watershed) or near it (e.g. around 1 km). The stable area should be located as close as possible to the area under investigation;

(c) The reference site should not have been influenced by erosion processes, which generally implies the need for a flat area;

(d) Highly bio-disturbed areas should be avoided.

Sometimes, due to the restricted area of permanent pasture around the study site, it may be necessary to select an area of flat undisturbed forest, ideally with a low canopy density. Generally the spatial variation of ^{137}Cs, and especially the resulting baseline value established, is higher in forested sites with a CV% of 19 to 47%, compared with grassland sites with a CV% of 5 to 41% [39, 40]. Despite this higher variability, forest areas can be used as a reference site if the problem of micro-variability is addressed by the sampling strategy. The soil sampling points should be selected taking account of the position of the trees, to avoid areas of concentrated stemflow input and large surface roots. However, because of the spatial variability of through fall beneath a forest canopy it is well known that undisturbed forested areas usually require a higher sample number to provide an acceptable estimate of the ^{137}Cs fallout input or reference inventory [52]. Sometimes, some atypical areas such as gardens, cemeteries, orchards, vineyards, and marshes [53] can also serve as suitable reference sites.

(ii) Special concerns for reference site selection in areas affected by Chernobyl fallout

Comprehensive guidance on use of the^{137}Cs method in Chernobyl affected areas has been provided [54].The major problem of reference site selection in areas affected by Chernobyl fallout is the magnitude and variability of ^{137}Cs contamination which may exceed the bomb-derived ^{137}Cs level. The Chernobyl accident released a great quantity of ^{137}Cs, but it did not reach the upper layers of the atmosphere and did not remain airborne long enough to circulate and to spread over the whole globe. Fallout occurred over a limited period (a few weeks) as compared to fallout of bomb-derived ^{137}Cs over a period of years. As the majority of fallout was associated with rainfall and only a minor portion was represented by dry fallout, the distribution of Chernobyl fallout reflects the irregular distribution of rainfall during the short period after the accident. Rainfall distribution is influenced by large scale factors such as those controlling circulation of air masses responsible for the regional weather differentiation and also by factors influencing the meso- and micro-scale variability in rainfall distribution such as orography and rain shadow effects, slope aspect and the impact of vegetation cover on infiltration as well as runoff micro-variability.

For these reasons, if there is a need to identify a reference site in an area affected by Chernobyl fallout, the following guidelines should be followed:

(a) The reference site should be as close as possible to the study site;

(b) Special attention should be given to the rainfall characteristics and distribution during the period shortly after the Chernobyl accident (26 April – 15 May 1986);

(c) A larger area should be sampled in order to identify any systematic spatial trend in the ^{137}Cs inventory, which would not be detectable over a shorter distance.

All of these issues should be taken into consideration and potential interactions should be evaluated. Experience has highlighted several issues which may be relevant for successful reference site selection in Chernobyl affected areas. For example, if rainfall after the Chernobyl accident was absent or very limited at the study site, it can be concluded, that dry fallout will have dominated the fallout input and this is likely to have been relatively uniform as compared to wet fallout associated with precipitation. If rainfall took place, but the wind was weak, the fallout could be still relatively uniform. However, if the wind was strong, considerable spatial variability of ^{137}Cs inputs should be expected between, for example,

wind-exposed slopes, plateau areas and slopes in a wind shadow. Even the presence of a forest boundary or a row of trees could influence the wind speed and the rainfall intensity sufficiently to affect fallout distribution.

In some cases conditions during the period of Chernobyl fallout resulted in such spatial variability of ^{137}Cs fallout, that the selection of an appropriate reference site may be impossible. Consequently, the quantification of soil redistribution rates with the use of conversion models is not possible. In such cases ^{137}Cs can only help to make qualitative studies of soil redistribution in the landscape as presented by Froehlich et al. [55]. In the study area in the Western Carpathians, the overall ^{137}Cs inventories were affected by Chernobyl fallout [55]. Here, the ^{137}Cs inventories at the reference site, situated on an undisturbed plateau, were smaller than on slopes affected by erosion. This was explained by increased rainfall receipt on wind facing slopes. Although the authors could not quantify the soil redistribution rates with the use of conversion models, the data on ^{137}Cs inventories were useful to study the spatial patterns of soil redistribution at terraced slopes [55]. The ^{137}Cs data helped, for example, to identify the deposition areas along the lower boundaries of terraces.

(iii) Alternative solutions to assess the magnitude of the initial ^{137}Cs fallout

The availability of appropriate reference sites continues to be a key limitation of the^{137}Cs method at some locations. Where difficulty is encountered, supporting information can be gained using the following approaches:

(a) The approximate reference value can be established using national or global long-term measurements of ^{137}Cs atmospheric fallout e.g. [56-58]. For example, the temporal history of ^{137}Cs release from the record of cumulative atmospheric fallout input since the global introduction of ^{137}Cs in the environment has been used to study sediment accumulation in the sea and lakes [8];

(b) In areas where the direct long-term measurements of atmospheric fallout are not available, the reference value can be estimated as a function of the annual rainfall. Several Equations directly relating ^{137}Cs atmospheric fallout to the average annual precipitation of the study area have been developed in Canada, Europe and Australia [11, 43];

(c) It is possible to estimate the ^{137}Cs inventory for a study site using the software developed by Walling and co-workers [32] (see Paper 5 of this TECDOC). The required parameters for a predicted inventory are: the site location (longitude and latitude) and the annual precipitation.

(iv) Reference site sampling approach

The two key objectives of soil sampling at the reference site are (1) to establish the reference inventory (Bq m^{-2}) and (2) determine the depth distribution of the ^{137}Cs activity to support application of conversion models (see Paper 5 of this TECDOC). In the first case, sampling commonly involves the use of bulk cores, whereas depth incremental sampling is required to establish the depth distribution. This could involve the use of a scraper plate, sectioned cores or the excavation of a soil pit and collection of samples from the exposed face of the pit.

For reference inventory samples, the maximum penetration depth of ^{137}Cs should first be determined to ensure that the complete ^{137}Cs inventory will be represented by the core samples. This is achieved through depth incremental sampling. At undisturbed pasture and

forest sites most of the ^{137}Cs should be concentrated within the top10 centimetres of the soil profile. At a typical reference site, no ^{137}Cs will be found below 25-30 cm [6, 59, 60]. When the depth distribution of ^{137}Cs is known, bulk core samples can be collected. The depth of the core samples should exceed the actual depth of the ^{137}Cs layer by at least 5 cm, in order to ensure that all ^{137}Cs inventory is included in the sample. The following guidelines should be followed when collecting cores from the reference site:

(a) Reference sites should be sampled using a systematic grid design according to the size of the site. The collection of three replicate cores within 1 m of each sampling point should be encouraged. Afterwards, the cores may be bulked and the counting time adjusted according to the ^{137}Cs activity;

(b) Different authors recommend different numbers of sampling points. For example, Pennock [61] recommended that between 15 and 30 sampling points will usually be necessary to provide an accurate estimate of central tendency. Sutherland [39, 62] suggested that approximately 11 sampling points would generally be adequate for many reference locations, assuming that independent random samples are selected. In order to have a standardised approach, a minimum of 10 to 15 soil samples should be collected for statistical evaluation. If the standard deviation obtained for this sample set proves too high (CV% > 30%), more samples should be taken. However, to establish the spatial variability of the initial ^{137}Cs fallout, the use of geostatistics is needed and then more samples – minimum of 50 – using an integrated multi-grid design will be required [2];

(c) It is also useful to take additional samples from the reference site to analyse and characterise the physical and chemical soil proprieties.

Similar considerations apply to establishing the ^{137}Cs depth distribution at the reference site. It is important that this should be representative of the site. Where sectioned cores are used, a number of cores should be sectioned to establish the degree of variability of the depth distribution and the mean distribution. Alternatively the cores could be sectioned and the individual sections bulked to provide a spatially-averaged depth distribution. Where a scraper plate is used, the much larger surface area involved relative to cores, reduces the problems associated with the micro-scale variability of the inventory. However, it is preferable to sample more than a single point in order to ensure that a representative depth distribution is obtained.

2.4. Sampling strategies at the field scale

To express the spatial distribution of ^{137}Cs resulting from post-fallout soil redistribution, the sampling strategy must integrate the micro-scale spatial variability in ^{137}Cs inventories and the spatial variability of soil redistribution processes [31]. For cultivated sites, the micro-scale spatial variability is generally minimal and each sampling point can be represented by a single core. However, in uncultivated sites, where there is a potential for local variability due to bio-perturbation or variability in vegetation cover, it is recommended that multiple cores (2 to 3) are collected to represent the individual sample points. These cores can be bulked. Nevertheless, the key factor in designing a suitable sampling strategy is to collect representative samples within the field, which reflect the spatial variability of soil redistribution processes. In this context, two approaches are commonly adopted:

(i) Transect approach

This approach is based on the hypothesis that there is lateral uniformity in ^{137}Cs distribution along parallel transects and is suitable for fields or small areas characterised by simple topography where no significant across-slope curvature exists and where each point along the transect receives flow from only those points immediately upslope. This method is especially suited to relatively steep, short and homogeneous slopes. In these situations, a single transect can represent the variability of ^{137}Cs inventories. If significant plan curvature exists, a single transect is not sufficient and a series of equally spaced parallel transects should be used. Transects are generally aligned along the axis of greatest slope, and consist of a sequence of sampling points from the upslope to the downslope boundary. An example of multiple transect sampling is given in Fig. 6 which involves three transects. The number of samples taken along a transect will depend on the downslope length and the topography of the studied field. However, in a small field, a minimum of three samples are required to establish the ^{137}Cs inventories close to the upslope and downslope boundaries, in addition to the main body of the field. A distance of 10 to 20 m between the sampling points is generally used. The multiple transect approach is particularly convenient if resources are limited. It allows a more rational use of resources than the grid approach, because the variability is usually much higher along the slope than across the slope.

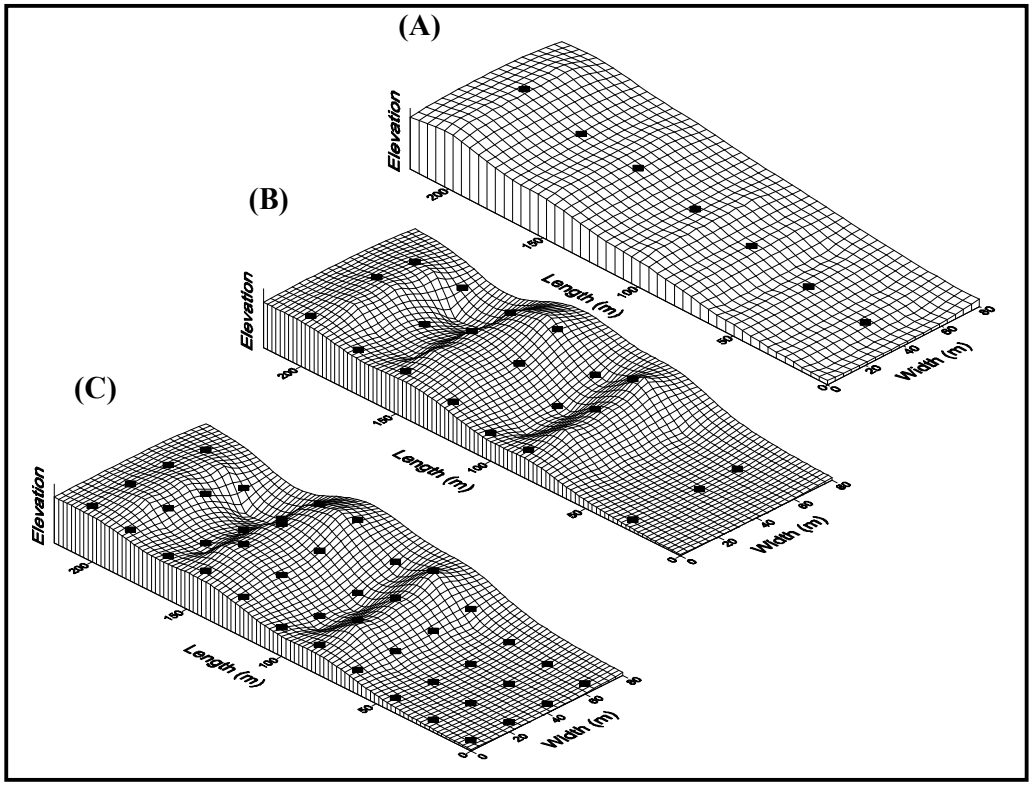

FIG. 6. Different sampling designs for collection of soil cores (A: Simple transect; B: Multiple transects; C: Grid).

(ii) Grid approach

When the topography is more complex, it is necessary to collect samples from a grid framework, covering the field with regularly spaced sampling points. Usually a square grid is used, but rectangular grids are also sometimes used. It is then possible to define effectively the spatial distribution of ^{137}Cs and the resulting soil redistribution pattern. The sampling density depends on the total area and is conditioned by the resource availability. However, a minimum density is required to establish the spatial distribution of the ^{137}Cs inventories. The number and spacing of the samples will influence the ^{137}Cs pattern obtained and the resulting assessment of the pattern of soil redistribution. Mabit et al. [63] reported a range of different grid sizes from published studies (e.g. 10 by 10 m [64]; 15 by 20 m [65]; 20 by 25 m [66]; 30 by 30 m [67]; 50 by 50 m [68]; and 100 by 100 m [69]).

2.5. Sampling strategies at the watershed scale

Assessing the severity and spatial extent of soil erosion over large areas is not an easy task. Soil movement mapping at scales exceeding that of the individual field is a complex process. This aspect is still under investigation and needs some refinement. Upscaling the use of FRNs for documenting soil and sediment redistribution to the watershed or catchment scale is one of the key concepts under investigation by the Soil and Water Management and Crop Nutrition Subprogramme of the Joint FAO/IAEA Division of Nuclear Techniques in Food and Agriculture through the new Coordinated Research Project (CRP) D1.20.11 entitled "*Integrated Isotopic Approaches for an Area-wide Precision Conservation to Control the Impacts of Agricultural Practices on Land Degradation and Soil Erosion*". This new CRP will be implemented during a five year cycle and started with the first Research Co-ordination Meeting (RCM) that took place in IAEA Vienna Headquarter from 8 to 12 June 2009. The second RCM to review initial progress was held in Rabat, Morocco from 27 September to 1 October 2010.

Nevertheless, based on a few existing studies at the watershed scale, some guidance can be provided. The experience gained from studies undertaken at the watershed scale has shown that the approach should be adjusted according to the size and heterogeneity of the watershed involved.

(i) Small homogenous watershed: a simplified approach

Based on previous studies e.g. [1, 70-72], an homogenous area (some hectares to a few square kilometres as a maximum) can be sampled using a grid (50 to 100 m) or a multiple transect approach incorporating information provided by topography, soil type and land use.

It is possible to balance the scientific objectives with economic constraints to reduce the costs of ^{137}Cs measurements in large-scale studies by increasing the dimensions of the sampling grid to some extent without a significant loss of information. However, the overall topography should always be taken into account prior to selecting a grid size [63].

For example, in the Lennoxville watershed (80 ha) in Canada, 539 soil samples were collected using a 25 by 30 m grid [73]. Two alternative sampling scenarios were tested involving two increased grid sizes (50 by 60 and 100 by 120 m). The soil redistribution map and the sediment budget were recalculated for both scenarios. This study suggested that it is possible to reduce to some extent the sampling density for ^{137}Cs and consequently the costs of the investigation without significant loss of information on the soil redistribution rates and their spatial distribution across the study area. Similar results were reported by Higgitt [74] with a slightly different procedure. Starting with an original 20 by 20 m grid, involving 83 sampling points, the author randomly removed a growing number of points to end up with 70, 60, 50 and 25 points, and calculated the resulting soil redistribution budgets of his study area. Except

for the most drastic scenario (n = 25), the reduction of the number of sampling points had no significant impact on the spatial distribution of the soil movement rates or on the soil redistribution budget.

However, it may be difficult to extend or generalize the results obtained from one watershed to other watersheds. Stratified random sampling may be a more appropriate approach, depending on topographic variability. Soil sampling could be significantly reduced in areas where the slope is essentially uniform, but should be increased in the case of more undulating topography.

(ii) Large watershed: the isosectors approach

The use of ^{137}Cs and other FRN measurements to study soil redistribution in small areas (a few hectares) generally involves soil sampling on a more or less regular grid basis or employing transects selected to the reflect the local topography [41, 63]. As the size of the watershed increases (more than 100 ha), a different sampling approach has to be adopted. In large watersheds, sampling using a regular grid is not possible because of the exponential increase of costs. A different approach based on so-called "isosectors" has, however, proved successful. With this approach, the area under investigation should be subdivided into homogeneous isosectors in order to facilitate the sampling strategy. This subdivision is based on use of soil and topographic-geomorphological maps, land use information obtained through satellite and/or aerial photographs and the use of Geographical Information Systems (GIS). A large watershed can be divided into isosectors presenting unique combinations of these parameters. With this approach, flat forested areas can be considered as stable with the soil redistribution budget assumed to be 0 t $ha^{-1}yr^{-1}$.

As an example, the Boyer River watershed in Canada (217 km^2) was delineated into six different isosectors using GIS and taking into account the land use, the topographic and soil information [34]. Within this watershed, two land use classes (i.e agricultural areas and forested flat areas with slope <2%), three soil texture classes (loam, sandy loam and sandy clay loam) and two slope classes (i.e. 0-2% and 2.15%) were identified.

Using these classes, six different isosectors were identified (see Fig. 7): (a) agricultural sandy loams with slopes < 2%; (b) agricultural sandy loams with slopes > 2%; (c) agricultural loams with slopes > 2%; (d) agricultural loams with slopes < 2%; (e) agricultural sandy clay loams with slopes <2% and (f) flat forested areas.

The next step was to select representative areas within each isosector for FRN sampling on a variable grid or multi-transects basis. The information provided by these representative fields was then extrapolated to the area of each relevant isosector.

For a large area with variable annual precipitation, there is clearly a need to employ additional reference sites to take account of the variation of the reference inventory across the study area. These should be located as close as possible to the sampled fields. These reference sites should be selected taking into account the criteria presented previously in this Paper.

At the watershed level, the collection of soil samples using a grid can be costly in terms of both time and resources. The sampling strategy must be optimized. To minimise sampling and analytical requirements, one of the fields selected to be representative of each isosector could be sampled using a grid approach and the other fields selected to be representative of the same isosector could be investigated using a single transect, if the conditions explained previously in this Paper are met. Alternatively, a selection of a typical sub-basin of the watershed including a reduced numbers of representative fields can be also investigated using the classical sampling strategy used at the field scale.

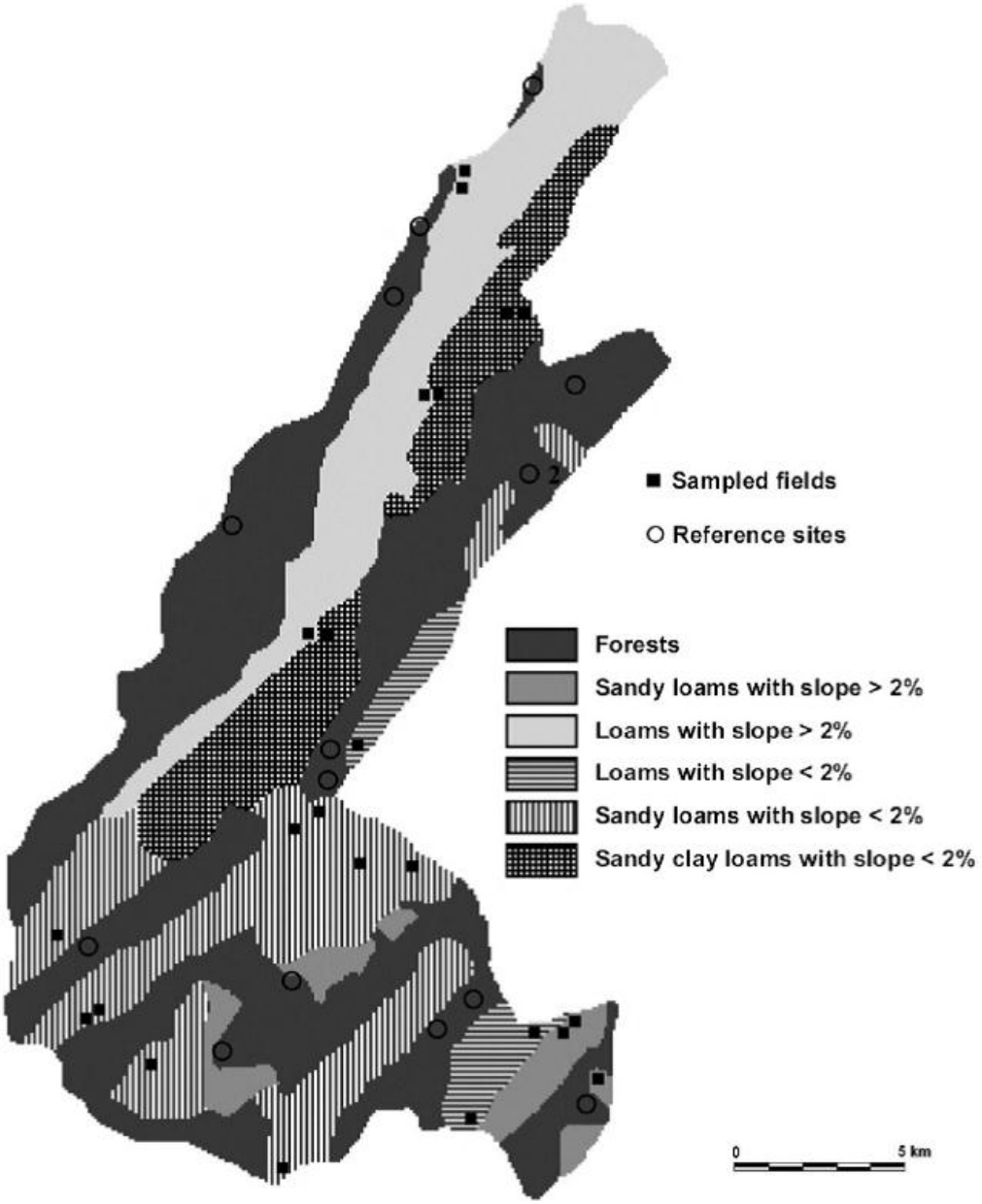

FIG. 7. The distribution of the six isosectors within the Boyer River watershed and the location of the sampled fields and the reference sites (Adapted from [34]).

2.6. Soil sample collection and recommended sampling tools

As the use of ^{137}Cs measurements in soil erosion and sedimentation investigation requires information on both bulk ^{137}Cs inventories (Bq m^{-2}) and the ^{137}Cs vertical depth distribution, two methods are commonly used to collect soil samples:

(i) Bulk sampling using cores

Generally, a steel cylinder is used as the corer. The diameter of the tube is usually 7 to 10 cm [75] with a wall thickness of 2-5 mm. The corer is constructed to cope with stony and compacted soil. To facilitate both the insertion of the core tube and sample extraction, the cutting edge of the tube should have a smaller internal diameter than the tube itself [31]. The tube can be inserted into the soil manually (e.g. using a hammer) or coupled with a mechanical percussion driver in hard soils. An example of such mechanical equipment is illustrated in Fig. 8, which shows a motorized 'Soil Column Cylinder Auger'. Small vehicles can also be equipped with a hydraulic driver or a motorized soil corer to facilitate soil collection and extraction in the field. Such mechanization can make sample collection much easier and faster.

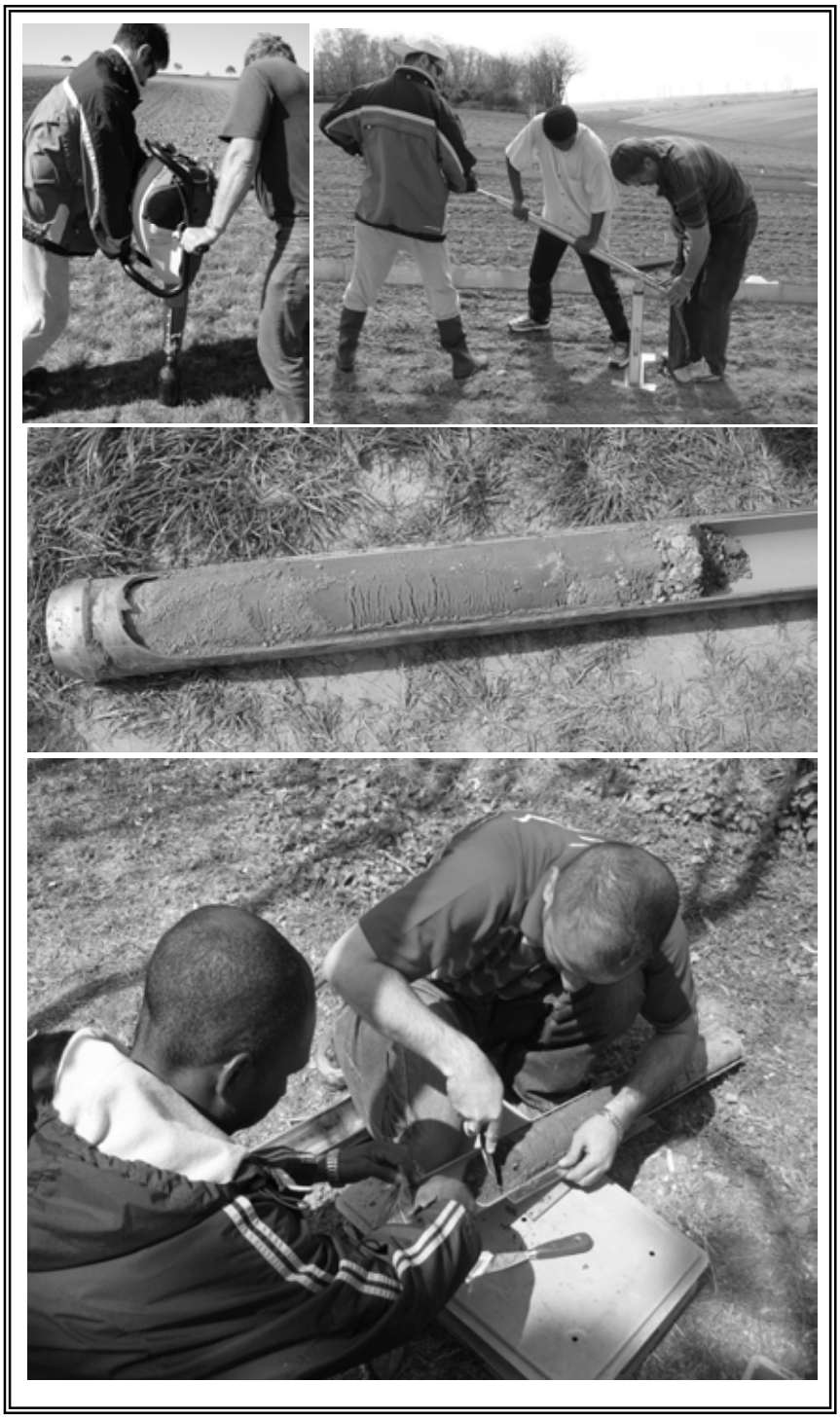

FIG. 8. Collection of soil samples by IAEA fellows and staff using a motorized soil column cylinder auger.

One of the problems related to the sampling process using a corer is the possible compaction of the soil sample within the core tube. Although it is advisable to avoid such compaction as far as possible, if the ^{137}Cs mass activity density is expressed in Bq kg^{-1} and the inventory is calculated on the basis of the sampled surface area and the total ^{137}Cs content of the core (Bq m^{-2}) problems associated with changes in bulk density are effectively avoided. Changes in bulk density introduced by coring will be much more important when cores are sectioned to determine the depth distribution. Lafond [76] compared soil surface dry bulk density

estimated from cylinders taken with a manual and hydraulic sampler under experimental conditions in Quebec (Canada). He concluded that the hydraulic sampler was able to reproduce with reliability dry bulk density and soil core length measurements [76]. Another important question concerns correct determination of the appropriate sampling depth. This issue is similar to that discussed previously for reference sites. The sampling depth should ensure that the whole soil profile containing ^{137}Cs is sampled. Therefore the ^{137}Cs vertical distribution should be tested by depth incremental sampling. When defining the sampling depth in a study field subject to soil redistribution, it should be recognized that the ^{137}Cs depth distribution is likely to be more variable than at reference sites, as the thickness of the ^{137}Cs contaminated layer may be reduced at eroded sites and increased at deposition sites. Therefore any reconnaissance depth incremental sampling should be undertaken at different topographic positions within the study site. The depth of bulk core samples will also depend on the land use of the study site. In areas under undisturbed pasture, sampling depths are likely to be less than in cultivated fields, although the depth required for the latter will vary according to the plough depth.

Summary of key points:

(a) *Reference sites*: The sampling depth should be around 30 cm.
(b) *Cultivated areas*: In eroding zones, the ^{137}Cs is mixed within the plough layer which generally ranges from 20 to 40 cm. The sampling should therefore extend to at least this depth. In depositional zones, the samples should be collected to a depth of 40 to 60 cm or even deeper, depending on the depth of the original plough layer and the expected magnitude of soil deposition.
(c) *Uncultivated areas*: A coring depth of 30 cm should be sufficient in eroding zones. However in depositional zones, the samples should be collected to a depth of 40 to 60 cm or even deeper, depending on the likely magnitude of soil deposition.

It is recommended that the ^{137}Cs vertical distribution in a soil is checked by collecting cores in eroded and depositional areas for depth incremental sectioning and analysis (protocol explained in the next paragraph), prior to sampling the whole field for ^{137}Cs inventory measurements.

(ii) Depth incremental sampling

Depth incremental sampling provides important information on the depth distribution (vertical distribution or profile) of ^{137}Cs. This is key information for the reference site as well as the study site. It is needed to determine the appropriate depth of bulk sampling at both reference and study sites, to ensure that the samples include the whole ^{137}Cs inventory. For the reference site, the shape of the ^{137}Cs vertical distribution provides valuable confirmation that the site is undisturbed and thus appropriate for establishing the local ^{137}Cs fallout input.

For the study site, the ^{137}Cs depth distribution provides the information necessary to define the required sampling depth in both eroding and depositional areas. Finally, information on the ^{137}Cs depth distribution is required for the application of conversion models within uncultivated sites (see Paper 5 of this TECDOC) and to determine parameters used by those models (e.g. mass relaxation depth).

A sectioned core provides the simplest means of defining the ^{137}Cs depth distribution. However, in order to provide a sufficient mass of sample from each depth increment for subsequent radiometric analysis, the diameter of the core tube generally needs to be greater than those used to collect bulk cores. A cylindrical steel tube with a diameter of 10 to 15 cm is commonly used. As with core tubes used for collecting bulk cores, it is advantageous if the

internal diameter of the cutting edge is slightly smaller than that of the core tube itself. Once collected, the core is then sectioned into incremental samples which can be counted separately. To easily extract the soil core, one of the best options is to use a specially designed core tube which splits into two longitudinal sections to allow access of the contents (Fig. 8). Soil increments of 2 to 5 cm are generally used. However, for a precise ^{137}Cs profile shape, it is better to cut the core at 2 cm intervals.

An alternative approach to obtaining depth incremental samples is to use a "scraper plate" (Fig. 9). This system has been widely used [31, 77-79]. The scraper plate has two components: a metal frame that is inserted into the soil surface and an adjustable metal scraping plate that can move along the frame and progressively scrape fixed soil depth increments from within the frame.

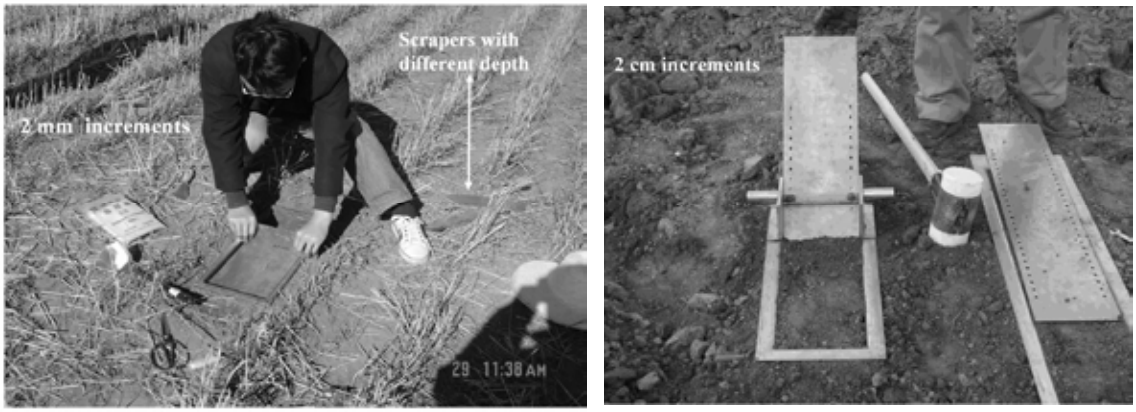

FIG. 9. Example of soil sampling in China using a scraper plate (Photo by: Yong Li, Chinese Academy of Agricultural Sciences).

3. Sample preparation and pre-treatment

Based on the protocol proposed [31, 41], sample preparation (Fig. 10) should involve the following steps:

(a) Each soil sample is firstly air dried or oven dried at around 60°C for 48 hours;

(b) The weight of the dried sample must be recorded (M_t);

(c) The sample is lightly ground or hand disaggregated. It is important to disaggregate mineral particles, organic concretions and any porous material. However, the soil should not be subjected to sufficient abrasion to break up individual particles [80];

(d) The sample is sieved or passed through a 2 mm mesh to separate soil particles (< 2 mm) from the coarser rock fragments (> 2 mm). The weights of both the fractions less and greater than 2 mm must be recorded (M_f and M_c). The bulk density of the soil sample (fine fraction) should be accurately calculated if this parameter is used for determining the ^{137}Cs areal activity or inventory;

(e) The weight of the sum fractions ($M_f + M_c$) is compared with the total sample weight (M_t). If the grinding has been undertaken with care, any discrepancy in weight will be only due to airborne loss of the fine fraction. The corrected fine fraction weight can therefore be calculated by subtracting the coarse fraction weight from the total weight ($M_t - M_c$);

(f) A representative sub-sample (e.g. 50 to 1500 g depending on the counting geometry) of the fine fraction is taken and packed for analysis. It is important that the fine fraction should be well mixed to ensure that this sub-sample is representative of the total mass of the fine fraction. Generally, depth incremental samples yield small quantities of material and are placed into a cylindrical container with a small volume (50 to 200 mL). Conversely, bulk cores yield large quantities and these are generally placed in 500 to 1500 ml "Marinelli" beakers.

FIG. 10. IAEA fellows pre-treating soil samples in the laboratory.

Two issues regarding the importance of the rock fragments in soil have been raised. Firstly, according to Auerswald and Schimmack [81], separation and analysis of the < 2mm fraction of soils with a significant rock-fragment content can generate errors in assessment of the radionuclide content of the original sample, since the rock fragment content of soil may vary spatially and the rock fragments may contain significant ^{137}Cs activity, particularly if fine clay particles adhere to the rock particles. These authors concluded that errors of several t ha^{-1} in soil loss calculations may result if heterogeneity and the ^{137}Cs concentration of the rock fragment are ignored. The second consideration is the effect of rock fragments on the bulk density of the whole samples. For stony areas, results vary significantly with sample volume, and the whole soil density may differ appreciably from the bulk density of fine particles. In these circumstances, the procedure described by Pennock and Appleby [41] can be adopted. Correction for the bulk density of the coarse material is most relevant for soils with significant rock fragments.

4. Gamma spectrometry measurements

4.1. Interaction of gamma rays with matter

As an introduction to the next section, a brief background to the interaction of gamma rays with matter is provided. In the energy region of 0.01 to 10 MeV, there are three types of processes by which gamma rays (photons) can be absorbed or scattered by matter:

(a) *Photoelectrical effect*: In this process, the primary photon (with energy of $h\nu_0$) is completely absorbed and a photoelectron is ejected with energy $T = h\nu_0 - B_e$, where B_e is the binding energy of the ejected atomic electron. The remainder of the energy appears as characteristic X-rays and auger electrons from the filling of vacancy in the inner (K or L) shell where the photoelectric reaction mostly takes place. This process occurs predominantly below energies of 0.1 MeV;

(b) *Compton effect*: This process is described as a simple two particle collision between a gamma ray and an electron with a low binding energy with the atom. The incident photon with initial energy of $h\nu_0$ transmits one part of its energy to the electron and is scattered at an angle denoted as θ. It has a lower energy after the collision ($h\nu < h\nu_0$) and the electron is deviated from the photon incident trajectory by an angle $\emptyset$, possessing a kinetic energy of $T = h\nu_0 - h\nu$. The fractional energy loss in individual Compton processes is quite large for energetic photons;

(c) *Pair production*: The third type of interaction becomes increasingly important above the incident energy of 1.02 MeV. The photon is completely absorbed and replaced by a positron and an electron pair whose total energy (kinetic plus rest mass) is just equal to $h\nu_0$. The process occurs only in the field of charged particles mainly in the nuclear field but also to some degree in the field of an electron.

4.2. High resolution gamma spectrometry in the laboratory

(i) General basis

Gamma spectrometry using germanium detectors (HPGe or Ge-Li) is an excellent analytical technique for measuring low level activities of natural (e.g. ^{226}Ra, ^{210}Pb, ^{40}K, etc.) or artificial radionuclides (e.g. ^{137}Cs, ^{60}Co, etc.) in environmental samples (e.g. soil, sediment, vegetation, water, etc.). The method allows both qualitative and quantitative determination of the radionuclides directly in the original sample, through the detection of gamma rays (photons), without the need for chemical separations. The simultaneous detection of several gamma emitters in the same sample material is possible using a shielded high resolution germanium semiconductor detector connected to a multichannel analyser (MCA). The interaction of gamma rays (photons) with the germanium crystal produces electric signals corresponding to the energy of the incoming photons. Signals are amplified and transmitted to the MCA. A gamma energy spectrum, characteristic of the gamma-emitting nuclides (Fig. 11) is produced. This is the result of the three effects described above (i.e. Photoelectric, Compton and Pair production effects) due to the interaction of gamma rays with the germanium crystal. The photoelectric effect is characterized by the presence of high resolution peaks (called full-energy peaks) associated with the γ-rays emitted by the radionuclides while the Compton effect is characterized by a continuum due to the interaction of the gamma rays with electrons of the atom. The conversion of the net peak area (counts per second) of the nuclide of interest, associated with the Photoelectric effect on activity (Bq kg^{-1}) as well as the processing of the overall collected spectral data are performed using a selected software package.

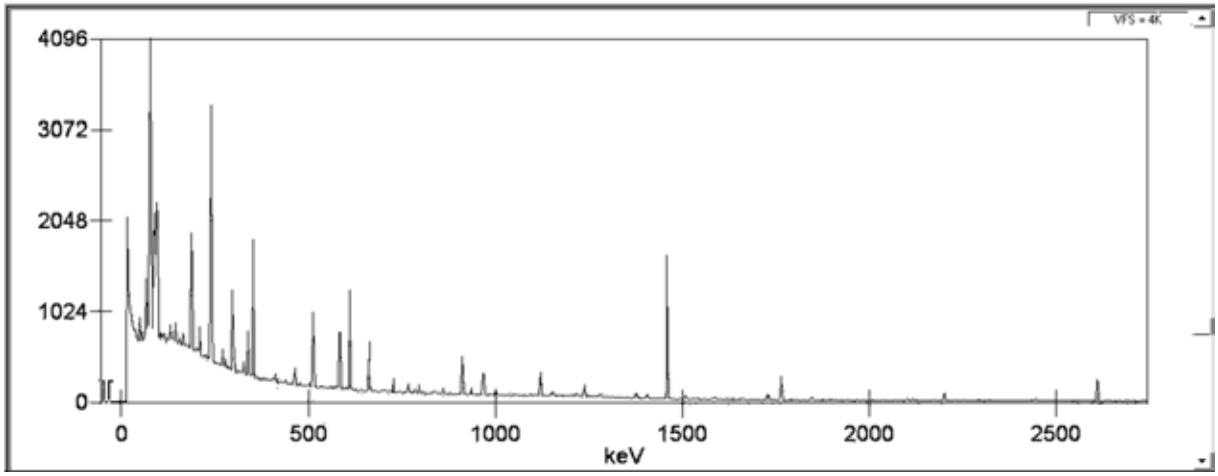

FIG. 11. An example of a gamma spectrum.

(ii) High purity germanium detectors

High purity germanium (HPGe) detectors are mostly used in gamma spectrometry and have many advantages as compared to older Germanium-Lithium (Ge-Li) detectors [82].They use semiconductor diodes having a p-i-n structure in which the intrinsic (i) region is sensitive to ionizing radiation, particularly x rays and gamma rays. Under reverse bias, an electric field extends across the intrinsic or depleted region. When photons interact with the material within the depleted volume of a detector, charge carriers (holes and electrons) are produced and are swept by the electric field to the p and n electrodes. This charge, which is in proportion to the energy deposited in the detector by the incoming photon, is converted into a voltage pulse by an integral charge sensitive preamplifier. The major constraint of germanium detectors is that they must be operated at very low temperatures. At higher temperatures, the electrons can easily cross the band gap in the crystal and reach the conduction band, where they are free to respond to the electric field. The system therefore produces too much electrical noise. To prevent this effect, HPGe detectors are connected to a cryostat cooling system situated generally inside a Dewar container filled with liquid nitrogen (T^o = 77.4 K) in order to reduce thermal excitations of valence electrons so that only a gamma ray interaction can give an electron the energy necessary to cross the band gap and reach the conduction band. Compared to Ge-Li detectors, the HPGe detectors can be allowed to warm up to room temperature when not in use. New electrical cooling systems have recently been developed and these have now become commercially available e.g. [83, 84]. They consist of an electrically powered cryostat which uses a pulse-tube cooler which is a relatively new concept in cryogenic coolers. The system has a compressor stage coupled to a heat exchanger in which there is a physical displacer that moves the compressed gas to effect the cooling cycle. The refrigerant used generally is pure helium - both CFC-free and non-flammable.

HPGe detectors commonly still use lithium diffusion to make a thick (~ 600 μm) donor contact n^+ and thin (~0.3 μm) boron implantation to make a receptor contact p^+. The shape, position and thickness of the contacts determine the detector configuration and in which energy range it can operate. HPGe detectors with a central p^+ contact are referred to as 'P-type' detectors while 'N-type' detectors have a n^+ central contact. A coaxial 'P-type' detector can operate in the energy range from 40 keV to 10 MeV and is largely suitable for measuring ^{137}Cs at 662 keV. However, for low energy photons such as the energy of ^{210}Pb at 46 keV, the efficiency of detection significantly decreases and the analysis of ^{210}Pb becomes critical. To overcome this difficulty, it is recommended to use the 'N-type' detector configuration which increases the efficiency considerably, especially below 100 keV, and makes it possible to

measure both low and high energy gamma rays. The energy range for such detectors is generally between 3 keV and 10 MeV. Various detectors (e.g. Fig. 12), depending on the application domain, are marketed by different suppliers. Additional details on the germanium detectors and their characteristics are reported e.g. [83, 84].

FIG. 12. Examples of HPGe detectors with shielding and electronic components at the IAEA Seibersdorf laboratory and at CNESTEN, Rabat, Morocco.

(iii) Gamma spectrometry systems in the laboratory

The different components of a gamma ray spectrometry system can be described as follows (see also Fig. 13):

(a) *A high purity germanium detector (HPGe) with cryostatic cooling*: A liquid nitrogen Dewar or electrically powered cryostat (described in the section above) will be needed. The performance of the detector is given by its relative efficiency, its energy resolution and the Peak-to-Compton ratio. The relative efficiency is a measure relative to that of a 75 x 75 mm NaI (sodium iodide) crystal and is normally based on the measurement of the 1.33 MeV peak of ^{60}Co. Its value depends on the crystal volume and the detector configuration. The energy resolution of the detector which is considered as the full energy peak at half maximum (FWHM) of the full energy peak of 1.33 MeV peak should be between 1.8 and 2.2 keV. The Peak-to-Compton ratio is the ratio of counts in the highest photo-peak channel to the counts in a typical channel just below the associated Compton edge and is conventionally quoted for the 1.33 MeV gamma ray photo-peak of ^{60}Co;

(b) *Shielding*: A detector shield with a cavity large enough to accommodate samples (up to 2 litres) will be needed. It is generally constructed of lead. The wall thickness is usually 10 cm in order to attenuate high-energy photons from all external sources. In addition, to attenuate lead photons coming from the lead shield, it is recommended to install inside the lead shielding a lining of either copper or steel with a thickness of 10 mm;

(c) *A preamplifier*: This is generally an integral part of the detector unit which takes the charge produced from the detector, integrates and amplifies this to produce a pulse, the amplitude of which is proportional to the total energy. The amplifier is located near

the detector in order to take advantage of the cooling which is necessary for the operation of the detector with low noise;

(d) *A high voltage power supply*: A bias voltage is applied across the detector volume to collect created charges within the germanium detector. This is usually in the range of ±1000 to 5000 V;

(e) *A linear amplifier*: This primarily takes the pulse signal from the preamplifier and considerably amplifies it. It also filters and shapes the incoming pulse to enhance the signal-to-noise ratio. High resolution spectroscopy amplifiers with a pile-up rejection and life-time correction are now commercially available;

(f) *An analogue to digital converter (ADC)*. The detector produces an analogue signal which is shaped by the amplifier. The ADC converts this analogue signal to a digital signal and can usually only process one incoming pulse at a time (from one detector). When several detectors are used, it is advisable to use a multiplexer or mixer-router which takes the separate counting chains from several individual inputs and routes them through to a single ADC;

(g) *A multichannel analyser (MCA)*. Usually incorporated into the computer system, an MCA registers the pulses emerging from the ADC in one of its channels according to their amplitudes i.e. the energies of gamma rays. It can operate with a minimum of 1024 channels and a maximum of 8192 channels. The number of channels usually used is 4096.

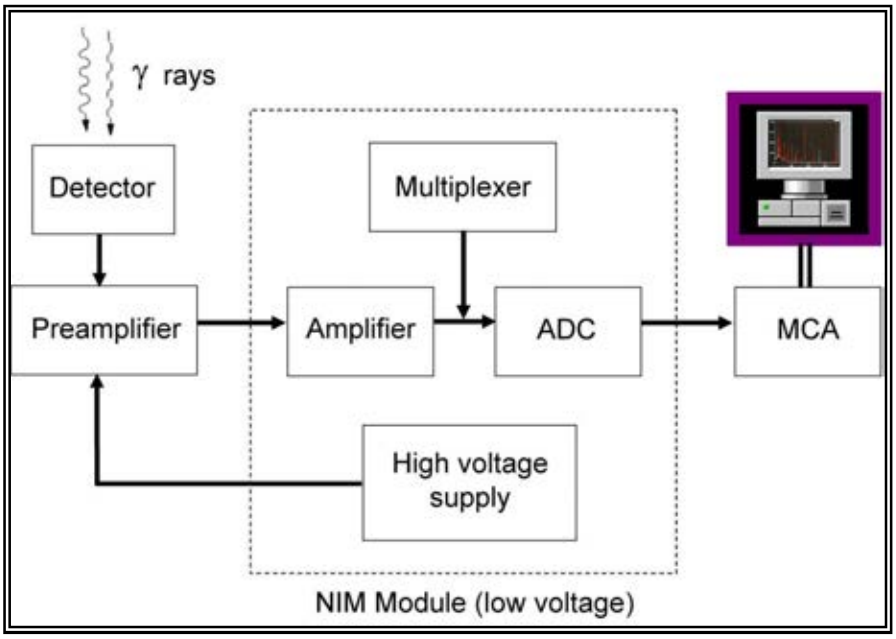

FIG. 13. The electronic components of a gamma spectrometry system.

(iv) Detector calibration

In order to accurately identify and quantify the radionuclides in a sample, it is necessary to calibrate the detector. This operation should be performed with great care, because the accuracy of all quantitative results will depend on it. The parameters of the electronic components should remain stable between calibration exercises. Any small changes in these parameters can have a direct impact on calibration. Both energy and efficiency calibrations need to be undertaken for gamma detectors as described below.

(a) *Energy calibration*: The energy calibration of a germanium detector system represents conversion of the channel number of the MCA to gamma ray energy. It is generally undertaken by measuring mixed standard sources containing known radionuclides with well-defined energies usually within the range from 60 to 2000 keV. Mixed gamma ray standards are available in various forms and containers from international suppliers e.g. [85, 86]. An example of the list of radionuclides from a current mixed gamma ray standard is given in Table 1. A radionuclide point source may also be used to perform the energy calibration of the detector. Standard sources should contain a selection of radionuclides with at least four different gamma energies. The curve of energy vs. the channel should be linear if the system is operating properly. The conversion factor (keV/channel) is adjusted by the gain of the amplifier. The value is usually fixed to 0.5 keV per channel;

(b) *Efficiency calibration and direct calibration*: Theoretical and experimental methods can be used to calibrate the detector for analysis and calculation of sample activity. However, it is recommended that a detector should be calibrated experimentally. The method is based on the measurement of the absolute efficiency. The efficiency depends on many parameters such as the gamma energy line, counting geometry (container form and distance from the detector), detector characteristics (e.g. relative efficiency) and the sample matrix (e.g. density and composition). Experimental efficiency is measured for each radionuclide contained in a mixed standard source of known radionuclides at their different energies, based on the certified activity of the radionuclide, the number of the detected events or gamma rays (counts/sec) and the characteristics of the nuclide (gamma intensity or emission probability and half-life). The standard must be prepared in the same counting geometry as the soil sample to be analysed. In addition, due to the self or auto-absorption effect (absorption of gamma rays by the soil matrix), which becomes important in low energy (< 200 keV) and for large volume samples, the density and composition of the standard should be as close as possible to that of the soil sample. The effect is not important if ^{137}Cs (γ of 662 keV) or ^{7}Be (γ of 478 keV) are measured, especially when small volumes of soil sample are used and there is not a big difference between the densities of the standard and the soil sample. However, the situation is critical for measuring ^{210}Pb (46 keV) and requires auto-absorption correction (see Paper 3 of this TECDOC). Correction related to the dead-time is automatically performed by the MCA by collecting data for a given live time. Generally, in the case of the measurement of low activities, the dead time effect is very low. Also, the coincidence summing correction is neglected when the activities are low.

In cases where the counting time is much lower than the half-life ($t_c < 0.01 \times t_{1/2}$), the efficiency can be expressed as follows:

$$\varepsilon = N / (A\, t_c\, I_\gamma) \qquad (2)$$

where:

ε = absolute efficiency;
N = net counts under the peak (net peak area) of the investigated nuclide (e.g. gamma ray energy of the ^{137}Cs: peak at 662 keV);
A = activity of the sample in Bq at the measurement time;
t_c = counting time;

I_γ = gamma intensity or emission probability
(e.g. 0.85 for ^{137}Cs gamma ray energy at 662 keV).

From the measured efficiency at different energies a specific curve can be used to fit the efficiency data to an analytical expression in order to obtain efficiencies for the gamma energies associated with the investigated radionuclides of the soil sample. An example of an efficiency curve is provided in Fig. 14.

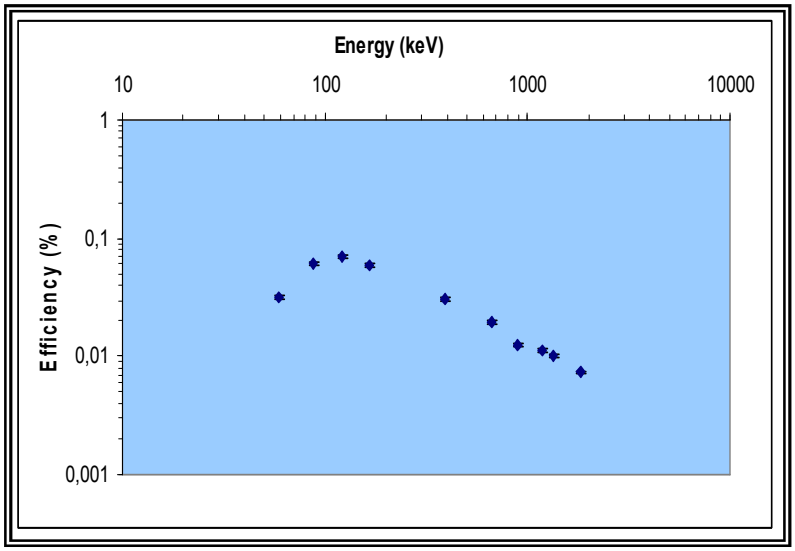

FIG. 14. Efficiency vs. energy under certain conditions using one of the CNESTEN's laboratory gamma detectors (HPGe, 'P' type 30%, cylindrical geometry 200 ml).

The points plotted on Fig. 14 represent the measured efficiencies of gamma energies corresponding to the radionuclides used for the efficiency calibration of a HPGe - P-type detector. A multi-gamma liquid source containing artificial nuclides such as ^{241}Am and ^{137}Cs was used as the standard. Their characteristics are detailed in Table 1.

TABLE 1. THE ARTIFICIAL RADIONUCLIDES (MULTI-GAMMA SOURCE) USED FOR THE DETECTOR CALIBRATION SHOWN IN FIG. 14

Nuclide	Half-life (days or years)	E_γ (keV)	Photons/decay
^{241}Am	432 yr	59.54	0.360
^{109}Cd	436 d	88.03	0.0368
^{57}Co	271.8 d	122.06	0.8559
		136.47	0.1059
^{139}Ce	137.6 d	165.85	0.800
^{203}Hg	46.6 d	279.20	0.813
^{51}Cr	27.7 d	320.08	0.0985
^{137}Cs	30.17 yr	661.66	0.850
^{54}Mn	312.5 d	834.84	0.99975
^{60}Co	1925.5 d	1173.24	0.9990
		1332.50	0.9998

Many analytical functions have been established to describe the dependence of the full-energy peak efficiency on the energy [87-90]. Between 200 and 2000 keV, the most frequently used

function is a linear relationship between efficiency (ε) and energy (E) on a log-log plot: $\log \varepsilon = a_1 + a_2 \log(E)$ where a_1 and a_2 are adjustable constants (fit parameters) which can be obtained from a linear regression analysis of the set of values [91]. An improvement of the fit in this range of energy can be obtained by the use of the polynomial fit:

$$\log\varepsilon = \sum_{j=0}^{n} a_j (\log E)^j \qquad (3)$$

The fit can be improved by increasing n to 3 or more [82]. The above functions to fit efficiency curves are generally automatically applied by software developed for spectrum evaluation and data processing.

The best method to calibrate a gamma detector is a direct calibration. In this case, the standard contains the same radionuclides as those investigated in the soil sample (e.g. ^{137}Cs). The detector is directly calibrated using standard sources with known activity. The key advantage of the direct method compared to the efficiency-curve approach is that it avoids any errors associated with establishing the efficiency curve and with the use of some nuclide characteristics (e.g. emission probability). Obviously, the counting geometry and matrix should be the same for the two samples (standard and soil sample).

(v) Counting geometry

A range of container shapes may be used to present soil samples to the detector. The geometry is selected according to the quantity of available sample material and the level of activity. It is recommended that a gamma laboratory should be able to use several containers with suitable configurations to maintain flexibility for sample analysis. Some examples of containers are cylindrical plastic/polyethylene containers with screw caps, 'Petri' dishes and aluminium containers of various volumes. 'Marinelli' beakers are used for large volumes of soil. Furthermore, the dimensions of the container should be appropriate for the dimensions of the detector and lead shielding.

(vi) Standards for ^{137}Cs

There are different ways to obtain a standard for measuring ^{137}Cs in soil samples:

(a) *Liquid ^{137}Cs source or liquid multi-gamma source (^{241}Am, ^{137}Cs, etc.)*: Certified activities are purchased from an international supplier e.g. [85, 86]. The standard is prepared in the laboratory from this parent source at different counting geometries in the laboratory. A certain quantity of these solutions is evaporated to dryness within an appropriate ground matrix (such as low activity sand). Matrixes with two or three different densities can be prepared;

(b) *Soil matrix with ^{137}Cs prepared by the supplier*: It is also possible to request a supplier to prepare a standard soil from a soil sample matrix containing ^{137}Cs at a certified activity in a range of geometries;

(c) *Use of reference materials*: The use of soil reference materials with known activities which are provided by international institutions or organisations e.g. [92] can constitute an alternative in the absence of certified standards or if the laboratory finds it difficult to prepare a suitable internal standard from certified sources. Count times are, however, generally longer to derive suitable peaks for calibration.

(vii) Spectral evaluation

Software packages are commercially available for the automatic treatment of gamma spectra. Descriptions of the major packages and their suppliers are provided by Wallbrink et al. [75] and Gilmore [93]. The operations usually performed by the computer programmes are as follows:

- Automatic peak search;
- Evaluation of the peak positions in terms of energy;
- Identification of radionuclides by the use of a nuclide library;
- Efficiency-calibration curve;
- Calculation of the net peak area;
- Calculation of activity concentrations in selected units;
- Calculation of the detection limits for specific nuclides.

However, despite the advantages of commercial software, the validity of the results obtained should be carefully checked, especially during the initial set-up [94]. Therefore, manual spectra evaluation should be applied from time to time to check data output and to ensure the quality of the results. For a typical peak (e.g. ^{137}Cs) resulting from gamma measurements, a manual procedure may be used as follows.

If the peak is located between the channel (energy) a_2 and b_1, the total count N_t is:

$$N_t = \sum_{i=a_2}^{b_1} N_i \tag{4}$$

$$N_b = \left(\sum_{i=a_1}^{a_2-1} N_i + \sum_{i=b_1+1}^{b_2} N_i\right) \frac{(b_1 - a_2 + 1)}{(a_2 - a_1 + b_2 - b_1)} \tag{5}$$

$$N = N_t - N_b \tag{6}$$

where:

N = net count or net peak area;
N_b = background count;
N_i = counts in the channel i;
N_t = total counts;
a_1, a_2, b_1 *and* b_2 = the number of the respective channel.

The regions a_1 *to* a_2 and b_1 *to* b_2 are representative of the background under the peak.

(viii) Activity calculations and uncertainties

The activity or concentration of a radionuclide (e.g. ^{137}Cs) in Bq kg^{-1} corrected to the date of sampling can be calculated using the following general expression:

from the efficiency calibration:

$$A = \frac{N\lambda t_c e^{\lambda t_0}}{\varepsilon I_\gamma M t_c (1 - e^{-\lambda t_c})}. \tag{7}$$

where:

A = activity or concentration of ^{137}Cs in Bq kg^{-1} at the sampling;
N = net peak area;
λ = decay constant ($\ln 2/t_{1/2}$), $t_{1/2}$ for ^{137}Cs is 30.17 yr;
t_c = counting time;
t_0 = time difference between sampling and starting the measurement;
M = mass of the soil sample (kg);
ε = absolute efficiency;
I_γ = emission probability (0.85 for ^{137}Cs).

As the counting time is much shorter than the ^{137}Cs decay period, the above Equation can be expressed as follows:

$$A = \frac{Ne^{\lambda t_0}}{\varepsilon I_\gamma M t_c}. \quad (8)$$

The relative uncertainty on the measured activity can be expressed as the quadratic sum of the relative uncertainties of the used parameters (N, M, ε and I_γ):

$$(\Delta A/A)^2 = (\Delta N/N)^2 + (\Delta M/M)^2 + (\Delta\varepsilon/\varepsilon)^2 + (\Delta I_\gamma/I_\gamma)^2 \quad (9)$$

$\Delta N/N$ is the relative uncertainty associated with the counting time

$$N = N_t - N_b \quad (10)$$

where:

N_t and N_b are the total count under the peak, and background count under the peak, respectively.

ΔN_t and ΔN_b are the standard deviations associated with total count and background count under the peak, respectively. If they are considered as normal probability distributions (Poisson distribution), then for an interval of 1σ, $\Delta N_t = \sqrt{N_t}$ and $\Delta N_b = \sqrt{N_b}$.

Therefore,

$$(\Delta N)^2 = (\Delta N_t)^2 + (\Delta N_b)^2 = N_t + N_b \quad (11)$$

$$\Delta N = \sqrt{N_t + N_b} \quad (12)$$

$$(\Delta N/N) = (\sqrt{N_t + N_b})/(N_t - N_b) \quad (13)$$

The value of the relative uncertainty $(\Delta N/N)$ depends on the statistical counting error. Normally, for the analysis of ^{137}Cs, the relative uncertainty should be lower than 5% at 1σ confidence interval.

$\Delta\varepsilon/\varepsilon$ is the relative uncertainty associated with the efficiency; it depends on the uncertainties on the certified activities and the counting statistics of the radionuclides in the standard. This value should be lower than 3%. The other source of uncertainties *(M* and I_γ*)* on the activity measurement is generally very low and can be neglected.

The areal activity, A_s in Bq m^{-2} or inventories are usually used to determine the total activity of ^{137}Cs in the whole core. It can be expressed as follows:

$$A_s = \frac{CM_t}{S} \tag{14}$$

where:

C = activity of the sub-sample of the core sample (Bq kg^{-1});
M_t = total mass of the whole core (kg);
S = area of the horizontal core cross section (m^2).

If the core is sectioned for measuring the ^{137}Cs profile, the areal activity is expressed as:

$$A_s = \frac{1}{S}\sum_i M_{T_i} C_i \tag{15}$$

where:

C_i = activity of the i^{th} sub-sample depth increment (Bq kg^{-1});
M_{T_i} = total mass of the i^{th} sample depth increment (kg);
S = area of the horizontal core cross (m^2).

The areal activity can also be calculated using bulk density information and the increment depth according to the following Equation:

$$A_s = \sum C_i.\rho_t.H_i \tag{16}$$

where:

C_i = activity of the i^{th} sample depth increment (Bq kg^{-1});
ρ_t = bulk density of the i^{th} sample depth increment (kg m^{-3});
H_i = depth of the i^{th} sample depth increment (m).

(ix) Background and detection limit

The background noise of the detection system is an important parameter which can interfere with the radionuclide measurement and exert an important effect on the detection limit and the accuracy of the measurement. Two main sources of background can be distinguished [95]: (a) Internal background linked to natural radioactivity (^{238}U, ^{235}U, ^{232}Th series and ^{40}K) coming from the material used to build the detector and natural radioactivity coming from the auxiliary equipment and shielding; (b) External background linked to natural radioactivity coming from the surrounding environment (earth surface, walls, floor, etc.), radiation coming from ^{222}Rn (gas) daughters and cosmic rays.

Materials commonly used in low internal background detectors are magnesium and copper, while aluminium is avoided [75]. For the external background, more attention should be devoted to the quality and thickness of shielding around the detector.

The detection limit is a term which expresses the detection capabilities of measurement systems under certain conditions [96, 97]. A generally accepted expression of the lower limit of detection (LLD) which contains a preselected risk of 5% of concluding falsely that activity is present and a 95% degree of confidence for detecting the presence of activity, is calculated as follows [98]:

$$\text{LLD} = 4.66 \frac{\sqrt{B}}{\varepsilon I_\gamma \sqrt{T}} \quad (17)$$

where:

B = background count rate (countss^{-1});
ε = absolute efficiency (gamma ray detection efficiency);
I_γ = emission probability of gamma rays;
T = counting time (s).

When introducing the mass (kg) of the sample (M), the minimum detectable concentration (MDC) also termed Minimum Detection Activity (MDA) in Bq kg^{-1} can be expressed as:

$$\text{MDC} = 4.66 \frac{\sqrt{B}}{\varepsilon I_\gamma M \sqrt{T}} \quad (18)$$

(x) Analytical quality control

Reliable results depend on precision (reproducibility) and accuracy (true value) of measurements [91]. Therefore, quality control measurements are necessary to confirm that the analytical results are reliable. The precision can easily be determined by internal measurement. The laboratory should operate a routine quality control programme to maintain reproducible results and make use of quality control charts. Such programmes check important parameters on a regular basis and involve:

- Checking the stability of the detector background;
- Checking the stability of the energy calibration and efficiency calibration;
- Using internal standards which incorporate the use of blind duplicates or triplicates, blanks and standards.
- The determination of accuracy requires more detailed actions [91]:

  - ✓ Analysis with different methods, analysts and techniques;
  - ✓ Control analysis with reference materials which are similar to the analysed materials;
  - ✓ Participation in inter-laboratory comparison exercises.

4.3. Measurements of in situ ^{137}Cs activity by portable gamma detector

^{137}Cs activity can also be easily assessed *in situ*, in the field, without sample collection, using a portable gamma spectrometer (Fig. 15). Counting times for *in situ* measurements are often significantly shorter than for laboratory measurements, and less soil disturbance is needed.

Furthermore, by measuring a larger volume of soil, the results are commonly less affected by small-scale variability. With *in situ* gamma spectrometry, the estimation of the activity must take account of the depth distribution of ^{137}Cs in the soil.

FIG. 15. In situ gamma measurement with IAEA fellows and staff during field experiments in the Mistelbach watershed (Austria).

This can be achieved by using a mathematical model of the expected depth distribution of the radionuclide in the soil or by interpreting the shape of the gamma spectrum [99, 100]. Knowledge of the soil attenuation properties, which depend on soil composition, moisture content and density, is also important, although such information is more important for radionuclides with gamma energies below 100 keV. Land use and soil erosion processes often lead to complexities of the depth distribution, making it difficult to assume a constant depth distribution function [99]. *In situ* gamma spectrometry can also be used to survey large areas in a relatively short time. For example, Mabit et al. [30] found that to obtain an acceptable *in situ* measurement of the ^{137}Cs activity – 6% counting error at 1σ – in the Mistelbach watershed in Austria, where the reference inventory is close to 1900 Bq m^{-2}, counting times of only 3600 s were required, as compared to 10000 s in the laboratory.

5. Data analysis, interpretation and presentation

5.1. Reference sites

Descriptive statistics (mean, standard deviation, coefficient of variation) to summarise the inventory measurements and the ^{137}Cs depth distribution should be established for the reference site. The validation of the estimate of the local ^{137}Cs fallout inventory is a key requirement for obtaining reliable estimates of soil redistribution rates. Several lines of evidence can be used to confirm the suitability of the reference site and the inventory obtained for the site. These include the following:

(a) A clear exponential decrease of ^{137}Cs content with depth should be obtained with 80 to 90% of the ^{137}Cs being found in the upper 20 cm of the soil profile;

(b) The variability of the inventories obtained for the multiple cores collected from the reference site, based on information provided by the descriptive statistics and the test of normality distribution as suggested by Owens et al. [59] and Sutherland [39, 62], should be as low as possible. A low coefficient of variation (CV% < 30%) is a good indicator of a stable and undisturbed reference site;

(c) The number of soil cores required to provide a reliable estimate of the reference inventory within a specified level of confidence can be calculated using a simple statistical function [39, 40, 62]. The minimum number of samples, N, required to estimate the population mean of ^{137}Cs reference inventory with an allowable error of ± 10% at the 95% level of confidence can be calculated using the following formula [62]:

$$N = \left(\frac{t_{(\alpha, n-1)} \cdot CV}{AE} \right)^2 \quad (19)$$

where:

N = the required number of soil samples;
t = the t value of the Student's t-test at 95% confidence ($\alpha = 0.05$);
CV = the coefficient of variation (decimal fraction);
AE = the allowable error (decimal fraction) = 0.1.

For example, the reference ^{137}Cs activity measured for cores from the reference site in the Lennoxville watershed located in Quebec, Canada, some 150 km east of Montreal, (n=9; CV =0.13; Student's value $t_{(0.05, 8)} = 2.31$; AE = 0.1) indicated that at least 9 cores were required to pass this test [73];

(d) The estimated value can also be compared with available estimates based on the annual precipitation and/or the direct yearly fallout data set if available. For example from Fig. 16, it can be seen that the average inventory of 2650 ± 333 Bq m^{-2} measured in the Lennoxville watershed (45°22´N, 71°51´W), is close to what could be expected and estimated from the local annual precipitation. If the estimated value from the yearly average rainfall would have been taken as the reference value, the ^{137}Cs initial fallout would have been overestimated by only 3% [73], which is within the analytical uncertainty.

5.2. Interpretation of the results of studies at the field scale

In a study field the ^{137}Cs inventories (Bq m^{-2}) associated with the sampling points and information on the ^{137}Cs depth profile for representative points (^{137}Cs concentration in Bq kg^{-1}vs. the soil depth in cm) should be documented. Inventories are calculated from the ^{137}Cs concentrations. Comparison of the inventories measured for the sampling points in the study field with that for the reference site allows eroding and depositional zones to be identified. The ^{137}Cs data thus provide a preliminary indication of the pattern of soil redistribution in relation to topography, land use and soil proprieties. The documentation of ^{137}Cs depth profiles associated with eroding or depositional points in cultivated and/or uncultivated fields provides confirmation of the likely validity of the bulk core measurements. The uncertainty associated with the values of the ^{137}Cs inventory will reflect the measurement uncertainty associated with the gamma spectrometry measurements as well as the variability introduced by the field sampling (see [40]).

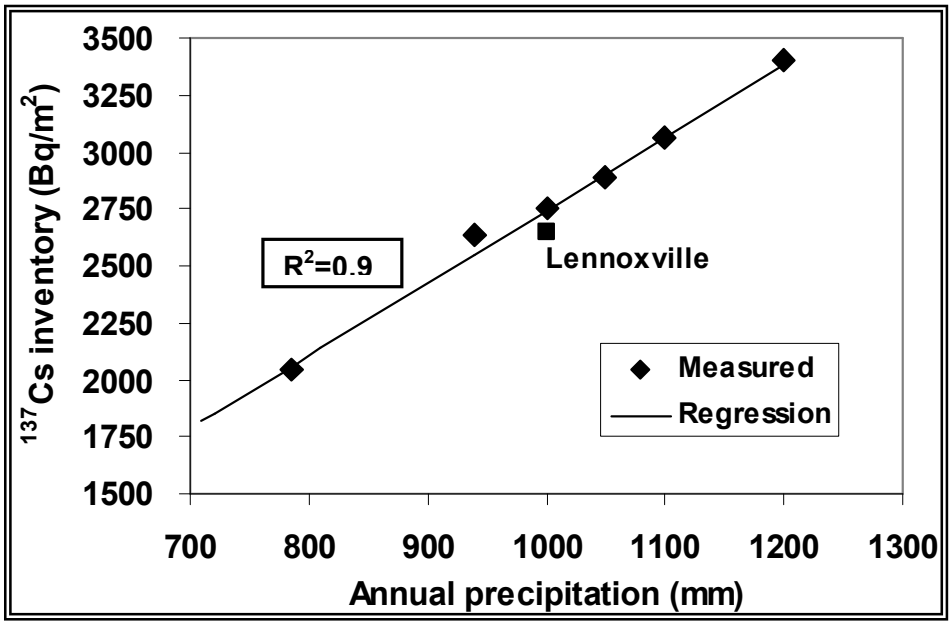

FIG. 16. The relationship between annual precipitation and the ^{137}Cs total inventory developed for eastern Canada [73].

Soil erosion or deposition rates for each sampling point are quantified using theoretical conversion models to convert the total activity of ^{137}Cs, i.e. the inventory (Bq m^{-2}), to erosion and/or deposition rates (t ha^{-1} yr^{-1}). Such models have been formulated for both cultivated and uncultivated soils and range from simple models (Proportional, Mass Balance I, Profile distribution models) to more complex models (Mass Balance II, Mass Balance III, Diffusion and Migration Models). One of the developed models, Mass Balance III, can distinguish and quantify both water erosion and tillage erosion. The Paper 5 of this TECDOC is devoted to this important aspect and shows how to estimate soil erosion and deposition rates using different models.

The data on soil redistribution rates obtained by FRNs from a study field can be presented with the aid of the following parameters [31, 101]:

- *Mean erosion in the eroding zone of the field:* the total mass of eroded soil divided by the area of the field affected by erosion;
- *Gross erosion of the whole field:* the total mass of eroded soil divided by the total area of the field;
- *Mean deposition in the depositional zone:* the total mass of deposited soil divided by the area of the field where deposition occurs;
- *Gross deposition in the whole field:* the total mass of deposited soil divided by the total area of the field;
- *Net erosion:* the amount of soil leaving the field representing the gross erosion minus the gross deposition;
- *Sediment delivery ratio:* the net erosion divided by the gross erosion.

An example of such calculations from a grid sampling programme, where each grid point is assumed to represent an equal area of the field, is given below.

$$\text{Eroding area} = T\frac{N_e}{N_t} \tag{20}$$

$$\text{Depositional area} = T\frac{N_d}{N_t} \quad (21)$$

$$\text{Mean erosion} = \frac{E}{N_e} \quad (22)$$

$$\text{Gross erosion} = \frac{E}{N_t} \quad (23)$$

$$\text{Mean deposition} = \frac{D}{N_d} \quad (24)$$

$$\text{Gross deposition} = \frac{D}{N_t} \quad (25)$$

$$\text{Net erosion} = \frac{E-D}{N_t} \quad (26)$$

$$\text{Sediment delivery ratio} = \frac{E-D}{E} \quad (27)$$

where:

T = Total area;
N_t = Total number of grid points;
N_e = Number of eroded points;
N_d = Number of points;
E = Sum of erosion estimates;
D = Sum of deposition estimates.

In order to distinguish between the soil redistribution processes, the erosion rates are commonly presented as negative values and the deposition rates as positive values. From data obtained on soil erosion and deposition rates, spatial variability in the soil redistribution rates can be represented. If a transect sampling is adopted, the variation can be represented by plotting a curve of soil redistribution rate (t ha^{-1} yr^{-1}) against the distance from the hilltop (m). When grid or multiple transect sampling is adopted, the spatial distribution of ^{137}Cs or soil redistribution rate can be mapped using data spatialisation tools. To understand better and explain the variations of the ^{137}Cs distribution and the related soil redistribution rate, it may prove useful to measure some key soil properties (e.g. soil texture, $CaCO_3$, pH, N, C, P, CEC and soil organic matter) [79].

A high erosion rate, indicated by a low ^{137}Cs inventory, is usually associated with a low level of soil organic matter (SOM). On the other hand, depositional areas show an accumulation of SOM. Several authors working under different environments have reported such results [2, 102-107]. This confirms that the physical degradation of soils through erosion is linked with a biochemical degradation that may decrease their productivity in the medium- to long-term. However, the interpretation of these parameters should be undertaken with care. Their differentiation may reflect controls other than soil redistribution, for example topographic position which effects soil development. Also, lower moisture availability on slopes can result in slower accumulation of soil organic matter so that the A horizons on the slopes are thinner and have a lower organic matter content than plateau areas or valley bottoms even before the onset of erosion and soil redistribution.

5.3. Interpretation of the results of studies at the watershed scale

Based on the sampling strategies used at the watershed scale, the net erosion of an entire watershed sampled using the isosector and the representative field concepts can be calculated using the following formula (adapted from [34]):

$$E_w = \left(\sum_{i=1}^{n} S_i . E_i \right) \Big/ S_{tot} \quad (28)$$

where:

E_w = Net erosion for the entire watershed or area (t^{-1} ha^{-1} yr^{-1});
n = Isosector number;
S_{tot} = Surface of the entire watershed or area (ha);
E_i = Average net erosion of the representative field(s) of the isosector $_i$ (t^{-1} ha^{-1} yr^{-1}).

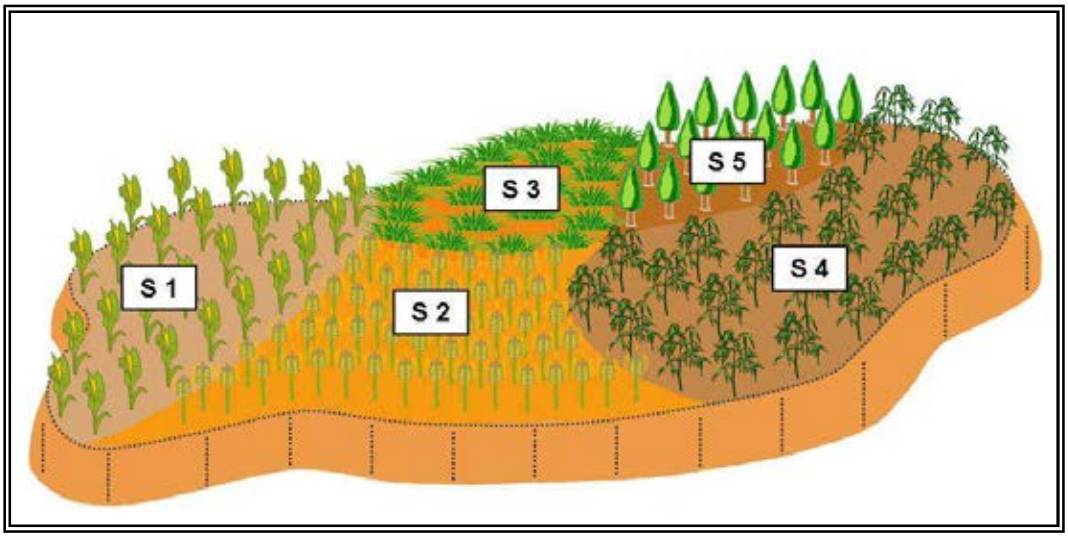

FIG. 17. A schematic watershed divided into 5 isosectors based on the land use.

For example, the E_w of the schematic watershed divided into 5 different isosectors presented in Fig. 17 can be evaluated according to the following:

$$E_w = [(S_1.E_1) + (S_2.E_2) + (S_3.E_3) + (S_4.E_4) + (S_5.E_5)] / (S_{tot}) \quad (29)$$

$$S_{tot} = S_1+S_2+S_3+S_4+S_5 \quad (30)$$

where:

$E_{1\text{-}5}$ = Net erosion for the isosectors numbered 1 to 5 (t^{-1} ha^{-1} yr^{-1});
$S_{1\text{-}5}$ = Surface area of the isosectors numbered 1 to 5 (ha).

With this approach the overall production of sediment (net erosion) from each isosector and then for the watershed can be provided.

5.4. Data spatialisation and soil redistribution mapping

The final step of the soil redistribution assessment by the ^{137}Cs method is the interpolation of data representing soil redistribution rates at sampled points and creation of a soil redistribution map. Production of a soil redistribution map requires a special statistical approach which can describe the spatial variability of soil redistribution. The accuracy of the resulting soil redistribution map depends on the number and the spatial distribution of the samples (e.g. transects, regular grid) [63]. Geostatistical approaches, in conjunction with variography, can assist with this task.

(i) Geostatistics and the variography concept

Soil parameters are not distributed randomly in the landscape; there is a spatial correlation that can explain their spatial distribution [108-110]. Soil redistribution rates estimated from ^{137}Cs inventories also follow this rule [111-113]. To represent this spatial correlation of variables, called the structure, geostatistical analysis can be undertaken using one specific tool, the variogram. Geostatistical methods provide a set of statistical tools for incorporating the spatial and temporal coordinates of observations in data processing [114 -116]. They are largely based on the concept of random function, and soil properties are regarded as a set of spatially-dependent random variables.

Geostatistical approaches enable the values of properties at unsampled places to be estimated from sparse sample data [117]. Geostatistical analysis has been used at the field scale and also at larger scales (areas of several square kilometres) for soil mapping and mapping of particular soil properties, especially the nutrient distribution and fertilizer demands [118].

The semivariogram and the variogram are the basic tools for the analysis of spatial structure. Structural analysis involves description and modelling of the estimated variogram. The variogram is a mathematical description of the relationship (structure) between the variance of pairs of observations (data points) and the distance separating these observations (h). It describes the between-population variance within a distance class (y-axis) according to the geographical distance between pairs of populations (x-axis) (Fig. 18).

The fitted curve minimizes the variance of the errors. The variogram model is used to define the weights of the Kriging function [111, 119] and the semivariance is an autocorrelation statistic defined as:

$$\gamma(h) = \frac{1}{2N(h)} \sum_{i=1}^{N(h)} \{Z(x_i)\ Z(x_i + h)\}^2 \qquad (31)$$

where:

$\gamma(h)$ = Semivariance for interval distance class or lag interval h;
$N(h)$ = Total number of sample couples or pairs of observations separated by a distance h;
$Z(x_i)$ = Measured sample value at point i;
$Z(x_i+h)$ = Measured sample value at point i+h.

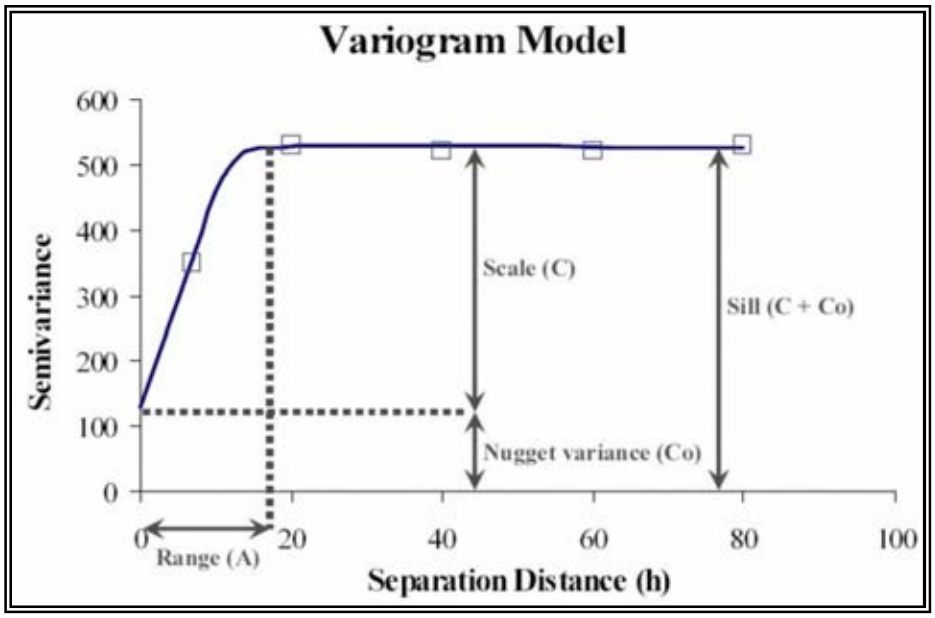

FIG. 18. Variogram parameters [120].

The variographic model can be described through different parameters (Fig. 18): the sill (C + Co), the nugget variance (Co), the scale (C) and the range (A). The sill corresponds to the model asymptote (scale and the nugget variance) and should be equal to the variance of the data set. The nugget variance represents they intercept for γ when h = 0. It is a non-zero value produced by various sources of unexplained error (e.g. measurement error, sampling error, inter-sample error and unexplained and inherent variability) for γ when h = 0. It represents an indication of short distance variation. The range is the value of h at which y attains the maximum value where the sill occurs and so represents the separation distance over which no more spatial dependence is apparent.

To build a 'reliable' variogram, different steps have to be followed. Different lag distances have to be tested until a sufficient number of pairs to represent the model are found. Four representative groups of pairs are enough to represent a relevant variogram with a significant coefficient of correlation (r^2) and a good nugget/sill ratio [112, 121].

The effective lag distance cannot be more than half of the maximum distance between data. Directional dependence has to be tested in the spatial autocorrelation. The isotrope (no directional dependence) or an isotrope (directional dependence) characteristic of the variogram has to be determined. If no anisotropy is found, it means that the value of the variable varies similarly in all directions and the semivariance depends only on the distance between sampling points [122, 123].

There are several types of models: unbounded such as the linear, gaussian, and exponential models or bounded such as the spherical model (Fig. 19).

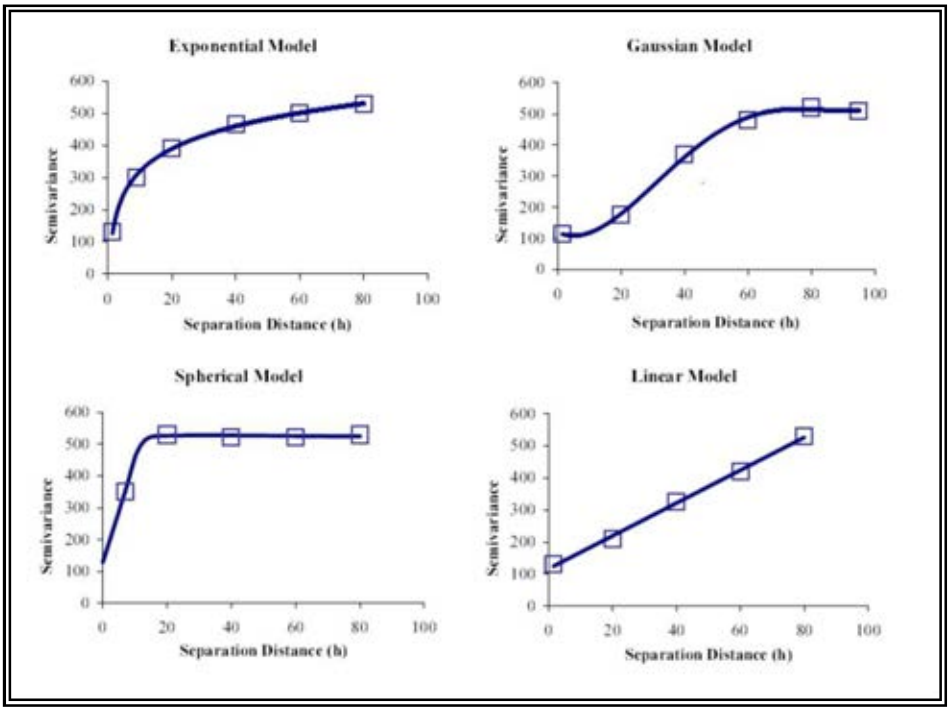

FIG. 19. Different variogram model forms [120].

The best variogram model (spherical, linear, etc.) and its parameters (nugget, sill, scale, range, etc.) have to be determined to validate the modelling of the spatial autocorrelation through the variogram's parameter optimisation. Two major indicators can be used: the coefficient of correlation (indication of how well the model fits the variogram data) and the scale to sill ratio (C/(C+Co)) which should approach 1. It means that Co (the nugget) should approach zero. Some authors also use the nugget to sill ratio (Co/(Co+C)), which should approach 0. If the 'nugget-to-sill' ratio is less than 25%, then the variable can be considered to have a strong spatial dependence. If this ratio is between 25 and 75%, the spatial dependence will be considered as moderate and if the ratio equals or exceeds 75%, then the spatial dependence will be considered as weak [124]. Some software like GS^+ [125] takes into account the distance between the group of pairs and the fitted model called the Residual Sums of Squares (RSS). The RSS is very useful as it allows the comparison of the different tested variograms.

To summarise, the numbers of pairs at each lag distance have to be ideally greater than 30, the coefficient of correlation (r^2) should be greater than 0.8 and the scale to sill ratio should approach 1, meaning that the nugget variance has to be as close as possible to the origin. Obviously, the variogram with the best RSS reduction has to be selected to represent the auto correlation between the data [120].

(ii) Data interpolation and map editing

Using two-dimensional space, the spatial structure of a variable (in our case, soil redistribution magnitude) can be visualized by maps. In order to produce maps, we need to interpolate the values at unsampled locations. In geostatistics, if there is a spatial correlation between the data, this prediction method is called 'Kriging'. Kriging is a method of interpolation named after a South African mining engineer, D.G. Krige, who developed the technique in an attempt to predict more accurately gold reserves in the early 1960s. Over the past several decades, Kriging has become a fundamental tool in the field of geostatistics. Kriging is based on the assumption that the parameter being interpolated can be considered as

a localized variable, the "regionalised variable theory" [126]. Kriging interpolation provides an optimal interpolation estimate for a given coordinate location and to obtain interpolations from observed values and their spatial relationships, as inferred from the variography [115, 116, 127]. Kriging uses nearby points weighted by distance from the interpolate location and the degree of autocorrelation or spatial structure for those distances, and calculates optimum weights at each sampling distance [128]. The Ordinary Kriging (OK) is an estimation technique known as the Best Linear Unbiased Estimator (BLUE) that has the great advantage of using the semivariogram information [114].

Other interpolation techniques (e.g. Inverse Distance Weighting (IDW), triangulation with linear interpolation, etc.) are fast and sometimes more 'user-friendly', but they do not take the spatial correlation of data into consideration and therefore oversimplify the reality. The IDW also called '*Inverse Distance to a Power'* is a weighted average interpolator which assigns more weight to nearby samples for estimating the attributes of the variable at unsampled places. Therefore, the weights are inversely proportional to a power of the distance. IDW behaves as an exact interpolator. The weights assigned to the data points are fractions with the sum of all the weights being equal to 1. Value of the power is frequently set to 2 [128]. As opposed to these deterministic data interpolation methods, Kriging is based on spatial correlation among the variables, as empirically tested and modelled from sample data. It also aims at minimizing the error variance, and provides an indication of the uncertainty of the estimate [129].

(a) *Software*: Geostatistical and spatial correlation analysis of soil redistribution can be performed directly with various GIS softwares, but in such cases there is a risk of not controlling all steps to build an accurate variogram. To avoid this, a preliminary software package to perform the variography steps e.g. GS^+ software [125] can be used, and the resulting variographic parameters and the fitted model can be introduced into a spatialisation software like Surfer 8.00 [130]. Semi-variance analysis can be performed using spatial modelling and interpolation techniques (OK, IDW power 1 and 2 to develop overlay maps. Cross validation should then be used to compare the prediction performances of the different interpolation methods. On the basis of the resulting map and the soil redistribution isolines, a sediment budget can be produced for the different interpolation algorithms. An example of a resulting map of the soil redistribution rates using OK is shown in Fig. 20;

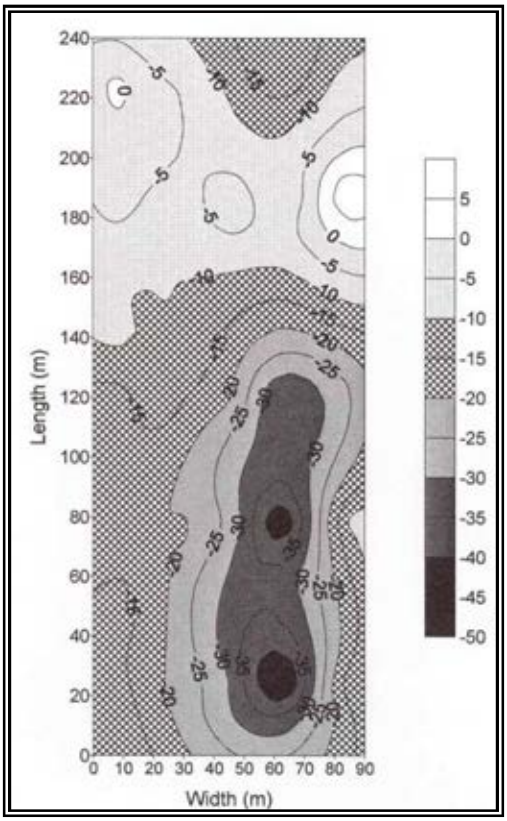

FIG. 20. Example of a soil redistribution map (t ha^{-1} yr^{-1}) created using Ordinary Kriging [2].

(b) *Validation of interpolation methods to map soil redistribution magnitude using variographic information*: Cross-validation analysis can be used for evaluating effective parameters for OK and IDW interpolations and to compare the different estimation techniques to determine the best approach for the precision of the predicted data. In cross-validation, each measured point in a spatial domain is individually removed from the domain and its value is estimated by Kriging and compared to the actual value, as though it were never there [125]. For an acceptable cross validation, the regression coefficient or the slope that measures the goodness of fit for the least squares model describing the linear regression equation needs to be as close as possible to 1. In the case of spatial structure, the r^2 (proportion of variation explained by the best-fit line) will be greater than 0.2. In general, Kriging is the best interpolation algorithm and provides the best predictor. Cross-validation analysis has shown that in the case of spatially structured data, OK is a better interpolation method than IDW1 or IDW2 for the assessment of unknown value in soil [120, 131 - 133]. For stable soil properties using cross validation procedure, OK performed best and Lognormal Ordinary Kriging could provide the best results when the parameter had a coefficient of skewness larger than 1.

To summarise, a simple protocol to spatialise variables can be applied to soil parameters, FRNs and resulting soil redistribution magnitudes (Fig. 21). Depending on the presence of a spatial structure and the information provided by the key parameters of the variogram, different interpolation methodologies can be adopted [120]. To take into account the spatial autocorrelation of the data, as documented in the literature, Kriging may be used. In the case of weak or absent spatial structure, the use of classical methods of interpolation (e.g. triangulation, IDW, etc.) is recommended [120]. In order to give some baseline values or

guidelines, it can be considered that the spatial dependence is weak if the coefficient of correlation (r^2) is less than 0.8 and if the 'nugget-to-sill' ratio is greater than 25%.

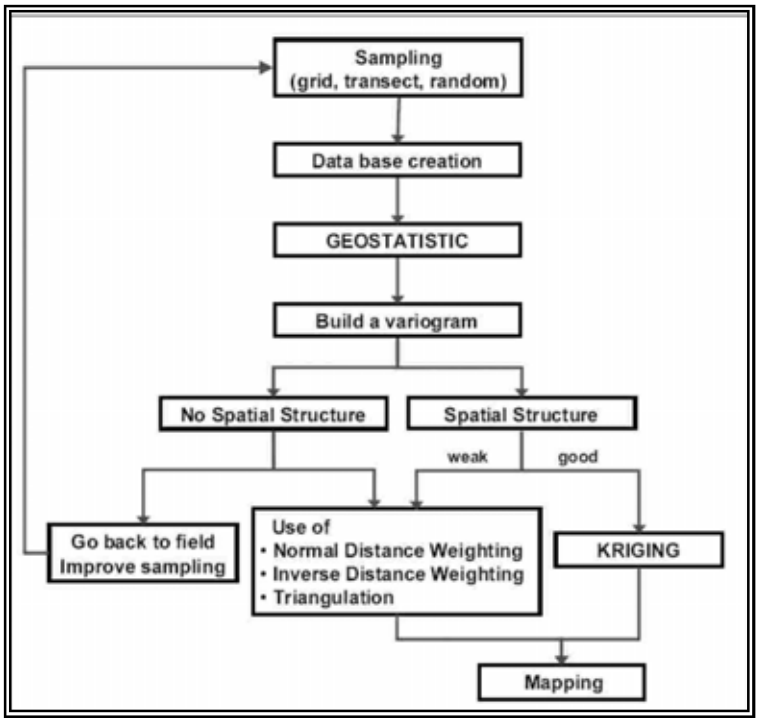

FIG. 21. Protocol for using a spatialisation approach [120].

Studies involving soil sampling following a regular grid are generally limited to a few hectares. Processing of areas larger than 1 km^2 with a similar approach would be too costly. A balance must then be reached between the scientific goals and the resource limitations. An oriented survey with geostatistics, depending on topographic variability, could then be a more appropriate approach for a soil spatial redistribution assessment.

REFERENCES

[1] BERNARD, C., MABIT L., WICHEREK, S., LAVERDIÈRE, M.R., Long-term soil redistribution in a small French watershed as estimated from ^{137}Cs data, J. Environ. Qual. 27 (1998) 1178–1183.

[2] MABIT, L., BERNARD, C., MAKHLOUF, M., LAVERDIÈRE M.R., Spatial variability of erosion and soil organic matter content estimated from ^{137}Cs measurements and geostatistics, Geoderma 145 (2008) 245–251.

[3] MABIT, L., FULAJTAR, E., "The use of ^{137}Cs to assess soil erosion and sedimentation processes: advantages and limitations", Book of the Extended Synopses of the International Conference on Environmental Radioactivity: From Measurements and Assessments to Regulation, IAEA-CN-145, IAEA, Vienna (2007) 338–339.

[4] RITCHIE, J.C., RITCHIE, C.A., Bibliography of publications of ^{137}Cs studies related to erosion and sediment deposition. Website (2008) http://www.ars.usda.gov/Main/docs.htm?docid=17939

[5] WALLING, D.E., "Use of ^{137}Cs and other fallout radionuclides in soil erosion investigations: Progress, problems and prospects", Use of ^{137}Cs in the Study of Soil Erosion and Sedimentation, IAEA-TECDOC-1028, IAEA, Vienna (1998) 39–64.
[6] WALLING, D.E., QUINE, T.A., "The use of fallout radionuclides in soil erosion investigations", Nuclear Techniques in Soil-Plant Studies for Sustainable Agriculture and Environmental Preservation,ST1/PUB/947, IAEA, Vienna (1995).
[7] ZAPATA, F. (Ed.), Handbook for the Assessment of Soil Erosion and Sedimentation using Environmental Radionuclides, Kluwer, Dordrecht, The Netherlands (2002) 219.
[8] RITCHIE, J.C., McHENRY, J.R., Application of radioactive fallout cesium-137 for measuring soil erosion and sediment accumulation rates and patterns: a review, J. Environ. Qual. 19 (1990) 215–233.
[9] WALLING, D.E, HE, Q., Use of fallout ^{137}Cs in investigations of overbank sediment deposition on river floodplains, Catena 29 (1997) 263–82.
[10] CARTER, M.W., MOGHISSI, A.A., Three decades of nuclear testing, Health Phys. 33 (1977) 55–71.
[11] BERNARD, C., MABIT, L., LAVERDIÈRE, M.R., WICHEREK, S., Césium-137 et érosion des sols, Cahiers Agricultures 7 (1998) 179–186.
[12] SUTHERLAND, R.A., DE JONG, E., "Quantification of soil redistribution in cultivated fields using caesium-137, Outlook, Saskatchewan, Canada", Soil Erosion- Experiments and Models (BRYAN, R.B., Ed.), Catena . 17 (1990) 177–193.
[13] DAVIS, J.J., "Cesium and its relationship to potassium in ecology", Radioecology (SCHULTZ, V., KLEMENT, A.W. Jr., Eds), Reinhold, New York (1963) 539–556.
[14] GARCIA AGUDO, E., Global distribution of ^{137}Cs inputs for soil erosion and sediment studies, IAEA-TECDOC-1028, IAEA, Vienna (1998) 117–121.
[15] UNSCEAR, "Radio-active contamination of the environment by nuclear tests", Rep. Suppl. 13 (A/7163),United Nations Scientific Committee on the Effects of Atomic Radiation, General Assembly, 24thSession, United Nations, New York (1969) 3–4.
[16] WALLING, D.E., "Recent advances in the use of environmental radionuclides in soil erosion investigations", Nuclear Techniques in Integrated Plant Nutrients, Water and Soil Management, Proc. Int. Symp., IAEA-CSP-11/C (2002) 279–301.
[17] ANSPAUGH, L.R., CATLIN, R.J., GOLDMAN, M., The global impact of the Chernobyl reactor accident, Science 242 (1988) 1513–1518.
[18] CAMBRAY, R.S., et al., Observations on radioactivity from the Chernobyl accident, Nucl. Energy 26 (1987) 77–101.
[19] MABIT, L., BERNARD, C., WICHEREK, S., LAVERDIÈRE, M.R.,"Les retombées de Tchernobyl, une réalité à prendre en compte lors de l'utilisation de la méthode du Césium-137", Paysages Agraires et Environnement. Principes Écologiques de Gestion en Europe et au Canada, CNRS (1999) 285–292.
[20] WORLD HEALTH ORGANIZATION, Updated background information on the nuclear reactor accident in Chernobyl, USSR, Summary Report of Measurement Results Relevant for Dose Assessment, Updated Revision No. 7, Copenhagen (1986).
[21] GOLOSOV, V.N., PANIN, A.V., MARKELOV, M.V., Chernobyl ^{137}Cs redistribution in the small basin of the Lokna River, Central Russia, Phys. Chem. Earth, Part A: Solid Earth and Geodesy 24 (1999) 881–885.
[22] EYMAN, L.D., KEVERN, N.R., Cesium-137 and stable cesium in a hypereutrophic lake, Health Phys. 28 (1975) 549–555.
[23] LOMENICK, T.F., TAMURA, T., Naturally occurring fixation of cesium-137 on sediments of lacustrine origin, Proc, Soil Sci. Soc. Am. 29 (1965) 383–387.
[24] DAHLMAN, R.C., FRANCIS, C.W., TAMURA, T., "Radiocesium cycling in vegetation and soil", Mineral Cycling in Southeastern Ecosystems, USAEC Symposium

Series, CONF-740513(HOWELL, F.G., GENTRY, J.B., SMITH, M.H., Eds), US Atomic Energy Commission, Washington, DC (1975) 462–481.
[25] ROGOWSKI, A.S., TAMURA, T., Environmental mobility of cesium-137, Radiat. Bot. 10 (1970) 35–45.
[26] ROGOWSKI, A.S., TAMURA, T., Erosional behaviour of cesium-137, Health Phys. 18 (1970) 467–477.
[27] HE, Q., WALLING, D.E., The distribution of fallout ^{137}Cs and ^{210}Pb in undisturbed and cultivated soils, Appl. Radiat. Isot. 48 (1997) 677–690.
[28] MABIT, L., Estimation de l'érosion hydrique des sols par la méthode du ^{137}Cs. Application aux bassins versants de Vierzy (France) et Lennoxville (Québec). Thèse de doctorat de géographie physique, Paris I Panthéon-Sorbonne (1999) 257.
[29] BENMANSOUR, M., et al., "Estimates of long and short term soil erosion rates on farmland in semi-arid West Morocco using caesium-137, excess lead-210 and beryllium-7 measurements", Impact of Soil Conservation Measures on Erosion Control and Soil Quality, IAEA-TECDOC-1665, IAEA, Vienna (2011) 159–174.
[30] MABIT, L., BENMANSOUR, M., WALLING D.E., Comparative advantages and limitations of fallout radionuclides (^{137}Cs, ^{210}Pb and ^{7}Be) to assess soil erosion and sedimentation, J. Environ. Radioact. 99 (2008) 1799–1807.
[31] WALLING, D.E., QUINE, T., Use of Caesium-137 as a Tracer of Erosion and Sedimentation: Handbook for the Application of the Caesium-137 Technique, Department of Geography, University of Exeter (1993) 196.
[32] WALLING, D.E., HE, Q., APPLEBY, P.G., "Conversion models for use in soil-erosion, soil-redistribution and sedimentation investigations", Handbook for the Assessment of Soil Erosion and Sedimentation using Environmental Radionuclides (ZAPATA, F., Ed.), Kluwer, Dordrecht, The Netherlands (2003) 111–164.
[33] SCHULLER, P., WALLING, D.E., SEPÚLVEDA, A., CASTILLO, A., PINO, I., Changes in soil erosion associated with the shift from conventional tillage to a no-tillage system, documented using ^{137}Cs measurements, Soil Till. Res. 94 (2007) 183–192.
[34] MABIT, L., BERNARD, C., LAVERDIÈRE, M.R., Assessment of erosion in the Boyer River watershed (Canada) using a GIS oriented sampling strategy and ^{137}Cs measurements, Catena 71 (2007) 242–249.
[35] ZUPANC, V., MABIT, L., Nuclear techniques support to assess erosion and sedimentation processes: preliminary results of the use of ^{137}Cs as soil tracer in Slovenia, Dela 33 (2010) 21−36.
[36] LOBB, D.A., KACHANOSKI, R.G., Modelling tillage erosion in the topographically complex landscapes of southwestern Ontario, Canada, Soil Till. Res. 51 (1999) 261–277.
[37] LOUGHRAN, R.J., BALOG, R.M., Re-sampling for soil-caesium-137 to assess soil losses after a 19-year interval in a Hunter Valley vineyard, New South Wales, Australia, Aust. Geogr. Stud. 44 (2006) 77–86.
[38] TIESSEN, K.H.D., et al., Using repeated measurements of ^{137}Cs and modelling to identify spatial patterns of tillage and water erosion within potato production in Atlantic Canada, Geoderma 153 (2009)104–118.
[39] SUTHERLAND, R.A., Caesium-137 soil sampling and inventory variability in reference samples; A literature survey, Hydrol. Process. 10 (1996) 43–53.
[40] OWENS, P.N., WALLING, D.E., Spatial variability of caesium-137 inventories at reference sites. An example from two contrasting sites in England and Zimbabwe, Appl. Radiat. Isot. 47 (1996) 699–707.
[41] PENNOCK, D.J., APPLEBY, P.G., "Site selection and sampling design", Handbook for the Assessment of Soil Erosion and Sedimentation using Environmental Radionuclides (Zapata, F., Ed.), Kluwer, Dordrecht, The Netherlands (2002) 15–40.

[42] EBERHARDT, L.L., THOMAS, J.M., Designing environmental field studies, Ecol. Monogr. 61 (1991) 53–73.
[43] BASHER, L.R., Surface erosion assessment using ^{137}Cs: examples from New Zealand, Acta Geol. Hispan. 35 (2000) 219–228.
[44] FULAJTAR, E., Assessment of soil erosion on arable land using the ^{137}Cs measurements: a case study from Jaslovské Bohunice, Slovakia, Soil Till. Res. 69 (2003) 139–152.
[45] MONTGOMERY, J.A., BUSACCA, A.J., FRAZIER, B.E., MCCOOL, D.K., Evaluating soil movement using cesium-137 and the revised universal soil loss equation, Soil Sci. Soc. Am. J. 61 (1997) 571–579.
[46] PENNOCK, D.J., DE JONG, E., Spatial pattern of soil redistribution in Boroll landscapes, Southern Saskatchewan, Can. J. Soil Sci. 150 (1990) 867–873.
[47] SOGON, S., PENVEN, M.J., BONTE, P., MUXART, T., Estimation of sediment yield and soil loss using suspended sediment load and ^{137}Cs measurements on agricultural land, Brie Plateau, France, Hydrobiologia 410 (1999) 251–261.
[48] PENNOCK, D.J., LEMMEN, D.S., DE JONG, E., Cesium-137 measured erosion rates for soils of five parent material groups in south western Saskatchewan, Can. J. Soil Sci.75 (1995) 205–210.
[49] FORSYTH, T.J., The use of cesium-137 measurements of soil erosion and farmers perceptions to indicate land degradation amongst shifting cultivators in northern Thailand, Mount. Res. Develop. 14 (1994) 229–244.
[50] LU, X.X., HIGGIT, D.L., Estimating erosion rates on sloping agricultural land in the Yangtze Three Gorges, China, from caesium-137 measurements, Catena 39 (2000) 33–51.
[51] ANDERSON, J.M., INGRAM, J.S.I., Tropical Soil Biology and Fertility. A Handbook of Methods, CAB International, Wallingford (1993).
[52] WALLBRINK, P.J., RODDY, B.P., OLLEY, J.M., A tracer budget quantifying soil redistribution on hillslopes after forest harvesting, Catena 47 (2002) 179-201.
[53] MABIT, L., BERNARD, C., WICHEREK, S., LAVERDIÈRE, M.R., "Vertical redistribution of radio-caesium (^{137}Cs) in an undisturbed organic soil of northeastern France", Applied Geomorphology, Theory and Practice (ALLISON, R.J., Ed.), John Wiley & Sons, UK (2002) 197–203.
[54] GOLOSOV, V.N., "Special consideration for areas affected by Chernobyl fallout", Handbook for the Assessment of Soil Erosion and Sedimentation using Environmental Radionuclides (ZAPATA, F., Ed.), Kluwer, Dordrecht, The Netherlands (2002) 165–183.
[55] FROEHLICH, W., HIGGITT, D.L., WALLING, D.E., "The use of cesium-137 to investigate soil erosion and sediment delivery from cultivated slopes in the Polish Carpathians", Farmland Erosion (WICHEREK, S., Ed.), Elsevier, Amsterdam (1993) 271–283.
[56] CAMBRAY, R.S., PLAYFORD, K., LEWIS, G.N.J., "Radioactive fallout in air and rain: results to the end of 1982", Rep. AERE-R-10859, U.K. Atomic Energy Authority, Harwell, UK (1983).
[57] CAMBRAY, R.S., PLAYFORD, K., LEWIS, G.N.J., "Radioactive fallout in air and rain: results to the end of 1984", Rep. AERE-R-11915, U.K. Atomic Energy Authority, Harwell, UK (1985).
[58] CAMBRAY, R.S., PLAYFORD, K., CARPENTER, R.C., "Radioactive fallout in air and rain: results to the end of 1988", Rep. AERE-R-10155, U.K. Atomic Energy Authority, Harwell, UK (1989).
[59] OWENS, P.N., WALLING, D.E., HE, Q., The behaviour of bomb-derived Caesium-137 fallout in catchment soils, J. Environ. Radioact. 32 (1996)169–191.

[60] WALLBRINK, P.J., MURRAY, A.S., OLLEY, J.M., Relating suspended sediment to its original soil depth using fallout radionuclides, Soil Sci. Soc. Am. J. 63 (1999) 369–378.
[61] PENNOCK, D.J., Suitability of ^{137}Cs redistribution as an indicator of soil quality, Acta Geol. Hisp. 35 (2000) 213–217.
[62] SUTHERLAND, R.A., Examination of caesium-137 areal activities in control (uneroded) locations, Soil Technol. 4 (1991) 33–50.
[63] MABIT, L., BERNARD, C., LAVERDIÈRE, M.R., "Influence of the sampling strategy on soil loss assessments from ^{137}Cs measurements", Man and Soil at the Third Millenium (RUBIO, J.L., MORGAN, R.P.C., ASINS, S., ANDREU, V., Eds), Geoforma Ediciones, Logroño, Spain (2002) 2083–2090.
[64] CAMPBELL, B.L., LOUGHRAN, R.J., ELLIOTT, G.L., SHELLY, D.J., "Mapping drainage basin sediment sources using caesium-137". Drainage Basin Sediment Delivery, International Association of Hydrological Sciences Publication No. 159 (1986) 437–446.
[65] MORRIS, C.D., LOUGHRAN, R.J., Distribution of caesium-137 in soils across a hillslope hollow, Hydrol. Process. 8 (1994) 531–541.
[66] QUINE, T.A., WALLING, D.E., "Use of Caesium-137 measurements to investigate relationships between erosion rates and topography", Landscape Sensitivity (THOMAS, D.S.G., ALLISON, R.J., Eds), John Wiley & Sons Ltd, Chichester (1993) 31−48.
[67] SOILEAU, J.M., HAJEK, B.F., TOUCHTON, J.T., Soil erosion and deposition evidence in a small watershed using cesium-137, Soil Sci. Soc. Am. J. 54 (1990) 1712–1719.
[68] PENNOCK, D.J., DE JONG, E., The influence of slope curvature on soil erosion and deposition in hummock terrain, Soil Sci. 144 (1987) 209–217.
[69] LONGMORE, M.E., O'LEARY, B.M., ROSE, C.W., CHANDICA, A.L., Mapping soil erosion and accumulation with the fallout isotope Caesium-137, Aust. J. Soil Res. 21 (1983) 373–385.
[70] HIGGITT, D.L., WALLING, D.E., "The value of caesium-137 measurements for estimating soil erosion and sediment delivery in an agricultural catchment, Avon, UK", Farm Land Erosion in Temperate Plains Environment and Hills (WICHEREK, S., Ed.), Elsevier, Amsterdam, The Netherlands (1993) 301–315.
[71] MABIT, L., BERNARD, C., LAVERDIÈRE, MR., WICHEREK, S., Assessment of soil erosion in a small agricultural basin of the St. Lawrence River watershed, Hydrobiologia 410 (1999) 263–268.
[72] WALLING, D.E., BRADLEY, S.B., WILKINSON, C.J., "A caesium-137 budget approach to the investigation of sediment delivery from a small agricultural drainage basin in Devon, UK", Drainage Basin Sediment Delivery, IAHS Publication No.159 (1986) 423–435.
[73] MABIT, L., BERNARD, C., LAVERDIÈRE, M.R., Quantification of soil redistribution and sediment budget in a Canadian watershed from fallout caesium-137 (^{137}Cs) data, Can. J. Soil Sci. 82 (2002) 423–431.
[74] HIGGITT, D.L., "The development and application of Caesium-137 measurements in erosion investigations", Sediment and Water Quality in River Catchments (FOSTER, I., GURNELL, A., WEBB, B., Eds), John Wiley & Sons, Chichester (1995) 287–305.
[75] WALLBRINK, P.J, WALLING, D.E, HE, Q., "Radionuclide measurement using HPGe Gamma Spectrometry", Handbook for the Assessment of Soil Erosion and Sedimentation using Environmental Radionuclides (ZAPATA, F., Ed.), Kluwer, Dordrecht, The Netherlands (2002) 67–95.
[76] LAFOND, J., Surface and subsurface soil sampling with a hydraulic impact hammer. Can. J. Soil Sci. 85 (2005) 693–697.

[77] CAMPBELL, B.L., LOUGHRAN, R.J., ELLIOTT, G.L., "A method for determining sediment budgets using caesium-137", International Association of Hydrological Sciences Publication No. 174 (1988) 171–179.
[78] LOUGHRAN, R.J., CAMPBELL, B.L., SHELLY, D.L., ELLIOT, G.L., Developing a sediment budget for a small drainage basin in Australia, Hydrol. Process. 6 (1992) 145–158.
[79] LOUGHRAN, R.J., PENNOCK, D.J., WALLING, D.E., "Spatial distribution of caesium-137", Handbook for the Assessment of Soil Erosion and Sedimentation using Environmental Radionuclides (ZAPATA, F., Ed.), Kluwer, Dordrecht, The Netherlands (2002) 97–109.
[80] BATES, T.E., "Soil handling and preparation", Soil Sampling and Methods of Analysis, (CARTER, M.R., Ed.), Lewis Publishers, Boca Raton (1993) 19–24.
[81] AUERSWALD, K., SCHIMMACK, W., Element-pool balances in soils containing rock fragments, Catena 40 (2000) 279–290.
[82] KNOLL, G.F., Radiation Detection and Measurements, 3rd ed, Wiley & Sons, New York (1999) 365.
[83] CANBERRA, Website (2010) http://www.Canberra.com
[84] ORTEC, Website (2010) http://ortec-online.com
[85] AMERSHAM, Website (2010) http://www6.gelifesciences.com
[86] THE NATIONAL INSTITUTE OF STANDARDS AND TECHNOLOGY, web site (2010) http://www.nist.gov/index.html
[87] GRAY, P.W., AHMAD, A., Linear classes of Ge(Li) detector efficiency functions, Nucl. Instrum. Methods Phys. Res., Sect.A, 237 (1985) 577−589.
[88] JÄCKEL, B., WESTMEIER, W., PATZELT, P., On the photopeak efficiency of germanium gamma-ray detectors, Nucl. Instrum. Methods Phys. Res., Sect. A 261 (1987) 543–548.
[89] MCNELLES, L.A., CAMPBELL, J.L., Absolute efficiency calibration of coaxial Ge(Li) detectors for the energy range 160–1330 keV, Nucl. Instrum. Methods Phys. Res., Sect. B, 109 (1973) 241–251.
[90] SANCHEZ-REYES, A.F., FEBRIÁN, M.I., BARÓ, J., TEJADA, J., Absolute efficiency calibration function for the energy range 63-3054 keV for a coaxial Ge(Li) detector, Nucl. Instrum. Methods Phys. Res., Sect. B, 28 (1987) 123–127.
[91] INTERNATIONAL ATOMIC ENERGY AGENCY, Measurement of Radionuclides in Food and Environment, Technical Report Series N° 295, IAEA, Vienna (1989) 169.
[92] INTERNATIONAL ATOMIC ENERGY AGENCY, website (2010) www.iaea.org/programmes/aqcs/
[93] GILMORE, G., Practical Gamma-ray Spectrometer, 2nd ed, Chichester and New York: John Wiley & Sons (2008) 408.
[94] SANDERSON, C.G., "An evaluation of commercial IBM PC Software for the analysis of low level gamma-ray spectra", Low-Level Techniques. Group-Int. Committee of Radionuclide Metrology. Wurenlingen, Switzerland (1987).
[95] MURRAY, A.S., MARTEN, R., JOHNSTON, A., MARTIN, P., Analysis for naturally occurring radionuclides at environmental concentrations by gamma spectrometry, J. Radioanal. Nucl. Chem. Articles 115 (1987) 263–288.
[96] HEAD, J.H., Minimum detectable photopeak areas in Ge(Li) spectra, Nucl. Instrum. Methods 98 (1972) 419−428.
[97] PASTERNACK, B.S., HARLEY, N.H., Detection limits for radionuclides in the analysis of multi-component gamma ray spectrometer data, Nucl. Instrum. Methods 91 (1971) 533–540.

[98] VOLCHOK, H.L., DE PLANQUE, G. (Eds), Limit of detection, EML Procedures Manual, Rep.HASL-300, 26th ed, Environmental Measurements Lab., New York, D-08-05 (1983).
[99] HE, Q., WALLING, D.E., Calibration of a field-portable gamma detector to obtain *in situ* measurements of the ^{137}Cs inventories of cultivated soils and floodplain sediments, Appl. Radiat. Isot. 52 (2000) 865−872.
[100] BENKE, R.R., KEARFOTT, K.J., An improved *in situ* method for determining depth distributions of gamma-ray emitting radionuclides, Nucl. Instrum. Methods Phys. Res., Sect. A 463 (2001) 393–412.
[101] QUINE, T.A., WALLING, D.E., Rates of soil erosion on arable fields in Britain: quantitative data from caesium-137 measurements, Soil Use Manag. 7 (1991) 169–176.
[102] DE JONG, E., WANG, C., REES, H.W., Soil redistribution on three cultivated New Brunswick hillslopes calculated from ^{137}Cs measurements, solum data and the USLE, Can. J. Soil Sci. 66 (1986) 721–730.
[103] LI, Y., LINDSTROM, M.J., Evaluating soil quality-soil redistribution relationship on terraces and steep hillslopes, Soil Sci. Soc. Am. J. 65 (2001) 1500–1508.
[104] MABIT, L., BERNARD, C., Relationship between soil ^{137}Cs inventories and chemical properties in a small intensively cropped watershed, Comptes Rendus de l'Académie des Sciences, Série IIa, Earth and Planetary Sciences 327 (1998) 527–532.
[105] MABIT, L., BERNARD, C., Spatial distribution and content of soil organic matter in an agricultural field in Eastern Canada, as estimated from geostatistical tools, Earth Surf. Process.Landf. 35 (2010) 278−283.
[106] RITCHIE, J.C., MCCARTY, G.W., VENTERIS, E.R., KASPAR, T.C., "Using soil redistribution to understand soil organic carbon redistribution and budgets", Sediment Budgets 2 (HOROWITZ, A.J., WALLING, D.E., Eds), International Association of Hydrological Sciences Publication 292, IAHS Press. Wallingford, UK (2005) 3–8.
[107] VERITY G.E., ANDERSON D.W., Soil erosion effects on soil quality and yield, Can. J. Soil Sci. 70 (1990) 471–484.
[108] GOOVAERTS, P., Geostatistical tools for characterizing the spatial variability of microbiological and physico-chemical soil properties, Biol. Fertil. Soils 27 (1998) 315−334.
[109] GOOVAERTS, P., Geostatistics in soil science: state of the art and perspectives, Geoderma 89 (1999) 1−45.
[110] GOOVAERTS, P., Geostatistical modelling of uncertainty in soil science, Geoderma 103 (2001) 3−26.
[111] MABIT, L., "The use of geostatistics in environmental sciences to spatialise fallout radionuclides to assess soil erosion/sedimentation (Part 1-Geostatistics concepts)", IAEA, Vienna, Soils Newsletter 29 (2) (2006) 22−23.
[112] MABIT, L., "Use of geostatistics to establish soil movement map and sediment budget using fallout radionuclides (FRN)", Effects of River Sediments and Channel Processes on Social, Economic and Environmental Safety, Proc. 10th International Symposium on River Sedimentation, 1-4 August 2007, Moscow, Russia. Publication of the Moscow University, Russia. Vol. I. (2007) 247−254.
[113] VAN DER PERK, M., SLÁVIK, O., FULAJTAR, E., Assessment of spatial variation of cesium-137 in small catchments, J. Environ. Qual. 31 (2002) 1930–1939.
[114] CRESSIE, N.A.C., Statistics for Spatial Data, Wiley, New York (1993).
[115] KANEVSKI, M., MAIGNAN, M. (Eds), Analysis and Modeling of Spatial Environmental Data, Environmental Sciences, Book + CD-Rom, EPFL Press (2004) 288.
[116] WACKERNAGEL, H., Multivariate Geostatistics, Springer-Verlag, Berlin (1995).

[117] OLIVER, M.A., WEBSTER, R., How geostatistics can help you, Soil Use Manag. 7 (1991) 206−217.
[118] YOST, R.S., UEHARA, G., FOX, R.L., Geostatistical analysis of soil chemical properties of large land areas. I. Semivariograms, Soil Sci. Soc. Am. J. 46 (1982) 1028−1032.
[119] WEBSTER, R., OLIVER, M.A., Geostatistics for Environmental Scientists, John Wiley and Sons Ltd., Chichester, UK (2001).
[120] MABIT, L., BERNARD, C., Assessment of spatial distribution of fallout radionuclides through geostatistics concept, J. Environ. Radioact. 97 (2007) 206−219.
[121] DINEL, H., NOLIN, M.C., Spatial and temporal variability of extractable lipids as influenced by cropping history, Soil Sci. Soc. Am. J. 64 (2000) 177−184.
[122] BURGOS, P., MADEJON, E., PEREZ-DE-MORA, A., CABRERA, F., Spatial variability of the chemical characteristics of a trace-element-contaminated soil before and after remediation, Geoderma 130 (2006) 157−175.
[123] EMERY, X., Ordinary multigaussian kriging for mapping conditional probabilities of soil properties, Geoderma 132 (2006) 75−88.
[124] CAMBARDELLA, C.A., et al., Field scale variability of soil properties in Central Iowa soils, Soil Sci. Soc. Am. J. 58 (1994) 1501−1511.
[125] GAMMA DESIGN SOFTWARE, GS+ Version 7, GeoStatistics for the Environmental Sciences, User's guide, Gamma Design Software, LLC (2004) 160.
[126] MATHERON, G., Principles of geostatistics, Econ. Geol. 58 (1963) 1246–1266.
[127] OLEA, R., (Ed.), Geostatistical Glossary and Multilingual Dictionary, Oxford University Press, New York, USA (1991).
[128] ISAAKS, E.H., SRIVASTAVA, R.M., An Introduction to Applied Geostatistics, Oxford University Press (1989).
[129] YOST, R.S., UEHARA, G., FOX, R.L., Geostatistical analysis of soil chemical properties of large land areas. II. Kriging, Soil Sci. Soc. Am. J. 46 (1982) 1033−1037.
[130] GOLDEN SOFTWARE, Surfer 8, Contouring and 3D Surface Mapping for Scientists and Engineers, User's guide, Golden Software, Inc. (2002) 640.
[131] PANAGOPOULOS, T., JESUS, J., ANTUNES, M.D.C., BELTRÃO, J., Analysis of spatial interpolation for optimising management of a salinized field cultivated with lettuce, Eur. J. Agron. 24 (2006) 1−10.
[132] ROBINSON, T.P., METTERNICHT, G., Testing the performance of spatial interpolation techniques for mapping soil properties, Comput. Electron. Agric. 50 (2006) 97−108.
[133] PERSICANI, D., Simulation and areal interpolation by different methods of atrazine transport, J. Environ. Manage. 44 (1995) 361−374.

THE USE OF EXCESS ^{210}Pb (^{210}Pb$_{ex}$) AS A SOIL AND SEDIMENT TRACER

M. BENMANSOUR
Centre National de l'Energie, des Sciences et des Techniques Nucléaires (CNESTEN), Rabat, Morocco

L. MABIT
Soil and Water Management and Crop Nutrition Subprogramme, Joint FAO/IAEA Division of Nuclear Techniques in Food and Agriculture,
Vienna - Seibersdorf

P.N. OWENS
Environmental Science Programme and Quesnel River Research Centre, University of Northern British Columbia,
Prince George, British Columbia, Canada

S. TARJAN
Radioanalytical Reference Laboratory, Central Agricultural Office Food and Feed Safety Directorate,
Budapest, Hungary

D.E. WALLING
Geography, College of Life and Environmental Sciences, University of Exeter,
Exeter, United Kingdom

Abstract

Lead-210 (^{210}Pb) is one of the fallout radionuclides offering the broadest spectrum for environmental applications due to its geogenic origin and relatively long half-life of around 22 years. For more than five decades, ^{210}Pb has been widely used for dating sediments and investigating sedimentation processes. It is only since the 1990s that studies have been using fallout ^{210}Pb for providing information on the magnitude of soil erosion and sedimentation in agricultural landscapes. As it is rapidly and strongly adsorbed at the soil surface, ^{210}Pb has an environmental behaviour similar to ^{137}Cs. The use of fallout ^{210}Pb for documenting soil redistribution rates involves the same advantages and limitations as ^{137}Cs. However, ^{210}Pb can extend the temporal scale, associated with other FRNs measurements, to provide a retrospective assessment of long-term soil redistribution rates over a period of up to 100 years. In addition, since the fallout of ^{210}Pb is continuous, its use does not face the problems associated with short- and medium-lived radioactive soil tracers. This paper summarizes the state-of-the-art related to the main assumptions, the requirements and the limitations which have to be recognised when using this FRN as a soil and sediment tracer. In particular, measurement of fallout ^{210}Pb by gamma spectrometry requires more accurate analytical measurements, as compared to ^{137}Cs, to be performed by skilled staff, and appropriate analytical quality assurance systems. Lessons learned and future research needs in the application of fallout ^{210}Pb are also presented and discussed in this paper.

1. General information

1.1. Origin and characteristics

With an atomic number of 82, lead (Pb) belongs to the heavy metals group. Lead has four natural stable isotopes: ^{206}Pb, ^{207}Pb, ^{208}Pb and ^{204}Pb with natural abundances of 23.6, 22.6, 52.3 and 1.4%, respectively. ^{206}Pb, ^{207}Pb and ^{208}Pb originate from the decay of ^{238}U, ^{235}U and ^{232}Th series or chains, respectively. These series also contain the radioisotopes of lead: ^{210}Pb, ^{214}Pb (^{238}U chain), ^{212}Pb (^{232}Th chain) and ^{211}Pb from ^{235}U series.

Lead-210 (^{210}Pb) is a very useful radioisotope element for environmental investigations such as dating and tracing. Since the 1970s measurements of ^{210}Pb have been used extensively for sediment dating in reservoirs, lakes, estuaries, flood plains and coastal marine environments and to determine sedimentation rates over the last 100-150 years in these environments e.g. [1-14]. Studies for source tracing, and for assessing rates and patterns of soil redistribution started in the mid-1990s e.g. [15-18]. Despite recent developments in the use of ^{210}Pb as a tracer of soil redistribution e.g. [19] more research is still needed if the technique is to realize its full potential and be considered a standard approach in this specific field of environmental research [20].

^{210}Pb is a natural geogenic radioisotope ($t_{1/2}$ = 22.26 years) occurring as one of the decay products of the ^{238}U series (i.e. – ^{226}Ra – ^{222}Rn – ^{218}Po – ^{214}Pb – ^{214}Bi – ^{214}Po – ^{210}Pb (see Fig. 1).

Theoretically ^{226}Ra and ^{210}Pb should be in secular equilibrium but owing to the diffusional behaviour of the noble gas daughter ^{222}Rn, disequilibrium can occur in natural materials. A proportion of ^{222}Rn ($t_{1/2}$ = 3.8 days) diffuses from geological soil materials into the air or upper soil layers leading to disequilibrium between the parent and daughter isotopes.

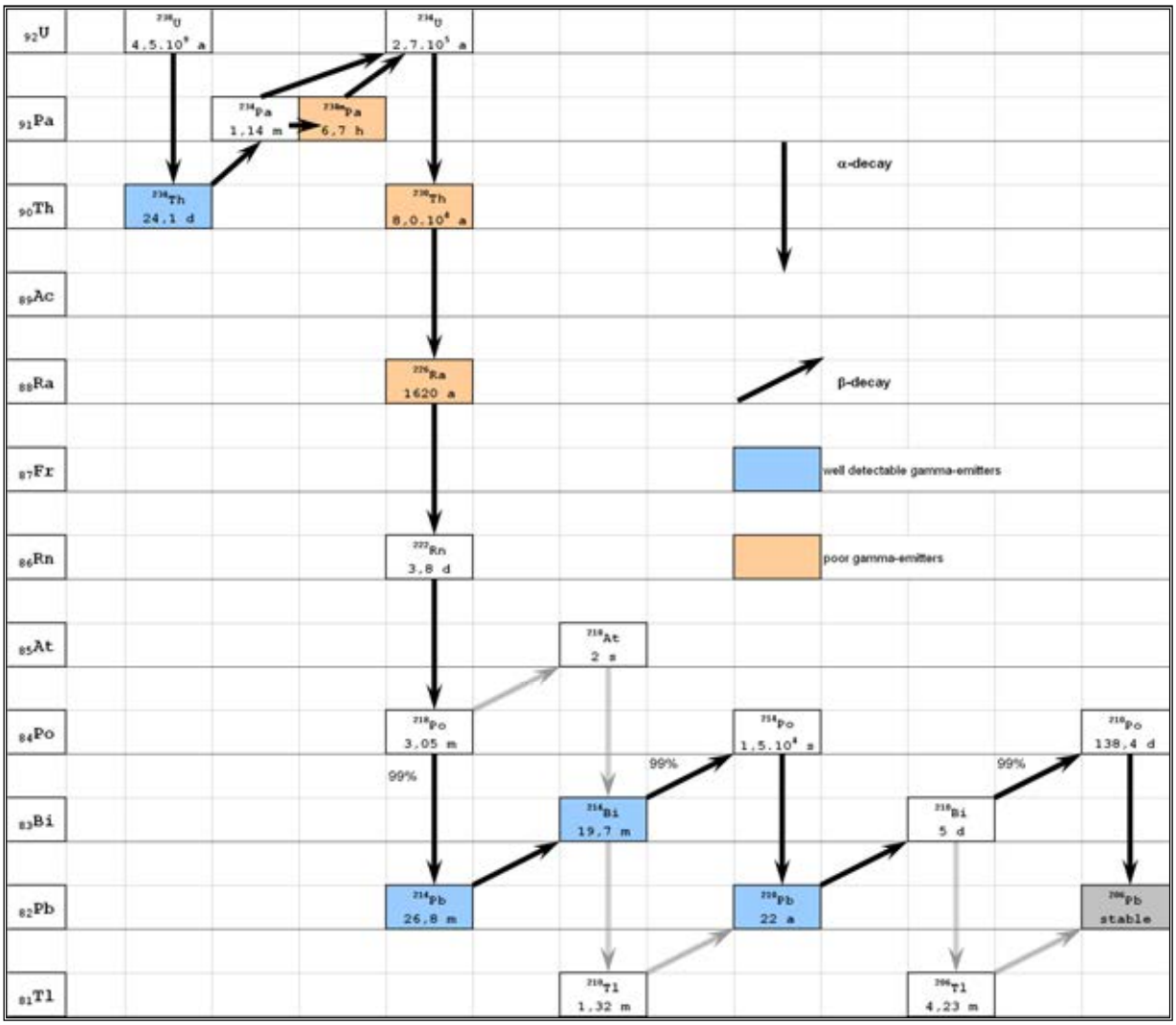

FIG. 1. The Uranium decay chain.

When ^{222}Rn escapes into the air its daughter products (including ^{210}Pb) are adsorbed onto the surface of aerosols and dust particles. These daughter isotopes reach the soil surface by wet and dry fallout and accumulate in the surface layers of the soil.

As a result of this process the surface soil layer contains a higher ^{210}Pb concentration than that expected from equilibrium with ^{226}Ra. The part of the ^{210}Pb which is in equilibrium with the ^{226}Ra activity is called 'supported ^{210}Pb'. Its activity will decrease with the half-life of ^{226}Ra (1620 years). The ^{210}Pb in excess of the equilibrium concentration is termed 'unsupported' or 'excess' (^{210}Pb$_{ex}$). ^{210}Pb$_{ex}$ decays by the real physical half-life of the ^{210}Pb isotope (~22 years).

^{210}Pb is a beta decay radionuclide, and 16% of its decay occurs at the ground level of the ^{210}Bi isotope. However 84% results in an excited nucleus which stabilizes by emission of low energy gamma rays (46.5 keV), and internal conversion of electrons to the ground state of ^{210}Bi ($t_{1/2}$ = 5 days) (Fig. 2) which in turn decays by emission of beta particles to a pure alpha emitter ^{210}Po ($t_{1/2}$ = 138 days) with an energy of 5.3 MeV.

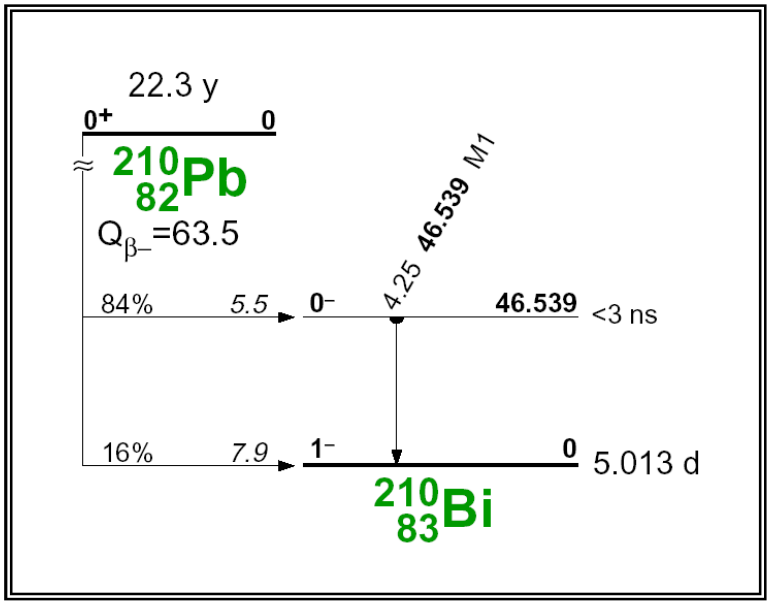

FIG. 2. Decay scheme of ^{210}Pb to ^{210}Bi.

In contrast to ^{137}Cs, the ^{210}Pb fallout flux is essentially continuous through time because of its natural origin. In some locations, seasonal and longer-term variations in ^{210}Pb concentrations in the air and in atmospheric fallout (rain, snow and dry deposition) have been recorded by long-term measurements e.g. [21].

The global pattern of ^{210}Pb fallout is characterized by a high spatial variability due to predominant west to east movement of air masses. This commonly results in: (i) low ^{210}Pb fallout in the western areas of the continents, where the air masses have travelled over the oceans and have had little opportunity to pick up ^{210}Pb, and (ii) much higher ^{210}Pb fallout in the eastern areas of continents, where the air masses will have passed over the continental interiors.

Seasonal variations of ^{210}Pb concentrations in the atmosphere have been reported in many parts of the world. For example, in Hungary, a monitoring programme was undertaken by the Central Radioanalytical Laboratory of the Food and Feed Safety Directorate from 1999 to the present [22]. The major objectives of this programme are to identify radionuclides, to obtain quantitative information on transfer processes, to evaluate the present situation, and to estimate the committed effective dose to humans due to ingestion. ^{210}Pb activities in the air were measured by gamma spectrometry, using filters to remove aerosols. In the autumn and winter seasons, the mean activity concentrations of ^{210}Pb (mBq m^{-3}) were slightly higher than those of the spring and summer seasons (Fig. 3).

Similar results were obtained in Egypt [23]. This seasonal variability can be related to the higher temperatures in spring and summer, which are usually accompanied by higher turbulence, leading to dilution of radioactivity in the lower layers. The same trend was also observed by Winkler and Rosner [24] who studied the seasonal and long-term variation of ^{210}Pb concentrations in air, the atmospheric deposition rate and the total deposition velocity in southern Germany from 1972 to 1999.

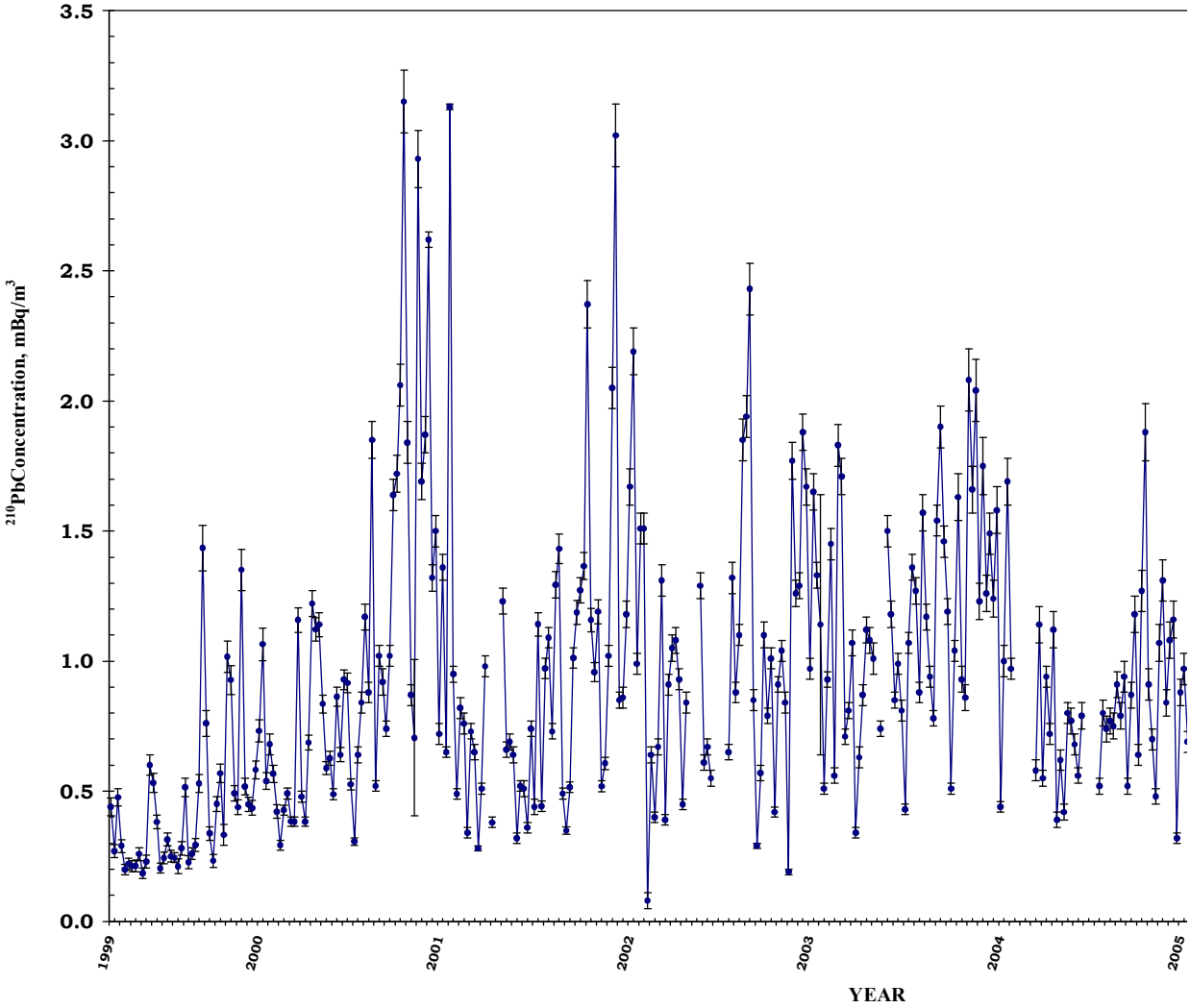

FIG. 3. Example of the variation of ^{210}Pb activity concentrations in air measured in Hungary from 1999 to 2005.

In addition, a significant correlation has been observed between mean annual rainfall (mm) and mean annual fluxes of ^{210}Pb (Bq m^{-2}) e.g. [24-26] suggesting that wet precipitation is mainly responsible for the scavenging of fallout radionuclides from the atmosphere. In southern Germany, for example, the mean annual ^{210}Pb deposition flux for the period 1981-1999 was 180 Bq m^{-2} yr^{-1} for a mean annual precipitation of 855 mm [24]. The minimum and maximum values for the same location were 120 and 250 Bq m^{-2} yr^{-1}. In Budapest (Hungary), the mean annual ^{210}Pb deposition flux for the period 1999-2006 was 81 Bq m^{-2} yr^{-1} for a mean annual precipitation of 476 mm, with minimum and maximum values for the same location of 44 and 100 Bq m^{-2} yr^{-1}, respectively [22]. At the global scale, the annual fallout flux of ^{210}Pb is reported to vary from 23 to 367 Bq m^{-2} yr^{-1}[2, 27, 28]. An overview of the global variation of the total annual deposition of ^{210}Pb is presented in Table 1.

TABLE 1. TOTAL ANNUAL DEPOSITION OF ^{210}Pb AT DIFFERENT LOCATIONS (ADAPTED FROM [27])

Location	Mean ^{210}Pb deposition rate (Bq m^{-2} yr^{-1})
Suva, Fiji	80
Auckland, New Zealand	50
Delhi, India	133
Calcutta, India	102
Bombay, India	250
Sydney, Australia	53
Alice Springs, Australia	57
Darwin, Australia	95
Hokkaido, Japan	367
Milford Haven, UK	85
Moscow, Russia	115
New Haven, USA	153

1.2. The environmental behaviour of ^{210}Pb in the soil and the general basis of the ^{210}Pb$_{ex}$ method for documenting soil redistribution

^{210}Pb$_{ex}$ has an environmental behaviour similar to ^{137}Cs. It is rapidly and strongly adsorbed at the soil surface. A strong affinity for sediment particles has been reported [29, 30]. Pb forms solid inner-sphere complexes with clay minerals [31], organic matter [32] and oxides [33]. In addition, Pb forms precipitates with a moderate to low solubility in soil, where Pb hydroxides and phosphates dominate in calcareous soils [34, 35].When reaching the soil surface as wet or dry fallout from the atmosphere, ^{210}Pb$_{ex}$ is rapidly adsorbed by clay minerals and organic matter, and like ^{137}Cs, its subsequent redistribution within the soil profile and across the landscape is controlled by erosion and sediment transport processes. Some investigations even highlighted that Pb is more strongly retained in soil than Cs e.g. [36]. The limited Pb uptake by plants [37] in combination with a strong affinity between the Pb atom and the surface of soil particles means that the post depositional redistribution of excess ^{210}Pb in the soil primarily reflects the redistribution of soil particles and associated organic and mineral complexes over time [38].

As in the case of ^{137}Cs, the general principle of using ^{210}Pb$_{ex}$ as a soil tracer is based on the comparison of the areal activity or inventory of ^{210}Pb$_{ex}$ (Bq m^{-2}) associated with the study area with the inventory of an undisturbed site or 'reference site'. The use of appropriate conversion models allows the quantification of soil erosion and deposition rates (t ha^{-1} yr^{-1}) associated with a period of ca. 100 years, which corresponds to a period of ~5 half-lives of ^{210}Pb, at which the activity is very low and detection constrained by analytical procedure. In areas of lower fallout, it should be recognised that the erosion signal may be dominated by ^{210}Pb fallout over the past 3 half-lives.

The vertical distributions of ^{210}Pb$_{ex}$ associated with undisturbed and cultivated soils are very similar to those documented for ^{137}Cs (Fig. 4 and 5). However, in contrast to the ^{137}Cs profile shape for undisturbed soil where the peak value is often located below the surface [39], the continuous input of ^{210}Pb$_{ex}$ results in a maximum activity occurring at the surface [16].

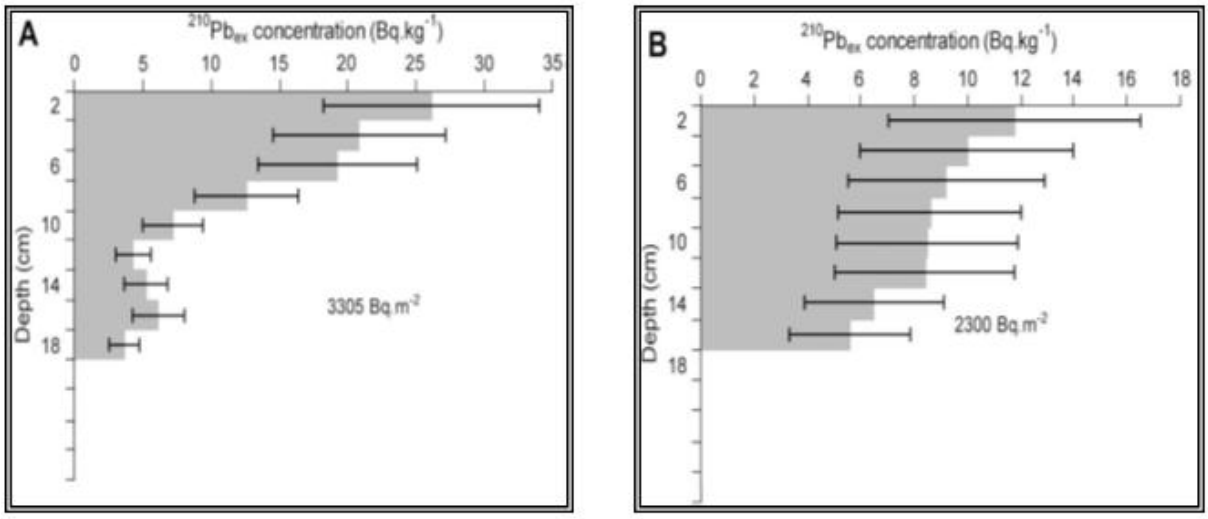

FIG. 4. Examples of $^{210}Pb_{ex}$ profiles in Morocco [40] (A: Undisturbed soil; B: Cultivated eroded soil).

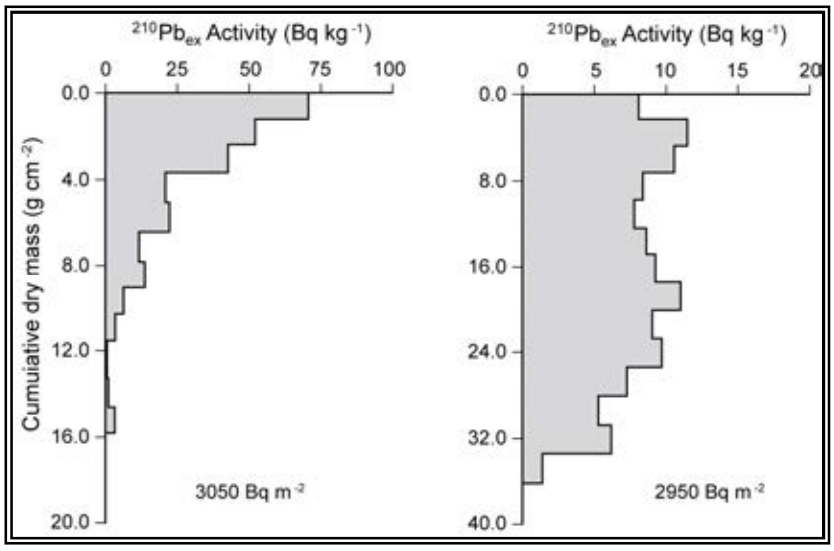

FIG. 5.Examples of $^{210}Pb_{ex}$ profiles from Jackmoor Brook catchment, Devon, UK. (A: Undisturbed soil; B: Cultivated eroded soil) (Based on [17]).

1.3. Advantages and limitations

The use of $^{210}Pb_{ex}$ determination for documenting soil redistribution rates on agricultural land retains the same general advantages as provided by ^{137}Cs (see Paper 2 of this TECDOC). In addition, it has the following further advantages:

(a) The use of $^{210}Pb_{ex}$ can extend the timescale associated with ^{137}Cs measurements, to provide a retrospective assessment of longer-term (up to 100 years) rates of soil redistribution;

(b) The $^{210}Pb_{ex}$ technique can be used in the southern hemisphere, where ^{137}Cs inventories are sometimes too low to permit precise measurements, as well as in areas affected by the Chernobyl accident, where additional radio-caesium fallout inputs in 1986 can complicate interpretation of ^{137}Cs measurements;

(c) The input of bomb-derived ^{137}Cs fallout has ceased and ^{137}Cs inventories are decreasing due to radioactive decay. In the future, the use of ^{137}Cs will no longer be possible, especially in the southern hemisphere. Since the fallout of $^{210}Pb_{ex}$ is effectively continuous, the use of this radionuclide does not face these problems.

The main constraints or limitations of the $^{210}Pb_{ex}$ approach include the following:

(a) Difficulties and constraints for measuring ^{210}Pb by laboratory gamma spectrometry;

(b) Additional sources of ^{222}Rn to the atmosphere may create problems. ^{222}Rn and its short-lived decay products are commonly present in the atmosphere at much lower levels than in the soil. However, increased activities can occur in the vicinity of volcanoes, thermal spas, and other sources of gas emanating from zones of the Earth's surface where rocks or minerals with high radium content are found;

(c) In some locations, the $^{210}Pb_{ex}$ content in soil has been found to be very low and even below detection limits. This could reflect either very high soil erosion rates or a low ^{210}Pb fallout deposition flux, and could clearly constitute a major limitation in some study areas. Where the total ^{210}Pb content of a soil is very close to the content of supported ^{210}Pb indicated by the ^{226}Ra content, the uncertainty associated with determining $^{210}Pb_{ex}$ may be too high. Limitations of the use of this isotope in some environmental applications such as sediment dating in New Zealand [41] as a soil tracer under certain conditions, including frozen soil and snow-melt [42] have already been reported. For example, due to a very low level of $^{210}Pb_{ex}$ coupled with a high variability (2.7 Bq kg^{-1} ± 115% (mean ± CV%); n = 11) and a high measurement uncertainty, it was not possible to use $^{210}Pb_{ex}$ to trace soil redistribution in a watershed in northern Austria [43]. It is likely that the precipitation in the area under investigation did not provide sufficient $^{210}Pb_{ex}$ input;

(d) Measurement of ^{210}Pb by *in-situ* gamma spectrometry detection is almost impossible due to the self-absorption of the low energy gamma ray 46.5 keV in soil. Effectively, assuming a soil density of 1.65 g cm^{-3} (composition tested: 68% of SiO_2, 10% of H_2O, 1% of C, 3% of Fe, 7% of Al and 11% of O_2) and based on the gamma attenuation law, 97% of the emitting gamma ray will be absorbed by the first 5 cm of the soil that is also coupled with an additional 3% absorption in dry air if the detector is placed at 1 m above ground level.

In order to better understand the constraints and/or limitations of the $^{210}Pb_{ex}$ approach, there is a need for future investigations to test and validate the use of $^{210}Pb_{ex}$ for documenting soil redistribution rates under a range of different environmental and climatic conditions.

2. Sampling design and sample collection

As fallout $^{210}Pb_{ex}$ has an almost identical environmental behaviour in soil to that of ^{137}Cs – strong adsorption to soil particulate matter and similar vertical distributions in both undisturbed and cultivated areas. The sampling design and soil sample collection procedure for the use of $^{210}Pb_{ex}$ as a soil tracer will be similar to those of the ^{137}Cs method presented in the Paper 2 of this TECDOC.

3. Sample preparation and radioactivity measurement

When preparing samples for measurement of ^{210}Pb activity, the same steps described for ^{137}Cs (see Paper 2 of this TECDOC) must be followed. In addition, where $^{210}Pb_{ex}$ is being used, and if ^{226}Ra, which reflects the activity of supported ^{210}Pb, is measured by gamma spectrometry using its daughters ^{214}Pb or ^{214}Bi, it is essential to ensure equilibrium with its direct gaseous daughter ^{222}Rn. To achieve equilibrium between ^{226}Ra and ^{222}Rn, samples should be placed in cylindrical containers or Marinelli beakers and sealed (e.g. with PVC tape or epoxy glue) for at least 21 days prior to performing gamma analysis. Care should be taken that the samples are in containers that can be effectively sealed to minimize radon escape. High Density Polyethylene (HDPE) or aluminium containers should be used for this purpose. Also, the void above the sample should be minimized so as to prevent radon from accumulating in that space and changing the ultimate counting efficiency for the photons of interest. The determination of $^{210}Pb_{ex}$ activity requires the measurement of total ^{210}Pb activity and ^{226}Ra activity, which is equivalent to supported ^{210}Pb:

$$^{210}Pb_{ex} = {}^{210}Pb - {}^{226}Ra \quad (1)$$

^{210}Pb can be measured by gamma spectrometry using HPGe detectors. However, the γ-rays are emitted at the low energy of 46.5 keV with a low emission probability of 4%. ^{226}Ra can also be measured by gamma spectrometry via the gamma ray energies of its daughters ^{214}Bi and ^{214}Pb at 609 keV and 351 keV, respectively. It can be measured directly through its gamma line at 186 keV, but this involves subtracting the contribution of ^{235}U, which emits a gamma ray in the same region as ^{226}Ra, leading to an interference of the two gamma rays. Hence the ^{214}Pb approach is preferred by most laboratories. The basis of gamma spectrometry has already been described in Paper 2 of this TECDOC. However, for the measurement of ^{210}Pb, some additional and specific information, as well as some constraints, should be considered.

3.1. Gamma detector configuration

Whereas ^{137}Cs is easily measured by gamma spectrometry using classical coaxial germanium 'P-type' detectors with an energy range from 40 keV to 10 MeV, ^{210}Pb analysis requires a detector with high efficiency and low background at the low energy range. 'N-type' germanium crystals are commonly used for measuring both high and low energy gamma rays. These detectors are of similar internal structure to other coaxial germanium detectors, with one important difference. Their electrodes are the opposite of the conventional coaxial detector, in that the 'P-type' electrode, (ion-implanted boron) is on the outside, and the 'N-type' contact (diffused lithium) is on the inside. There are two advantages to this electrode configuration, firstly window thickness, and secondly radiation damage resistance. The ion-implanted outside contact is extremely thin (0.3 μm) compared to a lithium-diffused contact. This, in conjunction with a thin 0.6 mm carbon composite cryostat window (aluminium and beryllium can be also used), extends the response to below 3 keV (usually this window is the closest part of the detector to the sensitive volume, and so it has a strong effect on the background). Beryllium and aluminium windows usually contain natural radionuclides like the ^{210}Pb isotope whereas carbon composite is an artificial material which is almost free from natural radionuclides. This configuration increases the detection efficiency especially below 100 keV, thereby allowing measurement of ^{210}Pb at 46.5 keV. Examples of such detectors able to measure both high and low energies (for ^{137}Cs and ^{210}Pb) can be provided by different

suppliers, such as [44] (e.g. reverse electrode (RGe) and XtRa (3 keV-10 MeV); broad energy germanium (3 keV-3 MeV)) or [45] (e.g. GMX "N-type" (3 keV-10 MeV)). Some key information is presented in Fig. 6 and additional characteristics of these detectors can be found on the respective web sites of the cited suppliers [44, 45].

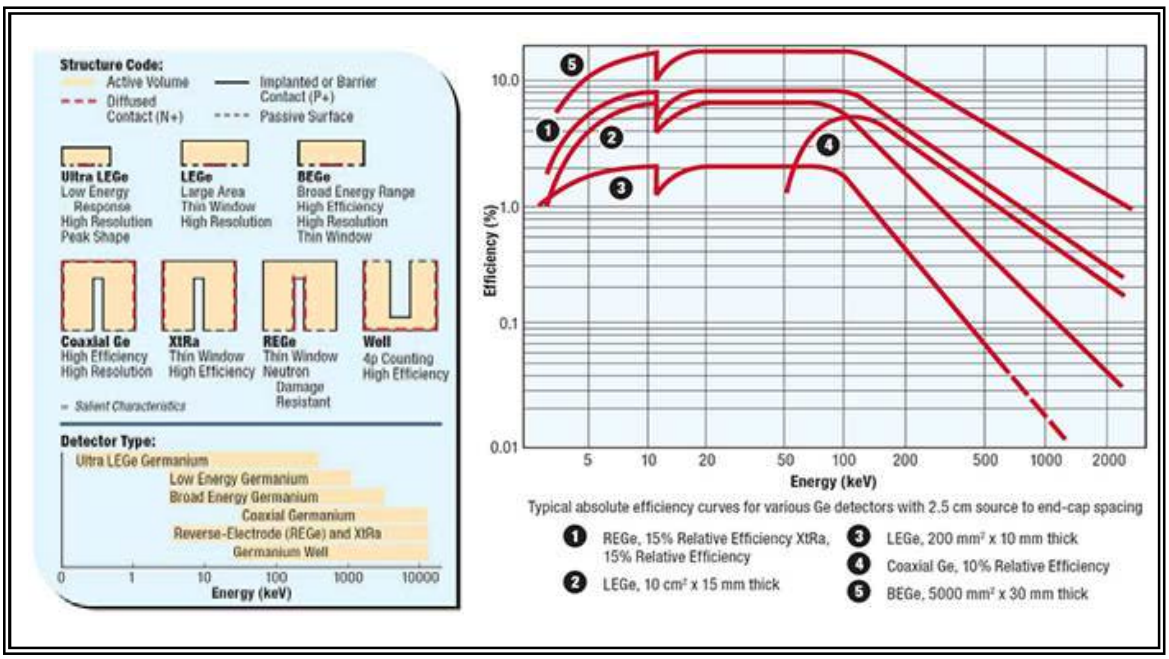

FIG. 6. Characteristics of various germanium detectors [44].

3.2. Efficiency calibration and the self-absorption effect

If the sample volume is large, a proportion of radiation can be attenuated before it actually leaves the sample medium. Self-absorption varies as a function of matrix chemical composition and density. Self-absorption is a noticeable factor in the low energy region (< 200 keV) and also the higher energy region if the sample volume is large. This effect was already mentioned in the Paper 2 of this TECDOC, where it was recommended that the bulk density and composition of the standard should be as close as possible to that of the soil sample. Although the auto-absorption effect is not so influential for ^{137}Cs measurement at 662 keV, its impact for $^{210}Pb_{ex}$ with an energy of 46.5 keV becomes important even if the densities and chemical composition of the soil sample and standard are similar.

An example of the difference between ^{210}Pb and ^{137}Cs is illustrated in Fig. 7 which presents the detection efficiencies of the photoelectric peak associated with gamma ray energies of 46.5 keV (^{210}Pb) and 662 keV (^{137}Cs) using cylindrical geometry (75 mL) for two standard matrixes analysed by a HPGe 'N-type' detector (45% relative efficiency, 2.0 keV energy resolution) at the CNESTEN laboratories in Morocco. The matrixes are a liquid multi-gamma source with a density of 1 g cm^{-3} and a sediment matrix (IAEA reference material IAEA-300) with a density of 1.28 g cm^{-3}. The variation in efficiency is important for the low energy of 46.5 keV, despite the small difference between the densities, while for the gamma line of 662 keV, efficiencies for the two densities are similar. The variation is around 15% and 2% for ^{210}Pb and ^{137}Cs, respectively. Different tests were performed [46] consisting of the measurement of over 70 radioactive standard bulk sources with different matrix densities (0.1 - 2.0 g cm^{-3}) and different shapes (cylindrical geometry of 50 cm^3 and two Marinelli beaker geometries of 450 and 1000 cm^3). The results showed that the dependence of the

photo-electric peak efficiency on the density is linear with a steeper slope for the low energies (< 200 keV). The energy range studied was 88-1836 keV.

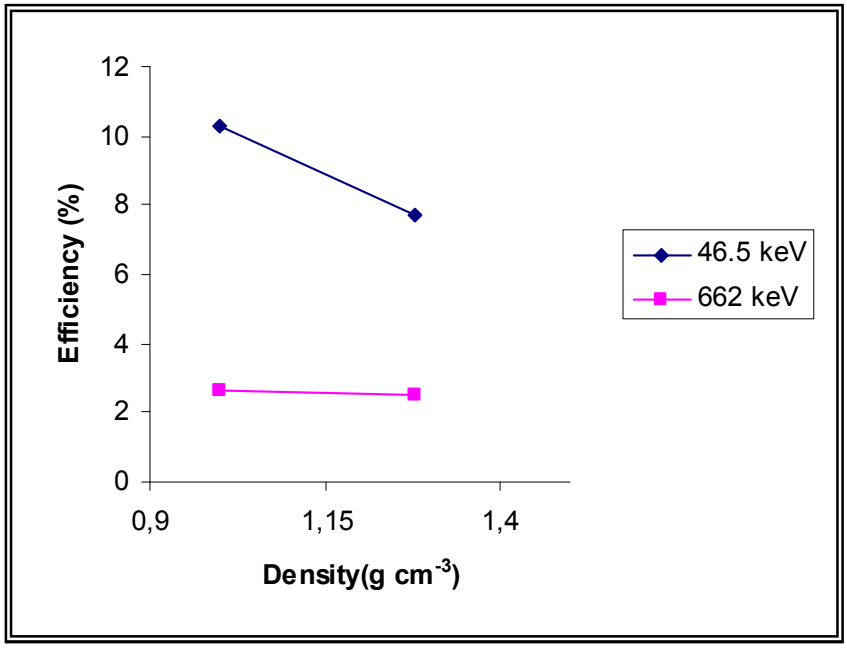

FIG. 7. Example of the variation of detection efficiency with matrix density for ^{137}Cs (662 keV) and ^{210}Pb (46.5 keV).

Ideally, standards of the same matrix as the samples should be used for instrument calibration. For analyses of ^{210}Pb by gamma spectrometry where the soil sample has a different matrix from the standard, it is necessary to apply a self-attenuation correction in order to obtain a precise determination of the activity concentration. Many studies have been undertaken to estimate the self-attenuation factor e.g. [46-53]. Experimental, theoretical and Monte-Carlo techniques have been proposed by these authors for the evaluation of the self-attenuation factor. A simplified experimental approach can be adopted e.g. [51, 53, 54]. This method is based on transmission measurements that can be easily undertaken in any laboratory. A point source with the same energy (^{210}Pb; $\gamma = 46.5$ keV) or similar energy (^{241}Am; $\gamma = 59.5$ keV) is positioned above the sample in the container located on the detector and above the air sample (identical empty container). The self-attenuation factor $F_{att,s}$ with respect to the air sample can be assumed to be:

$$F_{att,s} = -\frac{1-(I/I_0)}{Ln-(I/I_0)} \qquad (2)$$

where:

I *and* I_0 are the peak count rates for the unknown sample and air sample.

Generally, the efficiency calibration for volume samples is undertaken using a standard source. The relative self-attenuation factor F_{att} for a sample (s) with respect to a standard (st) is given by:

$$F_{att} = \frac{F_{att,s}}{F_{att,st}} \quad (3)$$

where:

$F_{att,s}$ *and* $F_{att,st}$ are the self-attenuation factors corresponding to the unknown sample and the standard, respectively, with respect to the air sample.

Therefore, a correction should be applied to the detection efficiency of the photoelectric peak ε_{st} at the energy of interest (e.g. 46.5 keV) associated with the standard. The efficiency ε_s corresponding to the unknown sample with a different matrix than the standard can be expressed as:

$$\varepsilon_s = F_{att}\varepsilon_{st} \quad (4)$$

3.3. Standards

As in the case of ^{137}Cs, there are a variety of ways to obtain or prepare a standard for ^{210}Pb, ^{214}Pb and ^{226}Ra, including:

- U-series standards from ore of known activities [55] provided by international suppliers of standards e.g. [56, 57] whereby the ore is diluted by weight into an inactive soil matrix (low-activity sand) at different masses and then ground and homogenised [55];
- Liquid standard source with known activities of ^{210}Pb and ^{226}Ra which can be diluted into inactive soil matrix at different masses;
- Soil standards containing ^{210}Pb, ^{226}Ra, ^{137}Cs prepared by international suppliers;
- IAEA Reference Materials (e.g. RGU1, RGTh-1, IAEA-327, Soil-6).

3.4. Background

Potential sources of background for gamma spectrometry using HPGe detectors have already been mentioned in the Paper 2 of this TECDOC. Particular attention should be devoted to background from natural radionuclides (natural series) which can constitute a constraint if ^{210}Pb and ^{226}Ra are analysed. The materials used for the detector and the shielding are sources of natural radioactivity. A low-background HPGe detector is recommended. In such detectors, there are only a few peaks from naturally occurring radionuclides visible typically at 1460 keV of ^{40}K and 2614 keV of ^{208}Tl [58]. The other common peaks are swamped by the continuous background generated by “bremsstrahlung” induced by muons and other high energy cosmogenic particles. To reduce lead photons originating from the lead shielding, it is common to add an additional graded lining with, for example, 1 mm of Sn or Cd and 1 mm of Cu. In addition, if the Compton background of the gamma spectrum is high, the 46.5 keV ^{210}Pb line is not easy to detect. Detectors with a good peak to Compton ratio can significantly improve the limit of detection.

3.5. Quality assurance and quality control

Multiple factors can affect the precision and accuracy of gamma measurement of soil samples especially when gamma-rays with low energies are measured. Since the ^{210}Pb gamma ray is in the low energy part of the spectrum with a relatively low emission probability, the determination of the total ^{210}Pb by gamma spectrometry in soil samples is more complicated than that of ^{137}Cs. The measurement uncertainty can be higher in the low energy photon spectra and strongly disturbed by the Compton scattering effect. The assurance of radioactive measurement quality is critically important for laboratories in many Member States, in order to achieve a reliable output. Indeed, measurements performed by laboratories worldwide should yield traceable, accurate, reliable and comparable results. Through the provision of reference materials, validated procedures, fellowship training in quality control and performance assessment by the organization of proficiency tests (PT) and inter-comparison exercises, the IAEA has been assisting laboratories in Member States in testing, improving and maintaining the reliability and the quality of analyses of radioactive material. Proficiency testing, which includes distribution of homogenous portions of the test material for analysis as an unknown, is a method for assessing and documenting the reliability and accuracy of the analytical data produced. In the framework of accreditation systems, the use of reference materials, both for quality control and proficiency testing, has therefore increased in recent years [59].

Following the recommendation of the first Research Coordination Meeting of the FAO/IAEA Coordinated Research Project (CRP) D1.50.08 "*Assess the effectiveness of soil conservation measures for sustainable watershed management using fallout radionuclides*" [60], a PT was organized in 2006 by the Chemistry Unit in collaboration with the Soil Science Unit of the IAEA's Laboratories [61]. This PT involved the determination of both ^{137}Cs and total ^{210}Pb in spiked soil samples using γ-spectrometry, and was organized to assess the validity and reliability of the analytical results of the 14 laboratories participating in the above-mentioned CRP, that was located in developed and developing countries (Argentina, Australia, Brazil, Canada, China, Chile, Japan, Morocco, Pakistan, Poland, Romania, Russian Federation, Turkey, United Kingdom, United States of America and Vietnam) [62]. Reference materials were distributed to the participating laboratories and, using a rating system, their analytical results were compared to the assigned reference values [61]. In the case of ^{137}Cs, most laboratories were able to produce acceptable analytical results, with a bias of $\leq$ 10%. However, the results for total ^{210}Pb demonstrated greater errors. While 66% of the 14 laboratories involved in the PT were able to measure^{137}Cs accurately, only 36% obtained acceptable results for total ^{210}Pb [61].

This inter-laboratory test underlines that further inter-comparison exercises should be organized by IAEA or regional laboratories to ensure the quality of the analytical data produced by Member States. As a result of the above-mentioned PT, some recommendations have been provided to improve the accuracy of gamma measurement of both ^{137}Cs and total ^{210}Pb [61]:

- Gamma measurement for FRNs should be undertaken according to the characteristics (geometry and energy range) of the gamma detector. A coaxial HPGe 'N-type' detector should be used if both ^{137}Cs and ^{210}Pb are measured in the same sample;
- A range of appropriate sample geometries for measurement should be used in the laboratory, in order to reach an acceptable level of the minimum detection limit [63, 64];

- A gamma detector with no impurities in the Ge detector end-cup should be installed in a low and stable background environment with reduced and minimized: cosmic rays and associated processes γ-rays from external natural radioactivity radon and daughters in the air electronic interferences and microphonic noise. To protect the measurement from external background, the lead shield should also have a minimum thickness of 100 mm;
- For efficiency calibration, the use of old reference materials or certified solutions with expired validity should be avoided;
- An appropriate matrix reference material for quality control and method validation should be used and an appropriate self-attenuation correction factor should be applied where appropriate e.g. [51, 53, 54];
- Gamma spectra should be analysed using appropriate software;
- Gamma detector calibration should be checked regularly with reference materials and blank samples. In order to assess the precision of gamma analysis, a quality control and quality assurance protocol, including regular measurement and records of backgrounds, should be produced and used to obtain accurate and valid measurement in the medium- and long-term;
- It is recommended that institutions dealing with γ-spectrometry run their own inter-comparison exercises at the local and regional levels to compare results on a regular basis with other institutions and include procedures to assess the accuracy and precision of analyses [65] (e.g. quality control using reference materials and/or certified reference materials with known activity levels);
- All sources of the uncertainty associated with measurement results should be listed and estimated. A practical example for the estimation of the uncertainty in gamma spectrometry can be found in [66].

3.6. Alternative approaches for measuring ^{210}Pb

The indirect approach to determining $^{210}Pb_{ex}$ activity from total ^{210}Pb and ^{226}Ra induces potential errors associated with the measurement of both ^{210}Pb and ^{226}Ra and results in a low precision for the final estimate of $^{210}Pb_{ex}$. The uncertainty associated with the estimate of $^{210}Pb_{ex}$ can reach 30 to 50%, especially where concentrations of $^{210}Pb_{ex}$ are low. Other methods of measuring total ^{210}Pb involve radiochemical separation. Alpha spectrometry and beta or liquid scintillation counting are more sensitive and can provide improved analytical precision [20, 67, 68]. They are, however, also labour-intensive and expensive.

For example, ^{210}Pb activity can be measured via its daughter ^{210}Po (half-life = 138 days), by using alpha spectrometry. The emitted alpha particle has an energy of 5.407 MeV. It is assumed that ^{210}Pb and ^{210}Po in soil are in equilibrium (see Fig. 1).

The method requires a total digestion of a small amount of soil (e.g. 0.2-0.5 g) generally combining several acids (HNO_3, HF, $HClO_4$ and HCl) and spontaneous deposition of polonium isotopes on silver discs [67]. ^{209}Po or ^{208}Po standard aqueous solutions (radiochemical tracer) are needed for radiochemical yield and activity determination. The alpha spectra of ^{210}Po using ^{209}Po as a tracer is shown in Fig. 8. The counting is generally performed by SSB (Silicon Surface Barrier) alpha detectors (Fig. 9) or PIPS (Passivated Implanted Planar Semiconductor) alpha detectors (Fig. 8).

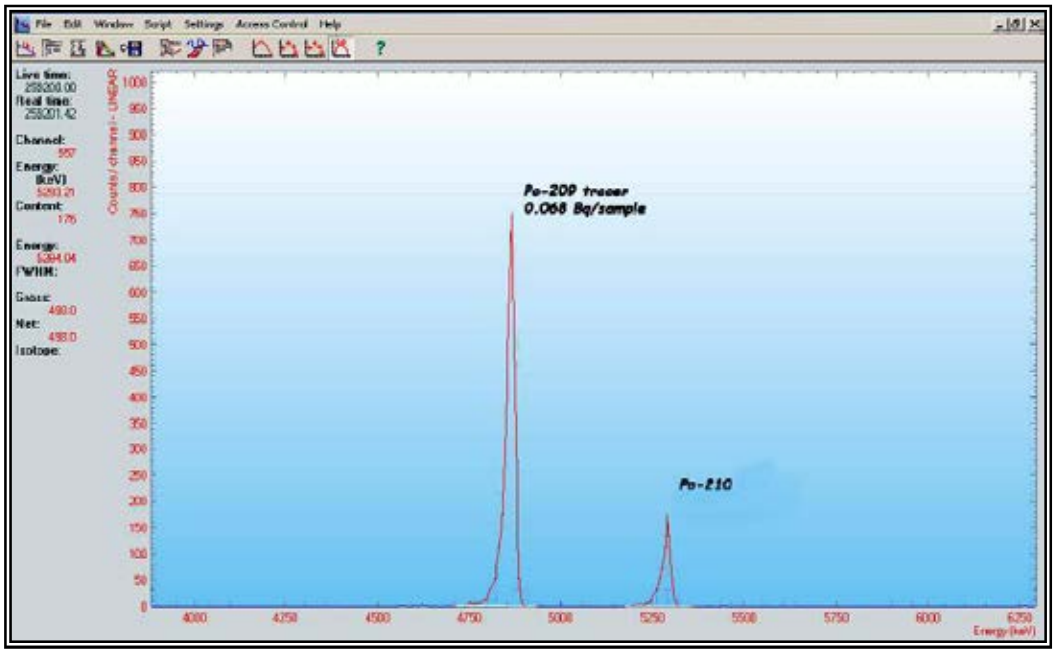

FIG. 8. The alpha spectrum of ^{210}Po by PIPS detector.

FIG. 9. Example of measurement of ^{210}Pb by HPGe ''N-type'' detector and alpha spectrometry (SSB detectors) via ^{210}Po at the CNESTEN laboratories.

A comparison of the analytical precision of alpha and gamma spectrometry measurements is provided in Fig. 10, which presents the relationship between relative uncertainty and $^{210}Pb_{ex}$ concentration under optimal laboratory conditions for alpha and gamma spectrometry determinations of total ^{210}Pb. At low activities, the difference between the two methods is high and alpha spectrometry performs much better than gamma analysis. The relative uncertainty associated with gamma spectrometry determination for a $^{210}Pb_{ex}$ activity of 10 Bq kg^{-1} can reach 40%, although for higher activities (>30 Bq kg^{-1}) uncertainties become acceptable (<15%) and when activities exceed 120 Bq kg^{-1}, uncertainty levels are close to those associated with alpha spectrometry. For additional information, see a recent comparison of alpha and gamma spectrometry for ^{210}Pb measurements [68].

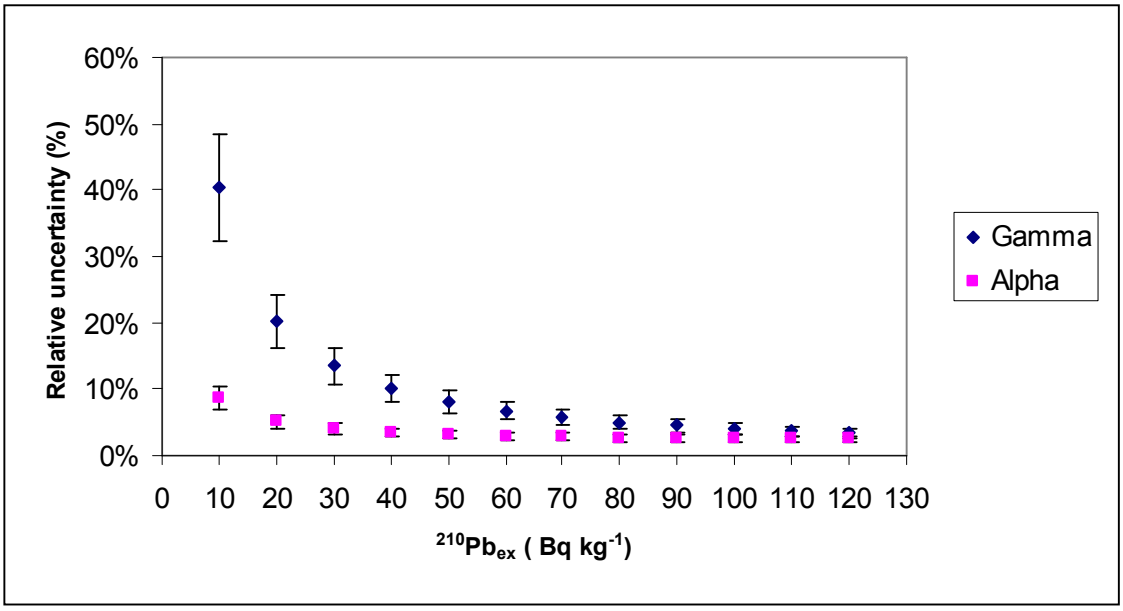

FIG. 10. Comparison of gamma and alpha spectrometry measurement uncertainty when used for determining the $^{210}Pb_{ex}$ activity of soil samples [20]. NB: The results plotted relate to measurements undertaken on individual samples. The uncertainty associated with gamma and alpha spectrometry measurements is reported at 2σ.

3.7. Example of the estimation of supported ^{210}Pb and unsupported $^{210}Pb_{ex}$ from gamma-spectrometry results

This sub-section describes step-by-step how gamma spectrometry can be used to estimate the concentration of supported and unsupported ^{210}Pb in an example of a typical soil sample and illustrates the importance of the equilibration of ^{222}Rn with ^{226}Ra prior to measurement. Firstly, small stones/gravel and visible organic matter were removed from the soil sample. The sample was then milled and sieved. A 60 cm^3 alumina sample holder was used and to prevent ^{222}Rn losses, the sample holder was sealed using two component epoxy glue. The mass of the sample was 30g and its density 0.5 g cm^{-3}. Measurements were carried out using a 30% relative efficiency 'N-type' HPGe detector. The sample distance to the detector was 5 mm. The sample was analysed twice. The spectra collection time was one day (80000 s). The first measurement was undertaken just after the boxing of the sample and the second after 30 days. Spectrum analysis was performed with the WINNER 6.0 software and using external density correction. The gamma rays of 295.24 and 351.92 keV are associated with ^{214}Pb, and the gamma rays of 46.5, 609.36 and 661.62 keV are associated with ^{210}Pb, ^{214}Bi and ^{137}Cs, respectively. The spectra are presented in Fig. 11.

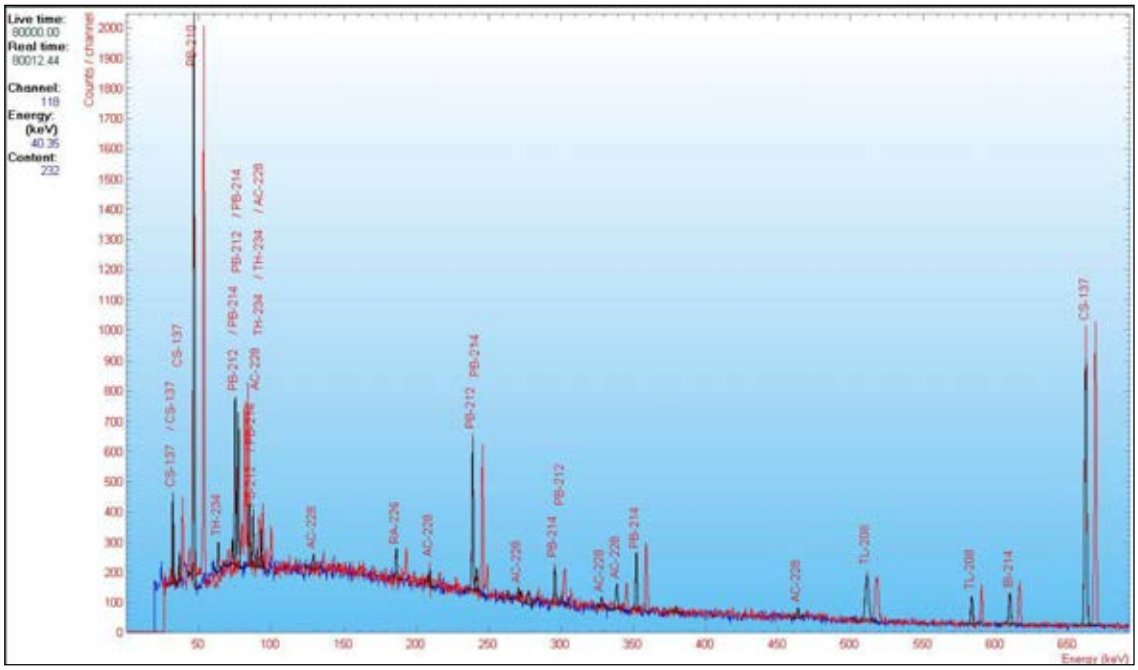

FIG. 11. Example of a gamma spectra before (black) and after (red) reaching the ^{226}Ra – ^{222}Rn equilibrium in a soil sample using "N-type" HPGe detector. Note that spectra are offset for clarity.

During the time elapsed between the two measurements, the intensity of the ^{222}Rn progeny peaks increased slightly (see overlaid spectra in Fig. 11) as reflected in the count numbers of the most important peaks (Table 2). The ^{210}Pb and ^{137}Cs peaks can be used as reference peaks because these areas are independent of the current status of the radioactive equilibrium between ^{226}Ra and its daughters.

TABLE 2. CHANGES IN THE PEAK AREA AFTER A ONE MONTH WAITING PERIOD

Peak energy (keV)	Net peak area on 08.08.2009	Net peak area on 03.09.2009	Difference (counts)	Difference (%)	u (peak area) (%)
46.5	5756	5892	136	2.31	5.2
295.24	339	480	141	29.38	4.6
351.92	620	861	241	27.99	3.4
609.36	290	460	170	36.96	4.7
661.62	4786	4808	22	0.46	1.4

In the case of ^{214}Pb and ^{214}Bi the changes between the two measurements are much stronger than the peak area uncertainty. We can therefore conclude that after processing ^{222}Rn and ^{226}Ra were not in secular equilibrium: ^{222}Rn concentrations were 30–35% below the equilibrium value. To assess the activity concentration of the supported ^{210}Pb, the ^{214}Pb and ^{214}Bi isotopes were used assuming the radioactive equilibrium of the ^{226}Ra and its progeny:

$$A_{^{210}Pb} = A_{^{214}Pb} = A_{^{214}Bi} = A_{^{226}Ra} \quad (5)$$

The unsupported part of the ^{210}Pb isotope is the part in excess of that supported by ^{226}Ra. This value can be obtained from the subtraction of the total ^{210}Pb and the ^{226}Ra (^{214}Pb or ^{214}Bi) activity:

$$A_{^{210}Pb_{ex}} = A_{^{210}Pb_{total}} - A_{^{226}Ra} \quad (6)$$

From the report printed by the software (see Table 2) the total ^{210}Pb was 747 Bq kg^{-1} ± 8.09% (60.4 Bq kg^{-1}) and the ^{214}Pb ~ ^{214}Bi ≈ ^{226}Ra was 23.1 Bq kg^{-1}± 20.2 % (4.7 Bq kg^{-1}) = supported ^{210}Pb. The unsupported part is 747 – 23.1 = 723.9 Bq kg^{-1}. The uncertainty of this part is calculated using the following Equation:

$$u(^{210}Pb_{ex}) = \sqrt{(u_{^{210}Pb_{total}})^2 + (u_{^{226}Ra})^2} \quad (7)$$

$$u(^{210}Pb_{ex}) = \sqrt{(60.4)^2 + (4.7)^2} = 60.58$$

which represents 8.4% when expressed as a percentage.

4. Data treatment

Conversion of ^{210}Pb$_{ex}$ inventories to soil erosion rates follows the same principles of the ^{137}Cs techniques (see Paper 2 of this TECDOC).

In order to derive estimates of soil redistribution rates, a mass balance conversion model can be applied to determinated ^{210}Pb$_{ex}$ inventories obtained for cultivated soils [10]. An adaptation of the diffusion and migration model developed for ^{137}Cs for use in uncultivated areas has also been successfully applied of ^{210}Pb$_{ex}$ inventories obtained from non-cultivated (e.g. pasture and rangeland) areas [69]. The full detailed description of these models including the different parameters needed is given in the Paper 5 of this TECDOC.

The combined use of FRNs should be encouraged to investigate medium- and long-term soil erosion rates in a study area. ^{210}Pb combined with ^{137}Cs can constitute a good approach to show the evolution of soil redistribution linked with land use change and the impact of agricultural practices over the last 100 years. If over this period, there is no soil redistribution variation, the spatial variation of ^{210}Pb$_{ex}$ inventories across a study site should be generally similar to that associated with ^{137}Cs inventories, since they both respond to similar redistribution processes.

An example of the comparison between ^{210}Pb$_{ex}$ and ^{137}Cs inventories in one study field in the UK is given in Fig. 12 [16]. Soil redistribution maps based on ^{137}Cs and ^{210}Pb$_{ex}$ data presented in Fig. 13 show a high degree of similarity, although the maximum rates of erosion estimated from the ^{210}Pb$_{ex}$ data are slightly greater than those generated by ^{137}Cs. A comparison of the estimates of the various soil redistribution rates derived from ^{137}Cs and ^{210}Pb$_{ex}$ determinations is provided in Table 3 [16]. These values also demonstrate close similarities (see also Paper 6 of this TECDOC).

TABLE 3. EXAMPLE OF SOIL REDISTRIBUTION RATE ESTIMATES FOR A STUDY FIELD BASED ON ^{137}Cs AND ^{210}Pb$_{ex}$ [16]

Parameter	^{137}Cs	^{210}Pb$_{ex}$
Percentage area eroding (%)	79	76
Percentage area depositing (%)	20	23
Mean erosion rate for the eroding area (t^{-1} ha^{-1} yr^{-1})	10	15
Mean deposition rate for the deposition zones (t^{-1} ha^{-1} yr^{-1})	7.5	9.5
Net erosion rate for the field (t^{-1} ha^{-1} yr^{-1})	6.5	9
Sediment delivery ratio (%)	81	81

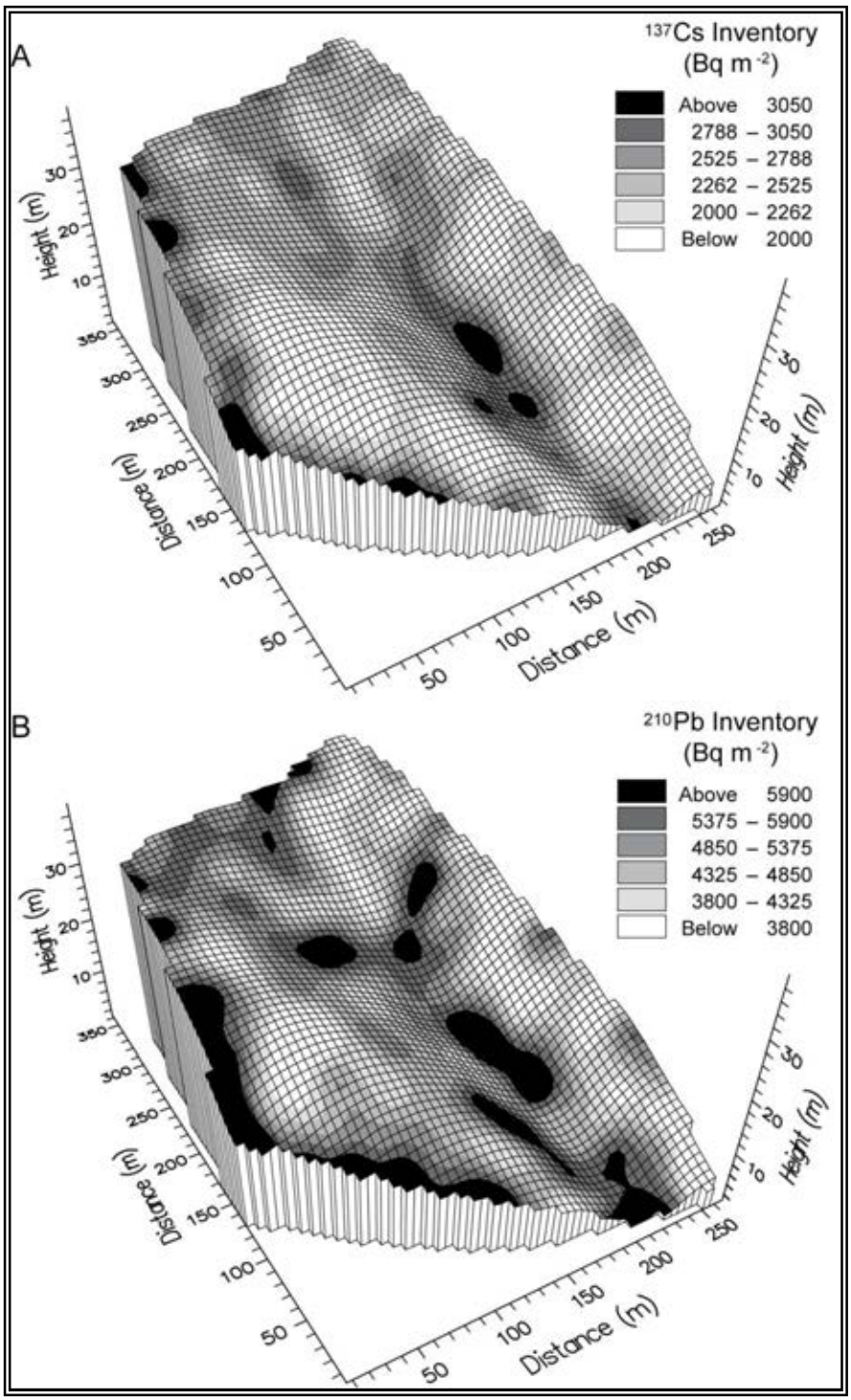

FIG. 12. Distribution of ^{137}Cs (A) and unsupported ^{210}Pb (B) inventories in a cultivated field at Butsford Barton near Colebrooke, Devon, UK [16].

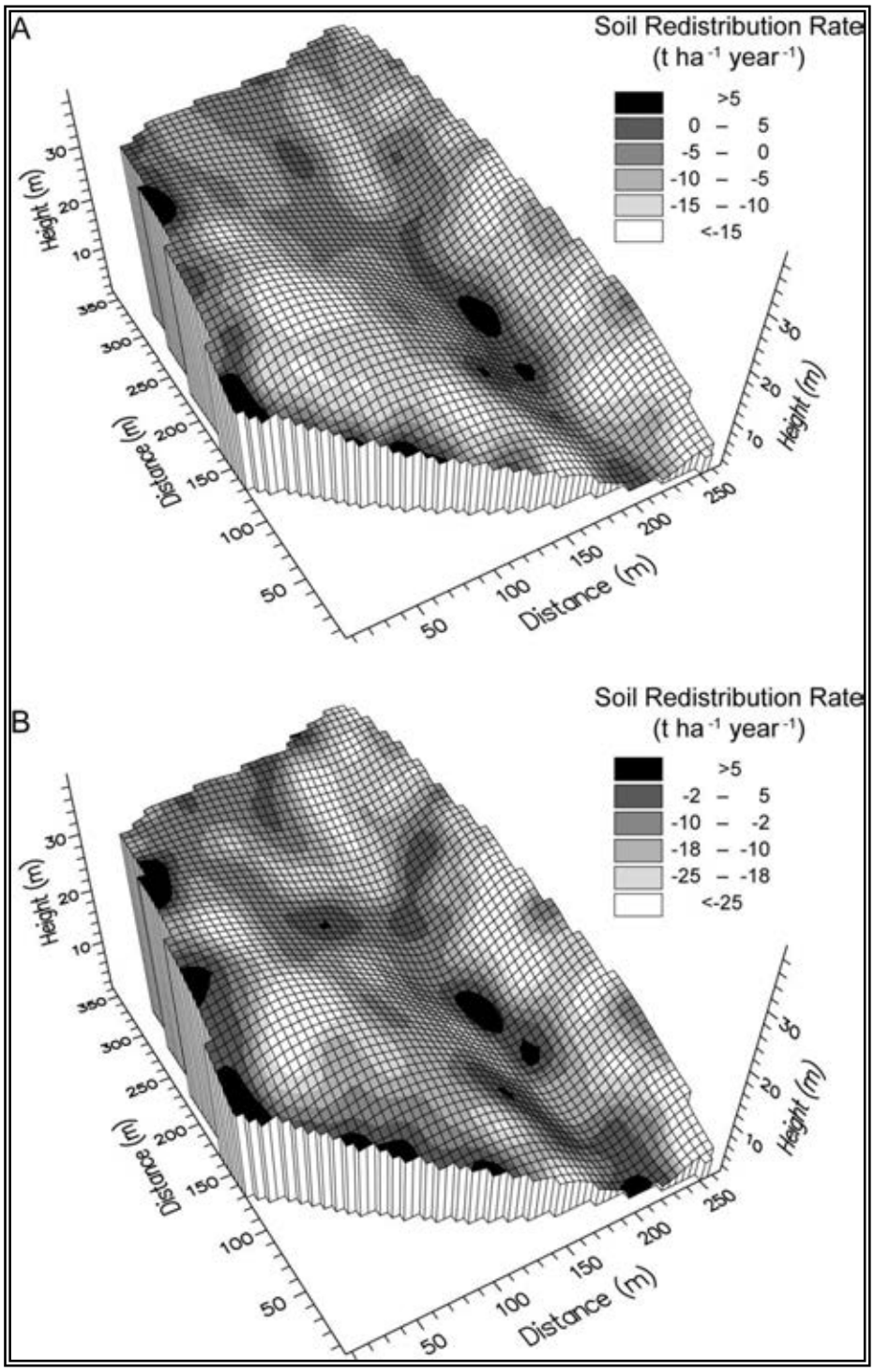

FIG. 13. Distribution of soil redistribution rates estimated using ^{137}Cs (A) and unsupported ^{210}Pb (B) measurements within a cultivated field at Butsford Barton near Colebrooke, Devon, UK [16].

5. A short overview of the use of $^{210}Pb_{ex}$ for establishing the chronology of sediment deposits

The present TECDOC is primarily concerned with the use of fallout radionuclides to study soil erosion/deposition in both cultivated and uncultivated areas. However, as indicated in the introduction, $^{210}Pb_{ex}$ has been extensively used to establish the chronology of sediment deposits and estimating the rate of accumulation of such deposits. This section aims to provide a brief overview of these applications.

The use of $^{210}Pb_{ex}$ to establish the chronology of a sediment deposit and to thereby estimate the sedimentation rate is founded on its fallout source and its known rate of decay ($t_{1/2}$ = 22.26 years). By establishing the rate of decline of $^{210}Pb_{ex}$ activity with depth in the core, it is possible to establish an age-depth relationship and to estimate the rate of sediment accumulation. If accumulation rates are high, the $^{210}Pb_{ex}$ activity will decline slowly with depth. If accumulation rates are low, the $^{210}Pb_{ex}$ activity will reduce rapidly with depth. In order to obtain precise estimates of the age of individual horizons it is necessary to take account of the source of the $^{210}Pb_{ex}$ and the manner of its incorporation into the accumulating sediment. In some situations, the freshly deposited sediment may have a constant $^{210}Pb_{ex}$ activity, but in others, for example where the main source of $^{210}Pb_{ex}$ is fallout to the surface of the water body or sediment surface, the activity of the deposited sediment will be influenced by the rate of sedimentation. In the latter case, a fixed amount of fallout may be mixed with a variable mass of sediment, resulting in a variable $^{210}Pb_{ex}$ activity in the freshly deposited sediment. Several different models have been developed to take account of these complexities when establishing the age-depth relationship. A full discussion of the approach and considerations is given by Appleby [70].

A range of models has been developed for deriving estimates of the age-depth relationship for a sediment core based on the $^{210}Pb_{ex}$ depth profile and the radioactive decay function [70]. The selection of an appropriate model depends on the nature of the sediment body e.g. lake deposits or river floodplain deposits, the environmental conditions and sedimentation processes. Knowledge of the likely behaviour of the sampled sediment is needed to ensure that the correct model is selected. There are a number of important assumptions associated with the approach more generally [71, 72] and these may be summarised as follows:

- $^{210}Pb_{ex}$ is quickly removed from the atmosphere and freshwater and sequestered in soils and sediments;
- $^{210}Pb_{ex}$ is immobile once deposited;
- $^{210}Pb_{ex}$ does not migrate down into the sedimentary column;
- Supported ^{210}Pb is in secular equilibrium with ^{226}Ra;
- $^{210}Pb_{ex}$ is independent of depth.

The most commonly used models are: the CFCS (Constant Flux and Constant Sedimentation Rate) model [1, 73], the CIC (Constant Initial Concentration) model [71] and the Constant Rate of Supply (CRS) model [74]. Descriptions of the models and the associated Equations are reported in the above references and [70]. The main distinction between the latter two models and the first model is that the influx rate of sediment can vary. The CRS model is the most widely accepted and used model. However, in deciding which model to use, consideration must also be given to the possibility that non-linearity in the ^{210}Pb record may be due to a number of other processes such as mixing of the superficial sediments by physical, biological, or chemical processes or interruptions to the normal process of sediment accumulation caused by in-wash or slump events [75]. Where there are significant differences between ^{210}Pb dates estimated by the CRS model and the CIC and CFCS models, the depth

distribution of other artificial fallout radionuclides such as ^{137}Cs and ^{241}Am produced by fallout from the atmospheric testing of nuclear weapons, can provide an independent means for confirming the depth of the sediment deposited in 1963, the year of peak fallout [75].

The models referred to above were developed primarily for use with cores collected from lakes. When attention is directed to sedimentation rates on river floodplains, the processes responsible for incorporating the $^{210}Pb_{ex}$ into the deposited sediment are likely to be more complex. In this case both direct fallout of $^{210}Pb_{ex}$ to the surface of the accreting floodplain and deposition of sediment mobilised from the surface of the upstream catchment during storm events and therefore already containing $^{210}Pb_{ex}$, are likely to be important [11]. In this situation it may be unreasonable to assume a constant flux or rate of supply or a constant initial concentration. A number of additional factors therefore need to be taken into consideration. Whereas the annual input of direct atmospheric fallout of ^{210}Pb to a lake is commonly assumed to be contained within the sediment deposited during that year, in the case of a floodplain, it will be distributed approximately exponentially with depth in the surface horizon of the existing floodplain sediment, which may itself be buried by further accretion during individual flood events [76]. In this case, the average sedimentation rate R (g cm^{-2} yr^{-1}) on the floodplain over the past ca. 100 years can be estimated by distinguishing the input of $^{210}Pb_{ex}$ associated with atmospheric fallout and deposited sediment and focussing on the latter, using the following Equation [11]:

$$R = \lambda_{Pb} \frac{A_{inv} - A_{inv,At}}{C_t} \qquad (8)$$

where:

λ_{Pb} is thedecay constant of ^{210}Pb;
A_{inv} is the $^{210}Pb_{ex}$ inventory (mBq cm^{-2}) determinated for a specific point on a floodplain;
$A_{inv,\,At}$ is the local fallout $^{210}Pb_{ex}$ inventory (mBq cm^{-2}), established by analysing soil samples collected from undisturbed land close to the floodplain above the inundation level;
C_t is the initial $^{210}Pb_{ex}$ concentration (mBq g^{-1}) in catchment-derived sediment.

This approach also has the advantage that only a single determination of the total $^{210}Pb_{ex}$ inventory of a floodplain core, rather than information on the depth distribution of $^{210}Pb_{ex}$ activity, is required. In addition, since only the total inventory of the sediment core is measured, the potential effects of biological activity in causing mixing within the sediment column and thus perturbing the $^{210}Pb_{ex}$ depth distribution are unimportant.

REFERENCES

[1] APPLEBY, P.G., OLDFIELD, F., The calculation of lead-210 dates assuming a constant rate supply of unsupported ^{210}Pb to the sediment, Catena 5 (1978) 1–8.

[2] ROBBINS, R.A., "Geochemical and geophysical application of radioactive lead", The Biogeochemistry of Lead in the Environment (NRIAGU, J.O., Ed.), Elsevier, Amsterdam (1978) 286–383.

[3] WISE, S.M., "Caesium-137 and Lead-210: a review of techniques and some applications in geomorphology", Timescales in Geomorphology, (CULLINGFORD, R.A., DAVIDSON, D.A., LEWIN, J., Eds), Wiley, New York (1980) 109–127.

[4] BENNINGER, L.K., KRISHNASWAMI, S., Sedimentary processes in the inner New York Bight: evidence from excess ^{210}Pb and ^{239,240}Pu, Earth Planet. Sci. Lett. 53 (1981) 158–174.
[5] OLDFIELD, F., APPLEBY, P.G., "The role of ^{210}Pb dating in sediment based erosion studies", Drainage Basin Erosion and Sedimentation, A conference on Erosion, Transportation and Sedimentation in Australian Drainage Basins, Newcastle, NSW (1984) 175–182.
[6] ROBBINS, R.A., MURDOCH, A., OLIVER, B.G., Transport and storage of ^{137}Cs and ^{210}Pb in sediments of lake St. Clair, Can. J. Fish. Aquat. Scie. 47 (1990) 572–587.
[7] ABRIL, J.M., GARCÍA-LEON, M., GARCÍA-TENORIO, R., SÁNCHEZ, C.I., EL-DAOUSHY, F., Dating of marine sediments by an incomplete mixing model, J. Environ. Radioact. 15 (1992) 135–151.
[8] WALLBRINK, P.J., OLLEY, J.M., HANCOCK, G., Estimating residence times for fine sediment in river channels using fallout Pb-210, IAHS Publ. 276 (2002) 425–433.
[9] WALLING, D.E., HE, Q., Rates of overbank sedimentation on the flood plains of several British rivers during the past 100 years, IAHS Publ. 224 (1994) 203–210.
[10] WALLING, D.E., HE, Q., Using fallout lead-210 measurements to estimate soil erosion on cultivated land, Soil Sci. Soc. Am. J. 63 (1999) 1404–1411.
[11] HE, Q., WALLING D.E., Use of fallout Pb-210 to investigate longer-term rates and patterns of overbank sediment deposition on the floodplains of lowland rivers, Earth Surf. Process. Landf. 21(1996) 141–154.
[12] BENMANSOUR, M., et al., "Distribution of anthropogenic radionuclides in Moroccan coastal waters and sediments", Radioactivity in the Environment - Book series– 8 (2006)145–150.
[13] LAISSAOUI, A., et al., Anthropogenic radionuclides in the water column and a sediment core from the Alboran Sea: Application to radiometric dating and reconstruction of historical water column radionuclide concentrations, J. Paleolimnol. 40 (2008) 823–833.
[14] SIMMS, A.D., et al., Use of ^{210}Pb and ^{137}Cs to simultaneously constrain ages and sources of post-dam sediments in the Cordeaux reservoir, Sydney, Australia, J. Environ. Radioact. 99 (2008) 1111–1120.
[15] HE, Q., OWENS, P.N., "Determination of suspended sediment provenance using caesium-137, unsupported lead-210 and radium-226: a numerical mixing model approach", Sediment and Water Quality in River Catchments, (FOSTER, I.D.L., GURNELL, A.M., WEBB, B.W., Eds), Wiley, Chichester (1995) 207–227.
[16] WALLING, D.E., HE, Q., QUINE, T., Use of caesium-137 and lead-210 as tracers in soil erosion investigation, IAHS Publ. 229 (1995) 163–172.
[17] HE, Q., WALLING, D.E., The distribution of fallout ^{137}Cs and ^{210}Pb in undisturbed and cultivated soils, Appl. Radiat. Isot. 48 (1997) 677–690.
[18] WALLING, D.E., HE, Q., "Changing rates of overbank sedimentation on the floodplains of British rivers over the past 100 years", Fluvial Processes and Environmental Change, (BROWN, A.G., QUINE, T.A., Eds), Wiley, Chichester (1999) 207–222.
[19] INTERNATIONAL ATOMIC ENERGY AGENCY, Rep. of the Third Research Co-ordination Meeting of the Coordinated Research Project "Assess the effectiveness of soil conservation techniques for sustainable watershed management using fallout radionuclides" Vienna, Austria (2006) 134.
[20] MABIT, L., BENMANSOUR, M., WALLING, D.E., Comparative advantages and limitations of the fallout radionuclides ^{137}Cs, ^{210}Pb$_{ex}$ and ^{7}Be for assessing soil erosion and sedimentation, J. Environ. Radioact. 99 (2008) 1799–1807.

[21] PREISS, N., MELIÉRÈ, M., POURCHET, M., A compilation of data on lead-210 concentration in surface air and fluxes at the air-surface and water-sediment interfaces, J. Geophys. Res. 101 (1996) 28847–28862.
[22] CRLFFSD, Central Radioanalytical Laboratory of Food and Feed Safety Directorate - Hungarian Agricultural Authority, Radioanalytical Monitoring Network of Ministry of Agriculture and Rural Development, Annual Rep. (2006).
[23] AHMED, A.A., et al., Seasonal variations of aerosol residence time in the lower atmospheric boundary layer, J. Environ. Radioact.77 (2004) 275–283.
[24] WINKLER, R., ROSNER, G., Seasonal and long-term variation of ^{210}Pb concentration in air, atmospheric deposition rate and total deposition velocity in south Germany, Sci. Total Environ. 263 (2000) 57–68.
[25] BASKARAN, M., A search of seasonal variability on the depositional fluxes of ^{7}Be and ^{210}Pb, J. Geophys. Res. 100 (D2) (1995) 2833–2840.
[26] CAILLET, S., ARPAGAUS, P., MONNA, F., DOMINIK, J., Factors controlling ^{7}Be and ^{210}Pb atmospheric deposition as revealed by sampling individual rain events in the region of Geneva, Switzerland, J. Environ. Radioact. 53 (2001) 241–256.
[27] TUREKIAN, K.Y., NOZAKI, Y., BENNINGER, L.K., Geochemistry of atmospheric radon and radon products, Ann. Rev. Earth Planet. Sci. 5 (1977) 227–255.
[28] APPLEBY, P.G., OLDFIELD, F., "Application of lead-210 to sedimentation studies", Uranium-Series Disequilibrium: Application to Earth, Marine and Environment Sciences, (IVANOVICH, M., HARMAN, R.S., Eds), Clarendon Press, Oxford (1992) 731–738.
[29] VAN HOOF, P.L., ANDREN, A.W., Partitioning and transport of ^{210}Pb in lake Michigan, J. Great Lakes Res. 15 (1989) 498–509.
[30] HE, Q., WALLING, D.E., Interpreting particle size effects in the adsorption of ^{137}Cs and unsupported ^{210}Pb by mineral soils and sediments, J. Environ. Radioact. 30 (1996) 117–137.
[31] STRAWN, D.G., SPARKS, D.L., The use of XAFS to distinguish between inner-and outer-sphere lead adsorption complexes on montmorillonite, J. Colloid Interf. Sci. 216 (1999) 257–269.
[32] STRAWN, D.G., SPARKS, D.L., Effect of soil organic matter on the kinetics and mechanism of Pb (II) sorption and desorption in soil, Soil Sci. Soc. Am. J. 64 (2000) 144–156.
[33] TRIVEDI, P., DYER, J.A., SPARKS, D.L., Lead sorption onto ferrihydrite. 1. A macroscopic and spectroscopic assessment, Environ. Sci. Technol. 37 (2003) 908–914.
[34] BRADL, H.B., Adsorption of heavy metal ions on soils and soils constituents, J. Colloid Interface Sci. 277 (2004) 1–18.
[35] EVANS, L.J., Chemistry of metal retention by soils, Environ. Sci. Technol. 23 (1989) 1046–1059.
[36] KLAMINDER, J., et al., Estimating the mean residence time of lead in the organic horizon of boreal forest soils using 210-lead, stable lead and a soil chronosequence, Biogeochem. 78 (2006) 31–49.
[37] KLAMINDER, J., BINDLER, R., EMTERYD, O., RENBERG, I., Uptakes and recycling of lead by boreal forest plants: Quantitative estimates from a site in northern Sweden, Geochim. Cosmochim. Acta, 69 (2005) 2485–2496.
[38] KLAMINDER, J., YOO, K., Contaminants as tracers for studying dynamics of soil formation: Mining an ocean of opportunities, Adv. Agron. 100 (2008) 15–57.
[39] OWENS, P.N., WALLING, D.E., HE, Q. The behaviour of bomb-derived caesium-137 fallout in catchment soils, J. Environ. Radioact. 32 (1996) 169–191.
[40] BENMANSOUR, M., et al., "Estimates of long and short term soil erosion rates on farmland in semi-arid West Morocco using caesium-137, excess lead-210 and

beryllium-7 measurements", Impact of Soil Conservation Measures on Erosion Control and Soil Quality, IAEA-TECDOC-1665, IAEA, Vienna (2011) 159–174.
[41] GRAHAM, I.J, DITCHBURN, R.G., BARRY, B.J., ^{210}Pb-^{137}Cs dating of glacial lake sediments, New Zeal. Sci. Rev. 61 (2004) 45–47.
[42] GOLOSOV, V.N., BELYAEV, V.R., MARKELOV, M.V., IVANOVA, N.N., KUZNETSOVA, Y.S., "Application of the radionuclide technique and other methods for assessing the effectiveness of soil conservation measures at the Novosil study site, Orel region, Central Russia", Impact of Soil Conservation Measures on Erosion Control and Soil Quality, IAEA-TECDOC-1665, IAEA, Vienna (2011) 131–157.
[43] MABIT, L., KLIK, A., BENMANSOUR, M., TOLOZA, A., GEISLER A., GERSTMANN, U.C., Assessment of erosion and deposition rates within an Austrian agricultural watershed by combining ^{137}Cs, ^{210}Pb$_{ex}$ and conventional measurements, Geoderma 150 (2009) 231–239.
[44] CANBERRA, Website http://www.Canberra.com. (2010).
[45] ORTEC, Websitehttp://ortec-online.com. (2010).
[46] BOSHKOVA, T., MINEV, L., Correction for self-attenuation in gamma-ray spectrometry of bulk samples, Appl. Radiat. Isot. 54 (2001) 777–783.
[47] SAN MIGUEL, E.G., PEREZ-MORENO, J.P., BOLIVAR, J.P., GARCIA-TENORIO, R., MARTIN, J.E., ^{210}Pb determination by gamma spectrometry in voluminal samples (cylindrical geometry), Nucl. Instrum. Methods Phys. Res., Sect. A, 493 (2002) 111–120.
[48] QUINDOS, L.S., et al., Correction by self-attenuation in gamma-ray spectrometry for environmental samples, J. Radioanal. Nucl. Chem. 270 (2006) 339–343.
[49] JODLOWSKI, P., Self-absorption correction in gamma-ray spectrometry of environmental samples - an overview of methods and correction values obtained for the selected geometries, Nukleonika 51 (2006) S21-S25.
[50] JODLOWSKI, P., Correction factors to account for minor sample height variations in gamma-ray spectrometry, Nucl. Instrum. Methods Phys. Res. Sect. A, 580 (2007) 238–241.
[51] KHATER, A.E.M., EBAID, Y.Y., A simplified gamma-ray self-attenuation correction in bulk samples, Appl. Radiat. Isot. 66 (2008) 407–413.
[52] SAIDOU, F.B, LAEDERMANN, J.P., BUCHILLIER, T., MOISE, K.N., FROIDEVAUX, P., Calibration of an HPGe detector and self-attenuation correction for ^{210}Pb: Verification by alpha spectrometry of ^{210}Po in environmental samples, Nucl. Instrum. Methods Phys. Res., Sect. A, 578 (2007) 515–522.
[53] ROBU, E., GIOVANI, C., Gamma-ray self-attenuation corrections in environmental samples, Roman. Rep. Phys. 61 (2009) 295–300.
[54] CUTSHALL, N.H., LARSEN, I.L., OLSEN, C.R., Direct analysis of ^{210}Pb in sediment samples: self-absorption corrections, Nucl. Instrum. Methods Phys. Res. 206 (1983) 309–312.
[55] WALLBRINK, P.J., WALLING, D.E., HE, Q., "Radionuclide measurements using HpGe gamma spectrometry", Handbook for the Assessment of Soil Erosion and Sedimentation Using Environmental Radionuclides, (ZAPATA, F., Ed.), Kluwer, Dordrecht (2002) 67–96.
[56] THE NATIONAL INSTITUTE OF STANDARDS ANDTECHNOLOGY, web site (2010) http://www.nist.gov/index.html
[57] AMERSHAM, Website (2010) http://www6.gelifesciences.com
[58] HULT, M., Low-level gamma spectrometry using Ge-detectors, Metrologie (2007) 87–S94.
[59] ISO/IEC, General Requirements for the Competence of Testing and Calibration Laboratories. Rep. 17025:2005, ISO, Geneva, Switzerland (2005).

[60] INTERNATIONAL ATOMIC ENERGY AGENCY, Rep. of the First Research Co-ordination Meeting of the Coordinated Research Project "Assess the effectiveness of soil conservation techniques for sustainable watershed management using fallout radionuclides", IAEA-311-D1-RC-888, IAEA, Vienna (2003) 82.
[61] SHAKHASHIRO, A., MABIT, L., Results of an IAEA inter-comparison exercise to assess ^{137}Cs and total ^{210}Pb analytical performance in soil, Appl. Radiat. Isot. 67 (2009) 139–146.
[62] INTERNATIONAL ATOMIC ENERGY AGENCY, Proficiency Test on the Determination of ^{137}Cs and ^{210}Pb in Spiked Soil, IAEA/AL/166, IAEA-CU-2006-02, IAEA, Vienna (2006) 51.
[63] MARTEN, R., Procedures for routine analysis of naturally occurring radio-nuclides in environmental samples by gamma ray spectrometry with HPGe detectors, Internal Rep. IR 76, Supervising Scientist for the Alligators Rivers Region, Jabiru (1993) JH/03/019.
[64] MURRAY, A.S., MARTEN, R., JOHNSTON, A., MARTIN, P., Analysis for naturally occurring radionuclides at environmental concentrations by gamma spectrometry. J. Radioanal. Nucl. Chem. 115 (1987) 263–288.
[65] INTERNATIONAL ATOMIC ENERGY AGENCY, Development and Use of Reference Materials and Quality Control Materials, IAEA-TECDOC-1350, IAEA, Vienna (2003) 113.
[66] INTERNATIONAL ATOMIC ENERGY AGENCY, Quantifying Uncertainty in Nuclear Analytical Measurements, IAEA TECDOC-1401, IAEA, Vienna (2004) 247.
[67] JIA, G., TORRI, G., Determination of ^{210}Pb and ^{210}Po in soil or rock samples containing refractory matrices, Appl. Radiat. Isot. 65 (2007) 1–8.
[68] ZABORSKA, A., CAROLL, J., PAPUCCI, C., PEMPKOWIAK, J., Intercomparison of alpha and gamma spectrometry techniques used in ^{210}Pb geochronology, J. Environ. Radioact. 93 (2007) 38–50.
[69] WALLING, D.E., COLLINS, A.L., SICHINGABULA, H.M., Using unsupported lead-210 measurements to investigate soil erosion and sediment delivery in a small Zambian catchment, Geomorphology. 52 (2003) 193–213.
[70] APPLEBY, P.G., "Chronostratigraphic techniques in recent sediments", Tracking Environmental Change using Lake Sediments, Volume 1, Basin Analysis, Coring, and Chronological Techniques, (LAST, W.L., SMOL, J.P., Eds), Kluwer, Dordrecht (2001) 171–203.
[71] PENNIGTON, W., TUTIN, T.C., CAMBRAY, R.S, EAKINS, J.D., HARKNESS, D.D., Radionuclide dating of recent sediments of Bleham Tarn, Freshwater Biol. 6 (1976) 317–331.
[72] NOLLER, J.S., "Lead-210 geochronology", Quaternary Geochronology: Methods and applications, American Geophysical Union, Washington (2000) 115–120.
[73] KRISHNASWAMI, S.D., LAL, D., MARTIN, J.M., MEYBECK, M., Geochronology of lake sediments, Earth Planet. Sci. Lett. 11 (1971) 407–414.
[74] APPLEBY, P.G., OLDFIELD, F., The assessment of ^{210}Pb from sites with varying sediment accumulations rates, Hydrobiol. 103 (1983) 29–35.
[75] WALLING, D.E., HE, Q., APPLEBY, P.G., "Conversion models", Handbook for the Assessment of Soil Erosion and Sedimentation Using Environmental Radionuclides, (ZAPATA, F., Ed.), Kluwer, Dordrecht, The Netherlands (2002) 111–162.
[76] HE, Q., Interpretation of Fallout Radionuclide Profiles in Sediments from Lake and Floodplain Environment, Ph. D Thesis, University of Exeter, UK (1993).

THE USE OF ^{7}Be AS A SHORT TERM SOIL REDISTRIBUTION TRACER

L. MABIT, A. TOLOZA
Soil and Water Management and Crop Nutrition Subprogramme, Joint FAO/IAEA Division of Nuclear Techniques in Food and Agriculture,
Vienna - Seibersdorf

M. BENMANSOUR
Centre National de l'Energie, des Sciences et des Techniques Nucléaires (CNESTEN)
Rabat, Morocco

W.H. BLAKE, A. TAYLOR
School of Geography, Earth and Environmental Sciences, Consolidated Radioisotope Facility (CORIF), University of Plymouth,
Plymouth, United Kingdom

S. TARJAN
Radioanalytical Reference Laboratory, Central Agricultural Office Food and Feed Safety Directorate
Budapest, Hungary

D.E. WALLING
Geography, College of Life and Environmental Sciences, University of Exeter,
Exeter, United Kingdom

Abstract

Beryllium-7 (^{7}Be) is a naturally occurring cosmogenic radionuclide produced in the stratosphere and troposphere and delivered to the Earth surface via wet and dry fallout. Comparison of global inventory measurements shows correlation with total precipitation. Its strong association with soil particles and short half-life of 53 days means that it is well suited to trace short-term (up to 6 months) soil and sediment redistribution processes. As with fallout ^{137}Cs and ^{210}Pb, soil redistribution estimates are based on a comparison of the total inventory at an eroding or deposition point to a reference site that has been stable, in the case of ^{7}Be, for more than 5 half-lives prior to the study. Key assumptions required and associated considerations when adopting ^{7}Be as a soil erosion tracer are explored in this paper. Theoretically, stable, eroding and aggrading sites should be clearly distinguishable in terms of the vertical depth profile distribution of ^{7}Be and the shape of the depth distribution is central to conversion of inventory to soil erosion estimates. It is proposed that application of ^{7}Be in a wider range of environments will lead to continued development and testing of conversion models for ^{7}Be for assessment of the impact of short-term changes in land use practices and the effectiveness of soil conservation measures for sustainable catchment management. Guidance is given in this paper on sampling strategies, sampling methods, sample preparation and analysis prior to conversion to soil redistribution estimates.

1. Origin and environmental behavior of ^{7}Be

1.1. Beryllium

Beryllium (Be) is a bivalent element with an atomic number of 4 and an atomic weight of 9. Beryllium belongs to the alkaline earth metal group. Beryllium is the 35th most abundant element in the Earth's crust, with an average content of about 6 mg kg^{-1} [1]. In its stable form, it is an essential constituent of about 100 out of about 4000 known minerals (e.g. Beryl) and is widely distributed in soils at low concentrations [2]. Beryllium has seven isotopes, of which only ^{9}Be (100% natural abundance) is stable. Beryllium has two main isotopes, ^{10}Be and ^{7}Be, which are both of cosmogenic origin. Beryllium-10 (half-life = 1.51 x 10^{6} yrs) and its daughter products have been used for measuring longer-term rates (over millennia) of physical erosion, chemical weathering [3-5], as well as variations in solar activity, age of ice cores dating [6], and global transport of air masses [7, 8]. As a short-lived fallout radionuclide, ^{7}Be offers the potential to trace soil redistribution over the short-term.

1.2. ^{7}Be production and fallout

^{7}Be ($t_{1/2}$ = 53.12 days) is a naturally occurring cosmogenic radionuclide produced in the stratosphere and troposphere as a result of nitrogen and oxygen spallation. Rates of production are dependent upon solar activity [9], and can therefore be influenced by latitude with increased production occurring at the poles owing to cosmic ray deflection towards polar regions. Production is also affected by altitude with higher levels of production occurring in the stratosphere than in the troposphere [10]. Variation according to the 11-year solar cycle can also occur with reduced production during the solar maximums owing to reduced flux of cosmic rays to the Earth's atmosphere [2]. Following its formation, ^{7}Be becomes associated with aerosols and is therefore subjected to atmospheric transport processes which can exhibit seasonal variations. Higher rates of ^{7}Be production in the stratosphere and longer residence times create a stratosphere-troposphere concentration gradient [11], and this gradient can be reduced during folding of the tropopause which encourages exchange of ^{7}Be from the stratosphere to the upper troposphere; this process is enhanced during the spring months at mid-latitudes [12, 13]. Vertical mixing within the troposphere may also occur through convective circulation during warmer months, which transports ^{7}Be enriched air from the upper troposphere to the lower troposphere [10, 14]. ^{7}Be is removed from the troposphere by wet scavenging [15] leading to depletion of concentrations during periods of increased precipitation. Concentrations in surface air masses can also, therefore, be influenced by seasonal climatic conditions [10]. An example of the seasonal variability of ^{7}Be is illustrated in Fig. 1 which represents the variation of ^{7}Be concentration (mBq m^{-3}) in the atmosphere in Budapest, Hungary, during the period 1999-2006 under a monitoring programme of radionuclides undertaken by the Central Radioanalytical Laboratory of Food Feed Safety Directorate - Hungarian Agricultural Authority [16]. ^{7}Be activities were measured by gamma spectrometry in aerosol samples collected by a high volume aerosol sampler (40 000 m^{3} $week^{-1}$) through a HEPA-5300 polypropylene filter designed directly for this type of sampling. Filters were measured after three days cooling time on a low background ''N-type'' HPGe γ-spectrometry system (acquisition time = 25 0000 s). From 1999 to 2006, the ^{7}Be concentration in the Budapest air ranged from 0.74 to 7.35 Bq kg^{-1}. High concentrations were generally obtained in spring and summer seasons (Fig. 1).

Wet deposition is the dominant pathway of ^{7}Be delivery to the Earth's surface with dry deposition accounting for around 10% to total fallout [15, 17, 18]. On an event basis,

deposition is correlated to the amount of rainfall received, and therefore seasonal depositional fluxes are closely correlated to rainfall with increases in surface inventories reflecting monthly rainfall volumes [17-19]. Activity concentrations in rainfall are not constant during an event with higher ^{7}Be concentrations often found at the start of an event reflecting washout from the troposphere [17]. Although low rainfall events have been found to exhibit higher ^{7}Be activity [12] concentrations are, however, found to be poorly correlated with rainfall volumes and shown to be independent of rainfall intensity [17, 19]. A complex combination of factors including solar activity, stratosphere-troposphere exchange and varying climatic conditions can therefore influence depositional fluxes by determining the concentration of ^{7}Be available for scavenging in the troposphere. This is highlighted in the range of rainfall concentration and depositional values detailed below and outlined in Table 1.

Rainfall activity concentrations for southeast Australia have been reported as ranging from 0.02 ± 0.003 to 5.9 ± 0.93 Bq L^{-1} [17], and within this range Ayub et al. [19] reported 0.7 ± 0.3 to 3.2 ± 0.7 Bq L^{-1} for a region of Argentina. These values correspond to northern hemisphere findings of 1.23 to 3.55 Bq L^{-1} reported by Short et al. [20] for the north of England. Annual deposition values for Australia have been reported as 1030 ± 100 Bq m^{-2} yr^{-1} [17], and 1070 ± 100 to 1362 ± 100 Bq m^{-2} yr^{-1} [18]. An annual depositional flux for Granada, Spain has been reported as 469 ± 145 Bq m^{-2} yr^{-1} [21]. Event depositional fluxes have a wide range with values between 0.03 to 108 Bq m^{-2} [17] and 1.1 to 120 Bq m^{-2} [19]. Net cumulative ^{7}Be surface inventories can be calculated by considering depositional fluxes and accounting for radioactive decay; A monthly cumulative inventory range of 180 to 540 Bq m^{-2} over a six year period was reported in Brisbane, Australia [18]. This is comparable to the inventory range of approximately 100 to 533 Bq m^{-2} reported for a winter period in southwest England [22].

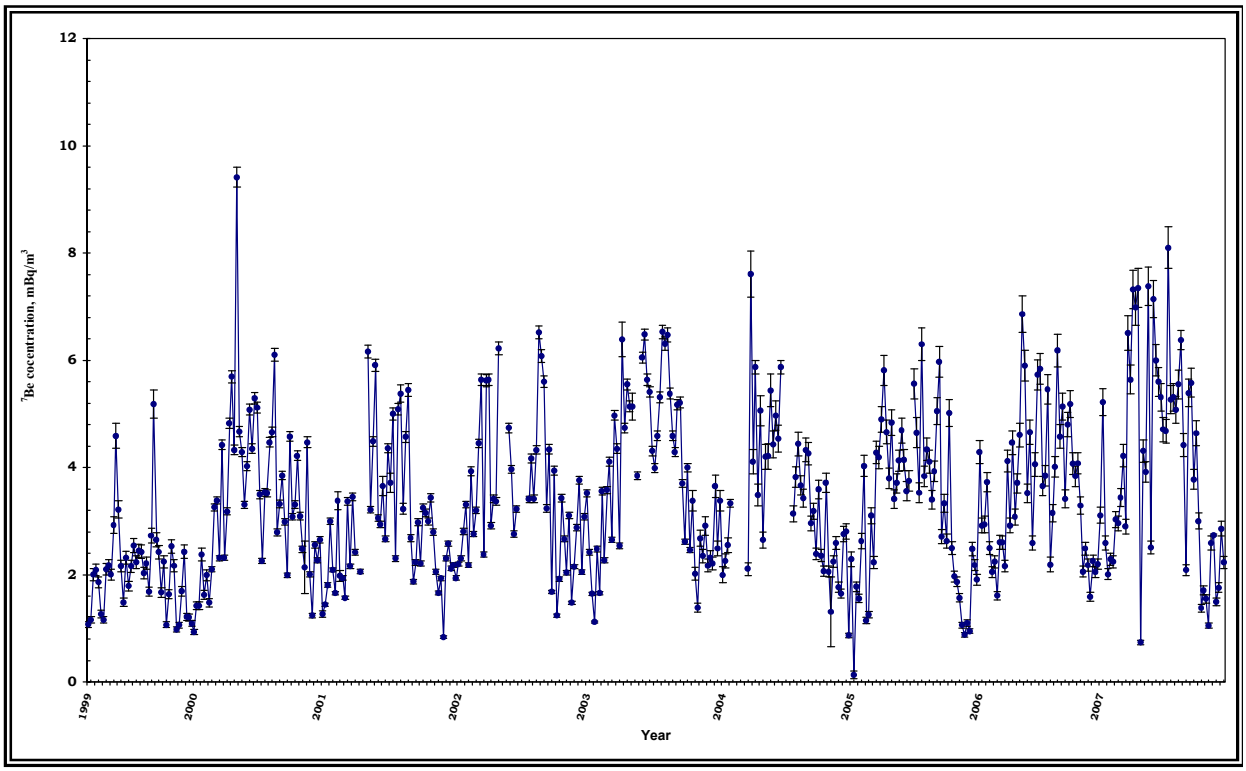

FIG. 1. Variation of ^{7}Be activity concentration in air at Budapest, Hungary from 1999 to 2007.

1.3. Geochemical behaviour of ^{7}Be in soil

Geogenic stable Be in soil material is largely present in oxide forms although it may be associated with carbonate complexes under alkaline conditions [3, 23]. Fallout ^{7}Be is delivered to the Earth's surface primarily in the form of Be^{2+}; owing to a high charge to radius ratio, Be^{2+} is highly competitive for particle exchange sites, and therefore demonstrates rapid adsorption upon contact with sediment particles [2]. This is reflected in ^{7}Be partition coefficient (K_d) values in excess of 10^4 under experimental and field conditions [24-26]. Variations in ^{7}Be K_d as a function of sediment type and pH have been demonstrated [27], showing a reduction in adsorption (and thus, K_d) under acidic conditions. Similar to many metals, ^{7}Be has an affinity with fine sediment fractions (< 63 μm) [28], and is likely to be associated with Fe/Mn and organic components of the soil matrix [29, 30]. Bioaccumulation of ^{7}Be in plants is unlikely to be the result of root uptake owing to shallow depth profiles exhibited by the radionuclide. Foliar interception of ^{7}Be fallout [31] and subsequent incorporation into the leaf structure is likely to be the main pathway for accumulation in flora. Once within the plant matrix, the mobility of ^{7}Be in representative natural solution is limited [23].

Table 1. Annual average ^{7}Be depositional fluxes and rainfall at different locations with comparable latitudes (Adapted from [21, 32])

Fallout (Bq m^{-2} y^{-1})	Location	Latitude	Rainfall (mm)	Reference
412	Malaga, Spain	36º N	308	[33]
469	Granada, Spain	37º N	452	[21]
528	Damascus, Syria	33º N	153	[34]
867	Arkansas, USA	38º N	1070	[35]
898	Chilton, UK	51º N	822	[36]
1030	Canberra, Australia	35º S	660	[17]
1249	Heidelberg, Germany	52º N	810	[37]
1267	Bombay, India	19º N	2277	[38]
1618	Milford Haven, UK	51º N	1328	[36]
2133	New Hamsphire, USA	41.5º N	na	[39]
2625	Devon, UK	51º N	901	[40]
2767	Massachusetts, USA	43º N	na	[39]
2850	Bermuda	33º N	1700	[41]
2968	Galvetson, Texas, USA	29º N	1390	[42]
3780	New Haven, Connecticut, USA	41º N	1240	[41]

na = data not available

1.4. ^{7}Be distribution in the soil profile

^{7}Be has been shown to have a strong affinity for most soils [43]. As a result ^{7}Be fallout is quickly and strongly fixed within the top few centimeters of the soil and the depth distribution is commonly characterized by an exponential decrease in activity with depth [44]. Because of its short half-life there is little opportunity for subsequent downward transfer and, if it is

found to greater depths, this is normally linked to downward transfer of soil particles by infiltrating rainwater via cracks and macropores, bio-perturbation and/or cultivation processes [31]. In the absence of significant vertical translocation, it is expected that the majority of the ^{7}Be will be found in the top 1 to 2 cm of the soil. In a recent study in Morocco, for example, the maximum depth of occurrence of ^{7}Be was 1.9 cm [45]. Because of its shallow distribution with the soil profile a special sampling device that allows the collection of very thin layers of soil (1-3 mm) is required to document the depth distribution. There are two ways to present the ^{7}Be soil profile distribution: (i) ^{7}Be mass activity concentration (Bq kg^{-1}) vs. depth and (ii) ^{7}Be areal activity density (Bq m^{-2}) vs. depth (also referred to as the inventory). For many purposes, it is preferable to express depth in terms of mass depth (kg m^{-2}), since this takes account of variations in the bulk density of individual depth increments.

Theoretically, stable, eroding and aggrading sites should be clearly distinguishable in terms of both their total inventory and the vertical profile distribution. The decline of activity concentration and areal activity density with depth has been shown in many studies to be approximately exponential in form [22, 46]. At sites that have experienced soil erosion, loss of ^{7}Be labelled soil from the surface will remove the upper section of the exponential profile leading to a reduction in overall inventory. In contrast, at downslope aggrading sites, addition of ^{7}Be labelled soil at the surface will lead to an increased inventory and non-exponential upper section to the depth profile, with the buried fallout profile underneath. Examples of typical ^{7}Be profile distributions in Chilean [47] and UK soils [48] are provided in Fig. 2 and 3, respectively.

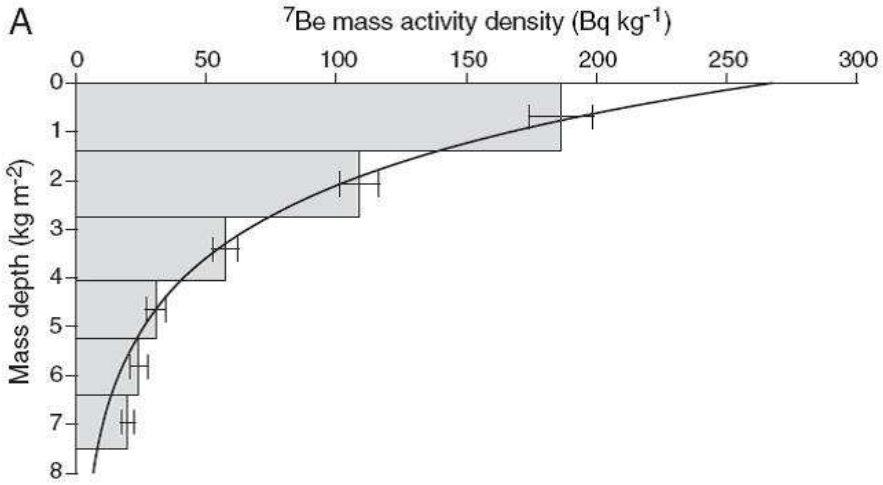

FIG. 2. Typical ^{7}Be depth profiles in a Chilean soil in a stable undisturbed site [47].

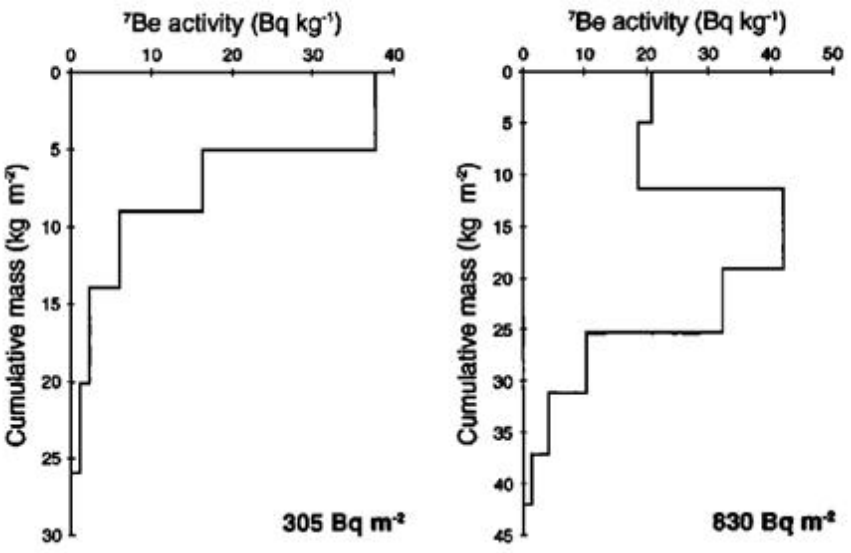

FIG. 3. Typical ^{7}Be profiles in UK associated with a) an eroding site b) an aggrading site [48].

1.5. Key considerations for use of ^{7}Be as a soil erosion tracer

The principles underlying the application of ^{7}Be in soil erosion measurements are essentially the same as those associated with the use of ^{137}Cs and $^{210}Pb_{ex}$ for estimating soil redistribution rates. While the ^{137}Cs data represent a retrospective assessment of mid-term soil redistribution (last 40-50 years) the ^{7}Be data are related to a particular event or series of events under investigation. By comparing the ^{7}Be inventories, or aerial activity density, (Bq m^{-2}) of selected sampling points in the study area with that of an adjacent reference inventory, erosional and depositional sites can be identified and rates of erosion and deposition estimated by using the appropriate conversion model (see Paper 5 of this TECDOC).

The potential to document the erosion and sedimentation rates associated with individual events and to thereby investigate the effectiveness of recent soil conservation practices or particular rainfall event impacts on agricultural land represents the major advantage of ^{7}Be over the assessments of longer-term erosion rates provided by ^{137}Cs or $^{210}Pb_{ex}$, although the latter will frequently provide an important longer-term context which can be beneficial when assessing the impacts of recent changes in soil management practice.

Key considerations when using ^{7}Be to assess soil redistribution include the following [45]:

(a) As traditionally applied, the use of ^{7}Be to document short-term soil redistribution rates focuses on individual events or short periods of heavy rainfall and involves a number of important assumptions. These include, firstly, that the input of ^{7}Be associated with the erosional event is spatially uniform, and, secondly, that any pre-existing ^{7}Be is uniformly distributed across the area under investigation [22]. The first assumption is commonly met at the scale of the individual field. The second assumption is frequently more difficult to meet. The necessary uniform spatial distribution of pre-existing ^{7}Be can generally be found in three situations; firstly, after a long dry period, when any pre-existing spatial variability of the ^{7}Be inventory will have been removed by radioactive decay, secondly, after an extended period with low intensity rainfall that has not resulted in erosion and soil redistribution and therefore redistribution of the existing ^{7}Be fallout input, or, thirdly, after a field has been ploughed and the existing

^{7}Be has been mixed within the plough layer and the activity is below the level of detection. As a more recent extension of the approach, the timescale can be increased to consider the effect of a series of events over an extended wet period or season by using a deconvolution approach incorporating information on ^{7}Be deposition during the study period on the variation of erosivity between individual events [49];

(b) The use of ^{7}Be in soil erosion investigations is commonly limited to bare soils because vegetation cover can cause small scale spatial variability in fallout inputs to the soil surface and also store a proportion of fallout. The former can be overcome to some extent through collection of spatially-integrated samples within target landscape units [30, 50];

(c) It is important that the depth distribution of ^{7}Be is measured at a non-eroding site within the study area since this depth profile provides a key parameter for the conversion model used to estimate soil redistribution rates. The criteria for selection of this site are similar to those for the reference site but additional care must be taken to ensure there are no signs of soil mobilization. Typically a flat area of the study field with no upslope contributing area is required. The depth profile of the reference site should be used with extreme caution since there is likely to be a difference in the structure and bulk density of the soil compared to the eroding sites (e.g. pasture vs. cultivated soil);

(d) The depth of sampling for collection of bulk cores requires careful consideration. The depth should be sufficient to include the total ^{7}Be inventory but it should be kept as small as possible to avoid excessive dilution of the ^{7}Be activity of the bulk sample by soil from below the zone containing ^{7}Be. Reduced activity will increase counting times and reduce the reliability of the results and may result in activities below the level of detection;

(e) Although the short half-life of ^{7}Be is a key characteristic of the radionuclide, it can represent a limitation. Soil redistribution can only be documented over short periods. If the period considered is too long, soil eroded during the early stages of the period will have only a limited effect on the final ^{7}Be inventory, compared to soil eroded close to the time of sample collection and the total erosion occurring during the period may be under-estimated. In addition, the relatively short time available to analyse samples, before activities are reduced below the level of detection by decay, means that, unless a substantial numbers of detectors are available, only a limited number of samples can be analysed. As storage times increase and the ^{7}Be activity of samples declines due to decay, progressively longer count times will be required. This is likely to limit the size of the area that can be investigated or the number of contrasting treatments that can be included in an experiment aimed at assessing their effectiveness in reducing erosion. It is clearly also important that all samples should be collected at the same time, since the occurrence of rainfall, and therefore additional fallout, during the sampling period could change the activity of those samples collected later in the period;

(f) In some cases, it may be difficult to establish the precise period covered by the erosional event investigated, due to the potential influence of preceding erosional events, not separated by a sufficiently long period or by a cultivation phase. In such instances, additional information on the temporal distribution of the ^{7}Be deposition flux and rainfall erosivity may be required [49], involving measurement of the ^{7}Be activity in precipitation and consideration of rainfall intensity, respectively;

(g) Fallout is dependent on the incidence of rainfall and inventories may be very low in arid and semi-arid areas. This could also be a problem in temperate or continental climates with extended dry periods;

(h) Sampling must be carefully planned to reflect the objectives of the study and to take account of the temporal distribution of rainfall and ^{7}Be fallout and the potential for spatial variability of ^{7}Be inventories inherited from preceding erosional events. A skilled, experienced and multidisciplinary team is required for studies involving ^{7}Be;

(i) There may be some environments where a significant proportion of the ^{7}Be fallout input delivered to the study site, i.e. in dry environments, during the event under investigation may not be totally adsorbed upon raindrop impact, if runoff is already occurring. This potential problem could be disregarded because it is reported that the ^{7}Be inputs received during later stages of a rainfall event are a relatively small proportion of the total ^{7}Be inventory, but this must be assessed on a case-by-case basis;

(j) There may be some environments where soil erosion occurs as a result of intense storm events that deliver a significant proportion of the ^{7}Be inventory; thus it is important to consider possible effects on radionuclide adsorption (delayed or occurring at some distance from the point of raindrop impact).

1.6. Sampling strategy and sampling procedures

The general approach adopted for the sampling strategy, when using fallout ^{7}Be as tracer for soil erosion investigations, is similar to that used for ^{137}Cs (see Paper 2 of this TECDOC). Firstly, as with ^{137}Cs and also $^{210}Pb_{ex}$, preliminary information on the study field must be collected and a preliminary visit to the site is recommended. Therefore, information on its location, short-term and long-term climatic and environmental information and variability are needed for later discussion and also for comparison with other studies. Similarities with and differences from ^{137}Cs and $^{210}Pb_{ex}$ in terms of both sampling strategy and sampling tools are described below in the following subsections.

Reference site

The reference inventories for a study area can be determined in two ways and it is recommended to use both methods and cross-check the information obtained:

(i) Collection of shallow soil cores from stable sites adjacent to the study area as for ^{137}Cs and $^{210}Pb_{ex}$

However, because of the short half-life of ^{7}Be, the reference site should ideally be devoid of vegetation, to avoid the effects of the plant cover in causing spatial variability in the inventory, or vegetation should be included in the sample and analysed accordingly. It is also possible to pre-prepare a reference site e.g. expose an area of bare soil on adjacent flat ground, although in this case it is important that the site should be prepared well in advance of the measurement of the reference inventory, in order to ensure that the measured inventory reflects the recent history of fallout input, and any effect linked to the disturbance of the site will disappear due to decay of the initial inventory.

(ii) Direct measurement of ^{7}Be delivery to the study area through analysis of rainfall samples associated with the period of time leading up to the event studied

Data required are records of daily rainfall and ^{7}Be activity concentration in rainfall to permit calculation of the accumulated inventory for a period of 5 half-lives prior to the studied event. Care should be taken to decay-correct ^{7}Be activities in precipitation on a day-by-day basis and report correctly the period covered by the measurements. The resulting time series of daily changes in the ^{7}Be inventory must reflect both fallout inputs and post depositional radioactive decay.

As for ^{137}Cs and $^{210}Pb_{ex}$, soil samples should be collected from a reference site ideally using a systematic grid with a minimum of 10 to 15 samples in order to accurately assess the value of the local reference inventory. Variability within the sample set must be quantified.

Study site

The sampling strategy at the field scale, as described in Paper 2 of this TECDOC, can be based on a transect or grid approach depending on the complexity of the topography, or a spatial-integration approach across landscape units [30, 50]. Most previous investigations of soil erosion on arable land using fallout ^{7}Be have been either at the plot or the field scale e.g. [22, 44, 47, 48, 51], and generally a grid approach has been adopted.

Soil samples must be collected at the same time as those from the reference site, immediately *after* the study event and *before* the site is disturbed by agricultural activities. In addition, it is recommended that rainwater samples are collected at the study site on a monthly basis in order to determine the temporal distribution of ^{7}Be deposition and to estimate the fallout ^{7}Be inventory at the sampling time. This information will serve to confirm the value of the reference inventory obtained from the reference cores and to establish ^{7}Be deposition dynamics during the erosional event(s) [45]. There are only a few studies at the watershed scale using ^{7}Be [52]. In this case, due to the short half-life of ^{7}Be and the possible spatial variability of the rainfall, the sampling for the selected fields should be performed during a short time period.

Sampling tools

There is a need to collect bulk soil samples from shallow depths, because the occurrence of ^{7}Be is restricted to the immediate surface layer of the soil. If the sample is not collected to a sufficient depth, it will not contain the full ^{7}Be inventory and soil erosion will be overestimated. Equally, however, if the sampling depth is too great, the inclusion of soil with a ^{7}Be activity below the level of detection may reduce the concentration of ^{7}Be in the overall sample affecting analytical precision. Careful planning is required, ideally with prior knowledge of the ^{7}Be depth profiled in the study area soil.

A major challenge in using the ^{7}Be approach is to achieve appropriate vertical sampling precision to establish the depth distribution. Sampling procedures and devices can represent an important potential constraint in the use of ^{7}Be. In addition, the need to characterize the exponential depth distribution at the reference site for use in the conversion model means that there is a need to section the core into small depth increments or to collect samples from small depth increments. A resolution of ca. 2 mm is frequently required but it is important to ensure that the sample is of sufficient mass to permit reliable measurements of the ^{7}Be activity by gamma spectrometry.

Various sampling tools have been used to meet this requirement [54]. The IAEA Soil Science Unit in collaboration with the Seibersdorf mechanical workshop has developed a prototype (Fig. 4 and 5) Fine Soil Increment Collector (FSIC) for this purpose [54]. The FSIC ensures

close control of the magnitude of the depth increment to be collected and facilitates the sectioning of the core by using a screw thread system (see Fig. 4).

In comparison with existing sampling tools, the FSIC has the following advantages: (i) it permits sampling of undisturbed topsoil samples; (ii) it is easily adjusted to collect soil at a high resolution (mm precision); (iii) it is simple to operate by an individual; (iv) it can be used in the field or laboratory; (v) it permits calculation of soil bulk density at high vertical resolution; (vi) sample size can be tailored to requirements; (vii) top-soil samples can be transported securely without disturbance. Other devices and or prototypes (e.g. 'adapted/modified' bulk density cylinder (e.g. Fig. 6) were developed and used in the United Kingdom, Chile and Morocco [44]. A scraper plate can also be used in non-stony areas [53], but it is generally harder to achieve mm precision with these tools.

FIG. 4. The Fine Soil Increment Collector being tested in the field.

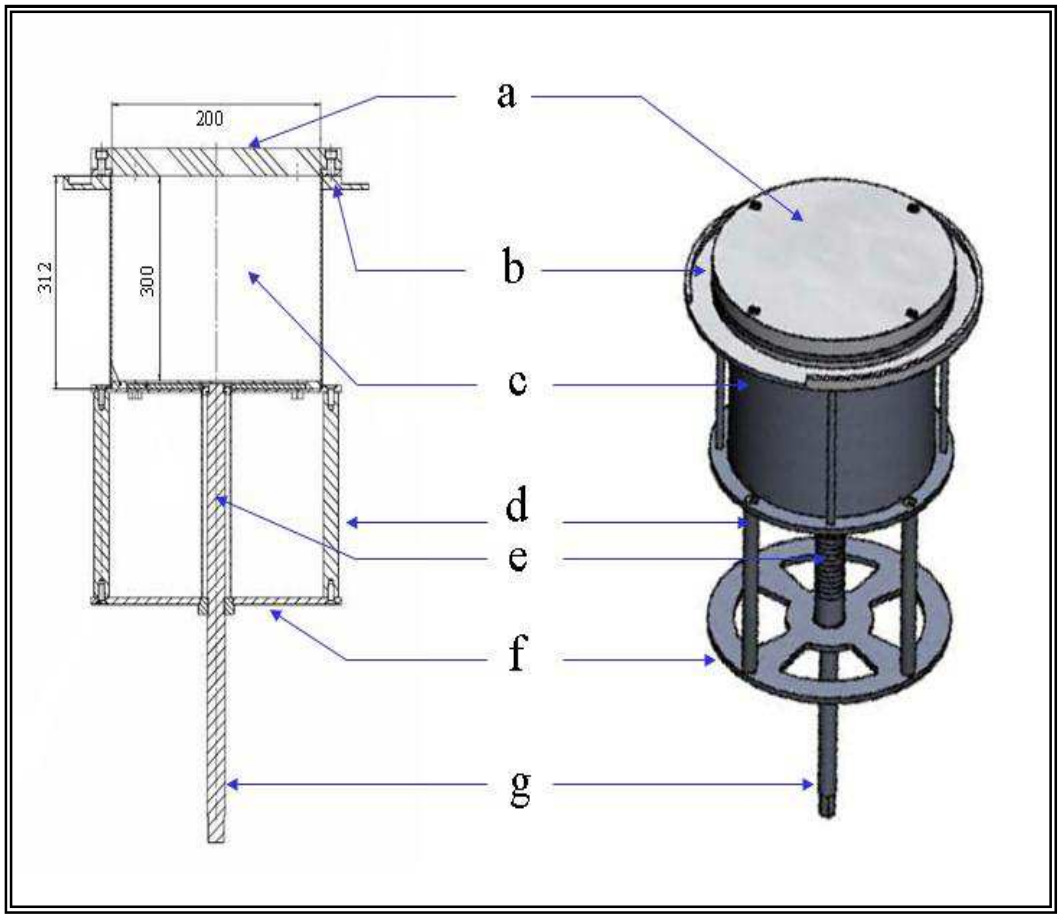

FIG. 5. The Fine Soil Increment Collector [54]: (a) Teflon / plastic cover; (b) Teflon / plastic guide to collect soil; (c) Stainless steel body cylinder; (d) Cylinder metal frames; (e) Graduated scale; (f) Circular metal maintain frame; (g) Screw thread.

FIG. 6. Surface sampling and 'modified' bulk density cylinder used for ^{7}Be investigations in Morocco.

2. Sample preparation and gamma spectrometry measurement

2.1. Sample preparation

Sample preparation and pre-treatment are simple and similar to the other FRNs (^{137}Cs and ^{210}Pb). Soil samples should be weighed then oven- or air-dried and reweighed to determine moisture content and total sample dry mass. The material should be lightly ground, homogenized and sieved to < 2 mm (see Paper 2 of this TECDOC for more details).

For measurement of ^{7}Be in rainfall, it is recommended that ^{7}Be is extracted from solution by co-precipitation with manganese dioxide (MnO_2) following methods detailed in [20]. The MnO_2 precipitate is filtered and analyzed as a thin source filter paper to maximize gamma counts and reduce analytical uncertainties. ^{7}Be recovery from rainwater was reported as approximately 96% [20]. The manganese dioxide precipitation method for acidified (HCl) rainwater is summarized below.

- 1ml of 0.2 M $KMnO_4$ is added per litre of water sample;
- The pH is adjusted to 8-10 with concentrated NH_4OH;
- 1ml per litre of water sample of 0.3 M $MnCl_2$ is slowly added while stirring to maintain the resulting MnO_2 precipitate in suspension;
- The precipitate is then allowed to flocculate and settle;
- The sample is then filtered through a 0.45 μm filter paper;
- The filter paper is dried and the precipitate fixed with cellophane prior to placing in a suitable container for gamma spectrometry.

2.2. Measurement by gamma spectrometry

^{7}Be is a gamma emitter with a γ–ray energy of 477.6 keV and an emission probability of 10.3%. ^{7}Be activity can be readily determined using a standard coaxial HPGe ‘‘P-type’’ detector by measuring the counts at 477.6 keV. As for ^{137}Cs, gamma detection of ^{7}Be is more straightforward than ^{210}Pb measurements that need special consideration and attention [55] (also see Paper 3 of this TECDOC). Nevertheless, the lower energy gamma lines measured for ^{7}Be combined with the lower emission probability have a higher spectral background in the peak region than those measured for ^{137}Cs and this will commonly result in higher uncertainty levels and detection limits for the same counting conditions. The basis for gamma spectrometry, as well as calibration procedures, is described in Paper 2 of this TECDOC.

The counting time must be sufficient to obtain an acceptable analytical precision at 2σ (< 10%) although it should be recognized that eroding sites with a low activity concentration will inevitably yield higher counting uncertainties and hence total uncertainty is often in excess of 10%.

^{7}Be has a short half-life (53.3 days), so the ^{7}Be activity should be corrected for decay between the collection period and counting time using the following Equation:

$$\lambda t \,/\, 1 - \exp(1 - \lambda t) \qquad (1)$$

where:

λ is the decay constant;
t the elapsed time.

Clearly it is desirable to start gamma measurements as quickly as possible after the collection and pre-treatment of the soil samples because of the short half-life of ^{7}Be and its potential low activity in rain water and soil (depending on study location and climatic parameters). Hence sample size needs to be given due consideration to maximize the number of counts acquired [56].

In situ measurements could provide an effective approach to obtaining the necessary information on ^{7}Be inventories from a study site, without the need for time-consuming sampling campaigns and associated laboratory measurements. However, based on the few existing studies, count times need to be at least twice as long as those required for ^{137}Cs, which represents an important constraint [45].

3. Data treatment

As with ^{137}Cs and $^{210}Pb_{ex}$ (see Papers 2 and 3 of this TECDOC), ^{7}Be inventories and vertical distributions in soil for both reference and study sites should be determined to permit similar analysis and treatment as for other FRNs. The analysis of the data generally includes the following points:

(a) Checking the ^{7}Be profile shapes for the reference and/or undisturbed study site location and estimation of the mass relaxation depth (e.g. h_o) (see Paper 5 of this TECDOC for model details);

(b) Establishment of the coefficient of variation for the reference inventory;

(c) Validation of the ^{7}Be reference inventory value by comparing the value obtained from the soil cores at the reference site and the fallout-derived ^{7}Be inventory from rainfall data and analysed rainfall samples;

(d) Comparison between inventories associated with the study fields and that of the reference site in order to identify erosional and depositional areas;

(e) Estimation of soil redistribution rates (t ha^{-1}) corresponding to the investigated period by converting the ^{7}Be inventory (Bq m^{-2}) measurements using the appropriate conversion model (see Paper 5 of this TECDOC);

(f) Establishment of a sediment budget (mean erosion, mean deposition, gross erosion, gross deposition, net erosion and sediment delivery) for the landscape unit being studied;

(g) Data spatialisation and soil redistribution mapping using geostatistics;

(h) Study of the influence of hydro-meteorological conditions if the impact of several events, or an entire wet season, are being investigated.

4. Applications in soil erosion and sedimentation studies from literature

^{7}Be, with its short half-life, offers a means of assessing rates and spatial patterns of soil erosion and deposition, on a rainfall event basis, thus providing a way to evaluate the short-term impact of conservation practices or shifts in land use on soil movement, against a background of medium-term data provided by ^{137}Cs.

The use of ^{7}Be as a catchment sediment fingerprinting tool was initiated in the early 1990s in Australian [17, 28, 46, 57] and UK catchments [58]. This was followed by application of ^{7}Be

as a tool for estimating event-based soil erosion data [22, 48]. The former studies demonstrated the ability of the methodology to distinguish between sediment mobilized by sheet erosion or rill erosion in erosion plot experiments, and to show the progressive development of rills during the course of a single simulated runoff event. In the latter studies, spatial patterns of ^{7}Be redistribution were used to estimate soil erosion and deposition rates within a field to determine the field-scale sediment delivery ratio. ^{7}Be analysis can also provide information regarding recent and seasonal sedimentation processes [59, 60] based on early work in coastal environments to assess sedimentation processes [25].

More recently, ^{7}Be as well as the other FRNs have been used to establish tracer-based sediment budgets and to trace soil redistribution in the landscape and export to stream networks. For example, this approach has been used to assess soil and associated organic materials redistribution after harvesting forested areas [47, 61, 62] and after severe wildfires [30, 50]. ^{7}Be has been also utilised to study specific components of the sediment budget, namely i) to trace the transport, storage and remobilization of fine sediment in river channels and ii) to estimate overbank sedimentation rates on river floodplains [63, 64]. Recent applications and development of the ^{7}Be methodology were undertaken under the IAEA/CRP D1-50-08 [65]. Particular application to investigate short-term erosion rates and sediment transfers with promising results includes the assessment of the impacts of tillage systems and forest harvest operations in several countries. e.g. Pakistan, Vietnam, Poland, UK, Chile, China, Morocco. More recently, an approach to extend the use of ^{7}Be to cover longer time periods (e.g. wet seasons) has been provided to overcome the problem of pre-event heterogeneity in soil inventories [49]. This involves new requirements e.g. to synthesise the temporal distribution of fallout input, to take into account of changes in h_0 to evaluate the temporal distribution of erosion during the study period [49].

TABLE 2. USE OF ^{7}Be AS A TRACER IN SOIL EROSION AND FINE SEDIMENT APPLICATIONS

Reference	Location	Study	Scale
[17, 28, 46, 57]	SE Australia	Sediment fingerprinting; erosion processes	Hillslope to channel
[58]	SW UK	Sediment fingerprinting; erosion processes	Hillslope to channel
[22, 48]	SW UK	Soil erosion (agriculture)	Hillslope
[63]	SW UK	Floodplain sedimentation	Floodplain*
[66]	Iowa, USA	Soil erosion (agriculture)	Hillslope plot
[64, 67, 68]	USA	Suspended sediment residence time and transport distance	Channel and wetland
[51]	China	Erosion processes	Plot
[30, 50]	SE Australia	Sediment budget (forest wildfire)	Small catchment‡
[47]	Central Chile	Soil erosion (logging)	Hillslope plot
[44]	Central Chile	Soil erosion (agriculture and burning)	Hillslope
[70]	W Morocco	Soil erosion (agriculture)	Hillslope plot
[71]	SW UK	Soil erosion (agriculture)	Hillslope transects
[62]	South central Chile	Soil erosion and sediment retention (logged hillslope)	Hillslope units

*as discrete landscape unit; ‡< 1 km^{2}

5. Concluding remarks

It should be recognized that ^{7}Be as well as $^{210}Pb_{ex}$ (see Paper 3 of this TECDOC) are still in their infancy as contemporary soil erosion and sediment tracers in comparison to ^{137}Cs. The physico-chemical behavior of ^{7}Be in different soils worldwide requires further investigation, before its full potential can be exploited with confidence at the larger catchment scale [45]. Application of ^{7}Be in a wider range of environments will lead to continued development and testing of conversion models for ^{7}Be (see Paper 5 of this TECDOC) to improve them accordingly for assessment of the impact of short-term changes in land use practices and the effectiveness of soil conservation measures for sustainable catchment management. There is a continuing need to refine the ^{7}Be technique to the same level as that of the ^{137}Cs technique and establish a standardized protocol or decision-support system for its application.

REFERENCES

[1] MASON, B., Principles of Geochemistry, John Wiley and Sons, Chichester, New York (1952) 276.

[2] KASTE, J.M., NORTON, S.A., HESS, CT., Environmental chemistry of Beryllium-7, Rev. Mineral. Geochem. 50 (2002) 271–289.

[3] BARG, E., LAL, D., PAVICH, M.J., CAFFEE, M.W., SOUTHON, J.R., Beryllium geochemistry in soils: evaluation of $^{10}Be/^{9}Be$ ratios in authigenic minerals as a basis for age models, Chem. Geol. 140 (1997) 237–258.

[4] CHAPPELL, J., ZHENG, H., FIFIELD, K., Yangtse River sediments and erosion rates from source to sink traced with cosmogenic ^{10}Be: Sediments from major rivers, Palaeogeogr. Palaeoclimatol. Palaeoecol. 241 (2006) 79–94.

[5] PAVICH, M. J., BROWN, L., VALETTE-SILVER, J.N., KLEIN, J., MIDDLETON, R., ^{10}Be analysis of a Quaternary weathering profile in the Virginia Peidmont, Geol. 13 (1985) 39.

[6] SJUNNESKOG, C., SCHERER, R., ALDAHAN, A., POSSNERT, G., ^{10}Be in glacial marine sediment of the Ross Sea, Antarctica, a potential tracer of depositional environment and sediment chronology, Nucl. Instrum. Methods Phys. Res., Sect. B 259 (2007) 576–583.

[7] PETERS, B., Cosmic-ray produced radioactive isotopes as tracers for studying large-scale atmospheric circulation, J. Atmos. Terrestr. Phys. 13 (1959) 351–37.

[8] ALDAHAN, A., POSSNERT, G., VINTERSVED, I., Atmospheric interactions at northern high latitudes from weekly Be-isotopes in surface air, Appl. Radiat. Isot. 54 (2001) 345–353.

[9] KIKUCHI, S., SAKURAI, H., GUNJI, S., TOKANAI, F., Temporal variation of ^{7}Be concentrations in atmosphere for 8 y from 2000 at Yamagata, Japan: solar influence on the Be-7 time series, J. Environ. Radioact. 100 (2009) 515–521.

[10] FEELY, H.W., LARSEN, R.J., SANDERSON, C.G., Factors that cause seasonal variations in Beryllium-7 concentrations in surface air, J. Environ. Radioact. 9 (1989), 223–249.

[11] DOERING, C., AKBER, R., Describing the annual cyclic behaviour of ^{7}Be concentrations in surface air in Oceania, J. Environ. Radioact. 99 (2008) 1703–1707.

[12] CAILLET, S., ARPAGAUS, P., MONNA, F., DOMINIK, J., Factors controlling ^{7}Be and ^{210}Pb atmospheric deposition as revealed by sampling individual rain events in the region of Geneva, Switzerland, J. Environ. Radioact. 53 (2001) 241–256.

[13] DAISH, S.R., DALE, A.A., DALE, C.J., MAY, R.,ROWE, J.E., The temporal variations of ^{7}Be, ^{210}Pb and ^{210}Po in air in England, J. Environ. Radioact. 84 (2005) 457–467.
[14] IOANNIDOU, A., MANOLOPOULOU, M., PAPASTEFANOU, C., Temporal changes of ^{7}Be and ^{210}Pb concentrations in surface air at temperate latitudes (40°N), Appl. Radiat. Isot. 63 (2005) 277–284.
[15] IOANNIDOU, A., PAPASTEFANOU, C., Precipitation scavenging of ^{7}Be and ^{137}Cs radionuclides in air, J. Environ. Radioact. 85 (2006) 121–136.
[16] CENTRAL RADIOANALYTICAL LABORATORY OF FOOD FEED SAFETY DIRECTORATE, Hungarian Agricultural Authority, Radioanalytical Monitoring Network of Ministry of Agriculture and Rural Development, Ann. Rep. (2006).
[17] WALLBRINK, P.J., MURRAY, A.S., Fallout of ^{7}Be in South Eastern Australia, J. Environ. Radioact. 25 (1994) 213–228.
[18] DOERING, C., AKBER, R., Beryllium-7 in near-surface air and deposition at Brisbane, Australia, J. Environ. Radioact. 99 (2008) 461–467.
[19] AYUB, J.J., et al., Short-term seasonal variability in ^{7}Be wet deposition in a semiarid ecosystem of central Argentina, J. Environ. Radioact. 100 (2009) 977–981.
[20] SHORT, D.B., APPLEBY, P.G., HILTON, J., Measurement of atmospheric fluxes of radionuclides at a UK site using both direct (rain) and indirect (soils) methods, Int. J. Environ. Pollut. 29 (2007) 392–404.
[21] GONZÁLEZ-GÓMEZ, C., et al., Seasonal variability in ^{7}Be depositional fluxes at Granada, Spain. Appl. Radiat. Isot. 64 (2006) 228–234.
[22] BLAKE, W.H., WALLING, D.E., HE, Q., Fallout beryllium-7 as a tracer in soil erosion investigations, Appl. Radiat. Isot. 51 (1999) 599–605.
[23] BETTOLI, M.G., et al., Preliminary investigations on ^{7}Be as a tracer in the study of environmental processes, J. Radioanal. Nucl. Chem. Articles 190 (1995) 137–147.
[24] HAWLEY, N., ROBBINS, J.A., EADIE, B.J., The partitioning of ^{7}Be in freshwater, Geochim. Cosmochim. Acta 50 (1986) 1127–1131.
[25] OLSEN, C.R., LARSEN, I.L., LOWRY, P.D., CUTSHALL, N.H., NICHOLS, M., Geochemistry and deposition of ^{7}Be in river estuarine and coastal waters, J. Geophys. Res. 91 (1986) 896–908.
[26] DIBB, J.E., RICE, D.L., The geochemistry of beryllium-7 in Chesapeake Bay, Estuar. Coast. Shelf Sci. 28 (1989) 379–394.
[27] YOU, C.F., LEE, T., LI, Y.H., The partition of Be between soil and water, Chem. Geol. 77 (1989) 105–118.
[28] WALLBRINK, P.J., MURRAY, A.S., Distribution of ^{7}Be in soils under different surface cover conditions and its potential for describing soil redistribution processes, Water Resourc. Res. 32 (1996) 467–476.
[29] BAI, Z., WAN, G., WANG, C., WAN, X., HUANG, R., Geochemical speciation of soil Be-7, Cs-137, Ra-226 and Ra-228 as tracers to particle transport, Pedosphere 7 (1997) 263–268.
[30] BLAKE, W.H., et al., Deriving hillslope sediment budgets in wildfire-affected forests using fallout radionuclide tracers, Geomorphology 104 (2009) 105–116.
[31] DOERING, C., AKBER, R., HEIJNIS, H., Vertical distributions of ^{210}Pb excess, ^{7}Be and ^{137}Cs in selected grass covered soils in Southeast Queensland, Australia, J. Environ. Radioact. 87 (2006) 135–147.
[32] RÓDENAS, C., GÓMEZ, J., QUINDÓS, L.S., FERNÁNDEZ, P.L., SOTO, J., ^{7}Be concentrations in air, rain water and soil in Cantabria (Spain), Appl. Radiat. Isot. 48 (1997) 545–548.

[33] DUEÑAS, C., FERNÁNDEZ, M.C., LIGER, E., CARRETERO, J., CAÑETE, S., Atmospheric deposition of ^{7}Be at a coastal Mediterranean station, J. Geophys. Res. 106 (D24) (2001) 34059–34065.
[34] OTHMAN, I., AL-MASRI, M.S., HASSAN, M., Fallout of ^{7}Be in Damascus City, J. Radioanal. Nucl. Chem. 238 (1998) 187–199.
[35] LEE, S.C., SALEH, A.I., BANAVALI, A.D., JONOUBY, L.J., KURODA, P.K., Beryllium-7 deposition at Fayetville, Arkansas, and excess Polonium-210 from the 1980 eruption of Mount St Helens, Geochem. J. 19 (1985) 317–322.
[36] PEIRSON, D.H., ^{7}Be in air and rain, J. Geophys. Res. 68 (1963) 3831–3832.
[37] SCHUMANN, G., STOEPPLER, M., Beryllium in the atmosphere, J. Geophys. Res. 68 (1963) 3827–3830.
[38] LAL, D., NIIJAMPURKAR, N., RAJAGOPALAN, G., SOMAYAJULU, B.L.K., Annual fallout of ^{32}Si, ^{210}Pb, ^{22}Na, ^{35}S and ^{7}Be in rains in India, Proc. Ind. Acad. Sci. 88a (1979) 29–40.
[39] BENÍTEZ-NELSON, C.R., BUESSLER, K.O., Phosphorous-32, phosphorous-37, beryllium-7 and lead-210: Atmospheric fluxes and utility in tracing stratosphere/troposphere exchange, J. Geophys. Res. 104 (1999) 11745–11754.
[40] BLAKE, W.H., The use of ^{7}Be as a Tracer in Sediment Budget Investigations, Ph. D thesis, University of Exeter, UK (2000).
[41] TUREKIAN, K.K., BENNINGER, L.K., DION, E.P., ^{7}Be and ^{210}Pb total deposition fluxes at New Haven, Connecticut and Bermuda, J. Geophys. Res. 88 (C9) (1983) 5411–5415
[42] BASKARAN, M., A search of seasonal variability on the depositional fluxes of ^{7}Be and ^{210}Pb, J. Geophys. Res. 100 (D2) (1995) 2833–2840.
[43] MATISOFF, G., BONNIWELL, E.C., WHITING, P.J., Soil erosion and sediment sources in a Ohio watershed using beryllium-7, cesium-137, and lead-210, J. Environ. Qual. 31 (2002) 54–61.
[44] SEPÚLVEDA, A., SCHULLER, P., WALLING, D.E., CASTILLO, A., Use of ^{7}Be to document soil erosion associated with a short period of extreme rainfall, J. Environ. Radioact. 99 (2008) 35–49.
[45] MABIT, L., BENMANSOUR, M., WALLING, D.E., Comparative advantages and limitations of fallout radionuclides (^{137}Cs, ^{210}Pb and ^{7}Be) to assess soil erosion and sedimentation, J. Environ. Radioact. 99 (2008) 1799–1807.
[46] WALLBRINK, P.J., MURRAY, A.S., Use of fallout nuclides as indicators of erosion processes, Hydrol. Process. 7 (1993) 297–304.
[47] SCHULLER, P., et al., Use of beryllium-7 to document soil redistribution following forest harvest operations, J. Environ. Qual. 35 (2006) 1756–1763.
[48] WALLING, D.E., HE, Q., BLAKE, W., Use of ^{7}Be and ^{137}Cs measurements to document short- and medium-term rates of water-induced soil erosion on agricultural land, Water Resourc. Res. 35 (1999) 3865–3874.
[49] WALLING, D.E., SCHULLER, P., ZHANG, Y., IROUMÉ, A., Extending the timescale for using beryllium-7 measurements to document soil redistribution by erosion, Water Resourc. Res. 45 (2009) W02418, doi:10.1029/2008WR007143.
[50] WALLBRINK, P.J., et al., "Using tracer based sediment budgets to assess redistribution of soil and organic material after severe bush fires", Sediment Budgets 2, (HOROWITZ, A.J., WALLING, D.E., Eds.), International Association of Hydrological Sciences Publication 292, IAHS Press, Wallingford, UK (2005) 223–230.
[51] YANG, M.Y., WALLING, D.E., TIAN, J.L., LIU, P.L., Partitioning the contributions of sheet and rill erosion using beryllium-7 and cesium-137, Soil Sci. Soc. Am. J. 70 (2006) 1579–1590.

[52] BAI, Z., et al., ^{7}Be distribution in surface soil of central Guizhou karst region and its erosion trace, Progr. Nat. Sci. 6 (1996) 700–710.
[53] LOUGHRAN, R.J., WALLBRINK, P.J., WALLING, D.E., APPLEBY, P.G., "Sampling methods", Handbook for the Assessment of Soil Erosion and Sedimentation using Environmental Radionuclides, (ZAPATA, F., Ed.), Kluwer, Dordrecht, The Netherlands (2002) 41–57.
[54] MABIT, L., TOLOZA, A., NIRSCHL, A., Development of a Fine Soil Increment Collector (FSIC) to solve the main limitation of the use of ^{7}Be as soil tracer, IAEA-Soils Newsletter 30 (2) (2008) 21–22.
[55] SHAKHASHIRO, A., MABIT, L., Results of an IAEA inter-comparison exercise to assess ^{137}Cs and total ^{210}Pb analytical performance in soil, Appl. Radiat. Isot. 67 (2009) 139–146.
[56] KOMURA, K., et al., Measurements of short-lived cosmic-ray-produced radionuclides in rainwater, J. Environ. Radioact. 96 (2007) 103–109.
[57] BURCH, G.J., et al., "Detection and prediction of sediment sources in catchments: Use of ^{7}Be and ^{137}Cs", Proc. Hydrology and Water Resources Symp., Australian National University, Canberra, Australia (1988) 146–151.
[58] WALLING, D.E., WOODWARD, J.C., "Use of radiometric fingerprints to derive information on suspended sediment sources", Erosion and Sediment Transport Monitoring Programmes in River Basins, (BOGEN, J., WALLING, D.E., DAY, T., Eds), IAHS Publ. 210 (1992) 153–164.
[59] BAI, Z.G., WAN, G.J., HUANG, R.G., LIU, T.S., A comparison on the accumulation characteristics of ^{7}Be and ^{137}Cs in lake sediments and surface soils in western Yunnan and central Guizhou, China, Catena 49 (2002) 253–270.
[60] PALINKAS, C.M., NITTROUER, C.A., WHEATCROFT, R.A., LANGONE, L., The use of ^{7}Be to identify event and seasonal sedimentation near the Po River delta, Adriatic Sea, Mar. Geol. 222/223 (2005) 95–112.
[61] WALLBRINK, P.J., RODDY, B.P., OLLEY, J.M., A tracer budget quantifying soil redistribution on hillslopes after forest harvesting, Catena 47 (2002) 179–201.
[62] SCHULLER, P., WALLING, D.E., IROUME, A., CASTILLO, A., Use of beryllium-7 to study the effectiveness of woody trash barriers in reducing sediment delivery to streams after forest clearcutting, Soil Till. Res. 110 (2010) 143–153.
[63] BLAKE, W.H., WALLING, D.E., HE, Q., Using cosmogenic Beryllium-7 as a tracer in sediment budget investigations, Geografiska Annaler 84 (2002) 89–102.
[64] MATISOFF, G., WILSON, C.G., WHITING, P.J., The ^{7}Be/^{210}Pb$_{xs}$ ratio as an indicator of suspended sediment age or fraction new sediment in suspension, Earth Surf. Process. Landf. 30 (2005) 1191–1201.
[65] INTERNATIONAL ATOMIC ENERGY AGENCY, Report of the third Research Co-ordination Meeting of the Coordinated Research Project "Assess the effectiveness of soil conservation techniques for sustainable watershed management using fallout radionuclides" Vienna, Austria (2006) 134.
[66] WILSON, C.G., MATISOFF, G., WHITING, P.J., Short-term erosion rates from a ^{7}Be inventory balance, Earth Surf. Process. Landf. 28 (2003) 967–977.
[67] WILSON, C.G., MATISOFF, G., WHITING, P.J., KLARER, D.M., Transport of fine sediment through a wetland using radionuclide tracers: Old woman creek, OH, J. Great Lakes Res. 31 (2005) 56–67.
[68] WHITING, P.J., MATISOFF, G., FORNES, W., SOSTER, F.M., Suspended sediment sources and transport distances in the Yellowstone River basin, Geol. Soc. Am. Bull. 117 (2005) 515–529.

[69] YANG, M.Y, TIAN, J.L., LIU, P.L., Investigating the spatial distribution of soil erosion and deposition in a small catchment on the Loess Plateau of China, using ^{137}Cs, Soil Till. Res. 87 (2006) 186–193.
[70] BENMANSOUR, M., et al., Estimates of long and short term soil erosion rates on farmland in semi-arid West Morocco using caesium-137, excess lead-210 and beryllium-7 measurements. In: Impact of soil conservation measures on erosion control and soil quality. IAEA-TECDOC-1665, IAEA, Vienna (2011) 159–174.
[71] PILLIDGE S., BLAKE W.H., WILLIAMS A., BRIGHT, D., Evaluating the role of buffer strips in arable catchments using fallout radionuclide tracers, Geophys. Res. Abstr. 10 (2008) EGU2008-A-12236.

CONVERSION MODELS AND RELATED SOFTWARE

D.E. WALLING,
Geography, College of Life and Environmental Sciences, University of Exeter, Exeter, United Kingdom

Y. ZHANG
ADAS,
Wolverhampton, United Kingdom

Q. He,
Geography, College of Life and Environmental Sciences, University of Exeter, Exeter, United Kingdom

Abstract

Within the framework of IAEA funded research networks, an attempt has been made to develop a generally applicable set of conversion models for use with ^{137}Cs, $^{210}Pb_{ex}$ and ^{7}Be measurements to estimate soil redistribution rates. The set of models includes six models for use with ^{137}Cs measurements, three models for use with $^{210}Pb_{ex}$ measurements and a single model for use with ^{7}Be measurements. All models have been developed for use with data collected from downslope transects. In the case of the six models for use with ^{137}Cs measurements, four are applicable to cultivated land. These include the proportional model, a simple mass balance model, a more comprehensive mass balance model, and a mass balance model that attempts to incorporate the effects of tillage. The other two models for use with ^{137}Cs measurements are applicable to uncultivated soils and include the profile distribution model and the diffusion and migration model. For $^{210}Pb_{ex}$, the three models include two that are applicable to cultivated land, namely a comprehensive mass balance model and a mass balance model incorporating tillage, and the diffusion and migration model, that is applicable to uncultivated land. The profile distribution model documented for ^{7}Be is applicable to both cultivated and uncultivated sites, as a result of the short half-life of this radionuclide. In order to facilitate the use of the models, a user-friendly software package, based on an Excel Add-in has been developed, guidelines for model selection and for establishing parameter values are provided. The model software contains several routines for estimating input variables.

1. Introduction

Many different approaches have been used to convert ^{137}Cs measurements to quantitative estimates of erosion and deposition rates [1-3]. Over the past decade progress has also been made in the development of similar conversion models for other fallout radionuclides and more particularly excess ^{210}Pb ($^{210}Pb_{ex}$) and ^{7}Be [4-6]. This paper provides an overview of the commonly used conversion models for use with ^{137}Cs, $^{210}Pb_{ex}$ and ^{7}Be and the development of user-friendly software for model implementation.

The development of the set of nine conversion models described in this contribution, and the associated software to assist in applying the models, was undertaken to support the implementation of the IAEA Coordinated Research Project on "Assessing the effectiveness of soil conservation techniques for sustainable watershed management using fallout radionuclides" (CRP D1-50-08).

The package of models can be directly downloaded free of charge from the internet site of the SWMCN Section in the *Models and Tool Kits* area: http://www-naweb.iaea.org/nafa/swmn/models-tool-kits.html.

2. Description of the conversion models

A brief description of the theoretical basis of the models incorporated into the software and some guidelines regarding the advantages and limitations of the individual models are presented in this paper. Since the conversion models developed for $^{210}Pb_{ex}$ and ^{7}Be were adapted from those used for ^{137}Cs, emphasis will be placed on the latter. The discussion of the models provided for $^{210}Pb_{ex}$ and ^{7}Be will focus on their differences from the conversion models employed for ^{137}Cs.

2.1. Models for use with ^{137}Cs measurements

The first four models described below are for application to cultivated soils and the last two for use with uncultivated soils (rangelands or permanent pasture).

(i) The proportional model

The proportional model is probably the simplest of the conversion models used for ^{137}Cs measurements. It is based on the premise that ^{137}Cs fallout inputs are completely mixed within the plough or cultivation layer and the simple assumption that the depth of soil removed by erosion is directly proportional to the fraction of the original ^{137}Cs inventory removed from the soil profile by erosion since the beginning of ^{137}Cs fallout or the onset of cultivation, whichever is later. Thus, if half of the ^{137}Cs input has been removed, the total soil loss over the period is assumed to be 50% of the plough depth. Division of this depth by the number of years elapsed since the beginning of significant ^{137}Cs fallout provides an estimate of the annual rate of surface lowering. Inclusion of a value for the bulk density of the soil makes it possible to calculate an erosion rate in units of mass per unit time (i.e. t ha^{-1} yr^{-1}). A particle size correction factor is often incorporated into the model to make allowance for the size selectivity of sediment mobilisation and the preferential association of ^{137}Cs with the finer fractions of the soil. The model can be represented as follows:

$$Y = 10\frac{B\,d\,X}{100\,T\,P} \qquad (1)$$

where:

Y is the mean annual soil loss (t ha^{-1} yr^{-1});
d is the depth of plough or cultivation layer (m);
B is the bulk density of soil (kg m^{-3});
X is the percentage reduction in total ^{137}Cs inventory (defined as $[(A_{ref}–A)/A_{ref}]\times100$);
A_{ref} is the local ^{137}Cs reference inventory (Bq m^{-2});
A is the measured total ^{137}Cs inventory at the sampling point (Bq m^{-2});
T is the time elapsed since the initiation of ^{137}Cs accumulation or the commencement of cultivation whichever is later (yr);
P is the particle size correction factor for erosion (see below).

An inference from the assumptions of the proportional model is that the ^{137}Cs concentration of the eroded sediment remains constant through time. The ^{137}Cs concentration of deposited sediment at a depositional point may therefore be assumed to be constant. In cases where the ^{137}Cs inventory A for a sampling point is greater than the local reference inventory A_{ref},

deposition of sediment may be assumed and the annual deposition rate Y' (t ha^{-1} yr^{-1}) may be estimated using the following Equation:

$$Y' = 10\frac{B\,d\,X'}{100T\,P'} \quad (2)$$

where:

X′ is the percentage increase in total ^{137}Cs inventory (defined as $[(A–A_{ref})/A_{ref}]\times100$);
P' is the particle size correction factor for deposition (see below).

The particle size correction factors P and P' are introduced to take account of the potential particle size selectivity of erosion and deposition processes. If erosion results in selective removal of fines, the eroded sediment is likely to be enriched in ^{137}Cs, since in most environments ^{137}Cs is preferentially associated with the fine fraction. Failure to take account of this in the conversion model will result in overestimation of erosion rates, because the reduction in the inventory will reflect the loss of a smaller mass of soil, by virtue of its increased ^{137}Cs content. Equally, deposition will frequently involve the deposition of coarser particles, which is likely to be characterized by a reduced ^{137}Cs content, when compared with the eroded soil. If this is not taken into account, deposition rates could be under estimated. P represents the ratio of the ^{137}Cs concentration in the sediment mobilized by erosion to that in the original soil and its value is generally 1.0 or greater. Similarly, P' represents the ratio of the ^{137}Cs concentration in deposited sediment to that of the mobilized sediment and its value is commonly less than 1.0. Further details on the estimation of P and P' are provided in this paper.

Advantages and limitations: The proportional model requires very little information to provide an estimate of the erosion or deposition rate at the sampling point. In addition to the values of ^{137}Cs inventory for the sampling points and the local reference inventory, only an estimate of the plough depth and a value for the bulk density of the soil are required. It is therefore easy to apply. However, the assumptions of this model are a considerable oversimplification of reality in terms of the accumulation of ^{137}Cs in the soil. The accumulation of ^{137}Cs takes place over several years and some of the fallout input will remain at the soil surface prior to incorporation into the soil profile by cultivation. If some of the ^{137}Cs accumulated on the surface is removed by erosion prior to incorporation into the profile the estimates of soil loss provided by the model will overestimate actual rates of soil loss. Perhaps more importantly, however, this model does not take into account the fact that the depth of the plough layer is maintained by incorporating soil from below the original plough depth as the surface is lowered by erosion. This in turn causes a progressive dilution of ^{137}Cs concentrations in the soil within the plough layer. As a result, the model is likely to underestimate the actual rates of soil loss. Similarly, if the model is used to estimate deposition rates, the values obtained will underestimate the actual deposition rates, since no account is taken of the progressive reduction in the ^{137}Cs content of the deposited soil as erosion proceeds upslope. In view of these fundamental limitations, use of the proportional model is not generally recommended. It is included in the software package to permit comparison of the results obtained with those provided by other more reliable models.

(ii) A simplified mass balance model (Mass Balance Model 1)

Mass balance models attempt to overcome some of the limitations of the simple proportional model by taking account of both inputs and losses of ^{137}Cs from the profile over the period since the onset of ^{137}Cs fallout and the progressive lowering of the base of the plough layer in response to removal of soil from the soil surface by erosion [7] proposed a simplified mass

balance model, which assumes that the total ^{137}Cs fallout occurred in 1963, instead of over the longer period extending from the mid-1950s to the mid-1970s. In its original form this simplified mass balance model did not take account of particle size effects but a correction factor *P* has been included in the model incorporated into the software.

For an eroding site ($A(t) < A_{ref}$), assuming a constant rate of surface lowering *R* (m yr^{-1}), the total ^{137}Cs inventory (A , Bq m^{-2}) at year *t* (yr) can be expressed as:

$$A(t) = A_{ref}(1 - P\frac{R}{d})^{t-1963} \quad (3)$$

By re-arranging Equations 5.1 and 5.3, the erosion rate *Y* (t ha^{-1} yr^{-1}) can be calculated as:

$$Y = \frac{10\ d\ B}{P}\left[1 - \left(1 - \frac{X}{100}\right)^{1/(t-1963)}\right] \quad (4)$$

where:

A_{ref} is the local reference inventory (Bq m^{-2});
Y is the mean annual erosion rate (t ha^{-1} yr^{-1});
d is the depth of the plough or cultivation layer (m);
B is the soil bulk density (kg m^{-3});
X is the percentage reduction in total ^{137}Cs inventory (defined as $[(A_{ref}-A)/A_{ref}]\times 100$);
P is the particle size correction factor.

For a depositional site ($A(t) > A_{ref}$), assuming a constant deposition rate R' (kg m^{-2} yr^{-1}) at the site, the sediment deposition rate can be estimated from the ^{137}Cs concentration of the deposited sediment $C_d(t')$ (Bq kg^{-1}) according to:

$$R' = \frac{A_{ex}(t)}{\int_{1963}^{t} C_d(t')\ e^{-\lambda(t-t')}\ dt'} = \frac{A(t) - A_{ref}}{\int_{1963}^{t} C_d(t')\ e^{-\lambda\cdot(t-t')}\ dt'} \quad (5)$$

where:

$A_{ex}(t)$ is the excess ^{137}Cs inventory of the sampling point over the reference inventory at year *t* (defined as the measured inventory less the local reference inventory) (Bq m^{-2});
$C_d(t')$ is the ^{137}Cs concentration of deposited sediment at year t' (Bq kg^{-1});
λ is the decay constant for ^{137}Cs (yr^{-1});
P' is the particle size correction factor.

Generally, the ^{137}Cs concentration $C_d(t')$ of deposited sediment can be assumed to be represented by the weighted mean of the ^{137}Cs concentration of sediment mobilised from the upslope contributing area. $C_d(t')$ and can therefore be calculated as:

$$C_d(t') = \frac{1}{\int_S R\ dS}\int_S P'\ C_e(t')\ R\ dS \quad (6)$$

where:

S is the upslope contributing area (m^2);

$C_e(t')$ is the ^{137}Cs concentration of sediment mobilised from an eroding point (Bq kg^{-1}), which can be calculated from Equation 5.3 according to:

$$C_e(t') = P\ \frac{A(t')}{d} = \frac{P}{d} A_{ref}(t') \left(1 - P\frac{R}{d}\right)^{t'-1963} = \frac{P}{d} A_{ref}(t)\ e^{\lambda\cdot(t-t')} \left(1 - P\frac{R}{d}\right)^{t'-1963} \quad (7)$$

where:

$A_{ref}(t)$ is A_{ref} in year t.

Advantages and limitations: The simplified mass balance model takes into account the progressive reduction in the ^{137}Cs concentration of the soil within the plough layer due to the incorporation of soil containing negligible ^{137}Cs from below the original plough depth and thus represents an improvement over the proportional model. This model is also easy to use and requires only information on plough depth. However, this model does not take into account the possible removal of freshly deposited ^{137}Cs fallout before its incorporation into the plough layer by cultivation, which may occur during rainfall events which produce surface runoff and therefore erosion. The assumption that the total ^{137}Cs fallout input occurs in 1963 is also an oversimplification. Since the model requires information on the ^{137}Cs concentration of soil eroded from upslope, the sampling points used with the model must be arranged along a downslope transect. Normally, a uniform spacing of sampling points is assumed. The first (upper) point on the transect should represent an eroding point.

(iii) Mass Balance Model 2

A more comprehensive mass balance model requires consideration of the time-variant fallout ^{137}Cs input and the fate of the freshly deposited fallout before its incorporation into the plough layer by cultivation.

For an eroding point ($A(t) < A_{ref}$), the change in the total ^{137}Cs inventory $A(t)$ with time can be represented as:

$$\frac{dA(t)}{dt} = (1 - \Gamma)\ I(t) - (\lambda + P\frac{R}{d})\ A(t) \quad (8)$$

where:

$A(t)$ is the cumulative ^{137}Cs activity per unit area (Bq m^{-2});
R is the erosion rate (kg m^{-2} yr^{-1});
d is the cumulative mass depth representing the average plough depth (kg m^{-2});
λ is the decay constant for ^{137}Cs (yr^{-1});
$I(t)$ is the annual ^{137}Cs deposition flux (Bq m^{-2} yr^{-1});
Γ is the proportion of the freshly deposited ^{137}Cs fallout removed by erosion before being mixed into the plough layer;
P is the particle size correction factor.

If an exponential distribution for the initial distribution of ^{137}Cs fallout at the surface of the soil profile can be assumed, following [8], Γ can be expressed as:

$$\Gamma = P\ \gamma\ (1 - e^{-R/H}) \quad (9)$$

where:

γ is the proportion of the annual ^{137}Cs input susceptible to removal by erosion;
H is the relaxation mass depth of the initial distribution of fallout ^{137}Cs in the soil profile (kg m^{-2}).

If t_0 (yr) represents the year when cultivation started, from Equations 5.8 and 5.9, the total ^{137}Cs inventory $A(t)$ at year t can be expressed as:

$$A(t) = A(t_0)\, e^{-(PR/d+\lambda)(t-t_0)} + \int_{t_0}^{t} (1 - P\gamma(1-e^{-R/H}))\, I(t')\, e^{-(PR/d+\lambda)(t-t')}\, dt' \qquad (10)$$

where:

$A(t_0)$ is the ^{137}Cs inventory (Bq m^{-2}) at t_0 (yr):

and

$$A(t_0) = \int_{1954}^{t_0} I(t')\, e^{-\lambda(t'-t_0)}\, dt' \qquad (11)$$

The erosion rate R can be estimated by solving Equation 5.10 numerically, when the ^{137}Cs deposition flux and values of the relevant parameters are known. The ^{137}Cs concentration of mobilised sediment $C_e(t')$ can be expressed as:

$$C_e(t') = \frac{I(t')}{R}\, P\gamma\,(1-e^{-R/H}) + P\frac{A(t')}{d} \qquad (12)$$

For a depositional point ($A(t) > A_{ref}$), assuming that the excess ^{137}Cs inventory A_{ex} (Bq m^{-2}) (defined as the measured total inventory $A(t)$ less the local direct fallout input A_{ref}) at an aggrading point is due to the accumulation of ^{137}Cs associated with deposited sediment, the excess ^{137}Cs inventory can be expressed as:

$$A_{ex} = \int_{t_0}^{t} R'\, C_d(t')\, e^{-\lambda(t-t')}\, dt' \qquad (13)$$

where:

R' is the deposition rate (kg m^{-2} yr^{-1});
$C_d(t')$ is the ^{137}Cs concentration of deposited sediment (Bq kg^{-1}).

$C_d(t')$ will reflect the mixing of sediment and its associated ^{137}Cs concentration mobilised from all the eroding points that converge on the aggrading point. $C_d(t')$ essentially comprises two components, the first of which is associated with the removal of the freshly deposited ^{137}Cs, and the second is associated with erosion of the accumulated ^{137}Cs stored in the soil. Again, $C_d(t')$ can be estimated from the ^{137}Cs concentrations of the mobilised sediment from the upslope eroding area S:

$$C_d(t') = \frac{1}{\int_S R\, dS} \int_S P'\, C_e(t')\, R\, dS \qquad (14)$$

From Equations 5.13 and 5.14, the mean soil deposition rate R' can be calculated from the following Equation:

$$R' = \frac{A_{ex}}{\int_{t_0}^{t} C_d(t')\, e^{-\lambda (t-t')}\, dt'} \qquad (15)$$

Advantages and limitations: The mass balance model described here takes account of both the temporal variation of the ^{137}Cs fallout input and its initial distribution in the surface soil, prior to incorporation into the plough layer by tillage. Results obtained using this model are likely to be more realistic than those provided by the simplified mass balance model 1 presented in the previous section. However, in order to use this model, information on the plough depth *h*, relaxation mass depth *H* and the parameter γ is required. Although the first is relatively easy to estimate from the ^{137}Cs depth distribution at a non-eroding point, the latter two are more difficult to specify. The relaxation mass depth *H* is best estimated experimentally for the local soil type and the parameter γ can be estimated from available long-term rainfall records and information on the timing of tillage operations at the study site. Since the model requires information on the ^{137}Cs concentration of soil eroded from upslope, the sampling points used with the model must be arranged along a downslope transect. Normally, a uniform spacing of sampling points is assumed. The first (upper) point on a transect should represent an eroding point.

(iv) A mass balance model incorporating soil movement by tillage (Mass Balance Model 3)

The mass balance models described previously do not take account of soil redistribution caused by tillage operations. As tillage results in the redistribution of soil in a field, the ^{137}Cs contained in the soil will also be redistributed, and such redistribution needs to be taken into account when using the ^{137}Cs measurements to derive estimates of rates of soil erosion by water. If the effects of tillage redistribution on ^{137}Cs inventories can be quantified and taken into account, the remaining component of redistribution will reflect the impact of water erosion.

The effect of tillage in redistributing soil can be represented by a downslope sediment flux. Following [9] the downslope sediment flux F_Q (kg m^{-1} yr^{-1}) from a unit contour length may be expressed as:

$$F_Q = \phi \sin\beta \qquad (16)$$

where:

β is the slope angle(°);
ϕ is a site-specific constant(kg m^{-1} yr^{-1}).

If a flow line down a slope is divided into several sections and each section can be approximated as a straight line, then for the ith section (from the hilltop), the net soil redistribution induced by tillage R_t (kg m^{-2} yr^{-1}) can be expressed as:

$$R_t = (F_{Q,out} - F_{Q,in})/L_i = \phi(\sin\beta_i - \sin\beta_{i-1})/L_i = R_{t,out} - R_{t,in} \qquad (17)$$

where:

L_i is the slope length of the ith segment (m);
$R_{t,out}$ and $R_{t,in}$ (kg m^{-2} yr^{-1}) are defined as:

$$\begin{aligned} R_{t,out} &= \phi \sin \beta_i / L_i \\ R_{t,in} &= \phi \sin \beta_{i-1} / L_i \end{aligned} \tag{18}$$

For a point experiencing water erosion [rate R_w (kg m^{-2} yr^{-1})], variation of the total ^{137}Cs inventory $A(t)$ (Bq m^{-2}) with time t can be expressed as:

$$\frac{dA(t)}{dt} = (1-\Gamma)\ I(t) + R_{t,in}\ C_{t,in}(t) - R_{t,out}\ C_{t,out}(t) - R_w\ C_{w,out}(t) - \lambda\ A(t) \tag{19}$$

where:

$C_{t,in}$, $C_{t,out}$ and $C_{w,out}$ are the ^{137}Cs concentrations of the sediment associated with tillage input, tillage output and water output, respectively (Bq kg^{-1}).

The net erosion rate R (kg m^{-2} yr^{-1}) is:

$$R = R_{t,out} - R_{t,in} + R_w \tag{20}$$

For a point experiencing water-induced deposition (rate R'_w, (kg m^{-2} yr^{-1})), variation of the total ^{137}Cs inventory with time can be expressed as:

$$\frac{dA(t)}{dt} = I(t) + R_{t,in}\ C_{t,in}(t) - R_{t,out}\ C_{t,out}(t) + R'_w\ C_{w,in}(t) - \lambda\ A(t) \tag{21}$$

where:

$C_{w,in}$ is the ^{137}Cs concentration of the sediment input from water-induced deposition (Bq kg^{-1}).

The net erosion rate R is:

$$R = R_{t,out} - R_{t,in} - R'_w \tag{22}$$

The ^{137}Cs concentration of the soil within the plough layer $C_s(t')$ (Bq kg^{-1}) can be expressed as:

$$\begin{aligned} C_s(t') &= \frac{A(t')}{d} \quad \text{for a net erosion site} \\ C_s(t') &= \frac{1}{d}\left[A(t') - \frac{|R|}{d}\int_{t_0}^{t-1} A(t'')\, e^{-\lambda t''}\, dt''\right] \text{ for a net deposition site} \end{aligned} \tag{23}$$

where:

$|R|$ (R<0) is the net deposition rate (kg m^{-2} yr^{-1}).

The relationships between C_s and $C_{t,in}$ and $C_{t,out}$ are as follows:

$$C_{t,in}(t') = C_{t,out}(t') = C_s(t')$$
$$C_{w,out}(t') = P\, C_s(t') + \frac{I(t')}{R_w} P\, \gamma\, (1 - e^{-R_w/H}) \quad (24)$$

while the ^{137}Cs concentration of water-derived deposited sediment $C_{w,in}(t')$ (Bq kg^{-1}) can be expressed as:

$$C_{w,in}(t') = \frac{1}{\int_S R\, dS} \int_S P'\, C_{w,out}(t')\, R\, dS \quad (25)$$

For a given point, the tillage-derived erosion or deposition rate ($R_{t,out}$–$R_{t,in}$) can be calculated from Equation 5.17 and the net soil erosion rate (R>0) or deposition rate (R<0) can be estimated by solving Equations 5.19, 5.20, 5.24 and 5.25 numerically.

Advantages and limitations: The mass balance model described here represents an important improvement over the two mass balance models presented previously in that it takes into account the effects of tillage-induced soil movement. The estimates of soil redistribution rates associated with water erosion provided by this model are likely to be closer to reality for cultivated soils than those provided by the other two mass balance models. However, this model requires more information than the previous two mass balance models. Furthermore, in its current form, the model can only be used for individual slope transects.

(v) The Profile Distribution Model (for uncultivated soils)

For uncultivated soils, the depth distribution of ^{137}Cs in the soil profile will be significantly different from that in cultivated soils where the ^{137}Cs is mixed within the plough or cultivation layer. In most situations, the depth distribution of ^{137}Cs in an undisturbed stable soil will exhibit a well-defined exponential decline with depth that may be described by the following function (see [1, 7]):

$$A'(x) = A_{ref}\ (1 - e^{-x/h_0}) \quad (26)$$

where:

$A'(x)$ is the amount of ^{137}Cs above the depth x (Bq m^{-2});
A_{ref} is the ^{137}Cs reference inventory (Bq m^{-2});
x is the depth from the soil surface (kg m^{-2});
h_0 is the coefficient describing profile shape (kg m^{-2}).

If it is assumed that the total ^{137}Cs fallout occurred in 1963 and that the depth distribution of the ^{137}Cs in the soil profile is independent of time, the *erosion rate Y* for an eroding point (with total ^{137}Cs inventory A_u (Bq m^{-2}) less than the local reference inventory A_{ref} (Bq m^{-2})) can be estimated as:

$$Y = \frac{10}{(t - 1963)\, P} \ln\left(1 - \frac{X}{100}\right) h_0 \quad (27)$$

where:

Y is the annual soil loss (t ha^{-1} yr^{-1});
t is the year of sample collection (yr);

X is the percentage ^{137}Cs loss in total inventory in respect to the local ^{137}Cs reference value (defined as $[(A_{ref}–A_u)/A_{ref}]\times100$);
A_u is the measured total ^{137}Cs inventory at the sampling point (Bq m^{-2});
P is the particle size correction factor.

For a depositional location, a tentative estimate of the deposition rate R' can be estimated from the excess ^{137}Cs inventory $A_{ex}(t)$ (Bq m^{-2}) (defined as $A_u–A_{ref}$) and the ^{137}Cs concentration of deposited sediment C_d:

$$R' = \frac{A_{ex}}{\int_{t_0}^{t} C_d(t')\, e^{-\lambda (t-t')}\, dt'} = \frac{A_u - A_{ref}}{\frac{P'}{\int_S R\, dS} \int_S A_{ref} \left(1 - e^{-R/h_0}\right) dS} \tag{28}$$

C_d can be calculated using the same approach as used in Equations 5.6 and 5.14.

Advantages and limitations: The profile shape model is simple and easy to use. However, this model involves a number of simplifying assumptions. Most importantly, it does not take account of the time-dependent behaviour of the ^{137}Cs fallout input and the progressive development (downward movement) of the depth distribution of the ^{137}Cs within the soil profile after deposition from the atmosphere. As such, it is likely to overestimate rates of soil loss, since the amount of ^{137}Cs removed with a given depth of soil is likely to be greater than suggested by the present-day depth distribution of ^{137}Cs in the soil.

(vi) The Diffusion and Migration Model (for uncultivated soils)

Although the depth distribution model described above can be used to obtain estimates of soil erosion or deposition rates for uncultivated soils, a more realistic approach needs to consider the time-dependent behaviour of the ^{137}Cs depth distribution, which reflects both the timing of the ^{137}Cs fallout input and the progressive redistribution and downward movement of ^{137}Cs in the soil profile after deposition from the atmosphere (e.g. [8, 10, 11]). Under certain circumstances, the redistribution of ^{137}Cs in uncultivated soils can be represented using a one-dimensional diffusion and migration model characterised by an effective diffusion coefficient and migration rate. For example, in some situations, the ^{137}Cs depth profile in uncultivated soils exhibits a broad concentration peak with the maximum concentration located below the soil surface. In this situation variation of the ^{137}Cs concentration $C_u(t)$ (Bq kg^{-1}) in surface soil with time t (yr) may be approximated as:

$$C_u(t) \approx \frac{I(t)}{H} + \int_0^{t-1} \frac{I(t')\, e^{-R/H}}{\sqrt{D\, \pi\, (t-t')}} e^{-V^2 (t-t')/(4D) - \lambda (t-t')}\, dt' \tag{29}$$

where:

D is the diffusion coefficient (kg^2 m^{-4} yr^{-1});
V is the downward migration rate of ^{137}Cs in the soil profile (kg m^{-2} yr^{-1}).

For an eroding point, if sheet erosion is assumed, then the erosion rate R may be estimated from the reduction in the ^{137}Cs inventory $A_{ls}(t)$ (Bq m^{-2}) [defined as the ^{137}Cs reference inventory A_{ref} less the measured total ^{137}Cs inventory A_u (Bq m^{-2})] and the ^{137}Cs concentration in the surface soil $C_u(t')$ given by Equation 5.29 according to:

$$\int_0^t P\, R\, C_u(t') e^{-\lambda (t-t')}\, dt' = A_{ls}(t) \tag{30}$$

For a depositional location, the deposition rate R' can be estimated from the ^{137}Cs concentration of deposited sediment $C_d(t')$ and the excess ^{137}Cs inventory $A_{ex}(t)$ (defined as the total measured ^{137}Cs inventory A_u less the local reference inventory A_{ref}) using the following relationship:

$$R' = \frac{A_{ex}}{\int_{t_0}^{t} C_d(t')\, e^{-\lambda (t-t')}\, dt'} = \frac{A_u - A_{ref}}{\int_{t_0}^{t} C_d(t')\, e^{-\lambda \cdot (t-t')}\, dt'} \qquad (31)$$

where $C_d(t')$ can be calculated from:

$$C_d(t') = \frac{1}{\int_S R\, dS} \int_S P'\, P\, C_u(t')\, R\, dS \qquad (32)$$

Advantages and limitations: Since the diffusion and migration model described here takes into account the time-dependent behaviour of both the ^{137}Cs fallout input and its subsequent redistribution or downward movement in the soil profile, it therefore represents an improvement over the profile shape model presented in the previous section. However, to use this model, more information on the behaviour of ^{137}Cs in undisturbed soils is needed. More particularly, estimates of the diffusion coefficient D and the migration rate V are required. These can be derived from detailed measurements of the ^{137}Cs depth distribution.

2.2. Models for use with $^{210}Pb_{ex}$ and ^{7}Be measurements

The use of $^{210}Pb_{ex}$ and ^{7}Be measurements for estimating soil redistribution rates is still in its infancy and not as well established as that of ^{137}Cs. The development of the conversion models for $^{210}Pb_{ex}$ and ^{7}Be presented here should therefore be seen as an attempt to promote the use of these two radionuclides in different environments and, in turn, to identify the shortcomings of the new models and to improve them accordingly.

(i) Conversion models for use with $^{210}Pb_{ex}$ measurements

$^{210}Pb_{ex}$ has a comparable half-life (22.3 years) to ^{137}Cs. However, its natural origin and its essential continuous input provide potential for deriving estimates of soil distribution rates averaged over longer periods (e.g. 100 years). Two mass balance models have been developed for use with the $^{210}Pb_{ex}$ inventories for samples collected from cultivated sites. They represent adaptations of mass balance models 2 and 3 developed for ^{137}Cs and described above. The second includes a tillage component, whereas the first does not. The migration and diffusion model for ^{137}Cs has also been modified for use with $^{210}Pb_{ex}$ measurements obtained for samples collected from uncultivated fields. The key modifications made to the ^{137}Cs conversion models are as follows:

- The modelling period has been set to extend back 100 years from the sampling date. It is assumed that any $^{210}Pb_{ex}$ deposition prior to this point in time will have become essentially insignificant due to decay. In theory, only around 4% of the original deposition will remain

after 100 years. The time of sampling is not used in the calculation. It is only relevant for interpreting the results obtained from the model;

- It is assumed that the annual $^{210}Pb_{ex}$ fallout remains effectively constant through time and that because the reference inventory will represent a steady state balance between input and decay, the reference inventory will remain the same through time. The deposition flux ($I_{(t)}$) can be determined from the local reference inventory (A_{ref}) as:

$$I_{(t)} = A_{ref} \ln(2) / 22.3 \quad (33)$$

- Due to its shorter half-life, the decay constant for $^{210}Pb_{ex}$ differs from that for ^{137}Cs.

Most of the parameters used in the conversion models for $^{210}Pb_{ex}$ inventories are very similar to those used for the ^{137}Cs models. However, a degree of caution is needed in their specification, since the behaviour of $^{210}Pb_{ex}$ in soils may differ from that of ^{137}Cs. Further information related to the application of $^{210}Pb_{ex}$ in soil erosion studies on cultivated land can be found in [5, 12].

(ii) Conversion models for ^{7}Be measurements

To use measurements of ^{7}Be inventories collected along a downslope transect to estimate erosion and deposition rates, the profile distribution model used for ^{137}Cs and described above has been modified as follows:

- The modelling period is reduced from decades to a single event or a short period encompassing several events;

- Annual natural decay is no longer important;

- The value for the profile shape factor h_0 is much lower (e.g. <20 kg m^{-2}). This value is likely to be similar to the value for the relaxation depth H used in the conversion models for ^{137}Cs and $^{210}Pb_{ex}$, since, by virtue of the short half-life of ^{7}Be, it effectively represents the relaxation depth of fresh fallout.

In all other respects, the application of the profile distribution model is essentially the same as its use for ^{137}Cs. A detailed discussion of the conversion model and its application can be found in [4, 6].

The calculations required when employing the approach to use ^{7}Be measurements for erosion assessment proposed by [13] have not been included in the software package, since this approach is used less commonly. It uses a mass balance for ^{7}Be to calculate soil redistribution and involves determination of the pre- and post-event ^{7}Be inventories in the soil, the fallout input of ^{7}Be during the event, and the profiles of ^{7}Be activity in the soil following the event.

2.3. Selecting a model for use with ^{137}Cs and $^{210}Pb_{ex}$ measurements

A single model is provided for use with ^{7}Be measurements, but for ^{137}Cs and $^{210}Pb_{ex}$, there is a choice of several conversion models. The discussion of the advantages and limitations of these different models provided in the previous sections will provide some help to users in making an appropriate choice. Factors that should be considered include:

- The intended use of the resulting estimated erosion and deposition rates;

- The land use history of the study sites;

- The availability of the relevant parameters and other data and the feasibility of obtaining these if they are not available.

While it is impossible to generalise as to which model is likely to be most appropriate for any specific project, some general guidelines are provided by the flow charts presented in Fig. 1. In addition to data availability, an understanding of site-specific radionuclide redistribution processes is an important prerequisite, when selecting a model. Collection of sectioned cores from some critical points / sites will not only help to refine the sampling strategy, but also yield valuable information about the on-going redistribution processes in the soil profile. For example, the depth of the maximum concentration down the profile for a reference site provides an indication of the migration rate for ^{137}Cs. The magnitude of the reduction in the inventory at the very top of a slope, where water erosion is likely to be negligible, can provide an indication of the intensity of tillage translocation.

2.4. Use of the Excel Add-in for implementing the ^{137}Cs, $^{210}Pb_{ex}$ and ^{7}Be conversion models

As indicated above, conversion of radionuclide inventories to estimates of erosion and depositional rates attempts to numerically infer the rate of removal or accretion of the radionuclide over a specific time period and thereby produce an estimate of the rate of soil redistribution. The complexities and uncertainties associated with the various soil redistribution processes means that the conversion models should initially be applied with caution and where possible the results obtained validated against independent information or evidence of the erosion and deposition rates involved. To facilitate the use of the conversion models described in the previous section, software has been developed for converting ^{137}Cs, $^{210}Pb_{ex}$ and ^{7}Be inventories to soil erosion and deposition rates using VBA (Visual Basic Application). The software has been designed to deal with point data collected along a single downslope transect that follows the flow line (direction of maximum slope), and assumes that there is no sediment contribution from upslope areas or significant across slope soil redistribution.

Implemented as a standard Add-in within Microsoft Excel, the software has the following features:

- It can take full advantages of the data management and data analysis functions available in Excel. The conversion results can be readily related to other environmental variables or factors for further analysis;

- To ensure meaningful model parameterisation, limitations have been placed on the acceptable ranges for individual parameters and default values have been provided. Procedures have also been included to derive or estimate some parameters;

- Conversion models for ^{137}Cs, $^{210}Pb_{ex}$ and ^{7}Be can be accessed with a uniform, consistent, interactive interface in a user-friendly manner. The design of the interfaces follows the logical sequence of data analysis, involving data input, parameter specification and output and storage of the results;

- There are no restrictions on folder names / paths, data file locations and, thus, the user is given flexibility in programme installation and data management.

The conversion models available within the Add-in are listed in Table 1.

TABLE 1. CONVERSION MODELS AVAILABLE WITHIN THE ADD-IN

FRN	Cultivated	Uncultivated (Pasture)
^{137}Cs	Proportional Model Simplified mass balance model (Mass Balance Model 1) Mass Balance Model 2 Mass balance model with tillage (Mass Balance Model 3)	Profile Shape Model Diffusion and Migration model
^{210}Pb	Mass Balance Model 2 Mass balance model with tillage (Mass Balance Model 3)	Diffusion and Migration model
^{7}Be	Profile Shape Model	

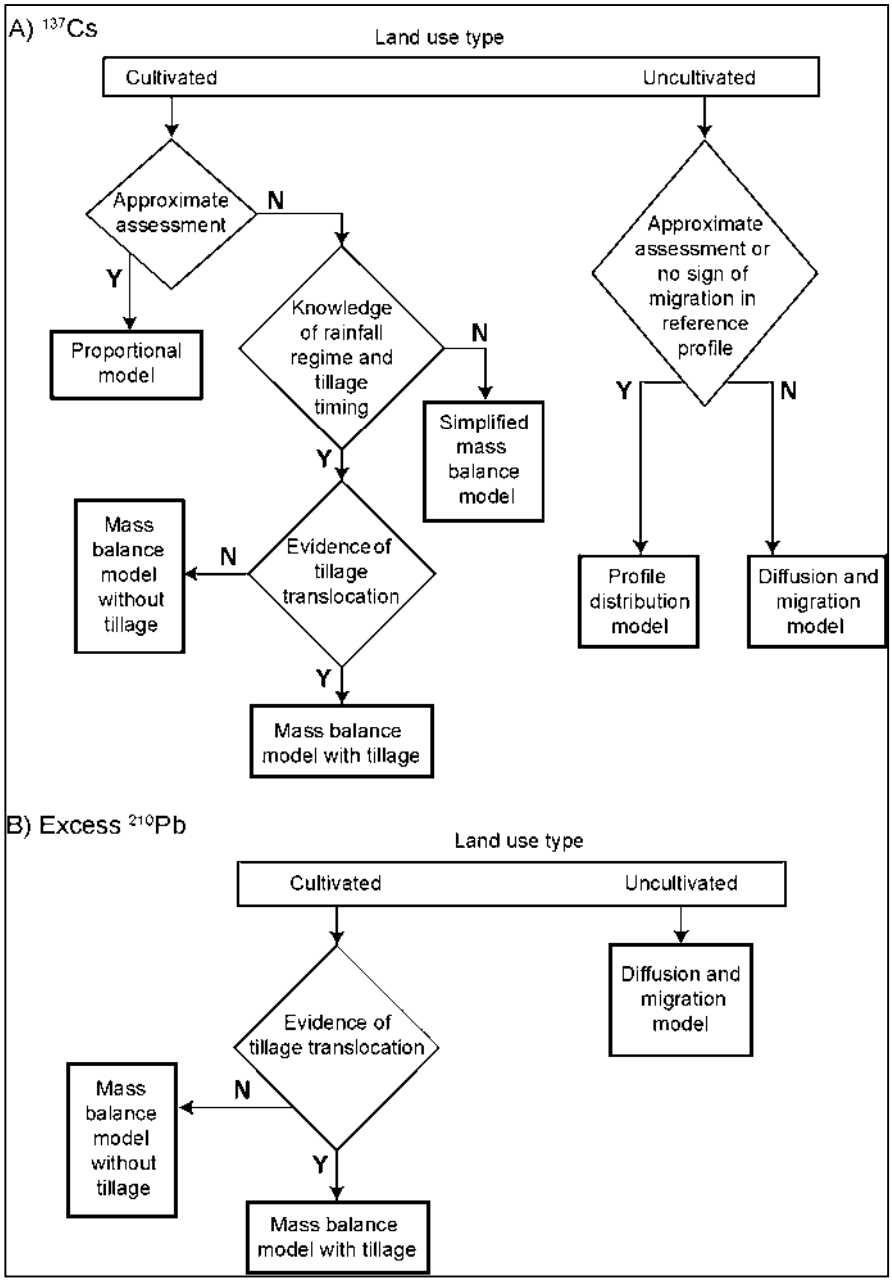

FIG. 1. General guidelines for choosing a conversion model for ^{137}Cs (A) and $^{210}Pb_{ex}$ (B).

For each model, the sample inventories, the reference inventory and the particle size correction factor (if it is available) are required. Other parameters and data requirements are detailed in Table 2.

TABLE 2. PARAMETERS AND DATA REQUIREMENTS FOR THE INDIVIDUAL MODELS

Model type	Parameter and data requirements
Proportional Model and Simplified mass balance model	Tillage depth, bulk density, year of tillage commencement
Mass Balance Model 2	Tillage depth, year of tillage commencement, proportion factor, relaxation depth, record of annual fallout flux [a]
Mass balance model with tillage (Mass Balance Model 3)	Tillage depth, tillage constant, proportion factor, relaxation depth, slope length and slope gradient for each section of the transect, record of annual fallout flux
Diffusion and Migration Model	Diffusion coefficient, relaxation depth, migration coefficient, record of annual fallout flux
Profile Shape Model	Profile shape factor

[a] *Only required for ^{137}Cs models*

It is clear that each model has its own specific set of parameters, although some parameters are common between models. More importantly, the models differ in their underlying assumptions, the process description and the representation of temporal variability. A sound understanding of the models and the meaning and derivation of their parameters is an essential precursor to their successful application. In order to assist in applying the appropriate model and to avoid their possible misuse, further information on the model parameters and the implementation of the model software is provided in the following sections.

2.5. Parameter specification and derivation

As with all models, the reliability of the conversion models outlined in the previous section depends heavily on the specification and derivation of the model parameters. Some of these are more difficult to derive and involve more uncertainty than others. Procedures for the derivation of the individual parameters are described in this section.

2.5.1. The reference inventory

The reference inventory is a critical parameter for any study using ^{137}Cs, $^{210}Pb_{ex}$ and ^{7}Be measurements to estimate soil redistribution rates. The value provided will govern whether a sampling point is designated as having undergone erosion or deposition, and the magnitude of the redistribution rates involved. For ^{137}Cs, an algorithm has been developed and included in the software to estimate a region-specific value for any area of the world, based on known relationships between the reference inventory, geographic location (longitude and latitude) and annual rainfall [14]. It must be emphasised that the predicted value is seen only as providing an estimate of the likely magnitude of the reference inventory at a study site and the value should not be used in the conversion models. It is necessary to obtain a reliable estimate of the local reference inventory, based on field measurements, prior to applying a conversion model. There are currently no procedures available to predict the likely magnitude of reference inventories for ^{210}Pb and ^{7}Be. It is recommended that the sampling of reference sites should include some depth incremental sampling, as well as the collection of bulk cores, in order to confirm that the site has not been disturbed (e.g. cultivated). The associated depth or profile distributions may also be needed to derive other parameters, such as the profile shape factor, and the migration and diffusion rate, etc.

2.5.2. *Particle size correction factors for eroding and depositional sites*

The particle size correction factors are incorporated into the conversion models, in order to take account of the potential grain size selectivity of erosion and sedimentation processes and the likely preferential association of the fallout radionuclides with the finer fractions of the soil or sediment. Thus, for example, if erosion is associated with the preferential removal of fine particles, which are characterized by high concentrations of the radionuclide, the erosion rate is likely to be overestimated if this is not taken into account. Equally, if deposition involves the preferential deposition of coarser particles with low radionuclide activity, the deposition rate may be under-estimated if this is not considered. However, although the need to incorporate particle size correction into conversion models is clear and P and P' are readily defined, there have been few attempts to derive these correction factors and they may prove difficult to establish. No standard procedure exists and potential approaches to estimating values of P and P' are likely to vary according to both the soil type and the radionuclide being considered, as well as the degree of selectivity associated with the sediment mobilisation (erosion and deposition) processes.

Since it may prove difficult to obtain the information on the ^{137}Cs concentration in soil mobilised by erosion and in deposited sediment, required to calculate P and P' directly, estimates of these parameters can be derived from information on the grain size composition of the surface soil, eroded sediment and deposited sediment, using the procedures described by [15]. If the specific surface area of mobilised sediment is S_{ms} (m^2 g^{-1}), and that of the original soil is S_{sl} (m^2 g^{-1}), P can be estimated as:

$$P = \left(\frac{S_{ms}}{S_{sl}} \right)^{\nu} \tag{34}$$

where:

ν is a constant with a value of ca. 0.65.

If the specific surface area of deposited sediment is S_{ds} (m^2 g^{-1}), P' can be estimated as:

$$P' = \left(\frac{S_{ds}}{S_{ms}} \right)^{\nu} \tag{35}$$

The value of ν in Equation 5.35 is the same as that in Equation 5.34. The following relationship therefore exists:

$$PP' = \left(\frac{S_{ms}}{S_{sl}} \right)^{\nu} \left(\frac{S_{ds}}{S_{ms}} \right)^{\nu} = \left(\frac{S_{ds}}{S_{sl}} \right)^{\nu} \tag{36}$$

Information on the specific surface area of a sediment sample can, in many cases, be provided directly by the current generation of laser granulometers that are widely used for grain size analysis. Such data are estimated from the grain size distribution, assuming spherical particles. Alternatively, equivalent values can be derived numerically from the grain size distribution, using information on the surface area of particles of different diameter.

Samples of mobilised sediment in surface runoff could be collected during erosion events and samples of deposited sediment could be collected from the surface of depositional areas immediately after such events. Alternatively, an indication of the likely size-selectivity of the

sediment mobilisation process could be obtained by comparing the grain size composition of the surface soil from eroded areas with that of areas with no erosion, and inferring the degree of size selectivity required to account for any coarsening of the surface soil in eroded areas. However, if this approach is taken, it would be necessary to consider whether coarsening of the soil in eroded areas reflected progressive removal of the surface horizons rather than size-selective erosion.

2.5.3. The relaxation depth

The relaxation depth H is used to represent the exponential depth distribution of fresh fallout in the surface soil. It is difficult to determine this value empirically. In the case of ^{137}Cs, the current fallout flux is negligible and it is impossible to replicate the situation during the main period of fallout in the late 1950s and the 1960s. In the case of $^{210}Pb_{ex}$, the fallout in out is continuous and it should be possible document the depth distribution of fresh fallout, if the pre-existing depth distribution is known and the pre-existing surface activity is low, as would be the case for a recently cultivated soil. Alternatively, H can be determined experimentally by simulating fallout input to the surface of a soil using a rainfall simulator and establishing the depth distribution of the applied fallout in the soil. In the absence of such empirical or experimental measurements, information on the depth distribution of ^{7}Be in the surface soil after an extended period of rainfall could be used to establish the likely value of H for ^{137}Cs or $^{210}Pb_{ex}$. Because of its short half-life, the depth distribution of ^{7}Be can be used as a surrogate for the depth distribution of fresh ^{137}Cs and $^{210}Pb_{ex}$ fallout, if the post fallout behaviour of the three radionuclides can be assumed to be similar. In the absence of any information, a value of 4.0 kg m^{-2} is frequently assumed for H, based on available empirical and experimental evidence. Further work is, however, required to determine the likely variation of H, according to soil type and other soil properties.

2.5.4. The proportion factor

The proportion factor represents the proportion of the annual radionuclide fallout that is susceptible to mobilisation by heavy rainfall, prior to its incorporation into the soil by tillage. This will depend on the temporal distribution of the local rainfall in relation to the timing of cultivation. In locations where the annual wet season and associated high intensity rainfall, which can generate surface runoff and thus mobilise sediment, occur shortly before the period of cultivation, the fallout input already accumulated at the soil surface as well as additional input directly associated with the high intensity rainfall events will be susceptible to removal by erosion. In these circumstances, the value for the proportional factor can be assumed to be ca. 1.0, if there is only one cultivation operation. In cases where the main period of high intensity rainfall events occurs immediately after cultivation has been completed and the remainder of the rainfall occurring during the year is unlikely to generate surface runoff, the fallout input accumulated at the soil surface before the occurrence of these events will have been incorporated into the plough layer by tillage, and only that directly associated with the intense rainfall occurring immediately after tillage will be susceptible to removal by erosion. Under these circumstances, the value of the proportion factor may be approximated by the ratio of the depth of rainfall associated with the main period of heavy rainfall, which produces surface runoff, to the total annual rainfall. If there is more than one cultivation operation each year, the temporal pattern of precipitation in relation to each cultivation operation needs to be considered.

2.5.5. The tillage constant

The potential significance of tillage translocation on within-field redistribution of fallout radionuclides has been emphasized by a number of recent studies [9, 16]. The contribution of tillage translocation to the redistribution of ^{137}Cs and $^{210}Pb_{ex}$ has been incorporated, albeit in a

simple manner, in mass balance model 3 by use of a tillage constant that represents a slope-independent specific soil flux. It is a lumped value for the time period under investigations (about 40 years for ^{137}Cs and 100 years for $^{210}Pb_{ex}$). No temporal and spatial variation is considered. While there are some data available on the value for the tillage constant associated with specific implements, the direct application of such values in the conversion models is frequently complicated by the need to account of the use of different implements over a period of several decades. An alternative approach to estimating the tillage constant is provided by considering the inventories of eroding sites located at the top of a slope where the contribution of water erosion and deposition can be treated as negligible, due to the lack of a significant upslope area to contribute runoff.

Assuming that there is no significant water erosion, the tillage erosion rate R_t (kg m^{-2} yr^{-1}) can be estimated from the measured total ^{137}Cs inventory $A_1(t)$ (Bq m^{-2}) of an eroding point using the following Equation (derived from Equation 5.10):

$$A_1(t) = A_1(t_0)\, e^{-(R_1/d+\lambda)(t-t_0)} + \int_{t_0}^{t} I(t')\, e^{-(R_1/d+\lambda)(t-t')}\, dt' \tag{37}$$

The tillage constant can be estimated from the erosion rate:

$$\phi = \frac{R_{t,out,1}\ L_1}{\sin\beta_1} = \frac{R_1\ L_1}{\sin\beta_1} \tag{38}$$

2.5.6. The profile shape factor, the migration rate and the diffusion coefficient

The profile shape factor (h_0) describes the rate of exponential decrease in inventory or radioactivity with depth for a soil profile from an uncultivated site. The larger the value of the profile shape factor, the deeper the ^{137}Cs or ^{7}Be penetration into the soil profile. If depth incremental samples are available for a reference site, h_0 can be estimated in Excel via curve-fitting. To estimate the value of h_0, an exponential function in the form of $f(z) = f(0)e^{-z/h_0}$ can be fitted to the relationship between sampling depth and mass concentration or inventory, where $f(0)$ is the fallout concentration (inventory) at the soil surface and z is the sampling depth in cumulative mass above.

The diffusion coefficient (D) and the migration rate (V) represent the evolution of the shape of the ^{137}Cs or $^{210}Pb_{ex}$ profile with time. High values of D and V will imply a deeper penetration of ^{137}Cs into the soil profile. Although more precise values of D and V can be obtained through solving the one-dimensional transport Equation (see Equation 5.15), in the case of ^{137}Cs they may be approximated using the following Equations:

$$V \approx \frac{W_p}{t - 1963} \tag{39}$$

$$D \approx \frac{\left(N_p - W_p\right)^2}{2 \times (t - 1963)} \tag{40}$$

where:

t is the year when the soil core was collected (yr);
W_p is the mass depth of the maximum ^{137}Cs concentration (kg m^{-2});

N_p is the mass depth at which the ^{137}Cs concentration reduces to $1/e$ of the maximum concentration (kg m^{-2}).

For ^{137}Cs, D (kg^2 m^{-4} yr^{-1}) and V (kg m^{-2} yr^{-1}) are normally in the range of 30-50 kg^2 m^{-4} yr^{-1} and 0.2-1.0 kg m^{-2} yr^{-1}, respectively. With ^{210}Pb$_{ex}$, D is related to V as follows [8]:

$$\frac{1}{h_0} = 0.5 \times \left(\sqrt{\frac{V^2}{D^2} + \frac{4\lambda}{D}} - \frac{V}{D}\right) \tag{41}$$

Assuming $V = 0$, since the maximum ^{210}Pb$_{ex}$ activity will commonly be found at the surface, rather than, as in the case of ^{137}Cs, just below the surface, D can be calculated using the above Equation. Routines have been developed for estimating h_0, D, and V for reference sites where values of depth incremental sample mass and corresponding values of mass concentration are available. These are activated when a migration and diffusion model is selected. It is important to note that the estimated values will be influenced by the thickness of the depth increment used in sectioning the core. Since soil erosion is a surface processes, it is vital to have detailed information near the top of the profile.

2.5.7. The annual deposition flux

Except for the simplified mass balance model, all other mass balance models use the annual deposition flux in their calculations. For ^{210}Pb$_{ex}$, the annual deposition flux is assumed to be effectively constant through time and it is calculated by the software, using the given reference inventory and assuming a steady-state between the annual input and the loss of the radionuclide by decay. For ^{137}Cs, the annual fallout deposition flux since 1954 must be provided. Few, if any, studies will have these data available for specific sites. The software therefore uses the given reference inventory value and generalised information on the temporal distribution of annual fallout to synthesise the annual series for a study site. Assuming that the study site has the same relative annual variation as that of the reference station used to characterize the temporal pattern of annual fallout, although different in absolute magnitude, the record of the local ^{137}Cs deposition flux $I(t)$ can be synthesised using the following Equation:

$$I(t) = \alpha \, I_n(t) \tag{42}$$

where:

$I_n(t)$ is the ^{137}Cs deposition flux for the reference station (Bq m^{-2} yr^{-1});
α is a scaling factor which can be calculated as follows:

$$\alpha = \frac{A_{ref}}{\int_{1954}^{t} I_n(t') \, e^{-\lambda(t-t')} \, dt} = \frac{A_{ref}}{A_n} \tag{43}$$

where:

A_n is the present total atmospheric fallout inventory for the ^{137}Cs deposition at the reference station (Bq m^{-2}).

The reference station file is a plain text file that contains a single column of numbers listing the annual flux in Bq m^{-2} from 1954. The default value for years after 1983 is zero. Representative station files for both the northern and south hemisphere, without Chernobyl-related ^{137}Cs inputs, are included in the help documentation. They can be copied, saved and modified. A customised annual deposition flux file can also be generated for those areas where the Chernobyl-related ^{137}Cs input is known to be significant, if the additional deposition flux that occurred in 1986 is known or can be estimated.

2.6. Management of the Add-in software and its application

2.6.1. System requirements and installation

The software distributed is a standard Microsoft (Ms) Excel Add-In. It consists of one Add-in file (named radiocalc.xla) and one rainfall data file if the approximate local reference inventory has to be estimated. The minimum software environment is a copy of Excel 97 operating on Windows 98 and Internet Explorer 5.0. It was originally developed on a PC with Windows 98 operating system running Excel 2000 and subsequently tested on the Windows XP, Vista and Windows 7 operating systems running Excel 2003. Though no extensive tests have been undertaken, it also appears to work in Excel 2007 and Excel 2010.

(i) Software installation

The software should be installed and removed through the built-in user interface for the management of Add-ins in Excel.

With the introduction of ribbon GUI (Graphic User Interface) from Excel 2007, its location has been changed. Separate instructions will be given for non-ribbon and ribbon interfaces below where necessary:

To install the programme, one only has to move the files to a user-preferred folder. Both files should be saved in one folder.

When you use the add-in for the first time, the following steps must be followed to prepare it for use:

1) Start Excel

2) Navigate the menu system to access the tools for the management of Addins. For non ribbon interface, it is via ‘Tools | Add-ins’. For ribbon interface, it is first ‘File | Options | Add-ins’ (or click the Office Button, the Excel Options button and then select Add_Ins from the side menu. When ‘View and manage Microsoft Add-ins’ is shown, choose ‘Excel Add-ins’ for the management option and then ‘Go…’ at the bottom.

3) With the tools available at the interface for management of the Add-ins, ‘Browse’ for the saved 'radiocalc.xla' and open it. It should, then, appear on the list. Make sure the leading box in front of the 'radiocalc.xla' is checked if necessary.

4) Close the Add-in window. For non-ribbon interface, a new menu item named 'radionuclide inventories conversion' should be added to the 'Tools' menu. For ribbon interface, it will appear on the tab for the Add-ins. Then, you can use the Add-in by simply clicking newly added menu item.

5) Apart from adding one entry to the Window's registry, no other files or modifications are to be made to the user's system files and configurations.

(ii) Removing the Add-in

Removal of the Add-in from your computer involves two steps:

6) Remove the added menu item from the menu system: navigate to the tools for management of the Add-ins as explained in step 2 Then, remove the Add-in by un-checking the leading box. The programme will also delete its entry to the Windows registry.

7) Remove the programme files: go to the folder and delete the files as usual.

When you go to the Add-in list next time, you may be prompted by the Excel to delete the Add-in from the list of available Add-ins. It is advised that users should avoid deleting the programme associated files before removing the added menu item.

2.6.2. Using the Add-in

(i) Input data management

The data for the sampling points should be entered into an Excel worksheet and listed in columns which run from the top to the bottom of the slope. The same numbers of entries will be expected for the values relating to sample inventory, particle size correction factor, etc. With the current version of the programme, an active worksheet is required for it to run. All input data are expected to be in this worksheet and the output results will also be saved in it.

(ii) Interaction with the interface

The interface of the Add-in should be familiar to any Microsoft Windows user. Designed as a tool for research purposes, it is assumed that the user knows how to deal with command buttons, option buttons, input boxes, etc., in a Windows operating system.

With this Add-in, users also have to select a particular set of values or range (multiple cells in a single column) for data input and output. This can be done by selecting the first cell in the range, holding down the mouse, dragging it over the cells, and releasing the mouse when you reach the last cell. If a mistake is made, one can simply click the first cell and start all over again. Where a range is expected, the text input box is locked (no keyboard entry will be allowed) to avoid error in its specification. Instead, an arrow-labelled button is provided to its right. The user simply clicks the button to select a range interactively from the active worksheet.

3. Conclusions

Conversion models are a key requirement in the use of fallout radionuclides to obtain information on soil redistribution rates, since they are able to convert measurements of the reduction or increase in the radionuclide inventory of a sampling point, relative to the local reference inventory, into a quantitative estimate of the erosion or deposition rate involved. A wide range of conversion models are available for use with ^{137}Cs measurements and a limited number of models are now being developed for use with $^{210}Pb_{ex}$ and ^{7}Be.

In order to facilitate the application of the models in a standardised manner, and to promote their use by the wider scientific community, a user-friendly software package, based on an Excel Add-in has been produced. It is hoped that the use of a standardised set of conversion models by other researchers from both developing and developed countries will facilitate exchange and comparison of results and that the wider testing of the conversion models will generate an improved understanding of their advantages and limitations and thus assist the further development and improvement of such models.

REFERENCES

[1] WALLING, D.E., QUINE, T.A., "Use of Caesium-137 as a Tracer of Erosion and Sedimentation", Handbook for the Application of the Caesium-137 Technique, University of Exeter, UK (1993) 195.

[2] WALLING, D.E., HE, Q., Improved models for estimating soil erosion rates from ^{137}Cs measurements, J. Environ. Qual. 28 (1999) 611–622.

[3] WALLING, D.E., HE, Q., APPLEBY, P.G., "Conversion models for use in soil-erosion, soil-redistribution and sedimentation investigations", Handbook for the Assessment of Soil Erosion and Sedimentation Using Environmental Radionuclides, (ZAPATA, F., Ed.), Kluwer, Dordrecht, The Netherlands (2003) 111–164.

[4] BLAKE, W.H., WALLING, D.E., HE, Q., Fallout beryllium-7 as a tracer in soil erosion investigations, Appl. Radiat. Isot. 51 (1999) 599–605.

[5] WALLING, D.E., HE, Q., Using fallout lead-210 measurements to estimate soil erosion on cultivated land, Soil Sci. Soc. Am. J. 63 (1999) 1404–1412.

[6] WALLING, D.E., HE, Q., BLAKE, W.H., Use of ^{7}Be and ^{137}Cs measurements to document short- and medium-term rates of water-induced soil erosion on agricultural land,Water Resourc. Res. 35 (1999) 3865–3874.

[7] ZHANG, X.B., HIGGITT, D.L., WALLING, D.E., A preliminary assessment of the potential for using caesium-137 to estimate rates of soil erosion in the Loess Plateau of China, Hydrol. Sci. J. 35 (1990) 267–276.

[8] HE, Q., WALLING, D.E., The distribution of fallout ^{137}Cs and ^{210}Pb in undisturbed and cultivated soils, Appl. Radiat. Isot. 48 (1997) 677–690.

[9] GOVERS, G., QUINE, T.A., DESMET, P.J.J., WALLING, D.E., The relative contribution of soil tillage and overland flow erosion to soil redistribution on agricultural land, Earth Surf. Process. Landf. 21 (1996) 929–946.

[10] PEGOYEV, A.N., FRIDMAN, S.D., Vertical profiles of cesium-137 in soils, Pochvovedeniye 8 (1978) 77–81.

[11] WALLING, D.E., HE, Q., "Towards improved interpretation of ^{137}Cs profiles in lake sediments", Geomorphology and Sedimentology of Lakes and Reservoirs, (MCMANUS, J., DUCK, R.W., Eds), Wiley, Chichester, UK (1993) 31–53.

[12] WALLING, D.E., COLLINS, A.L., SICHINGABULA, H.M., Using unsupported lead-210 measurements to investigate soil erosion and sediment delivery in a small Zambian catchment, Geomorphology. 52 (2003) 193–213.

[13] WILSON, C.G., MATISOFF, G., WHITING, P.J., Short-term erosion rates from a ^{7}Be inventory balance, Earth Surf. Process. Landf. 28 (2003) 967–977.
[14] WALLING, D.E., HE, Q., "The global distribution of bomb-derived ^{137}Cs reference inventories", Final Rep. IAEA Technical Contract 10361/RO-R1 (2000).
[15] HE, Q., WALLING, D.E., Interpreting particle size effects in the adsorption of ^{137}Cs and unsupported ^{210}Pb by mineral soils and sediments, J. Environ. Radioact. 30 (1996) 117–137.
[16] GOVERS, G., LOBB, D.A., QUINE, T.A., Tillage erosion and translocation: emergence of a new paradigm in soil erosion research, Soil Till. Res. 51 (1999) 167–174.

COMBINED USE OF ^{137}Cs AND $^{210}Pb_{ex}$ TO ASSESS LONG-TERM SOIL REDISTRIBUTION IN A SMALL AGRICULTURAL FIELD IN MOROCCO

M. BENMANSOUR, A. NOUIRA, A. ZOUAGUI
Centre National de l'Energie des Sciences et des Technique Nucleaires (CNESTEN)
Rabat, Morocco

L. MABIT
Soil and Water Management and Crop Nutrition Subprogramme, Joint FAO/IAEA Division of Nuclear Techniques in Food and Agriculture,
Vienna - Seibersdorf

H. BOUKSIRATE, R. MOUSSADEK, R. MRABET, H. IAAICH
Institut National de la Recherche Agronomique (INRA),
Rabat, Morocco

M. DUCHEMIN
Institut de Recherche et de Développement en Agroenvironment (IRDA),
Quebec, Canada

Abstract

In Morocco, over 15 million hectares of farmland are under serious threat and each year an additional 100 million tons of soil is lost. Despite the severity of land degradation, only limited data are available on the actual magnitude of soil erosion in this North-African country. The objective of this paper was to show how ^{137}Cs and $^{210}Pb_{ex}$ determinations can be combined for evaluating soil redistribution rates and establishing medium- and long-term sediment budgets for the last 50-60 to 100 years. This case study has been conducted in an agricultural field located in Marchouch at 68 km south east from Rabat (Morocco). The net soil erosion rates obtained were comparable, 14 t ha^{-1} yr^{-1} and 12 t ha^{-1} yr^{-1} for ^{137}Cs and $^{210}Pb_{ex}$ respectively. Soil redistribution patterns of the study field based on ^{137}Cs and $^{210}Pb_{ex}$ results were established using a simple spatialisation approach. The maps generated led to similar sediment delivery ratio of about 95% indicating that the soil erosion processes have not changed significantly at this site over the last 100 years. In addition, the findings of this research highlighted that water erosion is the leading process in this Moroccan cultivated field, with tillage erosion under the current experimental conditions being the main translocation process within the site without a significant and major impact on net erosion. This paper demonstrates the advantage in combining two fallout radionuclides to assess medium- and long-term soil redistribution under Mediterranean agricultural conditions.

1. Introduction

Due to the intensification of agricultural practices and specific bio-climatic conditions, more than 15 million hectares of the Moroccan agricultural land are under serious threat and each year around 100 million tons of soils are lost [1]. Despite the severity of land degradation in Morocco, only limited data are available on the actual magnitude of soil and water resource degradation and on soil erosion rates. Most of the previous research in this region has focused on conventional measurements of erosion (e.g. experimental plots, empirical erosion and modelling). Since the mid-1990s, several studies, however, have made use of ^{137}Cs as soil tracer in watersheds located in the northern and western parts of Morocco and also in the

neighbourhood of the Atlas Mountains [2-9]. Measured soil erosion rates in these studies ranged from 6 to 70 t ha^{-1} yr^{-1} with generally the highest soil erosion rates recorded in the north. However, to date there has only been limited use of $^{210}Pb_{ex}$ as soil tracer in Morocco [10].

The objectives of the investigation reported here were: (i) to test the combined use of ^{137}Cs and $^{210}Pb_{ex}$ to assess long-term soil redistribution rates in one experimental Moroccan agricultural field under a semi-arid climate located near Rabat and (ii) to establish a medium- and long-term sediment budget for this field.

2. Materials and methods

2.1. The study area

The 1 ha study area is an experimental agricultural field of the "Institut National de la Recherche Agronomique" (INRA) located in Marchouch, 68 km southeast from Rabat (Fig. 1). The mean annual precipitation is 405 mm of which 50% falls from December to March. The mean monthly temperature ranges from 10 to 23°C and the altitude above sea level is between 350 to 400 m.

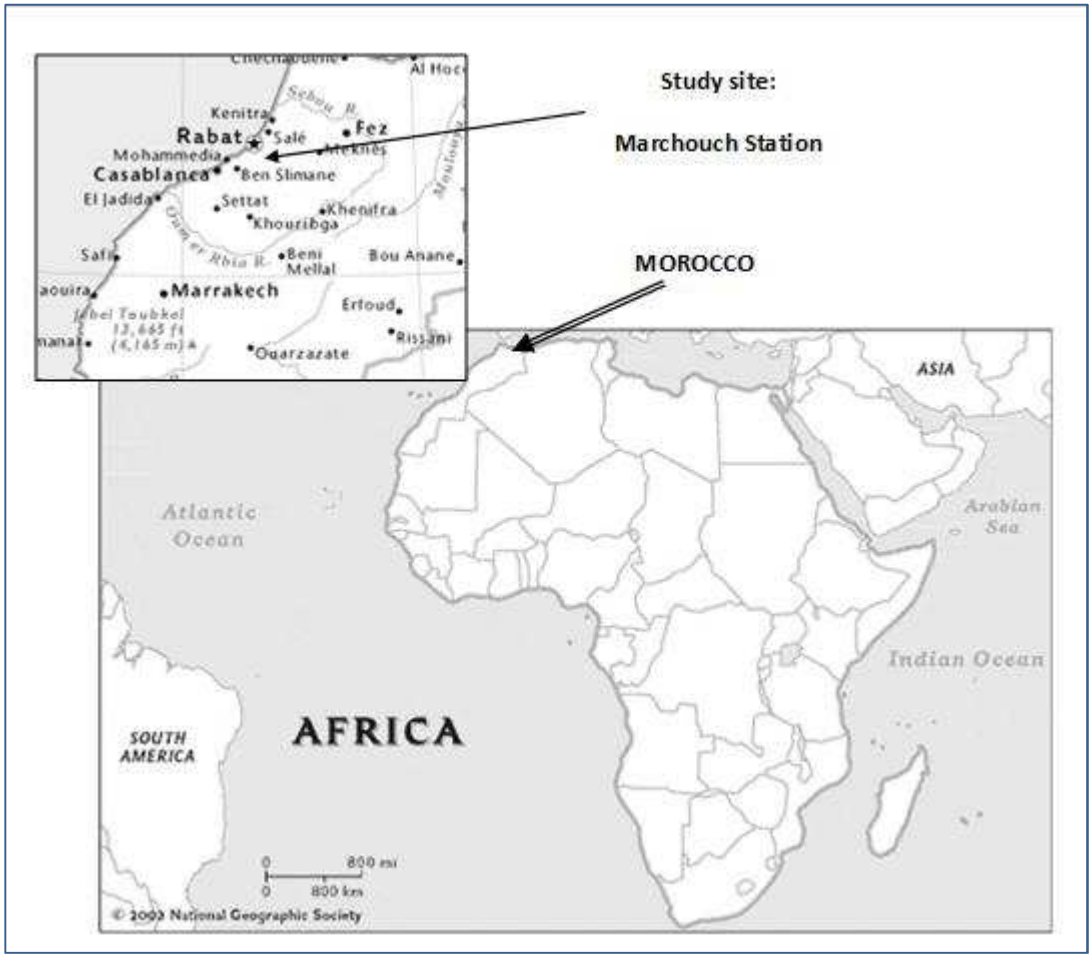

FIG. 1. Location of the Marchouch Station (6°42'W, 33°47'N).

Based on the USDA textural triangle, the soil of the field is a clay soil with a topsoil organic matter content of 25 g kg^{-1}. The mean slope gradient is 17% and the land use is dominated by cereals under conventional tillage with a plough depth of around 16 cm.

2.2. Soil sampling strategy

A transect approach was adopted to collect the soil samples in the experimental site (Fig. 2). A total of 45 core samples were collected along five parallel transects (T1, T2, T3, T4, T5) using a motorized soil column cylinder auger (Fig. 3). Bulk soil cores were collected to a depth of 40 cm to ensure that all ^{137}Cs and ^{210}Pb were taken into account. Section cores were also collected, sectioned at 1-2 cm increments, to obtain ^{137}Cs and ^{210}Pb vertical distributions.

The reference inventories of ^{137}Cs and ^{210}Pb were evaluated through collection of bulk and sectioned soil cores (n = 12) in an undisturbed pasture located 3 km from the study area.

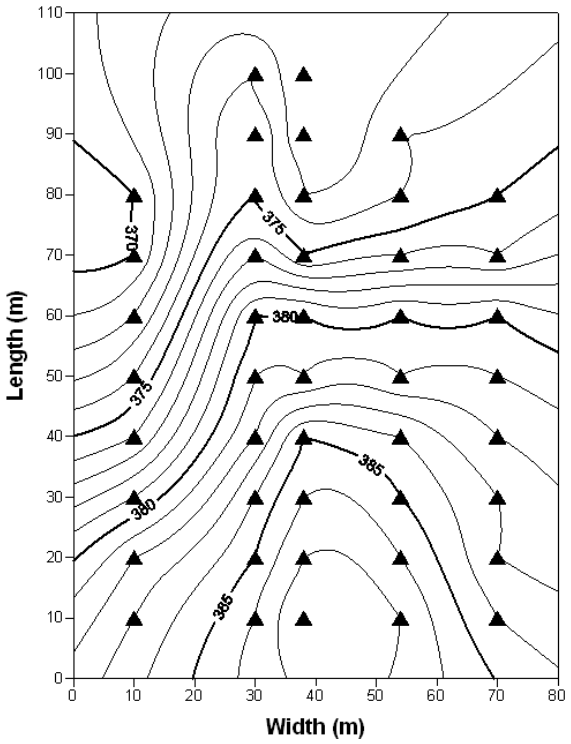

FIG. 2. Topography of the experimental field and the location of the sampled points.

FIG. 3. Soil sample collection using a soil column cylinder auger and pre-treatment of a soil core at the CNESTEN laboratory.

2.3. Sample pre-treatment and laboratory analysis

Soil samples were dried, sieved (< 2 mm) and homogenised prior to measurement of ^{137}Cs, ^{210}Pb and ^{226}Ra (from ^{214}Bi) by gamma spectrometry (see Papers 2 and 3 of this TECDOC). Two high resolution coaxial detectors ('P'-type 30% and 'N'-type 50%) were used for the γ-analysis. The detection systems were calibrated using certified multi-gamma source IAEA reference materials (IAEA 327, IAEA 375). Ground and homogenised soil samples were placed in Marinelli beakers (500 ml) or cylindrical containers (200 ml). ^{137}Cs, ^{210}Pb and ^{214}Bi activities were determined, respectively, from the net peak areas of gamma rays at 662, 46.5 and 609 keV. The counting time varied from 12 to 24 hr providing a precision of about 5 to 20% at the 95% confidence level. Under these experimental conditions, the minimum detection activity for ^{137}Cs and ^{210}Pb were 0.5 and 5 Bq kg^{-1}, respectively. Quality control procedures were applied using control charts (efficiency, resolution and background), certified reference materials and regular participation in inter-comparison exercises and proficiency tests organised by IAEA [11].

As indirect determination of $^{210}Pb_{ex}$ activity from total ^{210}Pb and ^{226}Ra gave a low precision with regards to the activity value (25 to 40%). To improve the precision of the ^{210}Pb determination, measurements by alpha spectrometry through ^{210}Po – daughter of ^{210}Pb – were performed for some soil samples with low $^{210}Pb_{ex}$ activities (see Paper 3 of this TECDOC for methodology).

2.4. FRN conversion models and data treatment

Activities of ^{137}Cs and $^{210}Pb_{ex}$ were converted into soil redistribution rates using the conversion model MBM 2 (see Paper 5 of this TECDOC). The parameters used in MBM2 for ^{137}Cs were: $\gamma = 0.6$, $H = 4.0$ kg m^{-2}, d = 217 kg m^{-2}, $A_{ref} = 1445$ Bq m^{-2}, p = p'= 1; and the parameters used in MBM2 for ^{210}Pb were: $\gamma = 0.6$, $H = 4.0$ kg m^{-2}, d = 217 kg m^{-2}, $A_{ref} = 3305$ Bq m^{-2}, I = 99 Bq m^{-2} yr^{-1}, p = p'= 1.

Soil redistribution rates obtained from ^{137}Cs and $^{210}Pb_{ex}$ were analyzed using geostatistical technique (see Paper 2 of this TECDOC) and the classical interpolation method, Inverse Distance Weighting (IDW).

IDW is a deterministic estimation method where unknown values are determined by a linear weighted moving averaging of values at known sampled points [12]. The formula used for IDW is:

$$Z^*(x_a) = \sum_{b=1}^{n} \lambda_b \cdot Z(x_b) \quad (1)$$

where:

$Z^*(x_a)$ is the estimated value Z for location x_a;
λ_b is the weighting factor assigned to the known variable Z for location x_b;
n is the number of observations.

The weighting factor λ_b is based on the inverse of the distance between locations of observed and estimated values [13]:

$$\lambda_b = \frac{1/d_b^{\alpha}}{\sum_{b=1}^{n} 1/d_b^{\alpha}} \quad (2)$$

where:

d_b is the distance between the measurement points of b and the points being estimated;
α is a positive real number called the power parameter, greater values of α assign greater influence to values closest to the interpolated point.

In IDW, the samples closer to the un-sampled location are more representative of the value to be estimated than samples further away. As the value of the power is traditionally set to 2 [14], IDW 2 was used in this Moroccan case study.

Geostatistical and spatial correlation analyses as well as variogram models were undertaken using the GS$^+$ version 7 software [15]. Using the protocol of Mabit and Bernard [16], maps of the spatial distribution of soil redistribution rates were derived using the GIS software Surfer 8.00 [17]. On the basis of the resulting maps, sediment budgets for the whole agricultural field under investigation were produced using the Surfer 8.00 package.

3. Results

3.1. Vertical distribution and inventories of ^{137}Cs and ^{210}Pb$_{ex}$

The depth distributions of ^{137}Cs and ^{210}Pb$_{ex}$ concentrations associated with the reference site are shown in Fig. 4. Most of the ^{137}Cs and ^{210}Pb$_{ex}$ were contained in the top 10 cm. The ^{137}Cs concentration in the reference site was the highest at the surface (0-3 cm) with a value of 13 Bq kg^{-1} while the ^{210}Pb$_{ex}$ concentration at the soil surface in the reference site was 25 Bq kg^{-1}.

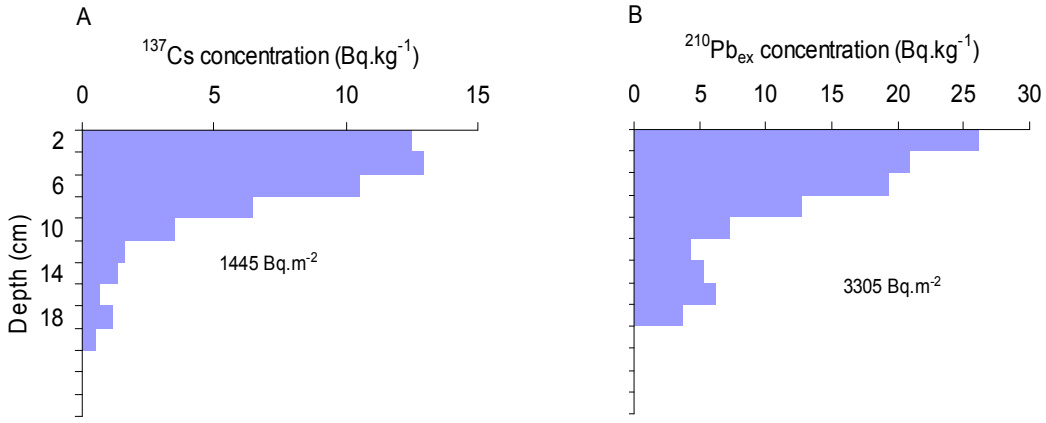

FIG. 4. Vertical distribution of ^{137}Cs (A) and $^{210}Pb_{ex}$ (B) in the reference site.

For the reference site, the vertical distributions associated with both radionuclides were similar with a clear exponential decrease with depth. Bio-perturbation processes induce a near-constant ^{137}Cs concentration in the upper 4 cm. This result can be explained by the origin of the ^{137}Cs fallout which ceased in the 1970s. However, the continuous inputs of $^{210}Pb_{ex}$ have maintained a maximum activity in the top 2 cm.

For the cultivated site, concentrations were almost uniform throughout the plough layer (~ 10-12 cm) as a result of mixing by tillage (Fig. 5). The concentrations derived from all explored points of the cultivated field ranged between 1.9 and 5.9 Bq kg^{-1} and between 2.2 and 16.7 Bq kg^{-1} for ^{137}Cs and $^{210}Pb_{ex}$, respectively. Similar ^{137}Cs and $^{210}Pb_{ex}$ profiles have been observed in other regions of the world in a variety of environments (see Papers 2 and 3 of this TECDOC). Along the five parallel transects, the ^{137}Cs inventory values were found to range from 600 to 1900 Bq m^{-2}.

For the undisturbed site, the mean ^{137}Cs reference inventory obtained from the 12 soil cores was estimated to be 1445 Bq m^{-2} with a CV of 18%. This variability compares well with those reported in existing literature reviews on reference sites [18-20] which indicated that the CV for reference pasture and grassland sites can range from 5.1 to 41%. Also, the reference inventory was comparable to those from previous Moroccan studies and a published correlation between mean annual precipitation and initial ^{137}Cs fallout in this region [4, 3, 7, 9, 21].

The ^{137}Cs activities of the soil cores collected in the cultivated field were lower than the reference inventory, particularly those of the upslope area, indicating soil loss. In contrast, ^{137}Cs inventories higher than the reference inventory were observed in the vicinity of the down slope boundaries, indicating soil deposition.

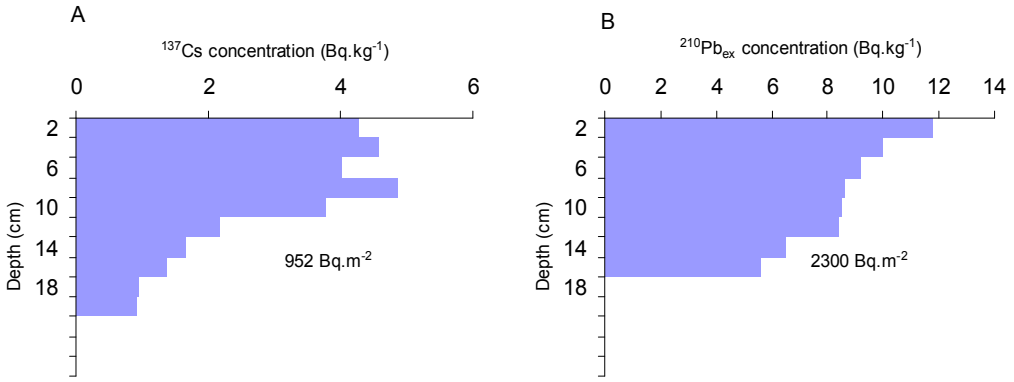

FIG. 5. Vertical distribution of ^{137}Cs (A) and $^{210}Pb_{ex}$ (B) in the cultivated field.

The $^{210}Pb_{ex}$ reference inventory was found to be 3305 Bq m^{-2} (Fig. 4) with a CV of 30%. The $^{210}Pb_{ex}$ inventories in the study field ranged between 1700 and 5000 Bq m^{-2}. As for ^{137}Cs, erosion could be observed at the upslope boundary while deposition was found at the down slope boundary. However the lateral variation of $^{210}Pb_{ex}$ inventories appeared to be more important than that of ^{137}Cs, as presented in Fig. 6, which represents the distributions of ^{137}Cs (A) and $^{210}Pb_{ex}$ (B) inventories along the five transects (T1, T2, T3, T4, T5). These fluctuations observed for $^{210}Pb_{ex}$ are due to the poor precision of the $^{210}Pb_{ex}$ measurements. Indeed, the mean relative uncertainties obtained for $^{210}Pb_{ex}$ ranged from 21.4 to 35.2% while those associated with ^{137}Cs activities ranged from 4.6 to 6.6% (see Table 1).

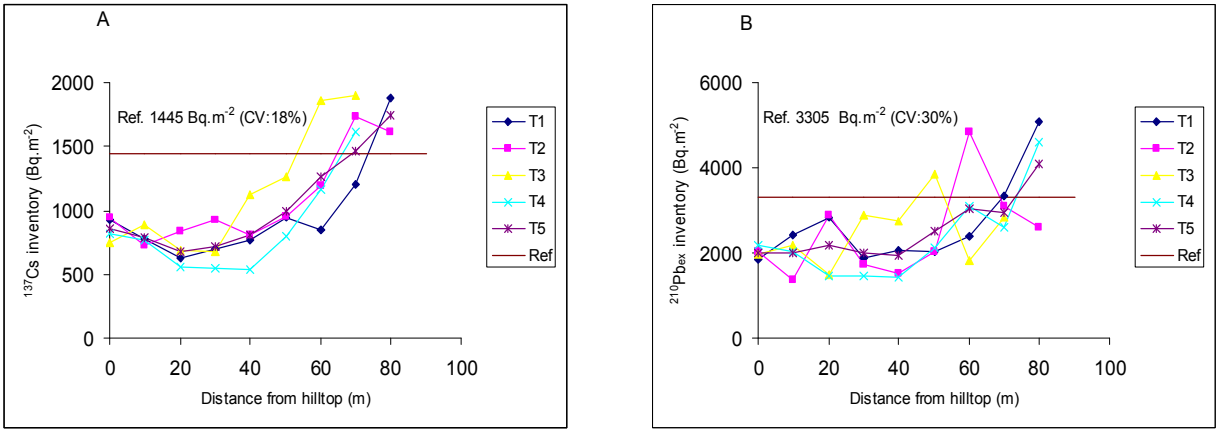

*FIG. 6. Distributions of ^{137}Cs (A) and $^{210}Pb_{ex}$ (B) inventories along the five transects (*i.e.*T1, T2, T3, T4, T5).*

TABLE 1. MEAN ^{137}Cs AND $^{210}Pb_{ex}$ INVENTORIES AND THEIR CORRESPONDING UNCERTAINTIES FOR EACH LEVEL

Distance from the top (m)	^{137}Cs		$^{210}Pb_{ex}$	
	Mean inventory (Bq m^{-2})	Mean relative uncertainty (%)	Mean inventory (Bq m^{-2})	Mean relative uncertainty (%)
10	858	5.6	2014	30.6
20	790	5.2	1995	33.2
30	677	6.6	2180	30.9
40	712	5.9	1992	34.1
50	809	6.1	1942	35.2
60	991	5.2	2513	26.9
70	1267	6.0	3033	25.1
80	1581	4.4	2968	26.1
90	1745	4.6	4082	21.4

3.2. Estimation of soil redistribution rates

The overall results (for all transects) obtained from ^{137}Cs measurements, converted to erosion rates using MBM 2 (see Paper 5 of this TECDOC), indicated that the erosion rates in the study field ranged from 4 and 30 t ha^{-1} yr^{-1}. The eroding zones in the upslope part of the field represented 82% of the total area, whereas soil deposition occurred at the lower slope position on the remaining 18% of the area. From $^{210}Pb_{ex}$ measurements, the erosion rates ranged between 8 and 27 t ha^{-1} yr^{-1}. The estimated eroding and depositional zones represented 84 and 16%, respectively.

Soil erosion and deposition rates estimated from ^{137}Cs and $^{210}Pb_{ex}$ measurements for the whole field (sediment budget), based on the average rate values of the five transects, were comparable (Table 1). The relatively high erosion rates can be mainly attributed to the steep slope of the field. The net soil erosion rates obtained from ^{137}Cs and $^{210}Pb_{ex}$ measurements were 14.3 and 12.1 t ha^{-1} yr^{-1}, respectively, resulting in a high sediment delivery ratio of 92 to 93%.

The RUSLE model [22] using the RUSLE 2 software [23] was applied in the same field to estimate rates of water-induced soil erosion. Generally, the prediction model provided comparable results to those obtained using ^{137}Cs and $^{210}Pb_{ex}$, in particular for soil erosion rate data [10, 24]. The gross and net erosion rates were 17.4 and 12.1 t ha^{-1} yr^{-1}. However, the sedimentation was observed to be higher (5.3 t ha^{-1} yr^{-1}) by the RUSLE 2 model than those estimated by ^{137}Cs or $^{210}Pb_{ex}$.

TABLE 2. SEDIMENT BUDGET AND SOIL REDISTRIBUTION ASSESSMENT FROM ^{137}Cs (A) AND $^{210}Pb_{ex}$ (B) USING THE SIMPLIFIED APPROACH

Soil redistribution magnitude (t ha^{-1} yr^{-1})	A	B
Mean erosion	17.9	15.0
Mean deposition	6.3	4.1
Gross erosion	15.4	12.9
Gross deposition	1.2	0.8
Net erosion	14.3	12.1
Sediment delivery ratio (%)	92	93

3.3. Assessment of soil redistribution rates derived from ^{137}Cs and $^{210}Pb_{ex}$ data using the spatialisation approach

Experimental variograms for soil redistribution rates calculated from the data provided by the ^{137}Cs and $^{210}Pb_{ex}$ results were fitted (see Paper 2 of this TECDOC). Following the optimization of variographic parameters [25] and the cross-validation analysis (see Paper 2 of this TECDOC), the geostatistical study of the data set highlighted a very weak autocorrelation with a high nugget effect, a non-significant coefficient of correlation ($r^2 < 0.4$) and a low ratio scale to sill close to 0.4 (Information related to variography parameters can be found in Paper 2 of this TECDOC). As suggested by Mabit and Bernard [16] in the case of weak or absent spatial structure, the use of classical methods of interpolation is recommended. Therefore, a simple spatialisation of the data set using IDW 2 to produce contour maps was used to spatialise the magnitude of soil redistribution based on ^{137}Cs and $^{210}Pb_{ex}$ data sets.

After IDW 2 interpolation, a complete soil movement budget was calculated for the whole field (Table 3). Contour maps of soil movements are shown in Fig.7. Two soil redistribution budgets for the agricultural field were established taking into account ^{137}Cs and $^{210}Pb_{ex}$ isotopic results (Table 3 and Fig.7).

TABLE 3. SEDIMENT BUDGET AND SOIL REDISTRIBUTION ASSESSMENT FROM ^{137}Cs (A) AND $^{210}Pb_{ex}$ (B) USING IDW 2 INTERPOLATION

Soil redistribution magnitude (t ha^{-1} yr^{-1})	A	B
Mean erosion	13.1	11
Mean deposition	3.5	3
Gross erosion	11	10.5
Gross deposition	0.3	0.1
Net erosion	11.7	10
Sediment delivery ratio (%)	94	95

Similar results were obtained for ^{137}Cs and $^{210}Pb_{ex}$. The sediment delivery ratio (SDR), corresponding to the ratio of the net erosion to the gross erosion rate represents 94 and 95%, respectively, using the ^{137}Cs and $^{210}Pb_{ex}$ approaches (Table 3). This means that most of the sediment mobilized in the field was moved out of the field. This is a logical result based on the fact that soil is cultivated in the direction of the slope which reached a gradient of 17%. This high SDR reflects the fact that the eroded area represents 93 to 96% of the field surface area using ^{137}Cs and $^{210}Pb_{ex}$, with the deposition area only 7 to 4%, respectively.

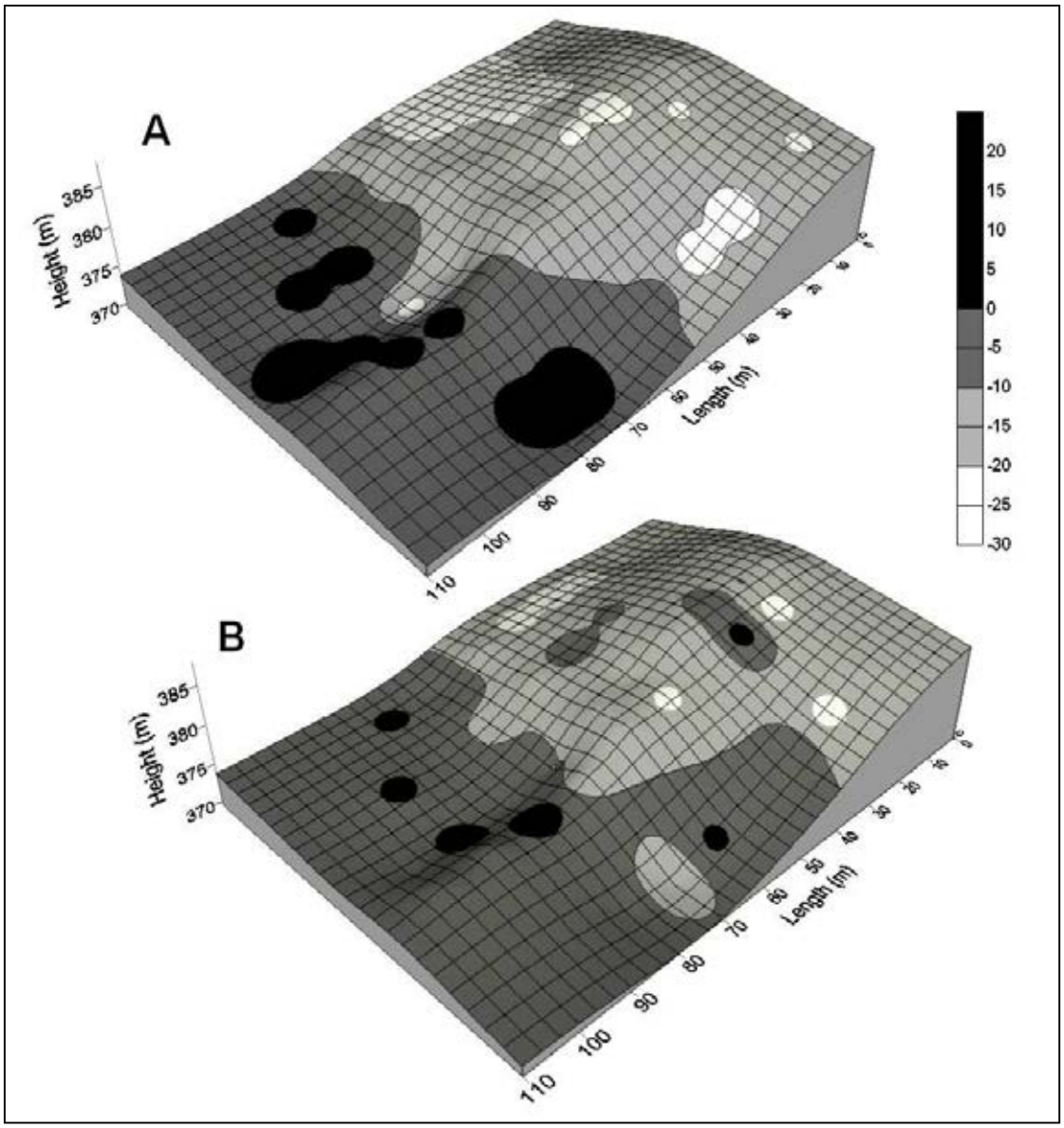

FIG. 7. Maps of soil redistribution in t ha^{-1} yr^{-1} using IDW 2 (from ^{137}Cs (A) and ^{210}Pb$_{ex}$ (B)).

4. Discussion and conclusions

This case study illustrates the potential for the combined use of fallout ^{137}Cs and ^{210}Pb$_{ex}$ to estimate long-term soil erosion rates in agricultural fields in Morocco and to establish sediment budgets and sediment delivery ratios (SDR) at the field scale. The ^{137}Cs technique provided more reliable results due to its good analytical precision with regard to the activity measurements compared to ^{210}Pb$_{ex}$. The overall data related to soil redistribution generated from the two techniques were similar despite the different periods for assessing soil erosion rates of 45 and 100 yrs for ^{137}Cs and ^{210}Pb$_{ex}$, respectively. These results indicate that the soil erosion rate did not change significantly during previous decades. For both the simplified approach and the spatialisation treatment of the data, soil redistribution descriptive parameters (e.g. mean erosion, mean deposition, gross erosion, net erosion, sediment delivery ratio) were in the same order of magnitude (see Tables 2 and 3).

Highly erosive rainfall and high soil temperatures accelerate the loss of soil organic matter and hence reduce the soil fertility and thus crop productivity in the study area. FRN data show that erosion is accentuated by unsustainable agricultural practices, increasing the pace of soil degradation in this area. The relatively high soil erosion rates in the study field are most likely the result of the steep topography, the clay-rich soil and the heavy rainfall during the winter season without major vegetative cover, but also the conventional tillage treatment practiced in the past. Comparable erosion rates ranging from 5 to 16 t ha^{-1} yr^{-1} were obtained in northern Morocco where climatic conditions are similar [4].

Improvement of the agricultural productivity under such conditions requires the use of appropriate soil conservation methods, which can also enhance the water availability for the crops. It can be achieved through the use of a production system which ensures agronomic and economic viability. For example, no-till practice appears to be a good method for soil and water conservation in this region. The non-disturbance of the soil-atmosphere interface permits the infiltration and evaporation of water to be controlled. No-till also minimizes erosion because crop seeds are planted directly through the crop residue layer and the soil surface is permanently covered by residues left from the previous crop. In addition the soil organic matter increases, improving soil structure.

REFERENCES

[1] SECRÉTARIAT d'ETAT CHARGÉ de l'EAU et de l'ENVIRONNMENT DÉPARTEMENT de l'ENVIRONNMENT., Rapport National sur l'Etat de l'Environnement du Maroc (2002) 292.

[2] BOUHLASSA, S., AZENFAR, A., MACHROUH, A., ^{137}Cs fallout as tracer of erosion and sedimentation in big catchment, Appl. Radiat. Isot. 46 (1994) 659–660.

[3] BOUHLASSA, S., MOUKHCHANE, M., AIACHI, A., Estimates of soil erosion and deposition of cultivated soil of Nakhla watershed, Morocco, using ^{137}Cs technique and calibration models, Acta Geol. Hisp. 35 (2000) 239–249.

[4] BENMANSOUR, M., IBN MAJAH, M., MARAH, H., MARFAK, T., WALLING, D.E., "Use of the ^{137}Cs technique in soil erosion in Morocco - Case study of the Zitouna basin in the north", International Symposium on Nuclear Techniques in Integrated Plant Nutrients, Water and Soil management, IAEA – CSP-11/C, IAEA, Vienna (2002) 308–315.

[5] BENMANSOUR, M., DUCHEMIN, M., NOUIRA, A., GALLICHAND, J., Emploi des radioéléments, de la modélisation et des mesures aux champs pour l'étude de l'érosion hydrique en milieu agricole (Maroc-Canada). Rapport, Convention Rep. P2-2092RR621, Agence Universitaire de la Francophonie (AUF) (2006) 25.

[6] BENMANSOUR, M., LAISSAOUI, A., BENBRAHIM, S., IBN MAJAH, M., CHAFIK, A., POVINEC, P., "Distribution of anthropogenic radionuclides in Moroccan coastal waters and sediments", Radioactivity in the Environment - Book series - 8 (2006) 145–150.

[7] NOUIRA, A., SAYOUTY, E.H., BENMANSOUR, M., Use of ^{137}Cs technique for soil erosion study in the agricultural region of Casablanca in Morocco, J. Environ. Radioact. 68 (2003) 11–26.

[8] NOUIRA, A., DUCHEMIN, M., BENMANSOUR, M., GALLICHAND, J., BOUKSIRATE, H., Efficacité du semis direct à contrer l'érosion hydrique en milieu agricole: Mise en évidence à l'aide des techniques des radioéléments, de la modélisation et de la mesure aux champs (Maroc-Canada), Actes des Journées Scientifiques Inter-Réseaux de l'Agence Universitaire de la Francophonie (AUF) (2007) 6.

[9] DAMNATI, B., IBRAHIMI, S., RADAKOVITCH, O., Utilisation du ^{137}Cs pour l'estimation des taux d'érosion dans un bassin versant du nord du Maroc, Sécheresse 15 (2004) 195–199.
[10] BENMANSOUR, M., NOUIRA, A., BENKDAD, A., IBN MAJAH, M., BOUKSIRAT, H., El OUMRI, M., MOSSADEK, R., DUCHEMIN, M., "Estimates of long and short term soil erosion rates on farmland in semi-arid West Morocco using caesium-137, excess lead-210 and beryllium-7 measurements", Impact of Soil Conservation Measures on Erosion Control and Soil Quality, IAEA-TECDOC-1665, IAEA, Vienna (2011) 159–174.
[11] SHAKHASHIRO, A., MABIT, L., Results of an IAEA inter-comparison exercise to assess ^{137}Cs and total ^{210}Pb analytical performance in soil. Appl. Radiat. Isot. 67 (2009) 139–146.
[12] MABIT, L., "Use of geostatistics to establish soil movement map and sediment budget using fallout radionuclides (FRN)", Proceedings of the 10th International Symposium on River Sedimentation, Effects of River Sediments and Channel Processes on Social, Economic and Environmental Safety. Volume I. Publication of the Moscow University, Moscow, Russia (2007) 247–254.
[13] CRESSIE, N.A.C., Statistics for Spatial Data, New York, Wiley (1993).
[14] ISAAKS, E.H., SRIVASTAVA, R.M., An Introduction to Applied Geostatistics, Oxford University Press, New York (1989) 561.
[15] GAMMA DESIGN SOFTWARE, GS$^+$ Version 7, GeoStatistics for the Environmental Sciences, User's guide, Gamma Design Software, LLC (2004) 160.
[16] MABIT, L., BERNARD, C., Assessment of spatial distribution of fallout radionuclides through geostatistics concept. J. Environ. Radioact. 97 (2007) 206–219.
[17] GOLDEN SOFTWARE, Surfer 8, Contouring and 3D Surface Mapping for Scientists and Engineers, User's guide, Golden Software, Inc. (2002) 640.
[18] SUTHERLAND, R.A., Examination of caesium-137 areal activities in control (uneroded) locations. Soil Technol. 4 (1991) 33–50.
[19] SUTHERLAND, R.A., Caesium-137 soil sampling and inventory variability in reference locations: a literature review, Hydrol. Process. 10 (1996) 43–53.
[20] OWENS, P.N., WALLING, D.E., Spatial variability of caesium-137 inventories at reference sites: an example from two contrasting sites in England and Zimbabwe, Appl. Radiat. Isot. 47 (1996) 699–707.
[21] NOUIRA, A., Application de la technique de ^{137}Cs pour l'étude de l'érosion et déposition du sol à l'échelle d'une parcelle culturale Ain Harouda et l'échelle du bassin versant de Trigrigra, Thèse de Doctorat, Faculté de Casablanca (2003).
[22] RENARD, K.G., FOSTER, G.R., WEESIES, G.A., McCOOL, D.K., YODER, D.C., Predicting Soil Erosion by Water: A Guide to Conservation Planning with the Revised Universal Soil Loss Equation (RUSLE), Agricultural Handbook 703, U.S. Department of Agricultural Research Service, Washington D.C. (1997) 404.
[23] USDA, Revised Universal Soil Loss Equation, Version 2 (RUSLE2), USDA-ARS National Soil Erosion Research Laboratory, Purdue University, West Lafayette (2005) (http://fargo.nserl.purdue.edu/rusle2_dataweb/RUSLE2_Index.htm)
[24] DUCHEMIN, M., BENMANSOUR, M., NOUIRA, A., GALICHAND, J., "Mesure et modélisation de l'erosion hydrique des sols agricoles au Maroc et au Québec", Proceeding of 14th International Soil Conservation Organisation Conference, Marrakech, Session Isotopes 11 (2006) 4.
[25] MABIT, L., "Erosion/disposition data derived from fallout radionuclides (FRNs) using geostatistics", Impact of Soil Conservation Measures on Erosion Control and Soil Quality, IAEA-TECDOC-1665, IAEA, Vienna (2011) 185–194. "

THE USE OF ^{7}Be AND ^{137}Cs IN SOIL REDISTRIBUTION INVESTIGATIONS IN CHILE

P. SCHULLER
Universidad Austral de Chile, Facultad de Ciencias, Instituto de Ciencias Químicas, Valdivia, Chile

D.E. WALLING
University of Exeter, College of Life and Environmental Sciences, Department of Geography, Exeter, United Kingdom

Abstract

This contribution provides summaries of several studies undertaken in Chile, which have used both ^{137}Cs and ^{7}Be to assemble information on rates of soil loss and soil redistribution on agricultural and forested land. The on-site and off-site problems associated with soil erosion are attracting increasing attention in Chile and lack of information on rates of soil loss and the impact of changing land use practices represent an important constraint on the development of soil conservation strategies and sustainable forest management practices. The use of fallout radionuclides to assemble such information has been actively promoted in Chile supported by the IAEA and such techniques are seen as offering considerable potential. The studies described cover, firstly, the use of both traditional and simplified sampling strategies to document soil redistribution rates under different land use and tillage systems and to estimate the relative contribution of both water and tillage-induced soil redistribution to total soil redistribution. In the second study, a novel approach, which permits the use of ^{137}Cs measurements to document the change in soil redistribution rates associated with a shift from a conventional mechanized tillage system to a no-tillage system, was developed and successfully tested. This involved both a standard and a simplified procedure. A complementary investigation was undertaken in the same area focusing attention on the erosional impact of burning crop residues as a component of no-till systems and the role of extreme events in soil redistribution. This required documentation of short-term soil redistribution rates and ^{7}Be measurements were successfully used to investigate the erosional impact of a 27 day period of extreme rainfall within a recently burnt field under no-tillage. In a third study ^{7}Be was also used as a tracer to investigate soil loss associated with the immediate post harvest period in a forest area.

1. Use of ^{137}Cs measurements to estimate tillage- and water-induced soil redistribution rates on agricultural land under different land use and tillage systems

To support soil conservation planning and sustainable crop production in Chile, there is an urgent need for reliable and rapidly obtainable information on the magnitude of soil loss from agricultural land under different land use and tillage systems. Taking advantage of the ^{137}Cs technique (see Paper 2 of this TECDOC), this study was undertaken to obtain spatially distributed information on time-integrated, medium-term average soil erosion and deposition rates for a period of about 45 years. Four study sites, with contrasting and constant land use (crop land and non-permanent grassland) and tillage systems (subsistence and commercial) over the last four decades were selected. Taking account of the relatively high ^{137}Cs areal activity densities documented in south-central Chile and the several important advantages of this radionuclide tracer technique for obtaining retrospective estimates of redistribution rates, compared with other traditional measurement methods, this investigation was the first attempt to use ^{137}Cs to investigate soil redistribution rates in Chile. The purpose of the research was to explore the applicability of the ^{137}Cs technique described by [1] and to trial a simplified and

faster approach for sampling and ^{137}Cs measurement aimed at estimating medium-term tillage, water-induced and total soil redistribution rates on agricultural land [2].

The four study sites were located in close proximity in the coastal mountains of south-central Chile (38°40'S; 72°30'W) and were characterized by an annual rainfall of 1600 mm and Palehumult (clay) soils. They represented:

- Crop land under a subsistence tillage system, chisel ploughed annually using animal traction, cultivated each year with different crops (site A);

- Crop land under a commercial tillage system - mechanically mouldboard ploughed annually with crop rotation (site B);

- Non-permanent grassland under a subsistence tillage system - chisel ploughed approximately every 6 years using animal traction (site C);

- Non-permanent grassland under a commercial tillage system - mechanically mouldboard ploughed approximately every 8 years (site D).

Further characteristics of the four study sites (A, B, C and D) are summarised in Table 1. It was not possible to select sites, which encompassed a complete slope for all the individual land use and tillage systems. The non-permanent grassland sites C and D represent only a portion of the slope profile.

The high clay content of the Palehumult soil and the limited incidence of macropores, together with the moderate rainfall at the study sites caused the total ^{137}Cs inventory to be restricted to a shallow surface soil layer, with a depth ranging from 0.12 m at eroded points to 0.34 m at depositional points. The ^{137}Cs mass activity density in the bulk soil samples varied from 0.3 to 5.3 Bq kg^{-1} [2].

For measurement of the ^{137}Cs areal activity density at the reference sites and at selected grid points in the study sites, bulk soil cores of 0.072 m diameter were collected using stainless steel cylindrical tubes inserted to at least the penetration depth of ^{137}Cs, i.e. the depth at which the ^{137}Cs concentration fell below the detection limit (previously determined by depth incremental soil sampling and analyses).

TABLE 1. STUDY SITE CHARACTERISTICS AND SAMPLING STRATEGY

Site code	A	B	C	D
Surface (m^2)	21000	4800	7000	1800
Slope length (m)	221	186	86	52
Mean slope (°)	5.7	4.5	5.1	16.7
Grid sampling method (individual point evaluation)				
Spacing of the sampling points (m x m)	16 x 20	7 x 10	10 x 10	6 x 6
Number of sampling points	84	72	77	60
Contour line sampling method (evaluation of composite samples)				
Contour lines	12	18	11	10
Sampling points per contour	7	4	7	6
Number of sampling points	84	72	77	60

Because the four study sites had been ploughed since the beginning of ^{137}Cs fallout, soil redistribution rates were documented using the Mass Balance Model Incorporating Soil

Movement by Tillage described by [1] (see Paper 5 of this TECDOC), which provides estimates of total soil redistribution and the components associated with water and tillage.

To estimate the reference areal activity density (inventory), four reference sites were selected near to the study sites. These reference sites were located above the investigated fields to avoid sediment input from those fields, in flat areas characterized by permanent grassland with minimum disturbance, i.e. minimally affected by soil redistribution since the onset of the global fallout. The number of cores collected from each reference site in 6 m by 6 m grids ranged between 15 and 16. The mean reference inventory measured at the undisturbed reference sites was 525 ± 12 Bq m^{-2}, σ = 94 Bq m^{-2}, n = 61, reference date January 1998 [2]. This value, whilst relatively low from a global perspective, was consistent with existing data on the dependence of ^{137}Cs areal activity density on the local mean annual precipitation for the 9th, 10th and 14th Regions of Chile [3].

Due to the difficulty in finding reference sites exhibiting the characteristics indicated above, four additional sites with similar characteristics, but frequently ploughed since the beginning of the ^{137}Cs fallout were evaluated as possible reference sites. The mean reference inventory documented for the same reference date at these sites, 435 ± 12 Bq m^{-2}, σ = 95 Bq m^{-2}, n = 60, was found to be significantly lower than that measured at the minimally disturbed reference sites. The measured values in regularly ploughed soils reflected soil loss as the result of repeated cultivation and harvest cycles. Therefore, the value of 525 ± 12 Bq m^{-2} for the minimally disturbed permanent grassland sites was used as the reference areal activity density for the sites investigated.

The additional parameters required to estimate soil redistribution when applying the Mass Balance Model Incorporating Soil Movement by Tillage were:

- *Plough depth*: estimated by ^{137}Cs analysis of soil samples collected at incremental depths: 0.12 m at chisel ploughed sites A and C; 0.17 m at mouldboard ploughed sites B and D;

- *Particle size distribution*: due to the fine texture of the investigated soils, no particle size correction was applied;

- *Proportion of the annual ^{137}Cs fallout susceptible to removal by erosion prior to tillage*: 0.5 for the annually ploughed sites A and B; 0.9 for the grassland areas C and D, ploughed every 6-8 years;

- *Constant related to the tillage practice*: 110, 210, 40 and 30 kg m^{-1} yr^{-1} for sites A, B, C and D, respectively.

Comprehensive descriptions of the methods used to determine the values of the parameters described above were reported by [2]. During the period mid-1997 to mid-1998, conventional grid-based sampling was used to evaluate the ^{137}Cs areal activity density at each sampling point, for establishing the spatial distribution of the ^{137}Cs inventories and soil redistribution rates at the four study sites using the conversion models described by [1] (see Paper 5 of this TECDOC).

Additionally, the feasibility of reducing the counting time required for ^{137}Cs analyses by measuring the ^{137}Cs areal activity density in composite soil samples, and using these data for estimating soil redistribution, was tested. From October to November 1999, soil samples were collected for this purpose at similar spacing as previously, but the cores were collected using a 0.035 m diameter auger from points located on transects along contour lines (Table 1). Afterwards all soil cores collected along a contour were mixed and homogenized using a Turbula Mixer Type T2 F and analysed for ^{137}Cs as a single composite sample. The contour-

based approach involved an important reduction of the number of samples analysed for ^{137}Cs when compared with the number of analyses required using the conventional grid-based sampling and analysis: from 84 to only 12 for site A, from 72 to 11 for site B, from 77 to 18 for site C, and from 60 to 10 for site D. The applicability of the approach based on composite samples collected along contours relies on the relative simple topography of the study fields and on the assumption of an approximately uniform lateral ^{137}Cs distribution along contour lines, due to the similar slope form and steepness at corresponding elevations.

The spatial distribution of the erosion and sedimentation rates based on individual ^{137}Cs measurements on samples collected from the sampling grid was reported by [2]. The spatial distribution of soil redistribution rates based on composite samples collected along contour lines was calculated by assigning to the grid points within the study fields the corresponding contour-based ^{137}Cs inventories estimates [2]. The similarity of the soil redistribution results obtained using the conventional approach based on individual measurement of ^{137}Cs at the grid points and the soil redistribution rates estimated using the contour-based ^{137}Cs method was reported by [2] and is additionally demonstrated by the strong correlation between the redistribution rates estimated for all sampling points using both approaches: $r = 0.962^{**}$, 0.958^{**}, 0.988^{**} and 0.955^{**}, for sites A, B, C and D, respectively. The integrated, spatially-weighted estimates of the total soil erosion and sedimentation rates for both sampling and evaluation strategies are summarised in Table 2. With the exception of the low net erosion rate and sediment delivery ratio obtained for site B using the contour-based evaluation, the spatially integrated values obtained with both methods are consistent within a ±20% uncertainty range. The results confirm the applicability of the simplified method for estimating soil redistribution rates under the relatively simple topographical conditions of the sites selected for the present study. Due to the similar slope form and steepness at corresponding elevations, an approximately uniform lateral ^{137}Cs distribution along contours could be initially assumed and afterwards effectively verified.

TABLE 2. ESTIMATES OF SOIL REDISTRIBUTION RATES FOR THE DIFFERENT SITES [2]

Sampling method	Area	Rate (t ha^{-1} yr^{-1})	Site A*		Site B		Site C		Site D	
Grid (individual point evaluation)	Eroding	Mean rate	12.7	(0.74)	9.3	(0.56)	2.7	(0.51)	2.9	(0.25)
	Sedimentation	Mean rate	7.3	(0.26)	8.7	(0.44)	9.8	(0.49)	6.8	(0.75)
	Total	Net erosion rate	7.5		1.3		**		**	
Contour line (evaluation using composite samples)	Eroding	Mean rate	11.4	(0.75)	6.3	(0.61)	2.8	(0.50)	4.3	(0.23)
	Sedimentation	Mean rate	5.8	(0.25)	9.1	(0.39)	11	(0.50)	6.7	(0.77)
	Total	Net erosion rate	7.2		0.3		**		**	

** Data in parentheses are the fraction of the total area affected by erosion or sedimentation*

** Net erosion rates are not provided for these sites, since they did not incorporate a complete slope profile.

For the subsistence tillage crop land (site A), the mean annual erosion rate for the eroded areas and the net erosion rate were found to be higher than for the commercially-managed crop field (site B), which was cultivated with more advanced technology. The higher rates for site A could be influenced by the intensive cultivation and ploughing procedure with annual ploughing downslope in the direction of maximum slope and the reduced vegetation cover during the rainy period following harvests. Site B was not isolated from the surrounding fields, and therefore part of the soil loss could be compensated by sediment input from adjacent upslope areas. In contrast, site A was totally isolated from adjacent uplope areas by

dense shrub fences resulting in a higher net soil loss compared with B. The mean soil erosion rates for the eroded areas at sites C and D were very similar. Nevertheless, the fraction of the total area affected by erosion was higher for site C, which exhibited limited vegetation cover during the rainy seasons, because of the intensive livestock grazing in this subsistence grassland site. Consequently, the gross erosion for site C was higher than for site D. Both grassland sites were not isolated from the surrounding fields and were affected by soil movement from and towards the adjacent sites. This could be the reason that the mean sedimentation rates for the aggrading areas in C and D are higher than the mean erosion rates for the eroding areas.

To validate the total erosion rates obtained using the ^{137}Cs Mass Balance Model Incorporating Soil Movement by Tillage, the estimated rates were compared with the annual sediment loss measured from 10 m by 1 m experimental erosion plots operated during 3 years in the upper sector of sites A and C, which were cultivated with the same crops and tillage practices and were characterised by the same annual precipitation as the areas associated with the ^{137}Cs measurements. Considering the uncertainty of the methods, the local mean total erosion rate estimated using the ^{137}Cs model at four points surrounding the installed erosion plots were found to be in very close agreement with the mean annual soil loss measured for the corresponding experimental plots [2]. The similarity of the results occurred despite the different time periods involved and the fact that the plot measurements relate to soil export from the plot and therefore provide an estimate of net soil loss. The soil redistribution rates estimated from the ^{137}Cs measurements at the four adjacent points represent the time-integrated average rate of soil loss for the last 45 years, which will reflect the magnitude and frequency of erosive events during that period.

The estimates of the total soil redistribution rates obtained from the ^{137}Cs results were also compared with soil redistribution rates estimated using pedological observations. The latter were assessed using a relative scale, because of the difficulty of determining the length of time that the sites had been cultivated and the depth of the reference horizons. The total rates documented using the Mass Balance Model Incorporating Soil Movement by Tillage showed similar relative magnitudes of soil redistribution rates to those estimated using pedological observations [4].

The Mass Balance Conversion Model Incorporating Soil Movement by Tillage, employed in this research permits separation and estimation of the contributions of tillage and water-induced soil redistribution to the total soil redistribution. To compare the erosion and sedimentation caused by tillage and water and the total soil redistribution estimated using both methods, the ^{137}Cs inventories measured in composite samples taken along contour line transects were compared with the mean inventories for the similar contour lines derived from analysis of individual samples taken using a grid pattern. In agreement with the similarity of these ^{137}Cs inventories estimated using both methods along a slope transect for each study site, and the strong correlation between these ^{137}Cs inventories ($r = 0.904^{**}$, 0.891^{**}, 0.985^{**}, and 0.994^{**}, at sites A, B, C, and D, respectively), [2] reported that the redistribution rates associated with tillage and water erosion, and the total soil redistribution rates estimated by the grid sampling method were similar and closely correlated at all four sites with the corresponding tillage- and water-induced rates and total soil redistribution rates estimated by the contour transect sampling. The variation of these soil redistribution rates along the slope transects allows the relative contribution of the tillage- and water-induced soil redistribution to the total redistribution to be estimated, providing information of the drivers of the erosion and sedimentation processes involved. For example the variation of the soil redistribution rates (tillage-induced, Rt; water-induced, Rw; and total redistribution rates, Rn) in relation to relative elevation along a slope transect from the cropland site A, based on individual grid points (top) and on the simplified contour method (bottom), are represented in

Fig. 1. This shows that the main driver of the total erosion documented at site A is the high water-induced soil erosion rates, which predominate along the slope transect, as compared to the tillage-induced rates. This is possibly due to the limited vegetation cover at the site during autumn and winter months, when about 72% of the rainfall occurs. High tillage-induced erosion rates were observed at the upper zone of the site due to annual chisel ploughing operations that moved the surface soil in a downslope direction and because sediment inputs from the upslope area were obstructed along this upper plot boundary by a dense shrub fence.

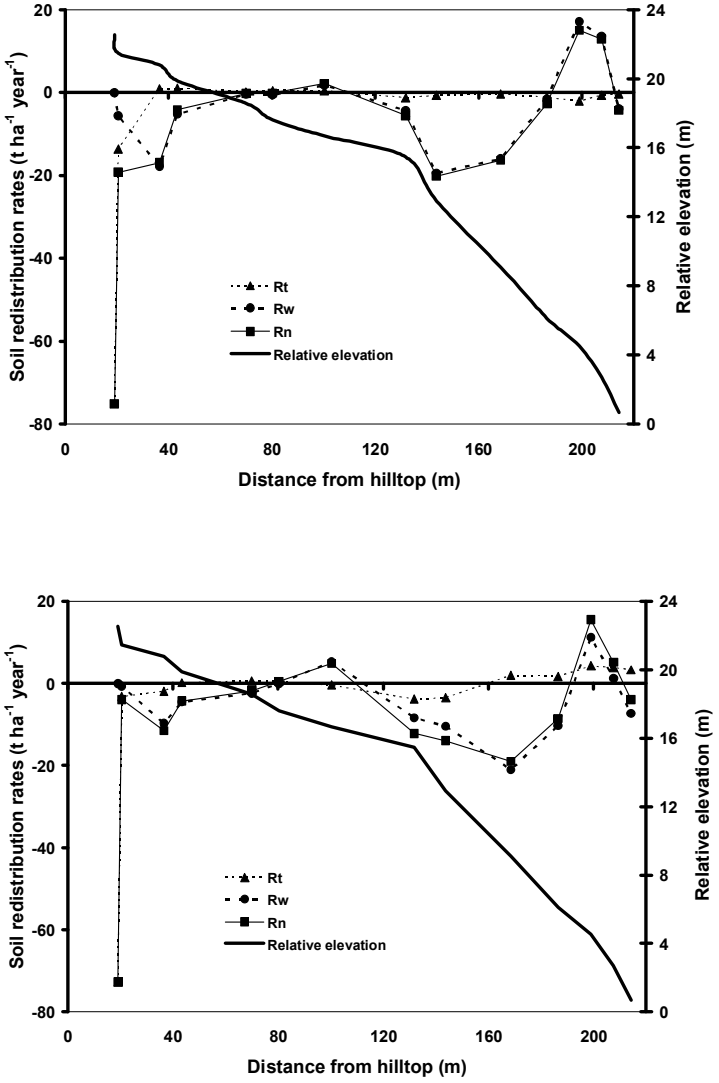

FIG. 1. Relative elevation and tillage-induced (Rt), water-induced (Rw), and total soil redistribution rates (Rn) along a slope transect from site A, based on individual grid points (top) and on contour-lines sampling (bottom) [2]. N.B. Negative values represent erosion rates and positive values sedimentation rates.

Local results of soil redistribution obtained using the ^{137}Cs Mass Balance Conversion Model Incorporating Soil Movement by Tillage were found to be in good agreement with the soil loss measured using conventional experimental erosion plots under the same precipitation, slope, land use and tillage system conditions. The soil redistribution rates show similar variation between different crops and tillage practices as that demonstrated by the estimates of rates of soil loss derived from pedological observations [2, 4]. Therefore, it is considered that mean medium-term results obtained by the ^{137}Cs conversion model provide meaningful

estimates of soil erosion and sedimentation rates and their spatial distribution for the study sites [2].

The simplified contour-based ^{137}Cs sampling procedure produces good estimates of the soil redistribution rates in areas exhibiting simple topography (with minimal cross-slope curvature), permitting a considerable reduction in laboratory measurement time. Within the study area, the simplified ^{137}Cs method permits rapid estimation of soil redistribution rates, providing the possibility of estimating soil redistribution over larger areas in a shorter time (see also [5]). The conventional grid-based sampling approach provides more detailed information concerning the variation of redistribution rates over the landscape than the simplified method. Nevertheless, such results are affected by the uncertainty associated with the measurements of ^{137}Cs inventory at each grid point, due to small-scale variability of the areal activity density. Therefore, the selection of an appropriate ^{137}Cs sampling strategy must take account of the resolution of the required information, and the scale and complexity of the relief of the local landscape.

Higher tillage- and water-induced erosion rates were observed on the annually ploughed crop lands (sites A and B) as compared to the grassland (sites C and D). Crop and grassland sites under subsistence management were characterised by greater soil loss than the commercially managed sites.

This study demonstrates that the ^{137}Cs approach possesses key advantages over conventional plot-based approaches for assembling information on soil redistribution rates and their spatial distribution at the landscape scale. The ^{137}Cs measurements are likely to generate more representative information for individual landscape units than the information provided by small plots, particularly when assessing net soil loss and sediment delivery to watercourses. The retrospective nature of the ^{137}Cs approaches can provide information relating to medium-term erosion rates operating in the landscape over the past ca. 45 years on the basis of a single visit to the site for the collection of soil samples. They permit comparison of total soil redistribution rates observed on agricultural land under different land use (cropland or grassland) and tillage systems (subsistence or commercial), and estimation of the relative contribution of water- and tillage-induced soil redistribution to the total soil redistribution rate. The present example shows that the ^{137}Cs technique can be seen as a very efficient method for documenting medium-term soil redistribution rates to support the planning of soil conservation and sustainable agricultural production under the climatic and soil conditions of the region of Chile investigated [2].

2. Use of ^{137}Cs and ^{7}Be measurements to estimate changes in soil erosion rates associated with a shift in the tillage system on cultivated land

2.1. A case study involving ^{137}Cs measurements to estimate the changes in soil redistribution rate associated with the shift from conventional (CT) to no-tillage (NT) system

Since 1970, the process of agricultural intensification has drastically increased soil erosion and associated soil degradation in the coastal mountains of south-central Chile. Due to conventional tillage with burning of crop residues (CT), over 80% of the soils under agriculture show evidence of compaction below the plough depth, and erosion rates are among the highest for any agricultural land in Chile. These problems have prompted a shift from CT to no-tillage without burning of crop residues (NT) systems. The implementation of NT has been reported to cause significant improvements in soil quality. However, there is still

a need to provide information on the precise magnitude of the decrease in soil loss associated with the shift from CT to NT systems [6]. To estimate the change in rates of soil redistribution associated with the shift from CT to NT a novel standard and a simplified approach for using the ^{137}Cs depth distribution were developed and applied by [7].

(i) The ^{137}Cs standard and simplified methods

The standard method is based on observation of the ^{137}Cs depth distribution in soil profiles. The medium-term erosion rate ($R_{NT} < 0$) or sedimentation rate ($R_{NT} > 0$) at selected sampling points, associated with the NT period (kg m^{-2} yr^{-1}), can be estimated by comparing the mass depth of the zone of homogeneous mixing of ^{137}Cs in the soil (*h(t),* kg m^{-2}) at the time of sampling (*t*, yr), with the estimated historical plough mass depth (*H*, kg m^{-2}) at the time of cessation of CT (*t′,* yr). Assuming that the whole study area was affected by erosion during the CT period and that no ^{137}Cs fallout occurred during the NT period, the depth of the zone of homogeneous mixing of ^{137}Cs in the soil at the time when CT ceased, *t′,* would be equal to the plough mass depth *H.* The reduction or increase in *h(t)* relative to *H* (i.e. *h(t) – H*, kg m^{-2}) represents the total amount of soil erosion or deposition occurring during the period extending from the time of introduction of the NT system (*t′*) to the time of sampling (*t*). The mean annual erosion or deposition rate R_{NT} (kg m^{-2} yr^{-1}) can therefore be estimated as:

$$R_{NT} = \frac{h(t) - H}{t - t'} \tag{7.1}$$

The total areal activity density ($A(t')$, Bq m^{-2}) at the measuring points at the end of the period of CT (or the beginning of the period of NT) can be estimated as:

$$A(t') = \left[A(t) - \{h(t) - H\}\overline{C}(t)\right]\exp\left[\ln(2)(t - t')/T_m\right] \tag{7.2}$$

where:

A(t) represents the areal activity density at each sampling point measured at the time of sampling (Bq m^{-2});
T_m is the half-life of ^{137}Cs (yr).

Comparison of the estimates of the total ^{137}Cs areal activity density at the end of the period of CT (*A(t')*) for the sampling points with the local areal activity density reference value at time *t'* enables the erosion rate during the period of CT ($R_{CT,}$ kg m^{-2} yr^{-1}) to be estimated for these points using one of the conversion models for cultivated soils documented by [1] (see Paper 5 of this TECDOC). The depth distributions of ^{137}Cs obtained for individual sampling points along a slope transect at a site under NT at the time of sampling, where the standard method was applied, indicated that only a small proportion of the total areal activity density was found below mass depth *h.*

The simplified approach is based on the significant linear relationship found between $A_h(t)$, the areal activity density above *h*, and the total areal activity density, *A(t)*, during the development of the standard method [7]:

$$A_h(t) = 1.006A(t) - 31.5 \qquad (r = 0.999^{**}) \tag{7.3}$$

where:

31.5 is a constant value representing the ^{137}Cs areal activity density which migrated below the mass depth of homogeneous mixing (Bq m^{-2});
h(t) refers to the time of sampling.

The well-defined relationship between these two variables makes it possible to estimate $A_h(t)$ for additional points at the study site, where only the total areal activity density, *A(t)*, has been measured using bulk (un-sectioned) cores, i.e. using a simpler method, than the standard method based on incremental soil sampling. Assuming that the ^{137}Cs mass activity density (*C(t)*, Bq kg^{-1}) is approximately constant down to depth *h* and that the bulk density of the soil will also be almost constant down to this depth, *h(t)* can be estimated using the relationship

$$h(t) = \frac{A_h(t)}{\overline{C}(t)} \qquad (7.4)$$

where:

$\overline{C}(t)$ is the mean ^{137}Cs mass activity density (Bq kg^{-1}) measured in the upper part of the soil profile (down to $h' \leq h$) at the sampling points and sampling date.

Using the relationship between *A(t)* and $A_h(t)$, and Equation 7.4, measurements of *A(t)* and $\overline{C}(t)$ at additional sampling points enables the key parameters for the ^{137}Cs depth distributions associated with the two tillage periods to be estimated for those points [7].

Consequently, the described methods permit estimation of the mean annual soil redistribution rates for the period under NT systems and additionally the mean erosion rate during the period of CT (R_{CT}) by using Equation 7.2 and one of the conversion models for cultivated soils documented by [1] (see Paper 5 of this TECDOC). The simplified approach was validated by [8], by demonstrating a very close correspondence between the results obtained using this method and those provided by the standard method for the same sampling points.

In the region of the study site, no Chernobyl fallout was detectable [3, 9] and global atmospheric bomb-derived deposition of ^{137}Cs was last recorded in 1983 [10-12]. Therefore, it can be safely assumed that the existing ^{137}Cs areal activity density was mixed homogeneously within the plough layer by CT prior to the implementation of the NT system. This is an important assumption of the approach proposed by [7-8].

(ii) Study site and soil sampling

The simplified method (based on empirical evidence obtained during the implementation of the standard method) was applied within a field located on a farm in the coastal mountains of south-central Chile (38º37´S; 73º04´W), characterized by Araucano series Ultisols (Typic Hapludult), a temperate climate and a mean annual precipitation of 1100 mm. The field had been cultivated annually for crop production and was under CT until May 1986, when there was a change to a NT system. A second site, located close to the site described above and with a similar soil type, but where CT had continued through the sampling year (2003), was selected to estimate the historical plough mass depth, *H* (kg m^{-2}). Depth increments of 1 cm were used around the expected plough depth, in order to define *H* as precisely as possible [8].

Samples were collected within an area of ca. 5,000 m^2, which was selected to be representative of a site affected by erosion during the period of CT. Initially, in 2001 and 2002, depth incremental samples were collected from points situated along a single slope transect, in order to implement the standard method and to establish the relationship between

A_h and A, required to use the simplified method. To apply the simplified method, bulk soil samples for determining the total ^{137}Cs areal activity density A and the ^{137}Cs mass activity density $\overline{C}$ down to $h' \leq h$, were collected during 2003, from between seven to eight points, located at 15 m intervals along four additional parallel slope transects extending down the upper and middle portions of the slope. At each point, three 25 cm long and two 8 cm long cores were collected using an 11 cm diameter corer, in order to determine A and $\overline{C}$, respectively.

To extend the area covered using the standard method through the use of the simplified method, A_h was estimated for the sampling points on the additional transects using the linear regression between $A_h(t)$ and $A(t)$ described in Equation 7.3. Soil redistribution rates during the NT period were estimated using Equations 7.4 and 7.1. The erosion rates associated with the period of CT were estimated using Equation 7.2 coupled with the Mass Balance Model Incorporating Soil Redistribution by Tillage developed by [1] (see Paper 5 of this TECDOC). The reference inventory used for the calculations was based on that determined previously for a neighbouring site, 525 ± 12 Bq m^{-2}, reference date 1998, taking account of the radioactive decay and the influence of local variation in annual precipitation.

(iii) Results

Using the information on the ^{137}Cs depth distribution observed at points susceptible to erosion located close to the experimental site, and where CT had continued to be practiced until the sampling year 2003, and based on the mean mass depth of the zone of ^{137}Cs homogeneous mixing in the plough layer of this annually ploughed soil, the historical plough depth H for the study site was estimated to be 170 kg m^{-2} [8].

The results obtained for the 29 sampling points in the study field using the simplified method, were combined with those obtained from the previous application of the standard method for a single slope transect (5 points) within the same area, to provide information from five slope transects [7-8]. The spatial patterns of the soil redistribution rates (negative values = erosion; positive values = deposition) obtained for the CT (I) and NT (II) periods [8], mapped using a kriging procedure, are shown in Fig. 2.

Summary statistics for the study area relating to the periods of CT and NT derived using an areal weighting procedure applied to the soil redistribution rates estimated for the 34 sampling points within the study area are presented in the first two columns of Table 3.

For the CT period, extending from the beginning of ^{137}Cs fallout in 1954 to the shift to NT practice in 1986, an area-weighted mean annual erosion rate for the study area of 11 t ha^{-1} yr^{-1} was estimated. This value is seen to be representative of the upper and middle portions of the study field, where erosion was expected to be the predominant soil redistribution process during the CT period. The results obtained corroborate this assumption, because all points investigated in the area evidenced erosion and the study area was therefore characterized by a sediment delivery ratio of 100%.

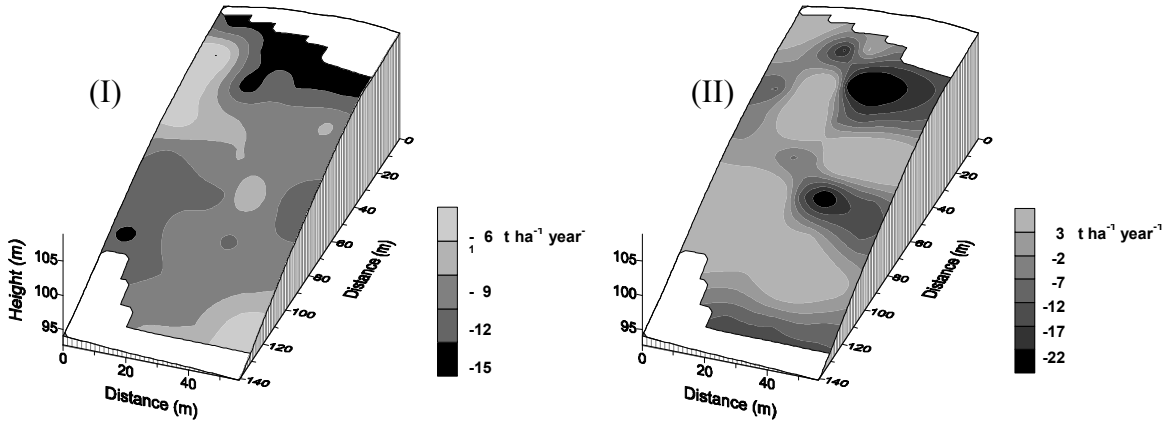

FIG. 2: Spatial patterns of mean annual soil redistribution rates based on ^{137}Cs measurements for the period of CT (I) and during the subsequent period of NT (II) [8].

TABLE 3: SOIL REDISTRIBUTION UNDER CT, NT AND NTWB. MEAN ANNUAL SOIL REDISTRIBUTION RATES FOR CT AND NT WERE BASED ON ^{137}Cs MEASUREMENTS. SOIL REDISTRIBUTION UNDER NTWB WAS ESTIMATED USING ^{7}Be MEASUREMENTS AFTER HEAVY RAINFALL [8, 13]

Parameter	Conventional tillage CT	No-till, no burning NT	No-till with burning NTWB
	Mean annual values for a 32 year period estimated using ^{137}Cs [8]	Mean annual values for a 16 year period estimated using ^{137}Cs [8]	Values documented for a 27 d period of heavy rainfall, estimated using ^{7}Be [13]
Years	1954-1986	1986-2003	May 2005
Period	32 yr	16 yr	27 d
Precipitation	~1100 mm yr^{-1}	~1100 mm yr^{-1}	400.5 mm
Length of the slope (m)	130	130	130
Sampling points	34	34	27
Eroding zone			
Mean erosion	11 ± 2 t ha^{-1} yr^{-1}	13 ± 2 t ha^{-1} yr^{-1}	18 ± 2 t ha^{-1}
Fraction of total area (%)	100	57	78
Aggrading zone			
Mean sedimentation	0 t ha^{-1} yr^{-1}	14 ± 2 t ha^{-1} yr^{-1}	9 ± 2 t ha^{-1}
Fraction of total area (%)	0	43	22
Total area			
Net erosion	11 ± 2 t ha^{-1} yr^{-1}	1.4 ± 2 t ha^{-1} yr^{-1}	12 ± 2 t ha^{-1}
Sediment delivery ratio (%)	100	19	86

During the NT period extending from 1986 to 2003, only 57% of the study area was affected by erosion and this was characterized by an area-weighted mean annual erosion rate of 13 t ha^{-1} yr^{-1}. The remainder of the area was affected by deposition, with an area-weighted mean annual deposition rate of 14 t ha^{-1} yr^{-1}. These results demonstrate that in the study area the shift from CT to a NT system caused soil erosion to decrease significantly to produce a net erosion rate of about 1.4 t ha^{-1} yr^{-1}, a gross erosion rate of 7.3 t ha^{-1} yr^{-1}, and a sediment delivery ratio of ca. 19%. Interestingly, the results obtained from the ^{137}Cs measurements show that within the study area, the shift to a NT system caused erosion rates in parts of the area to increase. The increase might reflect compaction in some areas as a result of the cessation of cultivation. This would most likely occur in those areas where previous erosion had caused the highest rates of soil loss and thus soil degradation (e.g. reduced organic matter

content and increased bulk density), and could result in local increases in surface runoff. However, this increase was coupled with a shift from erosion to deposition over more than 40% of the study area, with the result that the sediment delivery ratio decreased and both the gross and net soil loss from the study area decreased. In terms of soil degradation, the increased rates of soil loss over parts of the area must clearly be seen as undesirable, but more than 40% of the study area now experiences no soil loss and, equally important, the export of soil towards the stream network has been reduced to ca. 19% of that occurring during the period of CT. Overall, therefore, the introduction of NT management can be seen to have coincided with a significant reduction in both gross and net soil loss within the study area and to have greatly reduced the potential for diffuse source pollution of the local watercourses by eroded sediment [8].

Although the results presented above clearly demonstrate that the shift to a NT system coincided with a reduction of both gross and net erosion rates and the area subject to erosion, it is important to consider whether the change in soil erosion associated with the NT period could reflect the influence of other factors, such as annual rainfall. The mean annual rainfall for Temuco Airport (38º45'S; 72º38'W, some 45 km from the study site) over the period 1960 to 2003 was ca. 1230 mm, and therefore a little higher than the 1100 mm estimated from the available record for the study site. However, it is thought that both stations would have experienced similar trends in annual rainfall over the past 40 years. The years since 1986 at Temuco have generally been marked by reduced annual rainfall, with the mean for the period 1986 to 2003 being 1151 mm and ca. 11% lower than that for the preceding period extending from 1960 to 1985 (i.e. 1290 mm). The reduced annual rainfall associated with the period since the introduction of NT is likely to have contributed to the reduced soil loss during this period, but in view of the substantial length of the period and the occurrence of many years with annual rainfall totals similar to those associated with the preceding period under CT, it is suggested that the shift to a NT system represents the primary cause of the reduced rates of soil loss and sediment delivery estimated for the period under a NT system [8].

The use of the ^{137}Cs approach to estimate the influence of a change from CT to NT possesses four key advantages over conventional plot-based approaches for assembling such data. These are as follows [8]:

- The ability to generate information for individual landscape units that is likely to prove more representative than the information provided by small plots, particularly when assessing net soil loss and sediment delivery to watercourses;

- The ability to produce medium-term estimates of mean annual erosion rates associated with both CT and NT systems that will include the temporal variability of erosion rates;

- The ability to undertake 'before' (i.e. with CT) and 'after' (i.e. with NT) investigations on the same field or study area;

- The retrospective nature of the approach, which can provide information relating to medium-term erosion rates operating in the landscape over the past ca. 45 years on the basis of a single visit to the site for the collection of soil samples.

^{137}Cs measurements, as successfully employed in a study of a field located on a farm in south-central Chile, provide a valuable alternative to conventional techniques for assessing the impact of changes in tillage system on soil erosion rates. The results demonstrated a significant decrease in the rate of net soil loss and the portion of the study area subject to erosion, as well as in the sediment delivery ratio for the study area during the NT period. The shift from CT to a NT system was found to be associated with a decrease in the net soil

erosion rate of about one order of magnitude (from 11 to 1.4 t ha^{-1} yr^{-1}) and a reduction of the proportion of the eroded soil exported from the study area (the sediment delivery ratio) by 81% (from 100 to 19%). Additionally, the proportion of the study area subject to erosion decreased from 100 to 57%. The reduced soil loss has important benefits for the sustainable use of the soil resource. The reduced sediment delivery ratio will result in a reduction in sediment transfer to the local watercourses, which will in turn reduce the offsite effects of soil erosion and, more particularly, diffuse source pollution associated with sediment inputs to the stream network. These changes clearly demonstrate the potential environmental benefits of a shift from CT to a NT system. Since the simplified ^{137}Cs method requires far fewer measurements, it also allows data to be assembled for a larger number of sampling points and thus from a larger area, thereby providing a more rigorous and representative assessment of the changes in soil erosion rates associated with the change in tillage system.

2.2 Use of ^{7}Be measurements to estimate soil redistribution associated with a period of heavy rainfall occurring after the implementation of a system of no-till with burning of crop residues (NTWB)

(i) Methodology

This investigation was undertaken at the same field described previously, when the tillage system shifted from NT to no-till with burning (NTWB) two years after the study described above. The field had previously been under a NT system for 18 years. After harvesting in early 2005 (summer) and before the wet season began, the crop residues remaining on the field were burnt in March 2005, leaving the soil bare until the onset of a period of very heavy rainfall in early May 2005 (autumn). The rainfall record for the period between January 1 and June 1, 2005 is shown in Fig. 3.

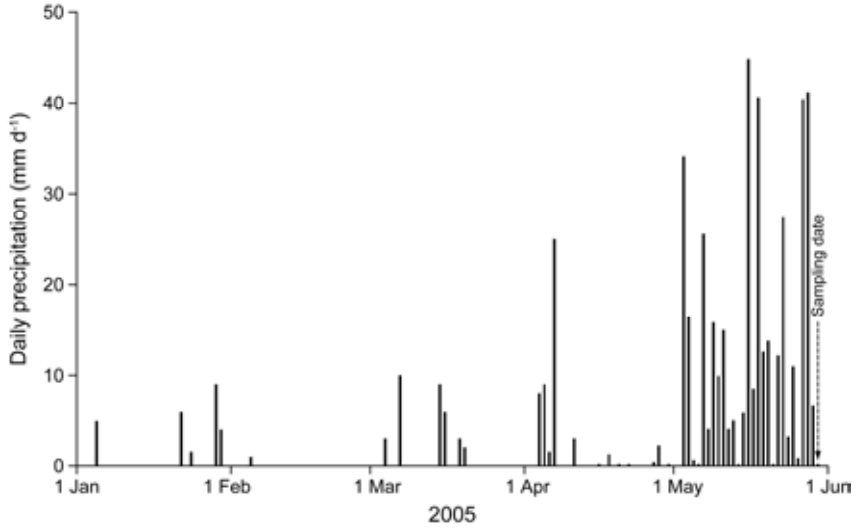

FIG. 3: Daily precipitation record for the study site from 1 January to 1 June, 2005. [13]. N.B. The arrow shows the date of collection of the soil samples used for ^{7}Be measurements.

After a prolonged dry period with little precipitation, a period with an unusually high amount of precipitation occurred, extending from 3 to 29 May, 2005. This period was characterized by a total rainfall of 400.5 mm in 27 days, including a 1-h period on 18 May with 11.4 mm of

rain. In the absence of a long rainfall record for the study site, it is not possible to provide a value for the recurrence interval of this period of heavy rainfall. However, based on the 52 year (624 month) record of monthly rainfall for the measuring station at Temuco Airport, some 45 km from the study site, it is estimated that a monthly rainfall total in excess of 400 mm was only recorded on three occasions, and therefore it can be considered as 'extreme rainfall' [13].

On May 30th, one day after cessation of the extreme rainfall period, the field was sampled for ^{7}Be measurements, using the method developed by [14] and [15] and also described by [16]. To measure the variation in areal activity density produced by erosion and deposition associated with the period of NTWB and heavy rainfall, across the same study area where the ^{137}Cs approach was applied, soil cores were collected from 9 sampling points located at 15 m intervals along each of three slope transects spaced 15 m apart, superimposed onto the grid used for the ^{137}Cs sampling. At each sampling point, two soil cores (11 cm in diameter and 4 cm long) were collected. To determine the reference areal activity density, A_{ref} (Bq m^{-2}) and the relaxation mass depth h_o (kg m^{-2}), two groups of nine cores, collected from a reference site, were sectioned into 2-mm slices, and the slices from each group representing specific depth increments were bulked for measurement as a single composite sample. The samples were analysed for their ^{7}Be content using gamma spectrometry.

(ii) Results

The mean reference inventory measured for the two groups of cores collected from the reference site was 473 ± 50 Bq m^{-2}. The linear regression between the natural logarithm of the mean areal activity density, $ln[A(x)]$, and the mean mass depth, x, based on the two groups of sectioned cores collected from the reference site showed a strong correlation (r = 0.997**), and confirmed the expected exponential decrease of the areal activity density with mass depth. The values for the relaxation mass depth, h_o, and the reference areal activity density, A_{ref}, obtained from this relationship were 3.4 ± 0.1 kg m^{-2} and 499 ± 10 Bq m^{-2}, respectively [13]. The depth distribution of the mean ^{7}Be areal activity density at the reference site $A(x) = 499exp(-x/3.4)$ is shown in Fig. 4.

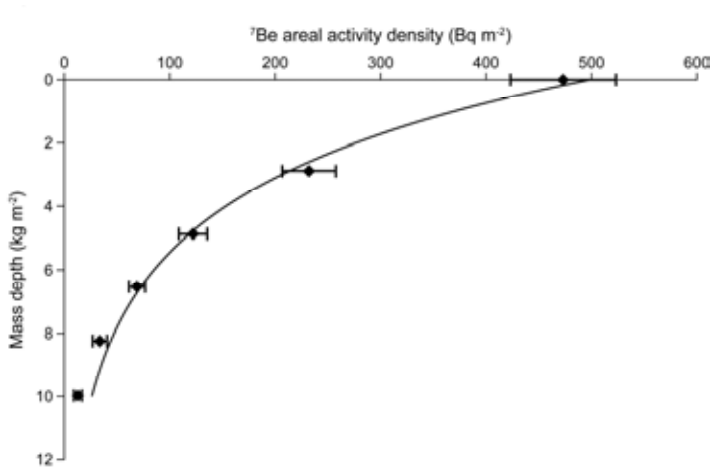

FIG. 4: Exponential decrease of ^{7}Be areal activity density with mass depth for the reference site [13].

Summary statistics for the magnitude of the soil redistribution associated with the period of heavy rainfall occurring in May 2005, estimated from the ^{7}Be measurements for 27 sampling

points located on three slope transects covering the same area studied previously using the ^{137}Cs approach, are reported in Table 3 (see final column). The results indicate that about 78% of the sampled area experienced erosion, whereas deposition occurred over 22% of the area. The mean erosion estimated for the eroding area was 18 t ha^{-1} and the mean sedimentation for the areas experiencing deposition was 9 t ha^{-1}. Combining these data, the net erosion from the sampled area was estimated to be 12 t ha^{-1}, indicating that a large proportion of the soil mobilised by erosion from the sampled area during the period of heavy rainfall was transported beyond that area [13].

^{7}Be measurements were successfully used within the same field used for the ^{137}Cs measurements, to investigate the influence on soil erosion of the shift from NT to a NTWB system, two years after the original study. The relatively high amount of net erosion associated with the period of NTWB and heavy rainfall could be seen as reflecting both the extreme nature of the rainfall and the impact of the burning in modifying the results obtained for the NT system. The results confirm the potential for using ^{7}Be measurements to estimate soil redistribution associated with individual periods of heavy rainfall. The ^{7}Be technique should therefore be seen as representing a valuable complement to ^{137}Cs measurements for soil erosion investigations in south-central Chile.

2.3. Combined use of ^{137}Cs and ^{7}Be measurements to compare the soil redistribution associated with the period of heavy rainfall occurring under a NTWB system, estimated using ^{7}Be measurements with that estimated for the CT and NT periods using ^{137}Cs measurements

A comparison of the estimates of soil redistribution at the study site for the period of NTWB and heavy rainfall that occurred in May 2005 with the medium-term mean annual rates of soil redistribution for the study site under both CT (1954-1986) and NT (1986-2003) using ^{137}Cs measurements is presented in Table 3. Based on this comparison, several observations, related to the impact of both the burning of the crop residue and the heavy rainfall associated with the May 2005 event on soil redistribution rates within the study area, can be made.

The magnitude of the values of short-term soil redistribution associated with the NTWB presented above can usefully be compared with the longer-term values of mean annual net erosion of 1.4 and 11 t ha^{-1} yr^{-1} for the study field under the NT system and the original CT system, respectively, reported by [8]. These data indicate that whilst the value of net erosion recorded for the 27 day period of extreme rainfall in May 2005 was an order of magnitude greater than the mean annual rate of net erosion reported for the field for the period of 16 years when it was managed with a NT system, it is not dissimilar to the mean annual rate of net erosion reported for the previous 32 years when the field was managed under a CT system [13].

The relatively high amount of net erosion associated with the period of NTWB and the heavy rainfall could be seen as reflecting both the extreme nature of the rainfall and the impact of burning in modifying the erosional response associated with the standard NT system. It is not possible to ascribe a relative importance to these two controls, due to their close interaction and the availability of only a single measurement of event-based soil redistribution for a period of heavy rainfall. A more comprehensive measurement programme, based on an experimental (factorial) design and involving several periods of rainfall of different magnitude with the presence and absence of burning, would be necessary to isolate the effects of the two controls.

The net erosion associated with the period of NTWB and heavy rainfall is of similar magnitude to the mean annual rate of net erosion from the study field during the period under CT. Because it reflects an extreme event, the net erosion associated with the period of heavy rainfall is expected to exceed the longer-term mean annual rate of net erosion associated with the NTWB system under normal precipitation conditions. It is therefore suggested that annual rates of soil erosion associated with the NTWB system under normal rainfall conditions are substantially less than under CT.

There are important differences between the magnitude and nature of the soil redistribution reported for the three periods in Table 3. Under conventional tillage, there was no net deposition of sediment within the sampled area. However, significant deposition occurred during both the period of NT and the period of heavy rainfall following the burning. In the case of the period under NT, the erosion rates for the eroding area were essentially the same as those estimated for the period of CT, but the occurrence of significant rates of deposition over nearly half (43%) of the sampled area resulted in a net erosion rate that is almost an order of magnitude less than that associated with the period under conventional tillage. The key impact of the introduction of the NT system was therefore to increase deposition of the sediment mobilised from the eroding areas, rather than to reduce rates of erosion from those areas. In the case of the period of heavy rainfall in May 2005, which followed the burning of the harvest residue, the soil mobilisation (t ha^{-1}) within the eroding zone was greater than the mean annual rates reported for the periods under NT and CT. However, in contrast to the situation under CT, some deposition occurred over 22% of the sampled area and, as a result the net erosion was similar to the mean annual rate of net erosion reported for the period under CT.

The application of ^{7}Be measurements to estimate gross and net erosion on agricultural land in south-central Chile, associated with a period of heavy rainfall following the burning of crop residues, clearly confirms the potential for using this technique. The information on event-related erosion generated by the ^{7}Be measurements provides a useful complement to that provided by the use of ^{137}Cs measurements to estimate the mean annual erosion rates associated with both CT and NT systems. In combination, the two radionuclides provided a valuable means of investigating soil erosion and assessing erosion risk in the study area. Although the use of ^{7}Be measurements involves a number of important requirements and assumptions, related to both the preceding conditions and the occurrence of a discrete period of heavy rainfall that can be expected to cause significant erosion, the approach is likely to be applicable in many parts of the world, in addition to south-central Chile.

3. The use of ^{7}Be measurements to estimate short-term event-based soil redistribution after final forest harvest operations

In south-central Chile, final harvesting in forestry plantations commonly takes place in the drier months of the year, between spring and summer. However, after clear-cutting and during the early stages of the establishment of a new plantation, soils remain bare during the rainy season and are, therefore, susceptible to significant soil redistribution processes. Several practices have been adopted to reduce erosional impacts and to limit the delivery of sediment to watercourses, in order to maintain soil and water quality standards [5, 17-18]. There is, however, an important need to assess the effectiveness of such management practices in reducing soil degradation and sediment export from the harvested forest slopes.

The potential for using naturally-occurring ^{7}Be fallout to estimate short-term soil redistribution on agricultural land has been reported by [14–15, 19-20] (see Paper 4 of this TECDOC). The present contribution is a summary of the results reported by an investigation

conducted by [16] aimed at exploring the potential for using ^{7}Be measurements as a basis for quantifying event-based soil redistribution following final forest harvest operations and thus for assessing the effectiveness of management practices in forest soils. The principles involved in using ^{7}Be to estimate patterns of soil redistribution would appear to overcome many of the limitations facing the use of ^{137}Cs in forest areas and more particularly, for estimating erosion following harvest operations. After harvesting, fallout inputs of ^{7}Be will not be influenced by canopy interception and can therefore be assumed to be homogeneously deposited on the soil within a local area receiving the same rainfall amount [16].

The conventional ^{7}Be approach [14-15] was applied to estimate soil redistribution associated with a period of heavy rainfall within an area of forest clear-cut after final harvesting in January 2003 (summer). The study site was located within the Forest Research Centre of the Universidad Austral de Chile (39º44´S; 73º11´W), in the River Region of Chile. The site is characterized by a Typic Paleudults (Ultisol) [21], a mean slope of about 22%, a temperate climate, and a mean annual rainfall of approximately 2300 mm [22]. Most precipitation falls between autumn and winter, when high rainfall intensities can occur.

During 2003 there was little rainfall at the experimental site until early August (winter). Between mid-August and mid-September, there was a period of very intense rainfall, producing a total of 311 mm in 25 days, including three 1 hour periods where rainfall intensity exceeded 13 mm h^{-1}, and caused visible erosion at the study site. On September 12th, immediately after the period of heavy rainfall, the soils of the study site were sampled for ^{7}Be measurement, in order to explore the potential for quantifying the soil redistribution that occurred during the preceding period.

A plot 3 m wide and 12 m long, with its longer side parallel to the predominant direction of water flow, located equidistant above and below two rows of woody harvest residue, was selected for detailed investigation. Forty shallow soil cores (4 cm deep) were collected from the plot at the intersections of a 0.5 m by 1 m grid, using 11 cm diameter cylindrical plastic core tubes. An adjacent flat area located within the harvested stand, that showed no evidence of erosion or deposition was selected as a reference site and two sets of six bulk cores were collected at the intersections of a 1 m by 1 m grid using the same plastic core tubes, in order to determine the reference areal activity density and to characterize the relaxation mass depth of ^{7}Be for the initial depth distribution [16].

In order to assess the validity of the soil redistribution amounts estimated using the ^{7}Be measurements, independent estimates of soil redistribution associated with the period of heavy rainfall were obtained for 30 regularly distributed points located within a grid superimposed on the same plot from which the soil cores were collected, using erosion pins. The metal erosion pins had been inserted into the soil at the intersections of a 0.5 m by 1 m grid on August 12th, immediately prior to the onset of the period of heavy rainfall. When inserted, 10 cm of the pin was left exposed above the soil surface and the position of the soil surface was measured again after the period of heavy rainfall using a Vernier caliper. These measurements were made on the same day as the soil cores for ^{7}Be analysis were collected. The mass depth (kg m^{-2}) of soil lost or gained at each pin position (grid intersection) was calculated by multiplying the change in the position of the soil surface, relative to the original 10 cm reference level, by the bulk density of the surface soil layer.

The function describing the downward decrease of the ^{7}Be areal activity density at the reference site was found to be $A(x) = 573\ exp(-x/2.14)$, i.e. A_{ref} = 573 Bq m^{-2}, and h_o = 2.14 kg m^{-2} [16].

A summary of the results obtained from the transects using the ^{7}Be method is provided in Table 4. Soil loss was indicated at 27 out of the 40 sampled points, which were characterized

by a mean erosion of 9.2 ± 1.8 t ha^{-1}. Sediment deposition was indicated at the remainder of the sampled points, for which the mean deposition was 7.2 ± 1.4 t ha^{-1}. The period of heavy rainfall resulted in a gross erosion of 6.2 ± 1.2 t ha^{-1} and a net erosion from the study plot of 3.9 ± 0.8 t ha^{-1}. The overall sediment delivery ratio for the plot was estimated to be 62%.

The significant amounts of erosion estimated by the ^{7}Be measurements demonstrate that, although the construction of linear woody trash barriers may be effective in reducing sediment delivery to watercourses, the soil redistribution occurring within the intervening areas could still represent a significant cause of soil degradation.

In Table 4, the values of soil redistribution provided by the ^{7}Be measurements are compared with those generated by the direct measurements using erosion pins. The net erosion of 3.2 ± 0.6 t ha^{-1} derived from the erosion pin measurements, is of a very similar magnitude to that provided by the ^{7}Be measurements. Equally, the values for the proportion of the measuring points characterized by erosion and deposition and the mean erosion and deposition amounts for those points are also very similar to those provided by the ^{7}Be technique, particularly when the uncertainties associated with these values and the associated standard errors are taken into account.

TABLE 4. SOIL REDISTRIBUTION USING ^{7}Be MEASUREMENTS AND DIRECT EROSION PIN MEASUREMENTS [16]

Parameter	Method	
	^{7}Be	Erosion pin
Number of sampling points	40	30
Eroding zone		
Mean erosion (t ha^{-1})	9.2 ± 1.8	11.4 ± 2.3
Fraction of total area	0.67	0.62
Aggrading zone		
Mean sedimentation (t ha^{-1})	7.2 ± 1.4	10.2 ± 2.0
Fraction of total area	0.33	0.38
Total area		
Net erosion (t ha^{-1})	3.9 ± 0.8	3.2 ± 0.6
Sediment delivery ratio (%)	62	45

The results provided by the ^{7}Be measurements and the erosion pins are not directly comparable, since the values relate to different points within the study plot and the erosion pin measurements covered only 75% of the plot area sampled by the ^{7}Be measurements. Because the results provided by the ^{7}Be measurements and the erosion pins relate to different positions within the plot, it is not possible to make a direct pairwise comparison between them. Additionally, whereas the erosion pins provide an estimate of surface lowering or accretion in the immediate vicinity of the pin, the ^{7}Be results represent an average amount of erosion or deposition for the 88.2 cm^2 surface area of the individual cores. Bearing in mind these considerations, the close similarities between the results provided by the ^{7}Be technique and the erosion pins appear to provide a clear validation of the results obtained from the ^{7}Be measurements [16].

The estimates of erosion provided by the ^{7}Be measurements confirm the potential for using this approach to collect information on the magnitude of event-based or short-term erosional losses and sediment redistribution within forest areas immediately after clear-felling. Although the approach has a number of limitations, including the need to ensure that the areal activity density was uniform across the study site immediately prior to the period of heavy

rainfall investigated and the need for specialist gamma counting facilities, it also offers a number of important advantages over the use of more conventional approaches, such as erosion plots and the use of erosion pins. In the case of erosion plots, high installation and operation costs, the need to install the plots well in advance of the study period, and uncertainties over the extent to which a small bounded plot is representative of the broader landscape will frequently limit their application. Similarly, with erosion pins, there is again a need to install the pins in advance of the period of measurement and important uncertainties exist regarding the extent to which the disturbance of the soil caused by inserting the pin and the disruption of the hydraulic conditions caused by the presence of the pin might produce unrepresentative results. Key advantages of the ^{7}Be approach include the ability to undertake retrospective investigations initiated after a period of heavy rain, the lack of a need for expensive field installations or the introduction of unrepresentative conditions, and the ability to undertake the necessary soil sampling during a single visit to the site, shortly after the period of heavy rainfall to be investigated. A clear advantage over the erosion plot is the ability to assemble spatially distributed information on amounts of erosion and deposition and thus to document soil redistribution within the study site, as well as the net soil loss from the site. Equally, an important advantage over the use of erosion pins for assembling spatially distributed data is the fact that the results represent average values for the surface area represented by the core, rather than the much smaller area represented by the pin, and are thus less likely to be influenced by small scale anomalies and/or variability associated with soil redistribution [16].

REFERENCES

[1] WALLING, D.E., HE, Q., Improved models for estimating soil erosion rates from ^{137}Cs measurements. J. Environ. Qual. 28 (1999) 611–622.

[2] SCHULLER, P., ELLIES, A., CASTILLO, A., SALAZAR, I., Use of ^{137}Cs to estimate tillage- and water-induced soil redistribution rates on agricultural land under different use and management in Central-South Chile. Soil Till. Res. 69 (2003) 69–83.

[3] SCHULLER, P., VOIGT, G., HANDL, J., ELLIES, A., OLIVA, L., Global weapons fallout ^{137}Cs in soils and transfer to vegetation in South Central Chile. J. Environ. Radioact. 62 (2002) 181–193.

[4] SCHULLER, P., SEPÚLVEDA, A., TRUMPER, R.E., CASTILLO, A., Application of the ^{137}Cs technique to quantify soil redistribution rates in Paleohumults from Central-South Chile. Acta Geol. Hisp. 35 (2000) 285–290.

[5] WALLBRINK, P.J., RODDY, B.P., OLLEY, J.M., A tracer budget quantifying soil redistribution on hillslopes after forest harvesting. Catena 47 (2002) 179–201.

[6] SCHULLER, P., WALLING, D.E., IROUME, A., CASTILLO, A., Fallout radionuclides ^{137}Cs and ^{7}Be as an important tool to evaluate effectiveness of no-tillage systems in Central-South Chile. IAEA Soils Newsletter 30 (2008) 8.

[7] SCHULLER, P., WALLING, D.E., SEPÚLVEDA, A., TRUMPER, R.E., ROUANET, J.L., PINO, I., CASTILLO, A., Use of ^{137}Cs measurements to estimate changes in soil erosion rates associated with changes in soil management practices on cultivated land. Appl. Radiat. Isot. 60 (2004) 759–766.

[8] SCHULLER, P., WALLING, D.E., SEPÚLVEDA, A., CASTILLO, A., PINO, I., Changes in soil erosion associated with the shift from conventional tillage to a no-tillage system, documented using ^{137}Cs measurements. Soil Till. Res. 94 (2007) 183–192.

[9] SCHULLER, P., LOVENGREEN, CH., HANDL, J., ^{137}Cs concentration in soil, prairie plants, and milk from sites in Southern Chile. Health Physics 64 (1993) 157–161.

[10] JUZDAN, Z.R., Worldwide Deposition of ^{90}Sr Through 1985. Environmental Measurements Laboratory, Report EML-515, U.S. Department of Energy, New York, NY 10014-3621 (1988).
[11] MONETTI, M.A., LARSEN, R.J., Worldwide Deposition of ^{90}Sr Through 1986. Environmental Measurements Laboratory, Report EML-533. U.S. Department of Energy, New York (1991).
[12] Environmental Measurements Laboratory. The Fallout Measurements Database Search Form (1999). http://www.eml.st.dhs.gov/databases/fallout/fallout_data_search.htm
[13] SEPÚLVEDA, A., SCHULLER, P., WALLING, D.E., CASTILLO, A., Use of ^{7}Be to document soil erosion associated with a short period of extreme rainfall. J. Environ. Radioact. 99 (2008) 35–49.
[14] WALLING, D. E., HE, Q., BLAKE, W., Use of ^{7}Be and ^{137}Cs measurements to document short- and medium-term rates of water-induced soil erosion on agricultural land. Water Resour. Res. 35 (1999) 3865–3874.
[15] BLAKE, W.H., WALLING, D.E., HE, Q., Fallout beryllium-7 as a tracer in soil erosion investigations. Appl. Radiat. Isot. 51 (1999) 599–605.
[16] SCHULLER, P., IROUMÉ, A., WALLING, D.E., MANCILLA, H.B., CASTILLO, A., TRUMPER, R.E., Use of ^{7}Be to document soil redistribution following forest harvest operations. J. Environ. Qual. 35 (2006) 1756–1763.
[17] PARK, S.W., MOSTAGHIMI, S., COOKE, R.A., MCCLELLAN, P.W., BMP impacts on watershed runoff, sediment, and nutrient yields. *Water Resources Bulletin,* American Water Resources Association 30 (1994) 1011–1023.
[18] GRIFFIN, C.B., Uncertainty analysis of BMP effectiveness for controlling nitrogen from urban nonpoint sources. *Water Resources Bulletin,* American Water Resources Association 31 (1995) 1041–1050.
[19] MATISOFF, G., BONNIWELL, E.C., WHITING, P.J., Soil erosion and sediment sources in an Ohio watershed using Beryllium-7, Cesium-137, and Lead-210. J. Environ. Qual. 31 (2002) 54–61.
[20] WILSON, C., MATISOFF, G., WHITING, P., Short-term erosion rates from a ^{7}Be inventory balance. Earth Surf. Process. Landf. 28 (2003) 967–977.
[21] Centro de Información de Recursos Naturales. Estudio agrológico, X Región. Descripción de suelos materiales y símbolos, Tomo I. Corporación de Fomento de la Producción, Santiago, Chile (2001).
[22] HUBER, A., Archivos meteorológicos. Universidad Austral de Chile, Valdivia, Chile (2004).

THE COMBINED USE OF ^{137}Cs AND STABLE ISOTOPES TO EVALUATE SOIL REDISTRIBUTION IN MOUNTAINOUS GRASSLANDS, SWITZERLAND

K. MEUSBURGER, C. ALEWELL, N. KONZ, M. SCHAUB
Department of Environmental Sciences, Environmental Geosciences, Basel University
Basel, Switzerland

L. MABIT
Soil and Water Management and Crop Nutrition Subprogramme, Joint FAO/IAEA Division of Nuclear Techniques in Food and Agriculture,
Vienna - Seibersdorf

Abstract

This paper aims to assess soil loss and the relevance of different soil erosion processes in a sub-alpine valley of the Central Swiss Alps (Urseren Valley). To reveal the relative importance of different soil erosion processes, different methods for soil erosion assessment were combined including ^{137}Cs laboratory based and in-situ measurements. The comparison of soil erosion rates for nine toposequences, determined by different assessment tools, showed the presence of significant discrepancies. Soil erosion rates measured with sediment traps during the growing seasons (2007 and 2008) and soil erosion modelling with the Water Erosion Prediction Project (WEPP) were below 1.5 t ha^{-1} yr^{-1}. In contrast, the Universal Soil Loss Equation (USLE) estimates were higher (i.e. 3.6 to 10.5 t ha^{-1} yr^{-1}), because its empirical factors are based on long-term measurements and in this study the single factors were adapted for mountainous areas. However, USLE does not consider winter and snowmelt processes and thus underestimates soil erosion rates. Consequently, ^{137}Cs based erosion rates indicated the highest erosion rates with maximum rates above 20 t ha^{-1} yr^{-1}, which is in accordance with the high visible erosion damage observed at the sites. The high erosion rates of the ^{137}Cs approach can be explained by the fact that ^{137}Cs integrates erosive processes during the winter season such as snow melt as well as intensive rain storm events with a long return period. These results indicate that in the Urseren Valley soil erosion processes during the growing season have minor contributions to annual soil erosion rates, if no extreme events occur. Replicate ^{137}Cs samples from the Urseren Valley highlighted a large variability in ^{137}Cs activities at meter scale. This small-scale heterogeneity is smoothed by the NaI detector in-situ measurements. After the correction of the in-situ data for soil moisture, a significant correlation (i.e. $R^2 = 0.86$; $p < 0.0001$) was found between ^{137}Cs activities estimated with in-situ NaI and laboratory GeLi detectors.

1. Introduction

Soil erosion is a severe problem in mountain ecosystems because once initiated, significant effort is required to stop, or even mitigate the process with remedial actions, due to the extreme topography. Because of the high degree of uncertainty connected with estimating soil erosion in mountainous regions, there is a demand for methods to describe and predict erosion of alpine soils from small to large scales [1]. Although a range of conventional assessment tools has been developed for Alpine systems [2-4], their ability to describe and predict changes in mountain soil stability and degradation has been questioned [5].

Datasets describing soil erosion in mountainous regions under natural precipitation regimes are scarce [6-8]. Moreover, existing studies focus on soil erosion measurement during the growing season as physical soil erosion measurement devices fail during the winter season. Hence, more data on soil erosion processes in alpine regions for longer time periods including

winter are needed. Such data would also support modelling approaches to quantify soil erosion in mountain areas. In the European Alps, only the Universal Soil Loss Equation (USLE) and the Pan-European Soil Erosion Risk Assessment (PESERA) models have been used to date [9, 10]. The validity of these models, however, has to be carefully considered for alpine regions [11, 12], especially the empirical USLE model, which was designed for the western USA. Moreover, soil erosion is affected by factors at a wide range of temporal and spatial scales [13]. It is therefore necessary to combine and cross-validate different methodological approaches for assessing soil erosion.

This study aims to address the above need for soil erosion data in alpine regions using a range of approaches i.e. direct monitoring through physical measurements, tracing with FRNs and stable isotopes, and modelling. The study was undertaken in the Urseren Valley (Switzerland), where the relevance of farming and the numbers of farmers have gradually decreased during the last decades [14]. The area was affected by fallout from the Chernobyl accident and hence the ^{137}Cs method can be used here to derive average soil redistribution rates for the period since 1986. The strength of the method is that it will integrate erosion rates over the entire year, but the technique is limited to sites where sheet and shallow rill erosion predominate, as deep rilling, gullying and land sliding involve redistribution of subsoil material having no ^{137}Cs content. Consequently, shallow landslides are not considered in this study, although they are a major source of soil erosion in the investigated site [15].

Alongside the ^{137}Cs approach, a stable isotope approach to evaluate early stage and long-term soil erosion is also proposed in this study. It has been reported in the literature that stable carbon isotope signatures can give information about the source area of suspended organic matter in rivers [16, 17] or runoff waters [18]. The present approach is to quantify soil erosion in hill slope transects from uplands (erosion source, oxic soils) to adjacent wetlands (erosion sink, anoxic soils) as they often occur in alpine environments.

Given that some methods are suited to quantify particular processes (e.g. sediment traps for sheet or rill erosion) and others to quantify overall net losses (e.g. inventories of ^{137}Cs), it is likely that the combination of approaches employed will yield additional knowledge about the relative importance of the different soil erosion processes. The advantages and disadvantages of the different methods and their suitability for alpine regions will be discussed in this paper.

2. Experimental design

2.1. Study area

The study area is located in the southern part of Central Switzerland in the Urseren Valley (Fig. 1). The bottom of the W-E extended mountain valley is approximately 1450 m above sea level surrounded by mountain ranges of altitudes up to 3200 m above sea level. The mean annual precipitation is 1516 mm (1986-2007, Source: MeteoSwiss) and the mean annual air temperature is 4.3 °C (1986-2007, Source: MeteoSwiss). The valley is snow covered for 5 to 6 months (from November to April) with a maximum snow depth in March. The precipitation maximum occurs in October, the minimum in February. Runoff is usually dominated by snowmelt in May and June. Nevertheless, summer and early autumn floods represent an important contribution to the flow regime. The valley mainly consists of grasslands. Upslope of villages there are small forest areas for avalanche protection. Avalanches are frequent because of the scarce forest cover and distinct topography. Land use is dominated by grazing and, in the lower reaches of the valley, by hay harvesting. Soils in the study area mainly

consist of podsols and cambisols [19]. A detailed description of the Urseren Valley is provided by [20].

Soil erosion was investigated at nine south-facing slope sections (Fig. 1), including three different grassland types each with three replicates: hayfields, (hf 1-3), pasture with dwarf shrubs (paw 1-3) and pasture without dwarf shrubs (pawo 1-3). The soil texture of hf2, paw2 and pawo1 was sandy loam, paw1 was loamy sand and hf1, hf3, pawo2, pawo3 and paw3 were silty loam. The vegetation of the hayfields was dominated by *Trifolium pratense L. ssp. Partense, Festuca sp.*, *Thymus serpyllum* and *Agrostis capillaries*. Pastures with dwarf shrubs were dominated by *Calluna vullgaris*, *Vaccinium myrtillus*, *Festuca violacea*, *Agrostis capillaries* and *Thymus serpyllum*. The dominant vegetation types in the pastures without dwarf shrubs were *Glubelaria cordifolia*, *Festuca sp.* and *Thymus serpyllum*. The slopes of all plots were in the range of 35 to 39°. During the study period, the pastured sites were stocked by cattle from June to September and dominated by horizontal cattle trails. The investigated sites were not affected by landslides.

The experimental design was based around five key work packages:

- Sediment yield measurement using sediment traps and cups for continuous acquisition of surface runoff, precipitation and soil moisture data;

- Characterisation of the experimental slope sections to support soil erosion modelling;

- Application of the soil erosion models WEPP and USLE;

- Use of ^{137}Cs as a tracer to quantify soil redistribution via both *in situ* and laboratory measurements;

- Measurement of stable C and O isotope ratios along transects to evaluate the relative importance of different sediment source areas.

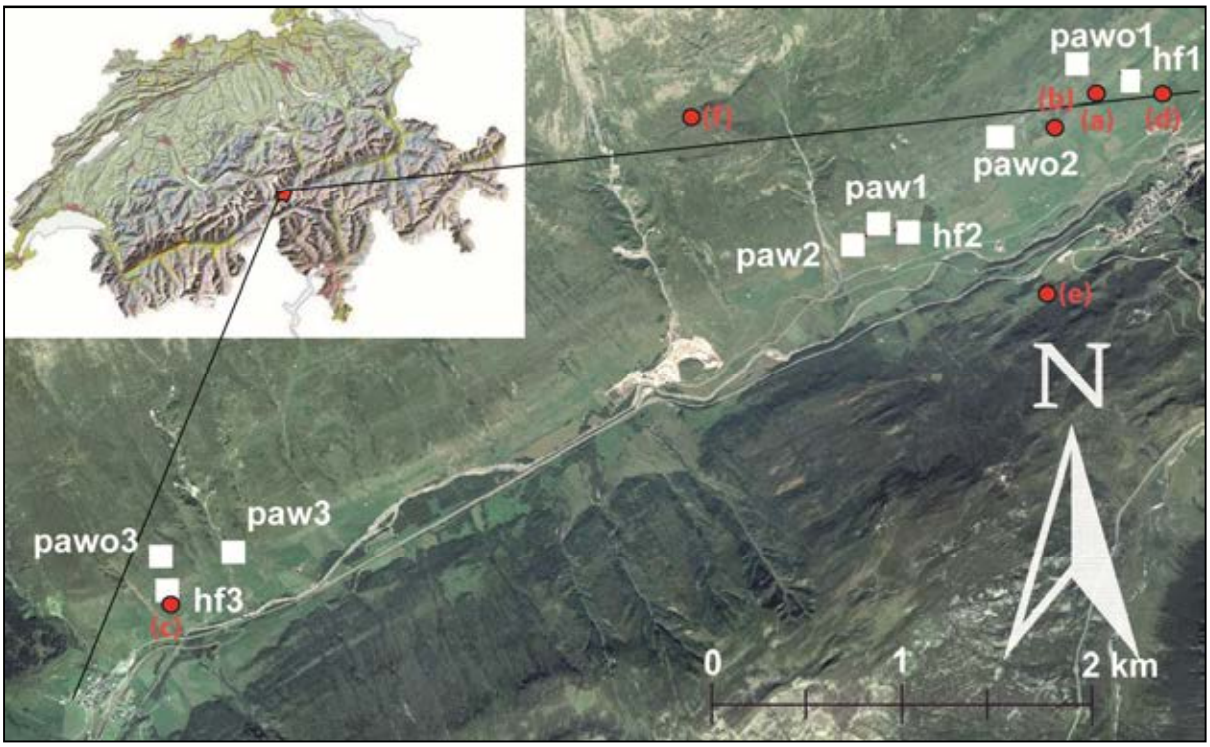

FIG. 1. The Urseren Valley study site (Central Swiss Alps) and the location of the nine slope sections with three grassland types: hayfield (hf), pasture (pawo) and pasture with dwarf shrubs (paw) and locations of stable isotope sampling (a) Spissen, (b) Bielen, (c) Laui and the corresponding reference wetlands (d) Oberes Moos, (e) Höh, (f) Lutersee and Spiessenälpetli (not shown here).

2.2. Determining spring and summer sediment yield with sediment traps and cups

Sediment traps were installed on each slope section in July 2006, one year before the study began. The slope sections were separated from upper slopes by large terraces. The contribution area of the sediment traps were 40 m^2 (2 m in width and 20 m in length). The upper boundary was delineated by plastic boards that were inserted to a depth of 20 cm. The plot locations were chosen to ensure that the topography clearly defined the side boundary i.e. they had neither a concave nor convex morphology. Thus, artificial side boundaries were not considered since they would have caused additional disturbance in stony soils and potentially channelized surface flow. The sediment traps [21] were extended by a v-shaped steel plate below a geotextile to concentrate and to measure surface runoff. Soil that flushed into the geotextile was collected every second week during the growing season from April to November in 2007 and 2008. In addition, precipitation, soil moisture and surface runoff were monitored every 10 minutes at one plot of each grassland type (hf3, pawo2, paw2). Precipitation was measured with tipping bucket (ECRN-50) rain gauges [22], soil moisture with a EC-5 sensor (Decagon Devices), and surface flow with a two-bowl tipping bucket (each bowl having 0.5 litre capacity). Further, 10 sediment cups [23] were installed along each plot. The sediment cups did not have fixed boundaries. Thus, the collected data was not quantitative as no contributing area was defined. Sediment cup yields were taken monthly as bulk samples per site.

2.3. Soil characterisation of the experimental sites

Vegetation and soil characteristics were determined for each plot to parameterise the soil erosion models. At each of the nine sites, 10 soil samples of the upper 5 cm were collected for particle size analyses using sieves between 32 and 1000 μm and a Sedigraph 5100 (Micromeritics) for the finer fractions. For the top 10 cm, soil bulk density and organic matter were measured three times for each plot. The soil total C content was measured with a Leco CHN analyzer 1000. The fractional vegetation cover was determined in April and September 2007. A grid of 1 m^2 with meshes of 0.1 m^2 was used. The fractional vegetation cover of each mesh was visually estimated and averaged for the entire square metre. This procedure was repeated four times for each plot. The maximum standard deviation was approximately 5%.

2.4. Soil erosion modelling using WEPP and USLE

The WEPP (Water Erosion Prediction Project) model is a well-established physically- based model for simulation of water erosion and sediment yield [24], and has already been successfully applied in the Italian Alps [25]. WEPP model parameters (vs. 2008) were determined through field characteristics (slope, plant species, fractional vegetation cover, initial saturation level), by laboratory analyses (grain size, organic matter) and by the WEPP internal database (rill- and inter-rill erodibility, effective hydraulic conductivity, cation exchange capacity). Measurements of the sediment traps, runoff and soil moisture were compared to WEPP simulations from April to November 2007. More detail on model parameterisation and application is presented in [26].

The empirical USLE model was originally developed for soil erosion assessment in the western USA. The coefficients required to run this model include topography (S and L factors), climate (R factor), soil (K factor), vegetation properties and land use (C and P factors). These coefficients were defined from a combination of field observations and laboratory analyses described above. The R factor (accounting for rainfall erosivity) was calculated according to [27], including a correction for snow accumulation [28], the S factor (accounting for slope steepness) was calculated after [29], the C factor (accounting for vegetation cover and land use) after the technical note of the United States Department of Agriculture [30]. The remaining factors, K (accounting for erodibility), P (accounting for conservation measures) and L (accounting for slope length), were calculated according to [31]. Climate input data for the models was available from the local meteorological station of MeteoSwiss in Andermatt. The main soil characteristics and all USLE factors are shown in Table 1.

Table 1. Measured and calculated parameters for the sites in the Urseren Valley, Switzerland (The relative standard deviation of organic matter is 17%. K is given in N h kg m^{-2} and R in N^{-1} H^{-1})

Parameter	Hayfield			Pasture (no dwarf shrubs)			Pasture (with dwarf shrubs)		
	1	2	3	1	2	3	1	2	3
Sand (g kg^{-1})	402	238	393	379	366	394	498	257	449
Silt (g kg^{-1})	473	588	438	505	471	456	376	635	409
Clay (g kg^{-1})	125	173	169	116	164	150	125	108	142
OM (g kg^{-1})	132	123	127	131	128	124	117	119	122
R	97.2	94.5	93.6	97.6	96.4	96.4	94.1	91.7	94.8
K	0.28	0.29	0.23	0.27	0.23	0.25	0.21	0.32	0.23
P (-)	1.0	1.0	1.0	0.9	0.9	0.9	0.9	0.9	0.9
S (-)	10.1	9.8	9.0	9.8	9.8	8.5	9.8	9.7	9.1
L (-)	2.2	0.9	2.3	1.2	1.4	1.8	1.4	1.3	1.3
C (-) x 10^{-2}	1.0	0.6	1.0	2.0	3.0	2.0	4.0	4.0	4.0

2.5. ^{137}Cs in situ measurements with a Sodium-Iodide detector

The main input of ^{137}Cs fallout to the study site occurred after the Chernobyl accident in 1986 [32]. *In situ* measurement of ^{137}Cs is a viable alternative to traditional gamma laboratory measurements in areas where soil collection is complicated and where high ^{137}Cs activity levels occur due to the Chernobyl accident [33]. However, results obtained need to be compared and verified with conventional laboratory gamma analyses.

A Sodium-Iodide (NaI) scintillation detector with a 50.8 x 50.8 mm crystal (Sarad, Dresden, Germany) was used for *in situ* ^{137}Cs measurements. The spectral resolution of the NaI detector is 9.7% at 661.7 keV FWHM. Peak area is specified by a Gaussian function over the region of interest (ROI). The background is separated from the peak area by a straight line between the beginning and end point of the ROI. The ROI was set to include the three interfering peaks ^{208}Tl at 583.2 keV, ^{214}Bi at 609.3 keV and ^{137}Cs at 661.7 keV. This multiplet was deconvolved to get peak areas of single peaks. As the determination of the ROI is subjective, the error on peak area was determined by using the mean standard deviation of peak areas of 20 tested spectra evaluated by five persons independently. The spectra were encrypted to avoid manipulation of evaluation. For the collection of field data, the NaI gamma spectrometer was placed perpendicular to the ground at a height of 25 cm for one hour. Three measurements were performed at each site.

2.6. ^{137}Cs laboratory measurements with a Germanium-Lithium detector

For *Germanium-Lithium* (GeLi) laboratory measurements soil samples were collected with a core sampler (Giddings Machine Company, Windsor, CO, USA) in the field. Soil samples were dried at 40 °C, passed through a 2 mm sieve and ground using a tungsten carbide swing grinder. The ground soil samples were filled into 25 ml sample containers (6.5 cm diameter) and measured for 8 hours. Analyses were performed with a Lithium-drifted Germanium detector (relative efficiency of 19%) at the Department for Physics and Astronomy, University of Basel. The detector was 48 mm in diameter and 50 mm in length. To reduce the amount of radiation from background sources, the samples were shielded by 4 cm thick lead during measurement. ^{137}Cs activity concentrations were determined using the InterWinner 5 gamma spectroscopy software (ITECH INSTRUMENTS LLC, Trenton, USA). The energy calibration of the GeLi detector was performed using a ^{152}Eu multi-source with peak line

positions at 122, 344, 778, 964 and 1408 keV. For efficiency calibration three reference samples enriched with known activities of ^{238}U, ^{232}Th and ^{40}K were used. These calibration samples were of the same geometry and a comparable density as the analysed soil samples. The resulting measurement uncertainty on ^{137}Cs was lower than 15% with a MDA of 0.1 Bq kg^{-1}.

2.7. Conversion of ^{137}Cs inventories to soil redistribution rates

To estimate the soil redistribution rates from ^{137}Cs inventories, reference sites and the depth distribution of the ^{137}Cs concentration are required (see Paper 2 of this TECDOC). Four potential reference sites near the valley bottom were evaluated. In unploughed grassland soils most of the ^{137}Cs is accumulated at the top of the soil profile or few centimetres below and the content decreases with depth [34-36]. The depth distribution at these sites was measured with a GeLi detector using soil cores sectioned into slices of 5 cm thickness. The GeLi laboratory measurements were used for the calculation of sedimentation rates in the wetlands. Soil redistribution rates were calculated using the profile distribution model (see Paper 5 of this TECDOC) assuming that the total ^{137}Cs fallout occurred in 1986.

Soil erosion estimates for the nine slopes were based on the NaI measurements. A layer model was used to convert the *in situ* ^{137}Cs activities to soil erosion rates, based on the following assumptions:

- a) ^{137}Cs fallout in 1986 was distributed homogenously over the catchment area and the resulting activity in the soil decreased exponentially with depth;

- b) ^{137}Cs distribution with depth can be represented by a layer-model. For 1986, ^{137}Cs activity at the surface was calculated by summing up the activities of single layers (derived from the exponential depth distribution). In this application, the shielding of upper soil layers needs to be taken into account using Beer's law.

The depth distribution of ^{137}Cs can be derived as follows:

$$Cs(z) = Cs(0) \times e^{-(-\log[0.5/ho])} \quad (1)$$

where:

Cs(0) is the ^{137}Cs concentration in the uppermost layer;
h_0 is the relaxation mass depth.

With knowledge of the activity at the surface and the shape of the ^{137}Cs depth distribution, the value of *Cs(0)* can be found by summing up the gamma radiation of *Cs(z)* seen at the surface and equating it to the measurement made by the NaI detector.

To evaluate the temporal dynamics of soil redistribution, the following aspects also required consideration in the conversion of inventory data to erosion rates:

- (a) The ^{137}Cs activity of each layer is reduced every year according to its radioactive decay (see Paper 2 of this TECDOC);

- (b) At eroding sites, the amount of soil removed needs to be estimated to explain the measured field activity. This is achieved by optimising the depth of the eroded soil layer

- (soil density is measured) to produce the measured activity. Considering the land use management, it was assumed that the upper soil layer (5 cm) is mixed by trampling and thus the ^{137}Cs activity for this layer was homogeneous.

2.8. The stable isotope approach for exploring sediment source areas

Stable carbon (C) isotope signatures can provide useful information about soil redistribution [37, 38]. However, stable carbon isotopes have never been used to track soil erosion in hill slope transects from uplands (erosion source) to adjacent wetlands (erosion sink) with no transition from C3 to C4 vegetation, as often occurs in alpine environments. Different carbon isotope signatures can be expected for uplands and adjacent wetlands and water bodies because in the aerobic environment of the uplands oxidative processes dominate during decomposition of plant material. Due to isotopic fractionation during those processes residues are increasingly enriched in the heavier carbon isotope (^{13}C) as the lighter ^{12}C will preferentially be involved in chemical reactions [39]. In contrast, wetland soils are characterized by anoxic conditions. The lack of oxygen results in an incomplete decomposition of organic material by anaerobic bacteria. Carbon compounds are preserved to a higher degree and keep their original (plant) isotopic signature. Therefore, $\delta^{13}C$ of soil organic carbon (SOC) in wetland soils can be assumed to be lighter than those of upland soils.

The latter relationship between $\delta^{13}C$ and decomposition of SOC might also be reflected in depth profiles. Increasing $\delta^{13}C$ with depth is typical for upland soils and is usually related either to kinetic fractionation during decomposition of soil organic matter resulting in an enrichment of ^{13}C in the residual material [40-42] or to soil age [18, 40, 43]. The isotopic composition of atmospheric CO_2 decreased from $\delta^{13}C$ values around –6.4 ‰ at the end of the eighteenth century to values around –7.6 ‰ in 1980 [44]. A further decrease to values around –8.1 ‰ in 2002 was measured by [45]. This decrease in $\delta^{13}C$ of 1.7 ‰ over the last 150 years (Suess effect) might be documented in wetland soils rather than in uplands due to their greater soil age (of up to several hundred years).

The underlying assumption of the approach presented here is that systematic differences between the isotopic fingerprint of upland and wetland soils exist. For upland soils, a clear increase of $\delta^{13}C$ with depth, due to decomposition processes taking place in the soil can be hypothesised (Fig. 2a) [40-42]. For an anaerobic environment in the wetland, where decomposition rates are small, a more or less constant $\delta^{13}C$ with depth can be hypothesised (Fig. 2a). SOC content and stable carbon isotope signatures of soils were assessed for their suitability to detect early stage soil erosion. Hill slope transects (Fig. 2b) from upland cambisols (A) to adjacent wetlands (B; with histosols and histic to mollic gleysols) differing in their intensity of visible soil erosion, and reference wetlands (C) without erosion influence were sampled.

Stable oxygen isotope signatures were also explored in a similar way. The stable oxygen isotope signature ($\delta^{18}O$) of soil is expected to be the result of a mixture of components within the soil with varying $\delta^{18}O$ signatures. Thus, the $\delta^{18}O$ of soils should provide information about the soil's substrate, especially about the relative contribution of organic matter vs. minerals. As there is no standard method available for measuring soil $\delta^{18}O$, the method for the measurement of single components using a high-temperature conversion elemental analyser (TC/EA) was adapted [46]. The $\delta^{18}O$ was measured in standard materials (IAEA 601, IAEA 602, Merck cellulose) and soils (organic and mineral soils) to determine a suitable pyrolysis temperature for soil analysis. A pyrolysis temperature was considered suitable when the yield of signal intensity (intensity of mass 28 per 100 mg) was at a maximum, the acquired raw $\delta^{18}O$ signature constant for the standard materials and when the quartz signal of the soil was

still negligible. After testing several substances within the temperature range of 1075 to 1375 °C, it was decided to use a pyrolysis temperature of 1325 °C for further measurements [46]. For the Urseren Valley a sequence of increasing $\delta^{18}O$ signatures from phyllosilicates to upland soils, wetland soils and vegetation was highlighted [46].

Stable carbon isotope analyses were accomplished using a continuous flow isotope ratio mass spectrometer (Delta^{plus} XP, ThermoFinnigan, Germany) coupled with a FLASH elemental analyser 1112 (ThermoFinnigan, Italy) combined with a CONFLO III interface (ThermoFinnigan, Germany), following standard processing techniques. The stable isotope ratios are reported as $\delta^{13}C$ values (‰) relative to V-PDB defined in terms of NBS 19 = 1.95 ‰. Oxygen isotope signatures were measured as CO with a high-temperature conversion elemental analyser (TC/EA, ThermoFinnigan, Germany) equipped with a zero blank autosampler (Costech Analytical Technologies, USA) and combined with a CONFLO III interface and a Delta^{plus} XP mass spectrometer (ThermoFinnigan).

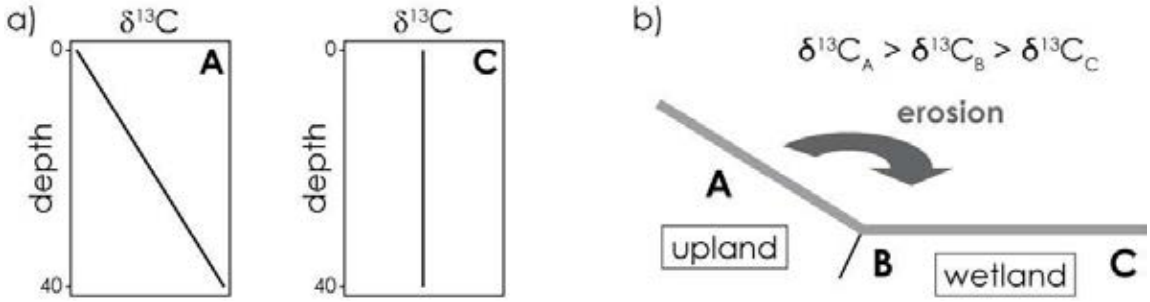

FIG. 2. (a) Theoretical $\delta^{13}C$ depth profiles at uplands (A) and undisturbed wetlands (C), and (b) theoretically expected influence of erosion on the $\delta^{13}C$ of wetlands disturbed by erosion (B).

3. Results and discussion

3.1. Soil erosion measurement with sediment traps and sediment cups

Monthly soil erosion magnitudes recorded with sediment traps during the 2007 and 2008 growing seasons were low, ranging from 0 kg ha^{-1} (hf2 and hf3 in September 2007) to 580 kg ha^{-1} (pawo2 in August 2007). Erosion rates measured with sediment traps did not differ significantly ($p > 0.05$, ANOVA) between grassland types (Fig. 3).

The erosion rates determined with the sediment traps were below 1.5 t ha^{-1} yr^{-1}. The latter is surprising considering the high visible erosion damage on the fields. However, measurements capture only erosion processes during the growing season. Furthermore, no extreme rain events occurred during the measurement period (2007-2008). The measured erosion rates are consistent with measured erosion rates for the growing season from Felix and Johannes [6] with 0.1 to 200 kg ha^{-1}. The authors concluded that their low erosion rates were based on low effective precipitation (rainfall that contributes to surface runoff) between 1 and 2%. The effective precipitation on the investigated plots was also low with a range of 0.6 and 2% during the 2007 and 2008 growing seasons, respectively.

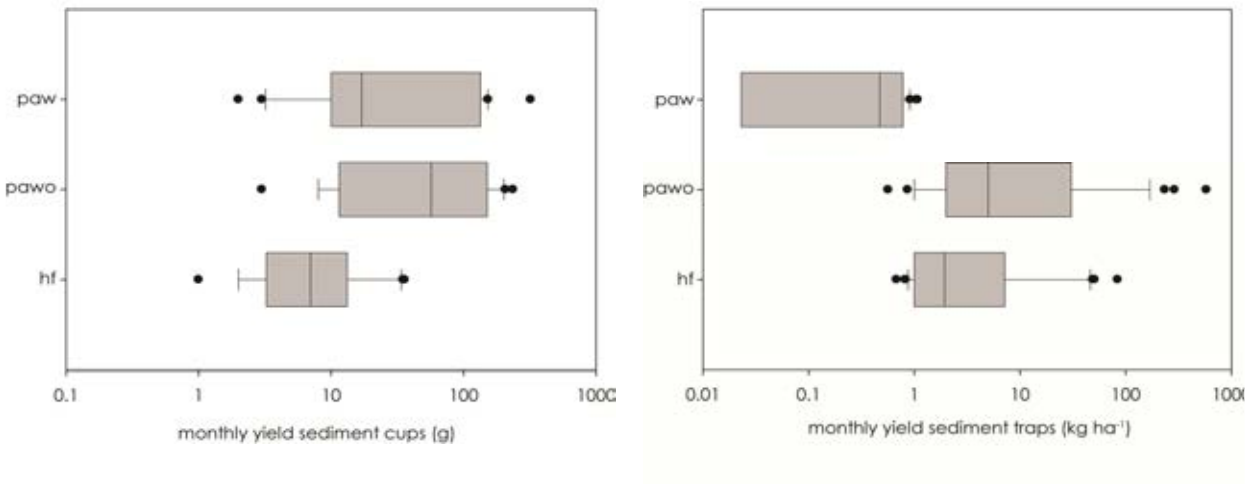

FIG. 3. Monthly sediment yield measured with sediment traps (left graph) and sediment cups (right graph) for three different grassland types: hayfield (hf), pasture (pawo) and pasture with dwarf shrubs (paw).

A mean (for six years) erosion rate of 20 t ha^{-1} yr^{-1} was measured (during the growing season) on grassland plots with clear signs of degradation (reduced vegetation cover) [47]. However, the authors reported that the effective precipitation during the measurement period was up to 60%. Generally, soil erosion measurement with sediment traps on subalpine grasslands is of limited use. Since erosion events are subject to a high spatial heterogeneity, it is critical to find a representative location for the installation of the sediment traps. A further problem of sediment traps is that they are not suitable for winter measurements because they will be destroyed by snow gliding and avalanches. Since soil erosion rates during the growing seasons were low and possibly transport limited (due to low effective precipitation caused by high infiltration rates), sediment cups were installed to test if there is small scale soil movement within the plots that is not captured, due to sedimentation occurring before the material reaches the sediment traps. Sediment cups are only suitable for a qualitative assessment of erosion activity but cannot give information on quantitative rates. Sediment cups indicated a comparable erosion magnitude for pasture with and without dwarf shrubs, but a lower magnitude for hayfields. The difference between the low erosion rates determined for pastures with dwarf shrubs with the sediment traps and the high erosion activity indicated by sediment cups point to small scale soil movement with detached particles not being transported down slope and, thus, not captured by sediment traps. Walling [48] concluded that generally 70 to 85% of the eroded material remains near the point of detachment.

3.2. Modelled estimates using WEPP and USLE

WEPP generally simulated the hydrology (soil moisture, surface runoff) of the sites sufficiently. However due to snow melt effect, the water availability in spring and early summer was overestimated. For the WEPP application, a distinction was made between short-term erosion prediction for a single growing season (2007) and long-term erosion prediction (1986-2007). The short-term simulated erosion rates for single growing seasons were very low with 0.3, 0.9 and 0.3 kg ha^{-1} for hf3, pawo2 and paw2, respectively, which is less than 0.0016 t ha^{-1} yr^{-1} (Fig. 4). WEPP simulated low to zero erosion during the growing season in spite of delayed snow melt, steep slopes and silt loam textures, which makes a soil prone to erosion. The simulated erosion rates were notably lower than the rates measured using the

sediment traps. Mean long-term erosion rates simulated with WEPP including the winter season ranged from 0.04 to 1.21 t ha^{-1} yr^{-1}. The simulated cumulative erosion rates for the growing seasons (from April 1986 to October 2007) are 30 to 500 times less than the cumulative annual erosion rates (from January 1986 to December 2007) (Table 2). The high erosion rates from November to March result from simulated overland flow on frozen ground.

TABLE 2. COMPARISON OF SIMULATED CUMULATIVE EROSION RATES (T HA^{-1}) FOR THE GROWING SEASONS (APRIL–OCTOBER) AND ANNUAL (JANUARY–DECEMBER) FROM 1986 TO 2007

Land use type	Growing season	Annual
Hayfield	0.005	0.154
Pasture (no dwarf shrubs)	0.04	20.9
Pasture (with dwarf shrubs)	0.14	4.4

The USLE provides long-term average soil erosion rates. The estimated erosion rates of USLE are high compared to the values of the sediment traps and the WEPP simulations (Fig. 4). The simulated values differed depending on grassland type. Mean average erosion rates were lowest for the hayfields with 3.6 ± 1.9 t ha^{-1} yr^{-1}. Estimates for pastures are higher with 10.5 ± 3.7 t ha^{-1} yr^{-1} for paw and 8.3 ± 2.0 t ha^{-1} yr^{-1} for pawo (Fig. 4).

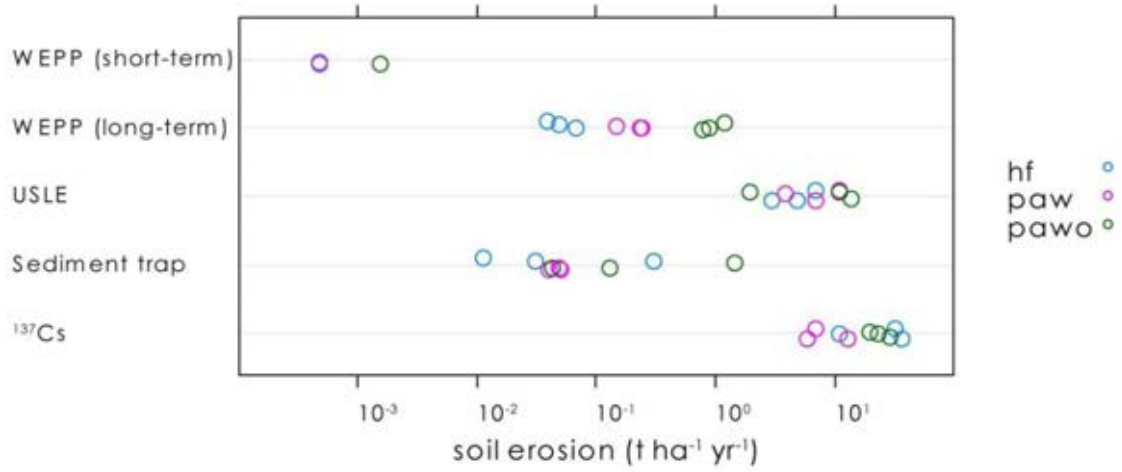

FIG. 4. Soil erosion rates in t ha^{-1} yr^{-1} estimated by different approaches.

3.3. Soil erosion information gained through use of ^{137}Cs in alpine areas

(i) Calibration of the *in situ* NaI detector

Replicate soil samples measured in the laboratory with the GeLi detector, showed a high variability in ^{137}Cs activities at the metre scale. This small scale heterogeneity determined with the GeLi detector was attenuated by *in situ* measurements with the NaI detector, which provides integrated estimates of ^{137}Cs within the field of view of each measurement.

The field of view and the increased shielding of the signal with penetration depth were determined for the detector calibration (Fig. 5). The depth distribution of ^{137}Cs was measured at a subdivided soil core (0-5, 5-10, 10-15 and 15-20 cm) by laboratory measurements

(GeLi detector). In accord with the reference site, the ^{137}Cs activity was observed to decrease exponentially with depth (Fig. 5a). Over 70% of the total ^{137}Cs inventory of the soil is held in the top 10 cm of the soil column (Fig. 5a).

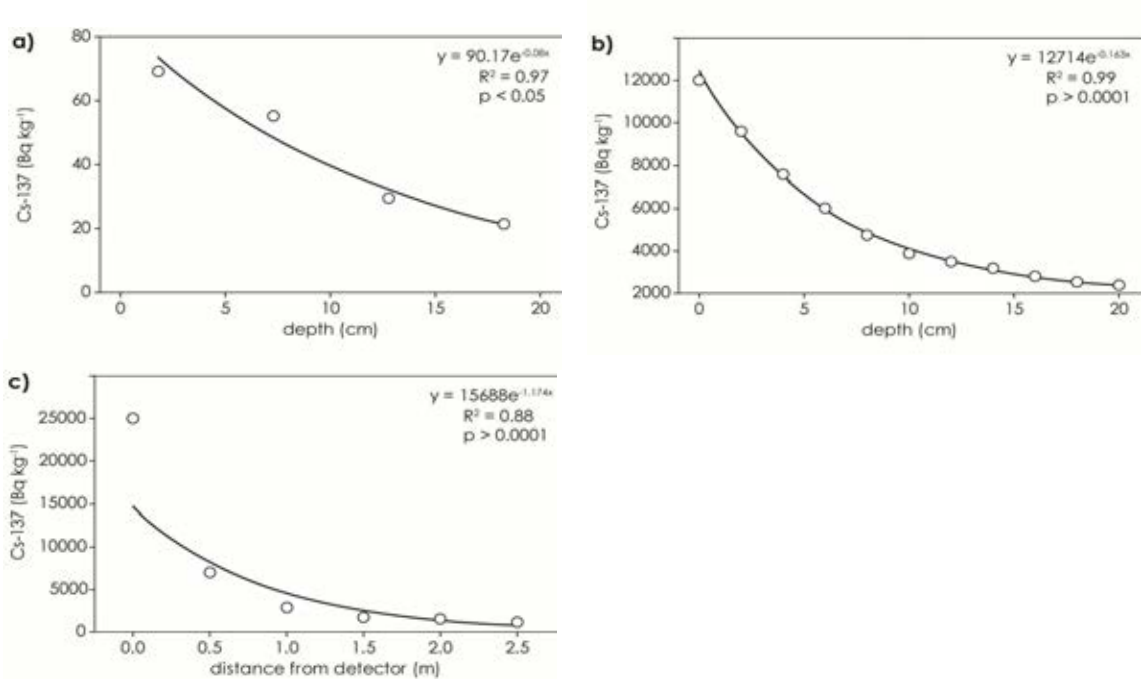

FIG. 5. (a) ^{137}Cs depth profile for an upland soil measured in the laboratory (GeLi detector). (b) Exponential decrease of the measured ^{137}Cs activity at the surface with increasing burial depth of the point source (NaI detector). (c) Exponential decrease of the measured ^{137}Cs activity with increasing distance between the point source and the detector (NaI detector).

A similar distribution was also observed [49] for the migration of ^{137}Cs deposited after the Chernobyl reactor accident in a grassland for 15 years. Hence, the contribution of radiation from deeper soil layers was estimated by repeated measurement of a buried ^{137}Cs point source (7.6 kBq on 08/2007) in steps of 2 cm between 0 and 20 cm soil depth by *in situ* NaI measurements. The radiation contributing to the total measured ^{137}Cs activity decreased exponentially with depth (Fig. 5b). Considering the decreasing ^{137}Cs content and decreasing detector yield with depth, the contribution of the top 10 cm to the total yield can be estimated to be ca. 90%. The field of view of the NaI detector was estimated in the field by repeated measurement of a ^{137}Cs point source (15.8 kBq on 08/2007) with increasing distance from the detector. The distance was increased by 0.5 m between measurements. With increasing distance of the point source to the detector, ^{137}Cs activity decreased exponentially (Fig. 5c). Under the assumption of a homogenous distribution, 90% of the measured ^{137}Cs activity originated from a circular area with a radius of 1 m around the detector (3.1 m^2).

The ^{137}Cs concentration within the field of view was determined by laboratory analysis of soil samples in order to calibrate the NaI system. Nine samples (0-10 cm depth) distributed over a circular area with 3 m of diameter around a NaI measurement were used (Fig. 6). The mean ^{137}Cs activity concentration was 58.8 ± 8.2 Bq kg^{-1} with a maximum of 68.2 and a minimum of 42.0 Bq kg^{-1}. The mean value of these nine measurements (GeLi) was used to convert the ^{137}Cs peak area (counts) determined from *in situ* measurement (NaI) to Bq kg^{-1}.

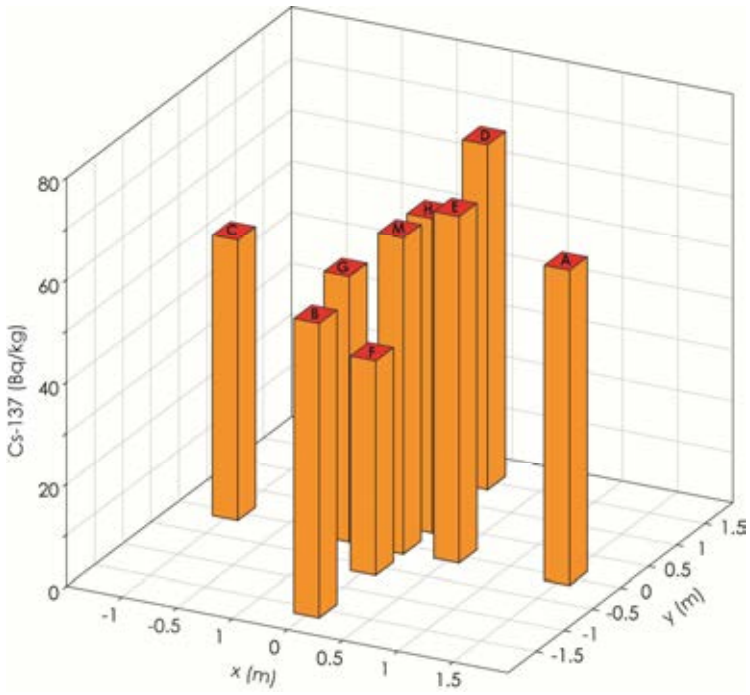

FIG. 6. Spatial heterogeneity of the ^{137}Cs distribution at the calibration site.

For the Urseren valley, no dependency of ^{137}Cs on pH, clay content and carbon content was observed [50]. However, a close relationship was determined between ^{137}Cs and soil moisture (Fig. 7). Thus, after soil moisture correction (using the Equation established in Fig. 7) the conversion should be valid for all further *in situ* measurements at comparable soils in the Urseren Valley. This was controlled with additional measurements at 12 sites demonstrating a significant correlation between the ^{137}Cs activities obtained from *in situ* NaI and laboratory GeLi measurements (Fig. 8; [50]). All ^{137}Cs activities refer to the year 2007. Spatial distribution of ^{137}Cs in grasslands is much more variable than in arable lands where ^{137}Cs is mechanically homogenized by ploughing. Therefore, interpretation of laboratory ^{137}Cs data of alpine grasslands is subject to errors relating to the small scale sampling [50]. *In situ* measurements integrate over 3.1 m^2 and average out small scale variability. However, it is critical that the depth distribution at the measurement location is associated to high uncertainties. More details on comparability of *in situ* and laboratory measurements and its application in the study site can be found in [50, 51-53].

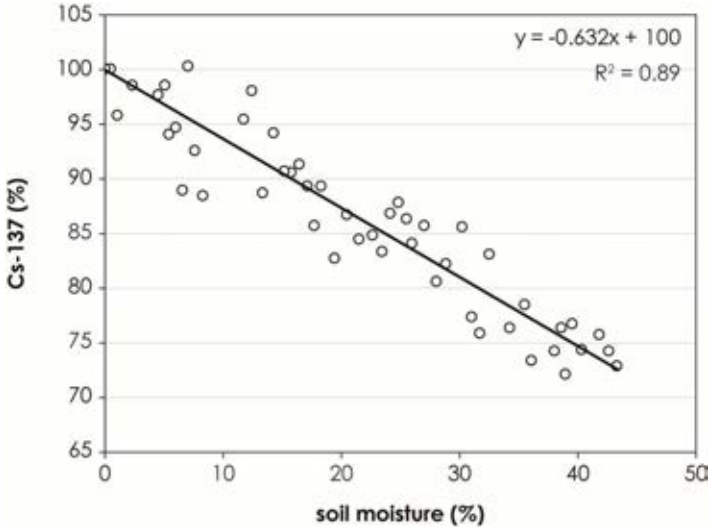

FIG. 7. Dependency of measured ^{137}Cs values on soil moisture. ^{137}Cs activity is given as % of ^{137}Cs activity measured for 0% soil moisture.

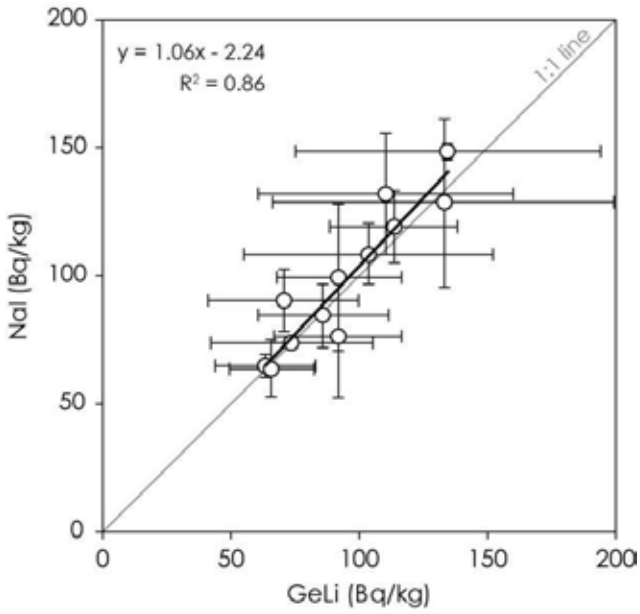

FIG. 8. Comparison of ^{137}Cs activities determined by in situ and gamma laboratory measurements. Error bars are standard errors on the mean estimate. They include the uncertainty in ^{137}Cs activity due to heterogeneity in ^{137}Cs distribution. Measurement uncertainty is comparable for both detectors with 15% for the GeLi detector and 17% for the NaI detector.

(iii) ^{137}Cs inventories and erosion rates

When ^{137}Cs measurements are converted to soil redistribution rates the question of suitable reference sites is crucial. Four reference sites were selected at the valley bottom where it could be assumed that neither erosion nor sedimentation occurs. Two of these reference sites were rejected due to ^{137}Cs depth profile features most likely linked to a flood event in 1987. For the two remaining sites, deposition of eroded soil can be excluded because of lateral

moraines protecting the reference sites from any upslope sediment input. Soil erosional export is also highly unlikely on these sites due to a slope angle of 0° and a constant vegetation cover since 1986. The latter could be confirmed from air photographs that were taken regularly since 1986. The mean ^{137}Cs activity of the reference sites is 146 ± 20 Bq kg^{-1}.

Resulting erosion rates based on *in situ* NaI measurements were between 6 and 37 t ha^{-1} yr^{-1} (Fig. 4). Mean ^{137}Cs activity based on *in situ* measurements were 91 Bq kg^{-1} for all hayfields, 94 Bq kg^{-1} for all pastures and 121 Bq kg^{-1} for all pastures with dwarf shrubs. Two hayfield sites showed the highest erosion rates due to the impacts of avalanche on hf3 [54] and mice activity on hf1. Pasture sites had higher erosion rates than pastures with dwarf shrubs. The latter might be due to increased sedimentation induced by dwarf shrubs which stabilize the soil and act as physical barriers, thus reducing transport of soil particles down slope. That dwarf shrubs might act as physical barriers was also noticed with sediment cup measurements, as described above.
Sediment traps and WEPP application both resulted in low erosion rates (less than 1.5 t ha^{-1} yr^{-1}) for the growing season (without an extreme rainfall event). However, the long-term erosion rates modelled with USLE (of up to 14 t ha^{-1} yr^{-1}) and WEPP (of up to 1.2 t ha^{-1} yr^{-1}) were controversial. The ^{137}Cs results showed that high soil erosion rates up to 37 t ha^{-1} yr^{-1} occur at the sites, which is consistent with the highly visible soil erosion damage. The high erosion rates must be due to winter processes (mainly mechanical translocation) because neither measurements during the growing season nor modelling include these processes.

3.4. Indication of soil erosion processes by stable isotope measurements

Carbon isotopic signature and SOC content of soil depth profiles were determined. A close correlation between δ^{13}C and carbon content ($r > 0.80$) was found for upland soils not affected by soil erosion, indicating that depth profiles of δ^{13}C of these upland soils mainly reflect decomposition of SOC [55]. Long-term disturbance of an upland soil was indicated by the decreasing correlation of δ^{13}C and SOC ($r \leq 0.80$). Consistent results were obtained in hill slope transects at three sites with a higher mean δ^{13}C signature of –26.6 ‰ in upland soils, an intermediate mean value of –27.5‰ for wetland soil horizons (0-12 cm) affected by erosion and representative of aerobic metabolism, and a reference wetland isotopic signature of –28.6 ‰, representative of anaerobic metabolism (Fig. 9). Carbon isotopic signature and SOC content were found to be sensitive indicators of short- and long-term soil erosion processes.

The results from this study show that the δ^{18}O values of upland soil samples differ significantly from wetland soil samples (Fig. 10). The latter can be related to the changing mixing ratio of the mineral and organic constituents of the soil. For wetlands affected by soil erosion, intermediate δ^{18}O signatures which lie between typical signatures for upland and wetland sites were found. This gives evidence for the input of upland soil material through erosion (Fig. 10).

By combining the ^{137}Cs approach (quantification of erosion rates) with stable carbon isotope signatures (process indicator of mixing vs. degradation of carbon pools) it was demonstrated that degradation of carbon occurs during soil erosion processes in the mountain grasslands under investigation. Transects from upland (erosion source) to wetland soils (erosion sinks) of sites affected by erosion were sampled. GeLi measurements of ^{137}Cs and conversion to sedimentation rates yielded an input of 2 and 4.6 t ha^{-1} yr^{-1} of soil material into the wetland sites [52]. Assuming no degradation of soil organic carbon during detachment and transport, the carbon isotope signature of SOC in the wetlands could only be explained with an assumed 500–600 and 350-400 years of erosion input into the Laui and Spissen wetlands, respectively

[52]. The latter is highly unlikely with alpine peat growth rates indicating that the upper horizons might have an age between 7 and 200 yr. It is not possible to conclude from the presented data that eroded SOC is generally degraded during detachment and transport. However, the proposed method may be suitable for gaining more information on process dynamics during soil erosion from oxic upland to anoxic wetland soils, sediments or water bodies.

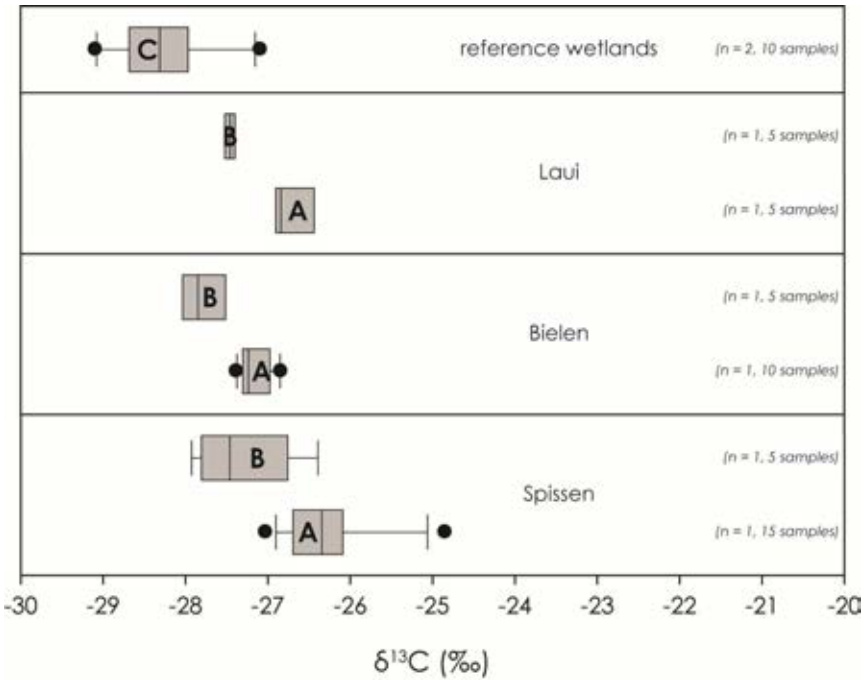

FIG. 9. $\delta^{13}C$ for three sites with upland soils (A) and adjacent wetlands with soil erosion influence (B) compared to a reference wetland (C)

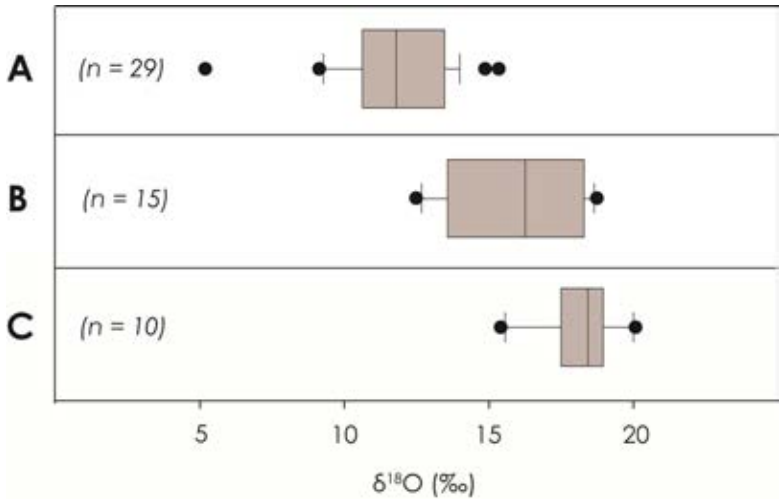

FIG. 10. Stable oxygen isotope signature of soil samples from sites in the Urseren Valley (A = upland, B = wetland with erosion influence, C = reference wetland unaffected by erosion).

4. Conclusion and outlook

The different erosion assessment tools used in this study delivered a wide range of erosion rates. Erosion values based on commonly used methods such as sediment traps and soil erosion modelling with WEPP are below 1.5 t ha^{-1} yr^{-1} implying low erosion risk. Direct measurement of erosion with sediment traps or sediment cups can only give information during the growing season. Modelling of erosion rates in mountain regions is hampered by the lack of a directly suited model. WEPP was successful in simulating the low to zero erosion activity during the growing season but failed to describe the high visible damage. The USLE estimates were higher because its empirical factors are based on long-term measurements and in this study, the R, L and S factors were adapted for mountainous areas. Use of empirically-based parameters produced more plausible long-term soil erosion estimates but the model does not consider winter and snowmelt processes and thus probably underestimates soil erosion rates. The physically-based WEPP model required detailed information on rainfall distribution and kinetic energy, overland flow hydraulics and soil properties. The assumptions made to generate these data might be of limited suitability for mountain areas. The same was shown for a comparison of catchment scale modelling of erosion rates in the Urseren Valley; the physically-based PESERA underestimated erosion rates by an order of magnitude, while the USLE came at least within the range of plausible erosion rates (judged by observed damage and ^{137}Cs rates [56]). Nevertheless, even the USLE simulated lower erosion rates than measured with ^{137}Cs.

Only the ^{137}Cs approach integrates erosion over a time period from April 1986 to the present, including erosive processes during the winter season and snow melt as well as during intensive rainstorm events. Thus, in the Urseren Valley erosion processes during the growing season seem to have a minor influence on annual soil erosion rates, in the absence of an extreme event. The deviation between the ^{137}Cs and the other approaches is most likely due to winter processes, most of all the mechanical translocation by snow movement (gliding, ablation and avalanches).

Stable carbon and oxygen isotopes were found to be useful as indicators of soil erosion as well as to differentiate long- and short-term soil erosive processes from upland to wetland soils. A combination of stable isotope data with ^{137}Cs data indicated that SOC is degraded during detachment and transport of eroded soil at the study site.

The use of multiple independent methods to evaluate soil erosion rates has highlighted the importance of comparing such techniques and validating the results from model estimates. Significant advantages in process understanding were gained when these techniques were used together. The results also indicate the need for a critical evaluation of model-based soil erosion estimates. The USLE and WEPP models have been widely applied, but their limited applicability for estimating erosion rates in mountain regions where snow gliding and avalanches cause mechanical soil translocation was clearly highlighted through this study. Measurements of erosion rates with ^{137}Cs indicated for the first time that subalpine grasslands are prone to very high erosion rates of up to 37 t ha^{-1} yr^{-1}, which explains the high visible erosion damage of the sites. Considering the vulnerability of the alpine areas for climate change, future research should aim at determining erosion induced by winter and snow processes. Furthermore, the understanding of winter and snow processes triggering soil erosion is crucial for future modelling of alpine systems.

ACKNOWLEDGEMENT

This work was supported by the Swiss National Science Foundation (SNF), project no. 200021-105579 and 200020-113331, by the State Secretariat for Education and Research (SER), in the framework of the European COST action no. 634: "On- and Off-site Environmental Impacts of Runoff and Erosion" and by the Swiss Federal Office for the Environment (Contract-no.: StoBoBio/810. 3129.004/05/0X). Spectra evaluation was done with software provided by H. Surbeck, University of Neuchâtel, Switzerland.

REFERENCES

[1] ASSELMAN, N.E.M., MIDDELKOOP, H., VAN DIJK, P.M., The impact of changes in climate and land use on soil erosion, transport and deposition of suspended sediment in the River Rhine, Hydrol. Process. 17 (2003) 3225–3244.

[2] LANGE, E., Integration of computerized visual simulation and visual assessment in environmental-planning, Landsc. Urban Plan. 30 (1994) 99–112.

[3] LASANTA, T., GONZÁLEZ-HIDALGO, J.C., VICENTE-SERRANO, S.M., SFERI, E., Using landscape ecology to evaluate an alternative management scenario in abandoned Mediterranean mountain areas, Landsc. Urban Plan. 78 (2006) 101–114.

[4] SCHNEEBERGER, N., BURGI, M., KIENAST, P.D.F., Rates of landscape change at the northern fringe of the Swiss Alps: Historical and recent tendencies, Landsc. Urban Plan. 80 (2007) 127–136.

[5] Bänninger, D., Brodbeck, M., Hohwieler, N., Meusburger, K., Alewell, C., Soil degradation in the Swiss Alps, Mount. Forum Bull. 6 (2006) 6–8.

[6] FELIX, R., JOHANNES, B., Bodenerosionsuntersuchungen auf Testparzellen im Kalkhochgebirge, Mitt. Österr. Geogr. Ges. 137 (1995) 76–92.

[7] DESCROIX, L., MATHYS, N., Processes, spatio-temporal factors and measurements of current erosion in the French Southern Alps: A review, Earth Surf. Process. Landf. 28 (2003) 993–1011.

[8] ISSELIN-NONDEDEU, F., BEDECARRATS, A., Influence of alpine plants growing on steep slopes on sediment trapping and transport by runoff, Catena 71 (2007) 330–339.

[9] JOINT RESEARCH CENTER ISPRA, Nature and extent of soil erosion in Europe, http://eusoils.jrc.it/ESDB_Archive/pesera/pesera_cd/sect_2_2.htm (2009).

[10] JOINT RESEARCH CENTER ISPRA, Soil erosion in the Alps (RUSLE), http://eusoils.jrc.ec.europa.eu/library/Themes/Erosion/ClimChalp/Rusle.html (2009).

[11] VAN ROMPAEY, A.J.J., BAZZOFFI, P., JONES, R.J.A., MONTANARELLA, L., GOVERS, J., Validation of Soil Erosion Risk Assessment in Italy, European Commission, Joint Research Centre, Luxembourg (2003).

[12] VAN ROMPAEY, A.J.J., et al., Validation of Soil Erosion Estimates at European scale, European Soil Bureau Research Report No. 13, Luxembourg (2003).

[13] HELMING, K., AUZET, A.V., FAVIS-MORTLOCK, D., Soil erosion patterns: evolution, spatio-temporal dynamics and connectivity, Earth Surf. Process. Landf. 30 (2005) 131–132.

[14] KAEGI, H.U., Die traditionelle Kulturlandschaft im Urserental: Beitrag zur alpinen Kulturgeographie, University of Zurich, Switzerland (1973).

[15] MEUSBURGER, K., ALEWELL, C., On the influence of temporal change on the validity of landslide susceptibility maps, Nat. Haz. Earth Syst. Sci. 9 (2009) 1495–1507.

[16] ONSTAD, G.D., CANFIELD, D.E., QUAY, P.D., HEDGES, J.I., Sources of particulate organic matter in rivers from the continental USA: Lignin phenol and stable carbon isotope compositions, Geochim. Cosmochim. Acta 64 (2000) 3539–3546.
[17] MASIELLO, C.A., DRUFFEL, E.R.M., Carbon isotope geochemistry of the Santa Clara River, Global Biogeochem. Cycl. 15 (2001) 407–416.
[18] BELLANGER, B., et al., Monitoring soil organic carbon erosion with delta C-13 and delta N-15 on experimental field plots in the Venezuelan Andes, Catena 58 (2004) 125–150.
[19] WORLD REFERENCE BASE FOR SOIL RESOURCES, World Soil Resources Reports No. 103, 2nd edn, FAO, Rome (2006).
[20] MEUSBURGER, K., ALEWELL, C., Impacts of anthropogenic and environmental factors on the occurrence of shallow landslides in an alpine catchment (Urseren Valley, Switzerland), Nat. Haz. Earth Syst. Sci. 8 (2008) 509–520.
[21] ROBICHAUD, P.R., BROWN, R.E., Silt Fences: An Economical Technique for Measuring Hillslope Soil Erosion. RMRSGTR-94, Rocky Mountain Research Station, USDA-Forest Service, United States Department of Agriculture (2002) 1–24.
[22] DECAGONDEVICES, http://www.decagon.com/ag_research/home/index.php (2007)
[23] VAN DIJK, A., BRUIJNZEEL, L.A., WIEGMAN, S.E., Measurements of rain splash on bench terraces in a humid tropical steepland environment, Hydrol. Process. 17 (2003) 513–535.
[24] FLANAGAN, D.C., NEARING, M.A., USDA-Water Erosion Prediction Project: Hillslope Profile and Watershed Model Documentation, National Soil Erosion Research Laboratory, West Lafayette, NSERL Rep. 10 (1995) 298.
[25] SIMONATO, T., BISCHETTI, G.B., CROSTA, G.B., Evaluating soil erosion with RUSLE and WEPP in an alpine environment (Dorena valley - Central Alps, Italy), Sustain. Land Manage. – Environ. Prot. 35 (2002) 481–494.
[26] KONZ, N., BÄNNINGER, D., NEARING, M., ALEWELL, C., Does WEPP meet the specificity of soil erosion in steep mountain regions? Hydrol. Earth Syst. Sci. Discuss. 6 (2009) 2153–2188.
[27] ROGLER, H., SCHWERTMANN, U., Rainfall erosivity and isoerodent map of Bavaria, Z. Kultur. Flur. 22 (1981) 99–112.
[28] SCHUEPP, M., Objective weather forecasts using statistical aids in Alps, Riv. Ital. Geofis. Sci. Affini 1 (1975) 32–36.
[29] RENARD, K.G., FOSTER, G.R., WEESIES, G.A., Predicting Soil Erosion by Water; a Guide to Conservation Planning with the Revised Universal Soil Loss Equation (RUSLE). United States Government Printing (1997) 384.
[30] UNITED STATES DEPARTMENT OF AGRICULTURE, Procedure for computing sheet and rill erosion on project areas, Soil Conservation Service, Technical Release No. 51, Rev. 2 (1977).
[31] WISCHMEIER, W.H., SMITH, D.D., Predicting Rainfall Erosion Losses - A Guide to Conservation Planning. Agricultural Handbook No. 537, Washington D.C (1978).
[32] DUBOIS, G., DE CORT, M., Mapping Cs-137 deposition: data validation methods and data interpretation, J. Environ. Radioact. 53 (2001) 271–289.
[33] GOLOSOV, V.N., et al., Application of a field-portable scintillation detector for studying the distribution of ^{137}Cs inventories in a small basin in Central Russia, J. Environ. Radioact. 48 (2000) 79–94.
[34] RITCHIE, J.C., MCHENRY, J.R., Application of radioactive fallout cesium-137 for measuring soil-erosion and sediment accumulation rates and patterns - a review, J. Environ. Qual. 19 (1990) 215–233.

[35] OWENS, P.N., WALLING, D.E., HE, Q., The behaviour of bomb-derived caesium-137 fallout in catchment soils, J. Environ. Radioact. 32 (1996) 169–191.
[36] RITCHIE, J.C., MCCARTY, G.W., Cesium-137 and soil carbon in a small agricultural watershed, Soil Till. Res. 69 (2003) 45–51.
[37] FOX, J.F., PAPANICOLAOU, A.N., The use of carbon and nitrogen isotopes to study watershed erosion processes, J. Am. Water Resourc. Assoc. 43 (2007) 1047–1064.
[38] TURNBULL, L., BRAZIER, R.E., WAINWRIGHT, J., DIXON, L., BOL, R., Use of carbon isotope analysis to understand semi-arid erosion dynamics and long-term semi-arid land degradation, Rapid Commun. Mass Spectrom. 22 (2008) 1697–1702.
[39] KENDALL, C., CALDWELL, E.A., Fundamentals of Isotope Geochemistry, Elsevier, Amsterdam (1998).
[40] BALESDENT, J., GIRARDIN, C., MARIOTTI, A., Site related $\delta^{13}C$ of tree leaves and soil organic matter in a temperate forest, Ecol. 74 (1993) 1713–1721.
[41] CHEN, Q.Q., et al., Soil organic matter turnover in the subtropical mountainous region of South China, Soil Sci. 167 (2002) 401–415.
[42] NOVAK, M., et al., Similarity between C, N and S stable isotope profiles in European spruce forest soils: implications for the use of delta S-34 as a tracer, Appl. Geochem. 18 (2003) 765–779.
[43] BIRD, M.I., HABERLE, S.G., CHIVAS, A.R., Effect of altitude on the carbon-isotope composition of forest and grassland soils from Papua-New-Guinea, Global Biogeochem. Cycl. 8 (1994) 13–22.
[44] FRIEDLI, H., LOTSCHER, H., OESCHGER, H., SIEGENTHALER, U., STAUFFER, B., Ice core record of the C-13/C-12 ratio of atmospheric CO_2 in the past two centuries, Nature 324 (1986) 237–238.
[45] KEELING, C.D., et al., "Atmospheric CO_2 and $^{13}CO_2$ exchange with the terrestrial biosphere and oceans from 1978 to 2000: observations and carbon cycle implications", A History of Atmospheric CO_2 and Its Effects on Plants, Animals, and Ecosystems, Ecol. Studies, Springer, Berlin 177 (2005) 83–113.
[46] SCHAUB, M., SETH, B., ALEWELL, C., Determination of delta O-18 in soils: measuring conditions and a potential application, Rapid Commun. Mass Spectrom. 23 (2009) 313–318.
[47] FRANKENBERG, P., GEIER, B., PROSWITZ, E., SCHÜTZ, J., SEELING, S., Untersuchungen zu Bodenerosion und Massenbewegungen im Gunzesrieder Tal/Oberallgäu, Eur. J. Forest Res. 114 (1995) 214–231.
[48] WALLING, D.E., The sediment delivery problem, J. Hydrol. 65 (1983) 209–237.
[49] SCHIMMACK, W., SCHULTZ, W., Migration of fallout radiocaesium in a grassland soil from 1986 to 2001 - Part 1: Activity-depth profiles of Cs-134 and Cs-137, Sci. Total Environ. 368 (2006) 853–862.
[50] SCHAUB, M., KONZ, N., MEUSBURGER, K., ALEWELL, C., Application of *in situ* measurement to determine ^{137}Cs in the Swiss Alps, J. Environ. Radioact. 101 (2010) 369–376.
[51] ALEWELL, C., MEUSBURGER, K., BRODBECK, M., BÄNNINGER, D., Methods to describe and predict soil erosion in mountain regions, Landsc. Urban Plan. 88 (2008) 46–53.
[52] ALEWELL, C., SCHAUB, M., CONEN, F., A method to detect soil carbon degradation during soil erosion, Biogeosci. 6 (2009) 2541–2547.
[53] KONZ, N., SCHAUB, M., PRASUHN, V., BÄNNINGER, D., ALEWELL, C., Cesium-137-based erosion-rate determination of a steep mountainous region, J. Plant Nutr. Soil Sci. 172 (2009) 615–622.
[54] AMBUEHL, E., 100 Jahre Einschneien und ausapern in Andermatt, Sonderausdruck aus dem Quartalsheft 4 (1961) *"Die Alpen"*.

[55] SCHAUB, M., ALEWELL, C., Stable carbon isotopes as an indicator for soil degradation in an alpine environment (Urseren Valley, Switzerland), Rapid Commun. Mass Spectrom. 23 (2009) 1499–1507.
[56] MEUSBURGER, K., KONZ, N., SCHAUB, M., ALEWELL, C., Soil erosion modelled with USLE and PESERA using QuickBird derived vegetation parameters in an alpine catchment, Int. J. Appl. Earth Observ. Geoinform. 12 (2010) 208–215.

USE OF ^{137}Cs, $^{210}Pb_{ex}$ AND ^{7}Be FOR DOCUMENTING SOIL REDISTRIBUTION: THE FUTURE

L. MABIT, G. DERCON
Soil and Water Management and Crop Nutrition Subprogramme, Joint FAO/IAEA Division of Nuclear Techniques in Food and Agriculture,
Vienna - Seibersdorf

M. BENMANSOUR
Centre National de l'Energie, des Sciences et des Techniques Nucléaires (CNESTEN), Rabat, Morocco

D.E. WALLING
Geography, College of Life and Environmental Sciences, University of Exeter, Exeter, United Kingdom

Abstract

Although ^{137}Cs and to some extent $^{210}Pb_{ex}$ based methodologies are well established, there remains a need for further investigations aimed at exploring the optimal use of ^{7}Be. The information generated by the ^{7}Be measurements can provide a useful complement to ^{137}Cs and fallout ^{210}Pb measurements to assess the effectiveness of different soil conservation practices. The conjunctive use of two or even three fallout radionuclides (FRNs) can generate valuable information on the erosional history of a site by generating datasets for different timescales. This approach needs to be developed further and validated under a range of different agro-ecological conditions. Another promising opportunity is the integration of FRNs and compound specific stable isotope techniques (CSSI) as fingerprinting technologies to identify critical agricultural areas of soil loss. An important and logical next step is the up-scaling of FRN-based methodologies from the field to the watershed level. To assist in integrating and interpreting the spatial complexity of the landscape, FRNs should be used more widely and at a larger scale for contributing more directly to decision making. An additional challenge for the users of FRNs will be to promote their transition and evolution from validated research tool to decision support tool.

1. Comparative advantages and limitations of ^{137}Cs, ^{210}Pb and ^{7}Be methodologies

The comparative advantages and limitations regarding the use of all three FRN-based methodologies (^{137}Cs, ^{210}Pb and ^{7}Be) in soil redistribution studies are summarized in Table 1. Based on this comparison, it is recommended that due to its simplicity with regard to soil sampling and measurement procedures, the transfer of FRN-based methodologies for erosion studies to Member States (MS) should focus initially on ^{137}Cs. Once the MS have built their capacity, ^{210}Pb and ^{7}Be can be introduced in order to build on that work and broaden the scope and potential afforded by the use of FRNs in soil redistribution investigations.

2. Future opportunities and needs in the use of ^{137}Cs, ^{210}Pb and ^{7}Be methodologies

2.1. Conjunctive use of FRNs

Although in many studies only a single radionuclide might be selected to meet the objectives, the conjunctive use of two or even three radionuclides can frequently provide more valuable information on the erosional history of a site, by generating datasets for different timescales. Based on their half-life and origin (Table 1), ^{137}Cs and ^{210}Pb can provide a basis for establishing the erosional history of a site over long- (100 years) and medium-term (50 years) periods [1] and the inclusion of ^{7}Be (days to months) provides the opportunity to consider shorter timescales [2-5]. The choice of FRN should therefore reflect the requirements of the study, in terms of both the timescales involved and its overall objectives [6].

Table 1. Comparative advantages and limitations of ^{137}Cs , $^{210}Pb_{ex}$ and ^{7}Be for quantifying soil erosion and redistribution (Adapted from [6])

FRN	Origin	Energy (keV)	Time		Sampling	Scale	Detector	Measurement		Sediment dating
			$t_{1/2}$	Span				Lab	In-situ	
^{137}Cs	Artific-ial man-made	662	30.2 yr	50 yr (MT)†	Simple	Plot to large water-shed	Normal HPGe γ	Easy	Easy	Feasible
^{210}Pb	Natural geo-genic	46	22.8 yr	100 yr (LT)†	Simple	Plot to water-shed	Broad energy range HPGe γ	More difficult	Limited and unreliable	Feasible
^{7}Be	Natural cosmo-genic	477	53.3 d	≤ 6 m (ST)*	Fine depth incre-mental	Local plot to field	Normal HPGe γ	Easy	Longer count time cf. ^{137}Cs	Feasible

** MT, medium-term; LT, long-term; ST, short-term erosion assessment; In some European countries the Chernobyl reactor accident provided the main input of ^{137}Cs into the landscape, and in these areas it is possible to estimate soil erosion and redistribution occurring since 1986. This represents a time scale of ca. 25 years which is significantly shorter than that provided by bomb fallout.*

2.2. The role of FRNs in assessing the effectiveness of soil conservation practices and environmental change

Work supported and promoted by an FAO/IAEA Coordinated Research Project (CRP) D1.50.08 (*Conservation Measures for Sustainable Watershed Management Using Fallout Radionuclides*) has demonstrated the potential for using ^{7}Be to assess the effectiveness of soil conservation measures in Chile, the US, the UK, Australia, Morocco and Vietnam [7]. The approach clearly involves a number of complexities, as it requires careful and detailed soil sampling and the need to monitor fallout inputs. To determine the effectiveness of soil conservation measures, it is necessary to have control areas for comparative purposes. However, the information generated by the ^{7}Be measurements provides a useful complement to ^{137}Cs measurements to assess the effects of different soil conservation practices.

In addition, ^{7}Be can provide a useful tool for investigating erosion associated with extreme weather events, which are expected to become more frequent as a result of climate change. The sequential sampling of ^{137}Cs inventories could provide another useful approach to

quantifying recent changes in soil redistribution in response to changes in both climate and land use and management, as demonstrated by work in Canada undertaken within the same CRP. However, the application of this approach is constrained by the need for periods of sufficient duration between measurement campaigns to ensure that the change in inventory is greater than the uncertainty associated with the sampling and laboratory measurement procedures.

2.3. Source fingerprinting procedures

Participants in CRP D1.50.08 from Australia, China, Japan, Poland, UK and USA have demonstrated the potential for using fingerprinting techniques for discriminating and quantifying the sources of suspended sediment transported by rivers and streams. Coupled with an appropriate experimental design, this approach could afford a powerful tool for assessing changes in sediment sources resulting from the introduction of soil conservation measures. This could involve a 'before' and 'after' study, where the relative importance of the potential sediment sources are assessed prior to treatment and the exercise is then repeated after treatment [8]. Equally, a paired catchment approach could be adopted, wherein one catchment serves as a control and the other is treated and the relative contributions of the potential sediment sources are determined in both catchments. If these approaches are adopted, it is important to also estimate the magnitude of the sediment output from the catchment or catchments, since source fingerprinting studies are only able to provide information on the relative contribution of different sources. Coupling of this information with information on the magnitude of the sediment output can provide quantitative information on changes in the amount of sediment mobilised from different sources and changes resulting from the introduction of soil conservation measures.

2.4. Up-scaling of the use of FRN-based methodologies from the field to the watershed level

Soil and water resources must be managed in an integrated way, in order to promote their sustainable use and to ensure environmental protection. Hence, the impacts of agricultural practices on the landscape and downstream communities need to be investigated at the watershed scale, which encompasses links between both upstream-downstream and upland-lowland environments. One of the major requirements for the further development of the application of FRNs in studying soil and sediment redistribution within watersheds is the fact that to date most studies have been conducted at the field scale, although some work has been undertaken in small basins ranging from a few hectares to a few km^2. An important and logical next step, which has to date been taken by only a few researchers using FRNs, is to upscale the assessment of the impact of agricultural activity on soil erosion and redistribution from the field to the watershed scale. This will require different sampling strategies and approaches. One of the possible options favoured by the authors is to analyse the watershed under investigation using GIS tools, and then divide it into sub-areas or classes representing similar agro-environmental conditions (soil, slope, land use) [9]. Representative fields can then be selected in each class, and sampled for application of FRN measurements. The results can then be generalized to the different classes and to the entire watershed. This should permit the establishment of a sediment budget, including an assessment of the sediment delivery ratio (SDR) and the net output. However, this approach needs to be developed further and validated under a range of different agro-environmental conditions (climate, soils, topography and

cropping systems). An approach for up-scaling to the national scale, where representative fields were sampled using transects, in a national sampling programme, in order to establish gross and net erosion rates has been described [10]. These data were in turn extrapolated to the national scale using a typology approach linked to available national databases on topography, soil types and land use, etc.

2.5. Evolution from research tools to decision support tools

If, in the future, FRNs are to be used more widely and at a larger scale and to contribute more directly to decision making, another great challenge for the users of FRNs will be to promote their transition and evolution from validated research tools to decision support tools.

2.6. Integration of FRN and compound specific stable isotope techniques

As indicated above, land degradation can be influenced by land use as well as by extreme weather events resulting from climate change. Adaptation to climate change will require the ability to identify the sources of mobilised sediment at an area-wide scale for the purposes of remediation, rehabilitation and sustainable agricultural and economic development. In this context, compound specific stable isotopes (CSSI) of carbon as well as other fingerprints associated with plants, animal manure and soil samples will be increasingly used to trace sources of soil loss/sediment production [11]. Combined use of Iso-Source and other advanced modelling tools that use several isotopes to identify sediment sources can provide the information needed to assess the effectiveness of different land use practices and soil conservation measures in response to changes in climate.

A CRP (D1.20.11: "Integrated Isotopic Approaches for an Area-wide Precision Conservation to Control the Impacts of Agricultural Practices on Land Degradation and Soil Erosion") on how to identify critical areas of soil loss has been implemented from 2009 to 2013. This CRP focused on the use of fingerprinting technologies, such as Compound Specific Stable Isotope (CSSI), in combination with the use of FRNs to establish key parameters of the sediment budget.

2.7. Other promising opportunities for the use of FRN methodologies

Several other areas, linked to refining the application of FRNs, are also currently being addressed by the scientific community [6]. These include:

- Testing assumptions relating to the initial distribution of fallout reaching the soil surface;
- Developing an improved understanding of the post-fallout behaviour of FRNs in soils and related environments (e.g. plant interception, preferential adsorption/desorption mechanisms);
- Provision of more rigorous guidelines for reference site selection;
- The wider application of *in situ* measurements for ^{7}Be and ^{137}Cs [12];
- Refinement of sampling methods for documenting FRN depth distributions, especially for ^{7}Be and ^{210}Pb;
- The improvement of laboratory procedures for measuring $^{210}Pb_{ex}$;

- Further improvement of the conversion models used to derive estimates of soil redistribution rates from measurements of FRN inventories;
- The use of interpolation and geostatistical tools to assist in the spatial extrapolation and mapping of results [13];
- Investigating the relationship between FRN activities and soil quality indicators [14].

3. Conclusion

The increasing worldwide use of FRNs for quantifying soil erosion and sedimentation within a wide range of agro-environments has clearly demonstrated the validity and potential of the approach. Furthermore, the many studies undertaken to date have demonstrated the potential advantages and limitations associated with individual FRNs. Although ^{137}Cs and to some extent $^{210}Pb_{ex}$ based methodologies are now well established, there remains a need for further investigations aimed at exploring the use of ^{7}Be, particularly in developing countries and in arid and semi-arid areas of the world. Notwithstanding the problems of interpretation that may occur when multiple erosion events occur within a short period, ^{7}Be offers considerable potential in providing a novel means of assessing erosion and soil redistribution associated with individual events, and establishing the effects of land use change and specific soil conservation measures. Because of the shorter timescales involved, ^{7}Be can provide a valuable complement to the use of ^{137}Cs and $^{210}Pb_{ex}$.

Measurement of FRNs by HPGe gamma spectrometry, however, particularly in the case of $^{210}Pb_{ex}$, requires skilled staff and appropriate analytical quality assurance systems, including standardised operating procedures. The selection and application of a particular FRN for quantifying soil erosion and redistribution should reflect the user's objectives, the advantages and limitations of each approach, and the human capacity and material resources available. The need to upscale the use of FRNs from the field to the watershed level will necessitate the application of additional tools (e.g. GIS, Global Positioning Systems (GPS) and Geostatistics) to assist in integrating and interpreting the spatial complexity of the landscape. More attention should be paid to combining FRNs with conventional methods. This approach has great potential that has yet to be fully exploited.

REFERENCES

[1] WALLING, D.E., COLLINS, A.L., SICHINGABULA, H.M., Using unsupported lead-210 measurements to investigate soil erosion and sediment delivery in a small Zambian catchment, Geomorphology 52 (2003) 193–213.

[2] BLAKE, W.H., WALLING D.E., HE, Q., beryllium-7 as a tracer in soil erosion investigations, Appl. Radiat. Isot. 51 (1999) 599–605.

[3] BLAKE, W.H., WALLBRINK, P.J., WILKINSON, S.N., HUMPHREYS, G.S., DOERR, S.H., SHAKESBY, R.A., TOMKINS, K.M., Deriving hillslope sediment budgets in wildfire-affected forests using fallout radionuclide tracers, Geomorphology. 104 (2009) 105–116.

[4] WALLING, D.E., HE, Q., BLAKE, W., Use of ^{7}Be and ^{137}Cs measurements to document short-and medium-term rates of water-induced soil erosion on agricultural land, Water Resourc. Res. 35 (1999) 3865–3874.

[5] SEPÚLVEDA, A., SCHULLER, P., WALLING, D.E., CASTILLO, A., Use of ^{7}Be to document soil erosion associated with a short period of extreme rainfall, J. Environ. Radioact. 99 (2008) 35–49.
[6] MABIT, L., BENMANSOUR, M., WALLING, D.E., Comparative advantages and limitations of the fallout radionuclides ^{137}Cs, ^{210}Pb$_{ex}$ and ^{7}Be for assessing soil erosion and sedimentation, J. Environ. Radioact. 99 (2008) 1799–1807.
[7] INTERNATIONAL ATOMIC ENERGY AGENCY, Impact of Soil Conservation Measures on Erosion Control and Soil Quality, IAEA-TECDOC-1665, IAEA, Vienna, Austria (2011).
[8] MERTEN, G.H., et al., "The effects of soil conservation on sediment yield and sediment source dynamics in a catchment in southern Brazil", Sediment Dynamics for a Changing Future, Proceedings of the Warsaw Symposium, June 2010, IAHS Publication No. 337 (2010) 59–67.
[9] MABIT, L., BERNARD, C., LAVERDIÈRE, M.R., Assessment of erosion in the Boyer River watershed (Canada) using a GIS oriented sampling strategy and ^{137}Cs measurements, Catena 71 (2007) 242–249.
[10] WALLING, D.E., ZHANG, Y., A national assessment of soil erosion based on caesium-137 measurements. Global Change–Changes for Soil Management, Adv. Geoecol. 4 (2010) 89–97.
[11] GIBBS, M.M., Identifying source soils in contemporary estuarine sediments: A new compound-specific isotope method, Estuar. Coasts 31 (2008) 344–359.
[12] TYLER, A.N., COPPLESTONE, D., Preliminary results from the first national *in situ* gamma spectrometry survey of the United Kingdom, J. Environ. Radioact. 96 (2007) 94–102.
[13] MABIT, L., BERNARD, C., Assessment of spatial distribution of fallout radionuclides through geostatistics concept, J. Environ. Radioact. 97 (2007) 206–219.
[14] LI, Y., et al., Changes in soil organic carbon induced by tillage and water erosion on a steep cultivated hillslope in the Chinese Loess Plateau from 1898–1954 and 1954–1998, J. Geophys. Res. 112 (2007) G01021, doi:10.1029/2005JG000107.

IAEA PUBLICATIONS ON SOIL AND WATER MANAGEMENT AND CROP NUTRITION

FOOD AND AGRICULTURE ORGANIZATION, Maximising the use of biological nitrogen fixation in agriculture. Developments in Plant and Soil Sciences No. 99. FAO, Rome, and Kluwer Academic Publishers, Dordrecht, FAO, Rome (2003).

FOOD AND AGRICULTURE ORGANIZATION, Use of phosphate rocks for sustainable agriculture. FAO Fertilizer and Plant Nutrition Bulletin 13. Joint FAO/IAEA Division of Nuclear Techniques in Food and Agriculture and the Land and Water Development Division-AGL, FAO, Rome (2004).

INTERNATIONAL ATOMIC ENERGY AGENCY, Assessment of Soil Phosphorus Status and Management of Phosphatic Fertilisers to Optimise Crop Production , IAEA-TECDOC-1272, IAEA, Vienna (2002).

INTERNATIONAL ATOMIC ENERGY AGENCY, Field Estimation of Soil Water Content, A Practical Guide to Methods, Instrumentation and Sensor Technology, Training Course Series No. 30. Also IAEATCS-30/CD - ISSN 1998-0973, IAEA, Vienna (2008).

INTERNATIONAL ATOMIC ENERGY AGENCY, Greater Agronomic Water Use Efficiency in Wheat and Rice Using Carbon Isotope Discrimination, IAEA-TECDOC-1671, ISBN978-92-0-123910-5, ISSN 1011-4289, IAEA, Vienna (2012).

INTERNATIONAL ATOMIC ENERGY AGENCY, Guidelines for the Use of Isotopes of Sulfur in Soil-Plant Studies, IAEA Training Course Series No. 20, IAEA, Vienna (2003).

INTERNATIONAL ATOMIC ENERGY AGENCY, Guidelines on Nitrogen Management in Agricultural Systems, Training Course Series No. 29: IAEA-TCS-29/CD - ISSN 1998-0973, IAEA, Vienna (2008).

INTERNATIONAL ATOMIC ENERGY AGENCY, Impact of Soil Conservation Measures on Erosion Control and Soil Quality, IAEA-TECDOC-1665, ISBN 978-92-0-113410-3, ISSN 1011-4289, IAEA, Vienna (2011).

INTERNATIONAL ATOMIC ENERGY AGENCY, Irradiated Sewage Sludge for Application to Cropland, IAEA-TECDOC-1317, IAEA, Vienna (2002).

INTERNATIONAL ATOMIC ENERGY AGENCY, Las Sondas de Neutrones y Gamma: Sus Aplicaciones en Agronomía, Segunda Edición, Colección Cursos de Capacitación No. 16, (2003).

INTERNATIONAL ATOMIC ENERGY AGENCY, Les Sondes à Neutrons et à Rayons Gamma: Leur Applications en Agronomie, Deuxième Édition, Collection Cours de Formation No.16 (2003).

INTERNATIONAL ATOMIC ENERGY AGENCY, Management of Agroforestry Systems for Enhancing Resource use Efficiency and Crop Productivity Details, IAEA IAEA-TECDOC Series No. 1606, ISBN 978-92-0-110908-8, IAEA, Vienna (2008).

INTERNATIONAL ATOMIC ENERGY AGENCY, Management of Agroforestry Systems for Enhancing Resource use Efficiency and Crop Productivity Details, IAEA-TECDOC-CD-1606, 2009, ISBN 978-92-0-150909-3, IAEA, Vienna (2009).

INTERNATIONAL ATOMIC ENERGY AGENCY, Management of Crop Residues for Sustainable Crop Production, IAEA-TECDOC-1354, IAEA, Vienna (2003).

INTERNATIONAL ATOMIC ENERGY AGENCY, Management Practices for Improving Sustainable Crop Production in Tropical Acid Soils Results of a Coordinated Research Project organized by the Joint FAO/IAEA Programme of Nuclear Techniques in Food and Agriculture, Proceedings Series, STI/PUB/1285. 277, (2007).

INTERNATIONAL ATOMIC ENERGY AGENCY, Neutron and Gamma Probes: Their Use in Agronomy, Second Edition, IAEA Training Course Series No. 16, IAEA, Vienna (2003).

INTERNATIONAL ATOMIC ENERGY AGENCY, Nuclear Techniques in Integrated Plant Nutrient, Water and Soil Management, Proc. Symp. Vienna, 2000 IAEA C+S Paper Series 11/P, IAEA, Vienna (2002).

INTERNATIONAL ATOMIC ENERGY AGENCY, Nutrient and water management practices for increasing crop production in rainfed arid/semi-arid areas, IAEA-TECDOC-1468, IAEA, Vienna (2005).

INTERNATIONAL ATOMIC ENERGY AGENCY, Use of Isotope and Radiation Methods in Soil and Water Management and Crop Nutrition - Manual IAEA Training Course Series No. 14, IAEA, Vienna (2001).

INTERNATIONAL ATOMIC ENERGY AGENCY, Use of Isotope and Radiation Methods in Soil and Water Management and Crop Nutrition, An interactive CD, (2004).

INTERNATIONAL ATOMIC ENERGY AGENCY, Water Balance and Fertigation for Crop Improvement in West Asia, IAEA-TECDOC-1266, IAEA, Vienna (2002).

CONTRIBUTORS TO DRAFTING AND REVIEW

Austria:

Chalk, P,	Soil and Water Management and Crop Nutrition Laboratory, Joint FAO/IAEA Division of Nuclear Techniques in Food and Agriculture, Seibersdorf
Chhem-Kieth, S,	Soil and Water Management and Crop Nutrition Laboratory, Joint FAO/IAEA Division of Nuclear Techniques in Food and Agriculture, Seibersdorf
Dercon, G,	Soil and Water Management and Crop Nutrition Laboratory, Joint FAO/IAEA Division of Nuclear Techniques in Food and Agriculture, Seibersdorf
Dornhofer, P,	Soil and Water Management and Crop Nutrition Laboratory, Joint FAO/IAEA Division of Nuclear Techniques in Food and Agriculture, Seibersdorf
Gonsalves, B,	Soil and Water Management and Crop Nutrition Laboratory, Joint FAO/IAEA Division of Nuclear Techniques in Food and Agriculture, Seibersdorf
Leon de Muellner, R,	Soil and Water Management and Crop Nutrition Laboratory, Joint FAO/IAEA Division of Nuclear Techniques in Food and Agriculture, Seibersdorf
Mabit, L,	Soil and Water Management and Crop Nutrition Laboratory, Joint FAO/IAEA Division of Nuclear Techniques in Food and Agriculture, Seibersdorf
Toloza, A,	Soil and Water Management and Crop Nutrition Laboratory, Joint FAO/IAEA Division of Nuclear Techniques in Food and Agriculture, Seibersdorf
Zapata, F,	Soil and Water Management and Crop Nutrition Section, Joint FAO/IAEA Division of Nuclear Techniques in Food and Agriculture, Vienna

Canada:

Bernard, C,	Ministère de l'Agriculture, des Pêcheries et de l'Alimentation du Québec, Quebec
Duchemin, M,	Institut de Recherche et de Développement en Agro-Environment (IRDA), Quebec
Owens, P.N,	Environmental Science Programme and Quesnel River Research Centre, University of Northern British Columbia Prince George, British Columbia

Chile:

Schuller, P,	Universidad Austral de Chile, Facultad de Ciencias, Instituto de Ciencias Químicas, Valdivia

Hungary:

Tarján, S,	Radioanalytical Reference Laboratory, Central Agricultural Office Food and Feed Safety Directorate, Budapest

Morocco:

Benmansour, M,	Centre National de l'Energie des Sciences et des Technique Nucleaires (CNESTEN), Rabat
Bouksirate, H,	Institut National de la Recherche Agronomique (INRA), Rabat
Iaaich, H,	Institut National de la Recherche Agronomique (INRA), Rabat
Moussadek, R,	Institut National de la Recherche Agronomique (INRA), Rabat
Mrabet, R,	Institut National de la Recherche Agronomique (INRA), Rabat
Nouira, A,	Centre National de l'Energie des Sciences et des Technique Nucleaires (CNESTEN), Rabat
Zouagui, A,	Centre National de l'Energie des Sciences et des Technique Nucleaires (CNESTEN), Rabat

Slovakia:

Fulajtar, E,	Soil Science and Conservation Research Institute, Bratislava

Switzerland:

Alewell, C,	Department of Environmental Sciences, Environmental Geosciences, Basel University
Konz, N,	Department of Environmental Sciences, Environmental Geosciences, Basel University
Meusburger, K,	Department of Environmental Sciences, Environmental Geosciences, Basel University
Schaub, M,	Department of Environmental Sciences, Environmental Geosciences, Basel University

United Kingdom:

Blake, W.H,	School of Geography, Earth and Environmental Sciences, University of Plymouth
He, Q,	University of Exeter, Department of Geography, Exeter
Tayor, A,	School of Geography, Earth and Environmental Sciences, University of Plymouth
Walling, D.E,	University of Exeter, Department of Geography, Exeter
Zhang, Y,	ADAS, Wolverhampton

IAEA
International Atomic Energy Agency

No. 23

ORDERING LOCALLY

In the following countries, IAEA priced publications may be purchased from the sources listed below or from major local booksellers.

Orders for unpriced publications should be made directly to the IAEA. The contact details are given at the end of this list.

AUSTRALIA
DA Information Services
648 Whitehorse Road, Mitcham, VIC 3132, AUSTRALIA
Telephone: +61 3 9210 7777 • Fax: +61 3 9210 7788
Email: books@dadirect.com.au • Web site: http://www.dadirect.com.au

BELGIUM
Jean de Lannoy
Avenue du Roi 202, 1190 Brussels, BELGIUM
Telephone: +32 2 5384 308 • Fax: +32 2 5380 841
Email: jean.de.lannoy@euronet.be • Web site: http://www.jean-de-lannoy.be

CANADA
Renouf Publishing Co. Ltd.
5369 Canotek Road, Ottawa, ON K1J 9J3, CANADA
Telephone: +1 613 745 2665 • Fax: +1 643 745 7660
Email: order@renoufbooks.com • Web site: http://www.renoufbooks.com

Bernan Associates
4501 Forbes Blvd., Suite 200, Lanham, MD 20706-4391, USA
Telephone: +1 800 865 3457 • Fax: +1 800 865 3450
Email: orders@bernan.com • Web site: http://www.bernan.com

CZECH REPUBLIC
Suweco CZ, spol. S.r.o.
Klecakova 347, 180 21 Prague 9, CZECH REPUBLIC
Telephone: +420 242 459 202 • Fax: +420 242 459 203
Email: nakup@suweco.cz • Web site: http://www.suweco.cz

FINLAND
Akateeminen Kirjakauppa
PO Box 128 (Keskuskatu 1), 00101 Helsinki, FINLAND
Telephone: +358 9 121 41 • Fax: +358 9 121 4450
Email: akatilaus@akateeminen.com • Web site: http://www.akateeminen.com

FRANCE
Form-Edit
5 rue Janssen, PO Box 25, 75921 Paris CEDEX, FRANCE
Telephone: +33 1 42 01 49 49 • Fax: +33 1 42 01 90 90
Email: fabien.boucard@formedit.fr • Web site: http://www.formedit.fr

Lavoisier SAS
14 rue de Provigny, 94236 Cachan CEDEX, FRANCE
Telephone: +33 1 47 40 67 00 • Fax: +33 1 47 40 67 02
Email: livres@lavoisier.fr • Web site: http://www.lavoisier.fr

L'Appel du livre
99 rue de Charonne, 75011 Paris, FRANCE
Telephone: +33 1 43 07 50 80 • Fax: +33 1 43 07 50 80
Email: livres@appeldulivre.fr • Web site: http://www.appeldulivre.fr

GERMANY
Goethe Buchhandlung Teubig GmbH
Schweitzer Fachinformationen
Willstätterstrasse 15, 40549 Düsseldorf, GERMANY
Telephone: +49 (0) 211 49 8740 • Fax: +49 (0) 211 49 87428
Email: s.dehaan@schweitzer-online.de • Web site: http://www.goethebuch.de

HUNGARY
Librotade Ltd., Book Import
PF 126, 1656 Budapest, HUNGARY
Telephone: +36 1 257 7777 • Fax: +36 1 257 7472
Email: books@librotade.hu • Web site: http://www.librotade.hu

INDIA
Allied Publishers
1st Floor, Dubash House, 15, J.N. Heredi Marg, Ballard Estate, Mumbai 400001, INDIA
Telephone: +91 22 2261 7926/27 • Fax: +91 22 2261 7928
Email: alliedpl@vsnl.com • Web site: http://www.alliedpublishers.com

Bookwell
3/79 Nirankari, Delhi 110009, INDIA
Telephone: +91 11 2760 1283/4536
Email: bkwell@nde.vsnl.net.in • Web site: http://www.bookwellindia.com

ITALY
Libreria Scientifica "AEIOU"
Via Vincenzo Maria Coronelli 6, 20146 Milan, ITALY
Telephone: +39 02 48 95 45 52 • Fax: +39 02 48 95 45 48
Email: info@libreriaaeiou.eu • Web site: http://www.libreriaaeiou.eu

JAPAN
Maruzen Co., Ltd.
1-9-18 Kaigan, Minato-ku, Tokyo 105-0022, JAPAN
Telephone: +81 3 6367 6047 • Fax: +81 3 6367 6160
Email: journal@maruzen.co.jp • Web site: http://maruzen.co.jp

NETHERLANDS
Martinus Nijhoff International
Koraalrood 50, Postbus 1853, 2700 CZ Zoetermeer, NETHERLANDS
Telephone: +31 793 684 400 • Fax: +31 793 615 698
Email: info@nijhoff.nl • Web site: http://www.nijhoff.nl

Swets Information Services Ltd.
PO Box 26, 2300 AA Leiden
Dellaertweg 9b, 2316 WZ Leiden, NETHERLANDS
Telephone: +31 88 4679 387 • Fax: +31 88 4679 388
Email: tbeysens@nl.swets.com • Web site: http://www.swets.com

SLOVENIA
Cankarjeva Zalozba dd
Kopitarjeva 2, 1515 Ljubljana, SLOVENIA
Telephone: +386 1 432 31 44 • Fax: +386 1 230 14 35
Email: import.books@cankarjeva-z.si • Web site: http://www.mladinska.com/cankarjeva_zalozba

SPAIN
Diaz de Santos, S.A.
Librerias Bookshop • Departamento de pedidos
Calle Albasanz 2, esquina Hermanos Garcia Noblejas 21, 28037 Madrid, SPAIN
Telephone: +34 917 43 48 90 • Fax: +34 917 43 4023
Email: compras@diazdesantos.es • Web site: http://www.diazdesantos.es

UNITED KINGDOM
The Stationery Office Ltd. (TSO)
PO Box 29, Norwich, Norfolk, NR3 1PD, UNITED KINGDOM
Telephone: +44 870 600 5552
Email (orders): books.orders@tso.co.uk • (enquiries): book.enquiries@tso.co.uk • Web site: http://www.tso.co.uk

UNITED STATES OF AMERICA
Bernan Associates
4501 Forbes Blvd., Suite 200, Lanham, MD 20706-4391, USA
Telephone: +1 800 865 3457 • Fax: +1 800 865 3450
Email: orders@bernan.com • Web site: http://www.bernan.com

Renouf Publishing Co. Ltd.
812 Proctor Avenue, Ogdensburg, NY 13669, USA
Telephone: +1 888 551 7470 • Fax: +1 888 551 7471
Email: orders@renoufbooks.com • Web site: http://www.renoufbooks.com

United Nations
300 East 42nd Street, IN-919J, New York, NY 1001, USA
Telephone: +1 212 963 8302 • Fax: 1 212 963 3489
Email: publications@un.org • Web site: http://www.unp.un.org

Orders for both priced and unpriced publications may be addressed directly to:

IAEA Publishing Section, Marketing and Sales Unit, International Atomic Energy Agency
Vienna International Centre, PO Box 100, 1400 Vienna, Austria
Telephone: +43 1 2600 22529 or 22488 • Fax: +43 1 2600 29302
Email: sales.publications@iaea.org • Web site: http://www.iaea.org/books

14-19351

International Atomic Energy Agency
Vienna
ISBN 978–92–0–105414–2
ISSN 1011–4289